Data-Driven Approaches to Modeling Heterogeneity and Variability Across Asymptomatic Brain and Cognitive Aging, Mild Cognitive Impairment, and Alzheimer's disease

by

Shannon Drouin

A thesis submitted in partial fulfillment of the requirements for the degree of

Doctor of Philosophy

Department of Psychology

University of Alberta

Abstract

Objective

We apply data-driven approaches to identify predictors of heterogeneous trajectories across normal aging, Mild Cognitive Impairment (MCI), and Alzheimer's disease (AD). In Study 1, we investigated predictors of left and right hippocampal (HC) volume trajectory classes. In Study 2, we identified the leading predictors of cognitive resilience, cognitive vulnerability, and brain/cognitive stability in varying contexts of morphometric brain changes. In Study 3, we examined the leading predictors of AD, MCI, and dementia from a set of risk factors/biomarkers including novel metabolomics markers.

Methods

Study 1 participants (n=351) were cognitively normal (CN) older adults from the Alzheimer's Disease Neuroimaging Initiative (ADNI) with longitudinal imaging and baseline biomarker/risk factor data. We applied latent class growth analysis (LCGA) to identify separable HC trajectory classes. We then applied a machine learning (ML) algorithm to identify leading biomarker predictors (from 38) discriminating the highest and lowest trajectory classes.

Study 2 participants (n=415) were CN older adults from ADNI with longitudinal imaging and baseline biomarker/risk factor data. We used LCGA for two foundational goals, identifying HC and cognitive trajectory classes. We applied ML algorithms to identify the leading predictors (from 42) of (a) cognitive resilience, (b) cognitive vulnerability, and (c) brain/cognitive stability.

Study 3 participants included two samples of three age- and sex-matched cohorts from the Comprehensive Assessment of Neurodegeneration in Aging study: cognitively unimpaired (CU; n_1=33; n_2=32), MCI (n_1=33; n_2=33), and AD (n_1=33; n_2=21). For each sample, we used three ML

algorithms and 111-112 risk factors/biomarkers, and metabolite predictors to identify the leading predictors of AD (CU-AD), MCI (CU-MCI), and dementia (MCI-AD).

Results

Study 1: We detected three trajectory classes for the left HC and three classes for the right HC (highest, middle, lowest). For the left HC, seven predictors from four modalities discriminated the lowest and highest HC trajectory classes: plasma Aβ1-40, plasma tau, plasma Aβ1-42, sex, education, depression, and body mass index. For the right HC, three predictors from two modalities discriminated the lowest and highest HC trajectory classes: sex, education, and plasma Aβ1-42.

Study 2: We first detected two HC trajectory classes and two cognitive trajectory classes (low and high). Based on differential combined class membership, we identified three target subgroups: cognitively resilient (*n*=72), cognitively vulnerable (*n*=144), and brain and cognitively stable (*n*=92). Cognitive resilience was predicted by higher CSF Aβ1-42, higher education, lower plasma Aβ1-42, lower CSF p-tau, lower plasma Aβ1-40, and lower age. Cognitive vulnerability was predicted by lower education, higher plasma Aβ1-40, higher BMI, higher age, lower glucose, higher plasma Aβ1-42. Brain/cognitive stability was predicted by higher CSF Aβ1-42, lower polygenic risk score, female sex, higher plasma Aβ1-42, higher pulse pressure, and lower age.

Study 3: We report leading predictors at a 40% model explanation criterion. AD was predicted by six biomarkers from three domains (sensory, imaging, and metabolomics) in Sample 1 and nine biomarkers from five domains (imaging, demographic, and clinical health, sensory, and metabolomics) in Sample 2. MCI was predicted by 12 biomarkers from three domains (metabolomics, clinical health, and imaging) in Sample 1 and 13 biomarkers from five

domains (metabolomics, clinical health, vascular/metabolic, imaging, and demographic) in Sample 2. Dementia was predicted by nine predictors from four domains (sensory, imaging, metabolomics, and vascular/metabolic) in Sample 1 and nine biomarkers from seven domains (imaging, demographic, clinical health, metabolomics, gait/function, lifestyle, and vascular/metabolic) in Sample 2.

Discussion

The overall aim of this dissertation research was to apply data-driven approaches to the prediction of heterogeneous trajectories and outcomes in brain/cognitive aging and dementia. Study 1 demonstrated that HC trajectory classes represent secondary phenotypes of brain aging that are predicted by a wide range of AD-related risk factors/biomarkers. Study 2 demonstrated that (a) cognitive trajectories can supplement HC trajectories and represent alternative pathways of brain and cognitive aging and (b) these pathways can be predicted by a similar roster of AD-related risk factors/biomarkers. Study 3 identified the leading predictors originating from established risk domains as well as novel metabolomics predictors that are associated with MCI, AD, and/or dementia. Overall, the dissertation research highlights the relative importance of risk factors/biomarkers and candidate metabolites in the prediction of both desirable (high HC trajectory classes, resilience, stability) and undesirable (low HC trajectory classes, cognitive vulnerability, MCI, AD, dementia) aging trajectories and outcomes.

Preface

Chapter 2 and Appendix A of this dissertation has been published as Drouin, S.M., McFall, G.P., Potvin, O., Bellec, P., Masellis, M., Duchesne, S., & Dixon, R.A. for the Alzheimer's Disease Neuroimaging Initiative, "Data-driven analyses of longitudinal hippocampal imaging trajectories: Discrimination and biomarker prediction of change classes," Journal of Alzheimer's Disease, 2022 (88), 97-115. https://doi.org/10.3233/JAD-215289. SMD, GPM, OP, SD, and RAD were responsible for the conception and background. SMD, GPM and RAD were responsible for the study plan. SMD, OP, SD, and GPM were responsible for data assembly and statistical analyses. SMD, GPM, and RAD were responsible for interpretation of the results. SMD drafted the manuscript. SMD, GPM, OP, PB, MM, SD, and RAD revised the manuscript prior to submission and following reviewer comments. All authors read and approved the final manuscript prior to submission. We present the final accepted version of the published manuscript.

Acknowledgements

I would first like to sincerely thank my supervisor, Dr. Roger A. Dixon, for his unwavering support and mentorship. I am extremely grateful for the kind support and expert guidance you have provided in these last years which have contributed to work I am extremely proud of. To members of my supervisory committee, Drs. Sandra Wiebe and Richard Camicioli, thank you for lending your time and expertise which has led to progress in both this dissertation work and my development as a researcher. I would also like to thank my mentors and colleagues, who have continuously provided insight, counsel, and laughs: Dr. Peggy McFall, Dr. Linzy Bohn, and Jill Friesen. Lastly, but not least, I would like to thank my family and friends for their continued support and encouragement during this demanding journey.

Funding Acknowledgement: The dissertation research was supported by grants to Roger A. Dixon. We would like to acknowledge: (a) Partnership support from the Canadian Consortium on Neurodegeneration in Aging and research funding from Alberta Innovates and the Canadian Institutes of Health Research (G2020000063) and (b) National Institutes of Health (National Institute on Aging; R01 AG088235). We acknowledge data from the Alzheimer's Disease Neuroimaging Initiative and the Canadian Consortium on Neurodegeneration in Aging COMPASS-ND Study. Shannon M. Drouin was supported by Alberta Innovates (Graduate Student Scholarship for Data-enabled Innovation; GSS-DEI).

Table of Contents

List of Tables

List of Figures

Chapter 1: Introduction

Characterized by vast variability in level and change as well as heterogeneous outcomes, pathways of brain and cognitive aging range from healthier (stable) trajectories to rapid decline and pathological changes associated with clinical syndromes (Bocancea et al., 2021; Dixon, Small, MacDonald, & McArdle, 2012; S. M. Drouin et al., 2022; Nyberg & Pudas, 2019). These aging trajectories differ not only across and within individuals, but also domains (e.g., memory, executive function), at-risk conditions (e.g., Type 2 diabetes, hypertension), sex, brain regions (e.g., cortical thickness, hippocampal volume), and asymptomatic and clinical phases of neurodegenerative disease (Ding et al., 2019; R. Dixon & M. Lachman, 2019; Ezzati et al., 2019; Giorgio et al., 2020; Heilman & Nadeau, 2019; Koran, Wagener, & Hohman, 2017; McCarrey, An, Kitner-Triolo, Ferrucci, & Resnick, 2016; Mielke et al., 2013; Minkova et al., 2017; Nyberg & Pudas, 2019; Pettigrew et al., 2016; Small, Dixon, & McArdle, 2011). Some of these non-normative (preclinical and clinical) outcomes include Alzheimer's disease (AD) and Mild Cognitive Impairment (MCI), the latter of which often precedes an AD diagnosis.

Global population aging and overall increases in average adult life expectancy have led to significant increases to aging-related morbidity rates, including that of AD and other neurodegenerative diseases. The most common form of dementia, the AD clinical syndrome is characterized by rapid and accelerating cognitive decline, especially in memory. Distinct neuropathology (i.e., beta-amyloid [Aβ] plaques and tau neurofibrillary tangles) as well as neurodegeneration (i.e., hippocampal atrophy, ventricular enlargement) distinguishes the disease biologically (D. Hu et al., 2021; Jack Jr et al., 2018; Seto, Weiner, Dumitrescu, & Hohman, 2021). Notably, global rates of dementia are expected to double every twenty years to reach 131.5 million by 2050 (Prince et al., 2015). The growing prevalence of AD and other forms of

dementias in older adults has become an urgent public health crisis with mounting societal, health, and economic costs. In Canada alone, close to one million older adults will be living with dementia by 2030 (*Navigating the Path Forward for Dementia in Canada: The Landmark Study Report #1*, 2022). In addition to the considerable amounts of healthcare resources necessary for this increasing proportion of older adults, health and opportunity costs for caregivers and other affected populations represent another aspect of the socioeconomic burden that is becoming a major and growing concern. For example, care partners to individuals with dementia in Canada contribute on average 26 hours a week of informal caregiving, representing a considerable economic impact on the current and future work force (*Navigating the Path Forward for Dementia in Canada: The Landmark Study Report #1*, 2022).

Despite the significant emphasis on identifying an efficacious treatment (e.g., drug therapy), therapeutic and clinical research has been generally unsuccessful in this regard (J. L. Cummings, Tong, & Ballard, 2019), with 99% of drug candidates being discontinued (Tatulian, 2022). Indeed, although there is a growing and strong focus on the development of disease-modifying drugs in the AD drug development pipeline (83% of clinical trial agents in 2021), most of these therapies have not successfully met phase III efficacy targets (J. Cummings, Lee, Zhong, Fonseca, & Taghva, 2021; J. L. Cummings et al., 2019). As of now, only two disease-modifying drugs has been approved by the US Food and Drug Administration (*aducanumab, lecanemab*) and expert opinion on their efficacy has been mixed at best (Tatulian, 2022). Possible reasons for the lack of success in clinical trials include the complex etiology and long prodromal period of AD (J. L. Cummings et al., 2019; Wilkins & Trushina, 2018). Specifically, AD-specific neuropathology (Aβ and tau) has been shown to accumulate decades prior to the onset of clinical symptoms such that current clinical therapeutics may be aimed at individuals too

late in the disease process to be effective (Wilkins & Trushina, 2018). As such, the identification of early signals and predictors of non-normative trajectories (i.e., exacerbated cognitive decline or regional brain atrophy) prior to diagnosis (and neuropathology accumulation) has become an emerging and important facet of brain and cognitive aging research (K. J. Anstey, R. Eramudugolla, D. E. Hosking, N. T. Lautenschlager, & R. A. Dixon, 2015; R. Dixon & M. Lachman, 2019). One important example of non-normative trajectories includes exacerbated hippocampal atrophy, a robust neuroimaging biomarker of AD-related neurodegeneration. Predictors of progressive atrophy of this key brain structure have been identified both cross-sectionally (Chetelat & Fouquet, 2013; O'Shea, Cohen, Porges, Nissim, & Woods, 2016) and longitudinally (S. M. Drouin et al., 2022; Gorbach et al., 2017; O'Shea et al., 2016; Rosano et al., 2012; Zhao et al., 2019). Selected examples of these predictors include a number of AD-related CSF and plasma biomarkers (S. M. Drouin et al., 2022; Stricker et al., 2012), education (Piras, Cherubini, Caltagirone, & Spalletta, 2011), smoking (Durazzo, Meyerhoff, & Nixon, 2013), and increased AD genetic risk (Chetelat & Fouquet, 2013; Kerchner et al., 2014; Warzok et al., 1998).

Similarly, the investigation of predictors and risk factors leading away from non-normative trajectories or pathways (and towards healthier and stable brain and cognitive aging) has been lauded as an important research direction (R. Dixon & M. Lachman, 2019; Kaup et al., 2015; McDermott, McFall, Andrews, Anstey, & Dixon, 2017). These factors may be non-modifiable (potential early identification or stratification variables for at-risk individuals) or modifiable (potential targets for preventative interventions prior to disease diagnosis) (R. Dixon & M. Lachman, 2019). Specifically, the identification of modifiable AD-related risk factors is especially important as this can both (a) facilitate the early detection of at-risk individuals and

(b) enable the targeting of specific factors. The latter goal is emphasized in a recent *Lancet* report describing 12 potentially modifiable risk factors across the lifespan which account for 40% of dementias globally (Livingston et al., 2020). These factors were lower education (in early life), hypertension, hearing impairment (< 25 dB), smoking, obesity (BMI > 30), depression, physical inactivity, diabetes, low social contact, excessive alcohol consumption (> 21 drinks per week), traumatic brain injury, and air pollution (i.e., high nitrogen dioxide concentration and fine ambient particulate matter) (Livingston et al., 2020). This report highlights the potential advantages of targeting specific factors—perhaps in combination—at the population and individual level in order to avoid or delay a considerable proportion of dementias worldwide (Livingston et al., 2020).

Moreover, a recent systematic review included a meta-analysis of numerous risk factors differentially for AD (34) and vascular dementia (VaD, 26) (Anstey, Ee, Eramudugolla, Jagger, & Peters, 2019). This review evaluated quality and breadth of evidence for such key modifiable risk factors as education, smoking, physical activity, diabetes, depression, obesity, hypertension and social engagement. Although these factors (and many others considered in the report) are repeatedly identified as associated with increased risk of AD and promoted as having the potential to be targeted in prevention protocols, the evidence base for differential influence varies across factor, domain, outcome, and generalizability (Anstey et al., 2019).

The consideration of sex and/or gender as risk factors has been increasingly encouraged in emerging ADRD research (Tierney, Curtis, Chertkow, & Rylett, 2017). Despite this, the majority of ADRD research studies were noted to not adequately measure or define sex and gender (Stites, Cao, Harkins, & Flatt, 2022). The inclusion of sex and gender in ADRD research is especially important for several reasons. First, women outnumber men in clinical diagnoses of

AD, with over 2/3 of cases being the former. Second, AD-related risk factors differ in both prevalence and impact across sex and gender. For example, some risk factors are sex-specific (e.g., menopause) and others occur more commonly in one sex or gender (e.g., increased risk of stroke for men versus women, lower mean education in women) (Mielke, Vemuri, & Rocca, 2014). Other risk factors, such as BMI, have been found to have a greater impact on one sex or gender. Specifically, a higher body mass index was found to be associated with better cognitive (executive function, memory, neurocognitive speed) trajectories in females but not males (L. Bohn, McFall, Wiebe, & Dixon, 2020). Other examples include the stronger risk effect of the Apolipoprotein E (*APOE*) ε4 allele for females versus males and the female-specific risk increasing effect of the Met66 allele of *Brain Derived Neurotrophic Factor* (Fukumoto et al., 2010). In summary, AD-related risk factors can be organized into meaningful clusters of risk domains, each associated with varying levels of risk for exacerbated decline in asymptomatic aging or transitions from normal to impaired aging. Specific examples of these domains include metabolic (e.g., Type II diabetes, body mass index [BMI]), medical history (e.g., depression, head injury), vascular (e.g., hypertension, atrial fibrillation), lifestyle (e.g., diet, physical activity, social engagement), genetic (e.g**.,** *APOE*), and demographic (e.g., sex, education) (Boyle, Buchman, Wilson, Leurgans, & Bennett, 2009; R. Dixon & M. Lachman, 2019; C. R. Jack et al., 2015; G. P. McFall, Bäckman, & Dixon, 2019; G. P. McFall et al., 2020; G. P. McFall et al., 2015b; Olaya, Bobak, Haro, & Demakakos, 2017; Shen, Zhou, Chen, Zhang, & Initiative, 2019; Waldstein et al., 2008; Zahodne et al., 2016). Importantly, some of these clusters of risk domains can vary in magnitude or prevalence by sex and/or gender.

Complementing the growing body of AD risk factor research have been substantial advances in an area that aims to identify biological and possibly mechanistic markers of

degenerative brain aging, impairment and AD diagnosis and progression (Adav & Wang, 2021; Habartová et al., 2019; Huan et al., 2018; Riedel et al., 2018; Sebastiani et al., 2017; Tam et al., 2019; Tanaka et al., 2020; Varma et al., 2018). These studies have produced promising evidence that biological markers may be independently predictive of exacerbated preclinical decline or disease diagnosis and progression, but may also operate interactively (e.g., as moderators) or in larger clusters, such as signatures (i.e., biological patterns), networks, panels, or composites (Badhwar et al., 2020a; Huan et al., 2018; Riedel et al., 2018; Sapkota et al., 2018; Schwarz et al., 2016; M. Wang et al., 2016). Like individual risk factors, such clusters of biological markers may include multiple modalities of AD-related risk or mechanisms (Fransquet & Ryan, 2018; Riedel et al., 2018; Sebastiani et al., 2017; Tanaka et al., 2020). For example, combinations of imaging, genetics, plasma, and CSF markers were found to be associated with varying levels of cognitive decline, brain atrophy, and clinical progression to AD (Riedel et al., 2018).

Among the promising recent approaches, panels of "omics"-based markers have been identified as strong predictors of AD (Adav & Wang, 2021; Badhwar et al., 2020a; Huan et al., 2018; Sapkota et al., 2018; Varma et al., 2018). Omics technologies involve the large-scale study of biological systems, such as genes (genomics), proteins (proteomics), lipids (lipidomics), and metabolites (metabolomics) (Adav & Wang, 2021). In addition to elucidating possible biochemical pathways towards (or away from) AD, metabolomics and other omics markers have been especially promising as candidate biomarkers in recent research (Bader et al., 2020; Habartová et al., 2019; Xianlin Han et al., 2011; Huan et al., 2018; Johnstone, Milward, Berretta, Moscato, & Initiative, 2012; Lista, Faltraco, Prvulovic, & Hampel, 2013; Trushina & Mielke, 2014; Varma et al., 2018). Examples include metabolite panels derived from saliva (three-metabolite panel) and serum (26-metabolite panel) found to accurately discriminate between

cognitively normal controls and AD (Huan et al., 2018; Varma et al., 2018). Similarly, metabolite panels have also been found to be associated with pre-AD syndromes such as MCI. Specifically, studies have identified panels including two (Huan et al., 2018), five (G. Wang et al., 2014), and 12 (Mapstone et al., 2017) metabolites which discriminate between normal controls and MCI. As these recent research efforts have captured some of the heterogeneity of AD from a multi-system biological perspective, they point towards the contributions of omics sciences to personalized and precision science approaches of AD-related prognosis and diagnosis (Clark, Dayon, Masoodi, Bowman, & Popp, 2021; Hampel et al., 2021). For example, a recent integrative multi-omics study identified specific molecular patterns associated with five different dimensions (latent factors) underlying heterogeneity in AD pathology (Clark et al., 2021) These latent factors captured AD heterogeneity across varying amounts multi-omics modalities (from 2-6), in so that each latent factor was associated with differing types core AD pathology. For all identified latent factors, proteins accounted for the most of the variance within the cohort (39.8%) and other (not one-carbon metabolites) accounted for the least (3.7%) (Clark et al., 2021).

Although considerable recent research has focused on predicting trajectories associated with the pre-clinical and clinical AD spectrum (i.e., MCI, AD), complementary research has focused on detecting signals of differential asymptomatic or typical aging, a long period that is especially vital for promoting brain health strategies and implementing risk reduction efforts (K. J. Anstey, 2014; Daffner, 2010; Nyberg & Pudas, 2019; Pudas et al., 2013; K. Yaffe et al., 2009). Notably, that aging outcomes range from the pathological to the non-pathological further highlights the dynamic heterogeneity of pre-outcome aging trajectories. In addition to impairment and neurodegenerative disease, aging trajectories encompass typical declines to very

stable and possibly improving (i.e., 'successful' or healthy aging) performance (Bocancea et al., 2021; Dixon et al., 2012; Nyberg & Pudas, 2019). Specifically, moderate declines in episodic memory and neurocognitive speed are considered typical with increasing age (Daffner, 2010; Dixon et al., 2012). Other changes in brain structure, such as some reductions in cortical gray matter volume, are also considered typical and not indicative of disease when moderate in presentation (Taki et al., 2011). Despite this expected general decline, stable (and high) cognitive trajectories amongst older adults have also been observed, indicating that the aging process is not consistently defined by decline (Dixon et al., 2012; Josefsson, de Luna, Pudas, Nilsson, & Nyberg, 2012; G. P. McFall, McDermott, & Dixon, 2019; Nyberg & Pudas, 2019). Representing an alternative pathway to even typical cognitive aging, subsets of older adults have been found to exhibit consistent high levels and maintenance despite increasing age or cognitive levels comparable to that of younger cohorts (i.e., stable/healthy aging) (Cosco, Prina, Perales, Stephan, & Brayne, 2014; Kok, Aartsen, Deeg, & Huisman, 2015; Lin et al., 2017; Martin et al., 2014; Nyberg & Pudas, 2019; Rogalski et al., 2020; Yu et al., 2019).

High levels and relative stability of memory and cognitive performance have also been observed in subsets of older adults, including in those who are at elevated risk for AD. Indeed, recent research has revealed that some older adults may continue to exhibit sustained levels of cognitive function even in the face of pertinent adversities, such as elevated AD-related neurodegeneration, neuropathology, or genetic risk (Aiello Bowles et al., 2019; K. J. Anstey & Dixon, 2021; Arenaza-Urquijo & Vemuri, 2018; Bocancea et al., 2021; R. Dixon & M. Lachman, 2019; D. Hu et al., 2021; McDermott et al., 2017; Montine et al., 2019; S. Negash, Wilson, et al., 2013; Seto et al., 2021). Coined 'cognitive resilience,' this phenomenon represents an opportunity for elucidating pathways away from AD in individuals who would otherwise be

considered at increased risk. Recent studies have identified several factors from different risk domains (e.g., demographic, functional, lifestyle) associated with cognitive and memory resilience (R. Dixon & M. Lachman, 2019; Kaup et al., 2015; McDermott et al., 2017; Perry et al., 2021). For example, four diverse risk factors (younger age, higher education, stronger grip strength, novel cognitive activity) were leading predictors of memory resilience in cognitively normal older adults who are at increased AD genetic risk (McDermott et al., 2017). Notably, the predictive risk factors also differed between females and males. Specifically, seven risk factors were selectively predictive for females (walking time, volunteering, pulse pressure, social visits, turning time, peak flow, living and marital status) and one for males (depressive symptoms) (McDermott et al., 2017). Other studies have identified predictors (e.g., higher literacy level, no recent negative life events) from several other domains to be associated with higher performing cognitive trajectories in those at greater genetic risk for AD (Kaup et al., 2015). Similarly, some subgroups of older adults have been found to maintain cognitive performance into older age and avoid AD-related adversities (stability). Research efforts aimed towards the study of brain and cognitive aging pathways, including resilience, in at-risk adults can aid in (a) advancing knowledge about potentially modifiable predictors of sustained healthy cognitive aging and (b) developing early interventions with risk-reducing lifestyle and other factors that promote stable (or less rapidly declining) cognitive trajectories.

The heterogeneous, multifactorial, and multi-directional nature of cognitive and brain aging has continued to encourage the use and application of varied approaches, methodologies, and theoretical perspectives. Cutting-edge approaches have been developed and proposed as necessary for optimizing the exploration and determination of the key factors (and their interactions) associated with the variable trajectories of aging (e.g., stable memory, memory

decline, memory resilience, clinical impairment). First, the investigation of factors from multiple modalities of risk have been consistently noted to outperform approaches considering one factor or even several factors from single domains (K. J. Anstey et al., 2015; Badhwar et al., 2020a; Fratiglioni, 1993; Hinrichs, Singh, Xu, Johnson, & Initiative, 2011; Korolev, Symonds, & Bozoki, 2016; Prakash et al., 2021; Sheppard & Coleman, 2020; Venugopalan, Tong, Hassanzadeh, & Wang, 2021). Due to the variability characterizing AD etiology, mechanisms, and clinical presentation, it is expected that risk factors from multiple modalities affect trajectories both independently and interactively (K. J. Anstey et al., 2015; Badhwar et al., 2020a; Baumgart et al., 2015; Fratiglioni, 1993; Hersi et al., 2017; Lipnicki et al., 2013; Mielke et al., 2014; Rusanen et al., 2010; Sachdev et al., 2012; Sheppard & Coleman, 2020; K. Yaffe et al., 2009). Accordingly, recent research has focused on testing large sets of biomarkers and risk factors from multiple modalities on pre-clinical and clinical outcomes (McDermott et al., 2017; G Peggy McFall et al., 2019; Sapkota et al., 2018; Sapkota, McFall, Masellis, & Dixon, 2021). Promising results include strong prediction performance of multi-modal biomarker networks in predicting AD as well as multi-modal (and sex-specific) risk factor clusters predicting memory resilience in asymptomatic older adults (McDermott et al., 2017; Sapkota et al., 2018). Similarly, strong prediction performance has been observed for indicators from multiple AD-related risk domains in the prediction of left and right hippocampal atrophy (S. M. Drouin et al., 2022).

Second, there are several emerging and sophisticated tools as well as approaches that are especially well-suited for this line of research. For example, the investigation of risk factors from multiple domains of risk simultaneously begets the use of analytical approaches that allow for non-linearity, high-order interactions, and a greater number of predictors than *n* (Jacobucci & Grimm, 2020; Pedregosa et al., 2011). Supervised machine learning techniques are a type of

data-driven analytic approach in which hypotheses are guided by existing data in a post-hoc manner. Specifically, supervised ML algorithms are trained on labeled data (i.e., known and identified outcomes) in order to create a predictive model (Breiman, 2001; Jacobucci & Grimm, 2020; Pedregosa et al., 2011). Depending on data characteristics, supervised machine learning algorithms can include random forest classification, support vector machines, and gradient boosting, decision trees, and artificial neural networks. These approaches are especially useful because of their ability to handle the above-noted complex data associations in a flexible and computationally competitive manner. In addition, person-oriented approaches feature an important data-driven component and are aimed at detecting similarities and patterns among individuals in an assumed heterogeneous population. As such, person-oriented approaches can be especially useful to detect and uncover subtypes or subgroups underlying population heterogeneity (Masyn, 2013a; Ram & Grimm, 2009).

These analytic approaches represent an emerging and important tool for understanding person-level characteristics in brain aging, cognitive impairment, and dementia research (Masyn, 2013a; G. P. McFall et al., 2019; Ram & Grimm, 2009). As such, these data-driven approaches can elucidate the vast variability in the level and change associated with aging trajectories and clinical outcomes. Valuable insights may be gained by identifying: (a) pathways towards healthier brain and cognitive aging, (b) pathways away from pathological outcomes (e.g., AD, clinical impairment), and (c) potential mechanisms of avoidance of clinical syndromes for those aging with or without elevated AD risk (e.g., *APOE* ε4+, amyloid beta positive, hippocampal atrophy) (Badhwar et al., 2020a; R. Dixon & M. Lachman, 2019; McDermott et al., 2017; G. P. McFall et al., 2019). Specifically, these approaches work to uncover heterogeneity, detect

unbiased subtypes which may not have been previously hypothesized, and identify relevant predictors despite complex data associations.

The Dissertation Research

My dissertation research focused on leveraging multi-modal datasets and applying data-driven approaches to explore multi-modal harbingers of heterogeneous and multifactorial trajectories in older age. Specifically, these trajectories or pathways included (a) left and right hippocampal volume trajectories, (b) cognitive resilience, cognitive vulnerability and brain/cognitive stability in varying contexts of morphometric brain changes, and (c) predictors of clinical diagnoses (AD) and preclinical classifications (MCI). I employed an array of data types such as imaging (e.g., structural magnetic resonance imaging [MRI]), AD-related genetic and other biomarkers (e.g., *APOE*, Omics-derived biomarkers), AD risk and protective factors (e.g., lifestyle, vascular health), and cognitive (e.g., episodic memory, executive function) in conjunction with large-scale cross-sectional and longitudinal datasets (Canadian Consortium on Neurodegeneration in Aging [CCNA] Comprehensive Assessment of Neurodegeneration and Dementia Study [COMPASS-ND], AD Neuroimaging Initiative [ADNI]). In order to explore potential independent, interactive and synergistic biomarker/risk factor associations with phenotypes of brain and cognitive aging, I applied data-driven approaches (e.g., machine learning) to these data from a multi-determinant perspective. In brief, the overarching goal of my dissertation work was to identify specific risk/protective factors and biomarkers that are associated with the varying and differential levels of cognitive and brain health exhibited across the pre-AD and AD spectrum (cognitively unimpaired aging, MCI, AD).

CHAPTER 2: STUDY 1

Data-Driven Analyses of Longitudinal Hippocampal Imaging Trajectories: Discrimination and Biomarker Prediction of Change Classes

This study has been published. It is presented in full and final manuscript form.

Full Reference:

Drouin, S.M., McFall, G.P., Potvin, O., Bellec, P., Masellis, M., Duchesne, S., & Dixon, R.A. for the Alzheimer's Disease Neuroimaging Initiative (2022). Data-driven analyses of longitudinal hippocampal imaging trajectories: Discrimination and biomarker prediction of change classes. *Journal of Alzheimer's Disease, 88,* 97-115. https://doi.org/10.3233/JAD-215289

Background

Hippocampal atrophy is a well-documented anatomical process that typically occurs during brain aging (De Leon et al., 1997; Potvin, Mouiha, Dieumegarde, Duchesne, & Initiative, 2016; Raz, Ghisletta, Rodrigue, Kennedy, & Lindenberger, 2010; Rusinek et al., 2003). However, aged individuals may vary in several indicators of hippocampal atrophy, including level (e.g., overall volume loss), slope (e.g. rate of volume loss), and associated clinical outcomes (e.g., memory impairment, Alzheimer's disease) (N. Fox, Scahill, Crum, & Rossor, 1999; N. C. Fox & Schott, 2004; Jack et al., 2000; Rusinek et al., 2003). In a distribution of cognitively normal (i.e., unimpaired or asymptomatic) older adults, hippocampal volume trajectories characterized by relatively lower levels and steeper decline may be suggestive of elevated risk for subsequent clinical transitions to Mild Cognitive Impairment (MCI) or Alzheimer's disease (AD) (Apostolova et al., 2012; Byun et al., 2015; Pini et al., 2016). Given its heterogeneity in level and change, further studies are required to ascertain and disentangle important features that characterize hippocampal atrophy in cognitively normal aging. Among the considerations are accumulating evidence of hippocampal hemispheric differences that are reflected in volume trajectories and various clinical outcomes (B. Ardekani, Hadid, Blessing, & Bachman, 2019; Minkova et al., 2017; Wachinger, Salat, Weiner, Reuter, & Initiative, 2016). For example, left and right hippocampal trajectories have been found to be differentially moderated by sex and *APOE* (McFall et al., unpublished data). Hemispheric differences in hippocampal subfields have also been observed between clinical cohorts (i.e., normal controls, subjective cognitive decline, MCI, and AD) (Zhao et al., 2019). We investigated this issue by deploying a sequence of two data-driven analytic approaches (i.e., latent class growth analysis, random forest classification) in parallel for the left (LHC) and right (RHC) hippocampi: (a) objectively

discriminating classes within a distribution of individualized volume longitudinal trajectories, and (b) identifying key biomarkers and risk factors that discriminated between the observed classes.

Previous hippocampal atrophy research has been conducted with both cross-sectional (comparing age or clinical groups at one time point) and longitudinal (following groups over two or more time points) designs (Apostolova et al., 2012; Jack et al., 2000; Jack et al., 2005; Raz et al., 2010; Y. Zhang et al., 2010). Although useful for determining average group differences or mean-level change in multiple domains of asymptomatic brain and cognitive aging, these variable-oriented approaches (i.e., focused on relationships between variables in assumed homogeneous populations) are not typically aimed at scrutinizing the well-established individual heterogeneity in either the level or slope of trajectories (Glisky, 2007; G. P. McFall et al., 2019; G. P. McFall et al., 2015a; Raz et al., 2010) as compared to person-oriented approaches (i.e., focused on similarities and patterns among individuals in an assumed heterogeneous population) (Masyn, 2013b). Recently, the growing interest in examining heterogeneity in brain aging and dementia (Badhwar et al., 2020b; Habes et al., 2020) has led to a corresponding effort to adapt data-driven technologies to the (a) examination of individualized trajectories of cognitive changes in older adults and (b) determination of possible underlying classes of trajectory patterns (Habes et al., 2020; G. P. McFall et al., 2019; Melis, Haaksma, & Muniz-Terrera, 2019). These latent classes, which are determined via application of algorithms based on performance intercept (level) and slope (rate of change) parameters (Masyn, 2013b), may later be clarified by identifying predictors most associated with reduced or exacerbated risk for cognitive decline or clinical impairment (Habes et al., 2020).

A growing body of neurocognitive aging and dementia research has demonstrated the viability of applying data-driven technologies to model heterogeneity in both cross-sectional and longitudinal (trajectory) distributions, including the identification of detectable asymptomatic classes and the determination of differential biomarker predictors (Habes et al., 2020; McDermott et al., 2017; G. P. McFall et al., 2019). One such longitudinal example in an AD sample identified atrophy subtypes associated with differing degrees of memory performance (Ferreira et al., 2017). In asymptomatic individuals, three cross-sectional biomarker profile subtypes were extracted from a combination of magnetic resonance imaging (MRI) data and cerebrospinal fluid (CSF) biomarkers (Nettiksimmons et al., 2010). One of these subtypes, similar in biomarker profile to a comparative AD group, was associated with accelerated cognitive decline and lower baseline scores on cognitive tests (Nettiksimmons et al., 2010). Although few studies have explored longitudinal data-driven subtypes (Habes et al., 2020), separate cross-sectional studies of cognitively unimpaired older adults have previously reported distinct imaging subtypes (Dong, Honnorat, Gaonkar, & Davatzikos, 2015; Eavani et al., 2018; Jung et al., 2016; Malpas, 2016; Orban et al., 2017; Tam et al., 2019). As both cognitively unimpaired aging and AD are characterized by progressive hippocampal atrophy, the possible presence of detectable longitudinal subtypes of hippocampal trajectories in cognitively normal older adults and their potential associations with AD-related risk factors merit further investigation.

Research on early detection of AD risk in asymptomatic older adults has identified a large number of modifiable and non-modifiable factors (e.g., *APOE* genetic risk, education, metabolic health, sex) which are associated with increased risk of (or protection from) accelerated cognitive decline, MCI, and AD (Jack Jr et al., 2018; Livingston et al., 2017; Sapkota

et al., 2018). Similarly, previous studies of normal aging and hippocampal atrophy in normal aging and clinical groups have identified predictors from multiple domains. For example, both traditional CSF AD-related biomarkers, such as baseline p-tau$_{181p}$ and Aβ1-42 (Henneman et al., 2009; Stricker et al., 2012), and such disparate lifestyle risk factors as smoking (Durazzo et al., 2013) and complex mental activity (Valenzuela, Sachdev, Wen, Chen, & Brodaty, 2008) have been associated with hippocampal atrophy. In addition, three CSF biomarkers (Henneman et al., 2009) have been previously used in a multiple linear regression model to predict longitudinal hippocampal atrophy. Although some recent biomarker reports have featured data-driven technologies applied to large numbers of predictors of AD outcomes (Beltrán et al., 2020), longitudinal studies of hippocampal atrophy in cognitively unimpaired older adults have not included a large number of biomarkers or biomarker domains. Previous reports have emphasized the need to include biomarkers from multiple modalities in prediction models over the use of a single biomarker or domain in order to achieve increased prediction accuracy (Falahati, Westman, & Simmons, 2014; Ritter et al., 2015).

We aimed to address a knowledge gap regarding hippocampal volume trajectories in cognitively asymptomatic aging. Specifically, the gap refers to the extent to which the heterogeneity of trajectory distributions can be clarified by the detection of underlying longitudinal latent classes and the determination of leading risk factor and biomarker predictors. Because hippocampal hemispheric atrophy differences have been reported both cross-sectionally (Cherbuin, Réglade-Meslin, Kumar, Sachdev, & Anstey, 2010; Minkova et al., 2017) and longitudinally (J. Barnes et al., 2005; Bernard et al., 2014; Koran et al., 2017), we implemented this aim by testing two main research goals, both of which included parallel analyses of LHC and RHC. For the first research goal (RG1), we analyzed distributions of hippocampal volume

trajectories (up to six time points, maximum of 7.2 years) for predominantly cognitively normal (asymptomatic) participants from the Alzheimer's Disease Neuroimaging Initiative (ADNI). We used latent class growth analyses (LCGA) to detect discriminable classes of trajectories. LCGA is a data-driven longitudinal quantitative modeling technology that applies an algorithm of level and slope to identify statistically separable trajectory classes. Our study focused on a brain aging phase not yet characterized by clinical impairment. Despite normal cognitive function, some individuals may exhibit relatively lower and declining hippocampal volume likely associated with increased risk of future cognitive decline or AD. Notably, membership in higher volume trajectory classes may indicate reduced risk for (or protection from) age-typical morphological shrinkage, membership in lower volume trajectory classes may indicate elevated risk for impending pathological changes. For our second research goal (RG2), we compiled a large, multi-modal set of 38 AD-related biomarkers and risk factors (e.g., CSF Aβ1-42, body mass index, hypertension, sex) from the ADNI database. Whereas most studies have investigated these factors independently or in relatively small clusters, we examine them simultaneously in the context of a competitive quantitative model. We used random forest analyses (RFA), a machine-learning technology for evaluating the relative importance of multiple biomarker and risk factors predictors to the discrimination of higher and lower classes of LHC and RHC atrophy trajectories.

Methods

Alzheimer's Disease Neuroimaging Initiative

Data used in preparation of this article were obtained and downloaded from the ADNI database (adni.loni.usc.edu on June 30 2020). The ADNI was launched in 2003 as a public-private partnership, led by Principal Investigator Michael W. Weiner, MD. The primary goal of

ADNI has been to test whether serial MRI, positron emission tomography, other biological markers, and clinical and neuropsychological assessment can be combined to measure the progression of MCI and early AD. For up-to-date information, see www.adni-info.org.

Participants

From the ADNI database, we used a subsample of older adults who were cognitively normal at baseline with at least one wave of successful MRI data that were processed with the longitudinal imaging pipeline by UCSF (files: UCSFFSL_02_01_16.csv, UCSFFSL51Y1_08_01_16.csv, and UCSFFSL51ALL_08_01_16.csv). The final sample consisted of 351 participants who were (a) cognitively unimpaired at baseline (Mean [*M*] age at baseline = 74.8, *SD* = 5.7, baseline range = 59.8-90.6 years, Mini-Mental State Examination [MMSE] *M* = 29.1; ADAS-Cog *M* = 9.2, 48.7% Female, 14% ε2+, 25% ε4+) and (b) followed for up to six times points (*M* interval between successive time points = 0.91 years [SD = 0.53]). The full distribution analyzed in this study populated a 35-year band of aging (ranging from 59.8 to 94.6 years). The total wave observations in this study were overwhelmingly cognitively normal (96.3%), with only 3.7% and 0.56% of observations being persons with MCI or AD respectively. As such, the present sample was uniformly CN at the outset of the study and predominantly CN throughout the remainder of the study period. Baseline participant characteristics and demographic information can be found in Table 1. Individuals were considered cognitively unimpaired at baseline if they: (a) had no memory complaints, (b) scored between 24-30 on the MMSE, (c) had a Clinical Dementia Rating (CDR) score of 0, and (d) scored equal to or above a cut-off based on years of education (3, 5, or 9 for 0-7, 8-15 and 16 or more) on the Logical Memory II subscale of the Wechsler Memory Scale-Revised (Petersen et al., 2010). The ADNI data collection procedures were in certified compliance with prevailing

human ethics guidelines and boards. All participants or authorized representatives provided informed written consent.

MRI Acquisition and Image Processing

MRI data were provided by the ADNI neuroimaging team and full details about the image processing can be found on adni.loni.usc.edu in the following file: UCSF_FreeSurfer_Methods_and_QC_OFFICIAL_20140131.pdf. Briefly, cortical reconstruction and volumetric segmentation was performed with the FreeSurfer image analysis suite, which is documented and freely available for download online (http://surfer.nmr.mgh.harvard.edu/). We used longitudinal pipelines (freesurfer.net) which uses each subject as their own control and processed the data using *FreeSurfer* 4.4 (1.5T) and *FreeSurfer* 5.1 (3T) (Reuter, Schmansky, Rosas, & Fischl, 2012). The technical details of these procedures are described in prior publications (A. Dale, Fischl, & Sereno, 1999; A. M. Dale & Sereno, 1993; Fischl & Dale, 2000; Fischl, Liu, & Dale, 2001; Fischl et al., 2002; Fischl, Salat, et al., 2004; Fischl, Sereno, & Dale, 1999; Fischl, Sereno, Tootell, & Dale, 1999; Fischl, van der Kouwe, et al., 2004; Xiao Han et al., 2006; Jovicich et al., 2006; Segonne et al., 2004). Briefly, this processing includes motion correction and averaging (Reuter, Rosas, & Fischl, 2010) of multiple volumetric T1 weighted images, removal of non-brain tissue using a hybrid watershed/surface deformation procedure (Segonne et al., 2004), automated Talairach transformation, segmentation of the subcortical white matter and deep gray matter volumetric structures (including hippocampus, amygdala, caudate, putamen, ventricles) (Fischl et al., 2002; Fischl, Salat, et al., 2004) intensity normalization (Sled, Zijdenbos, & Evans, 1998), tessellation of the gray matter white matter boundary, automated topology correction (Fischl et al., 2001; Segonne, Pacheco, & Fischl, 2007), and surface deformation following intensity gradients to optimally place the gray/white

and gray/cerebrospinal fluid borders at the location where the greatest shift in intensity defines the transition to the other tissue class (A. Dale et al., 1999; A. M. Dale & Sereno, 1993; Fischl & Dale, 2000). ADNI protocols have ensured that MRI harmonization is performed by using (a) a standardized protocol, harmonized across all three vendors (GE Healthcare, Siemens Medical Systems, Philips Healthcare); (b) the use of a geometric phantom for distortion evaluation; and (c) manual quality control of the image data (Gunter et al., 2009; Jack Jr et al., 2008).

Quality control was conducted by the ADNI neuroimaging team. We removed all failed segmentations, indicating a global failure due to extremely poor image quality, registration issues, gross misestimation of the hippocampus, or a processing error. In the present sample, 60.1% of the images were processed with the FreeSurfer 4.4 (1.5T) and 39.9% with the FreeSurfer 5.1 (3T) pipelines. Hippocampal volumes and estimated intracranial volume from the aseg file were used. We corrected LHC and RHC volume for head size at the individual level (and at each time point) using the following formula (Sundermann, Tran, Maki, Bondi, & Initiative, 2018):

$$\frac{Hippocampal\ volume}{Intra-cranial\ volume}\ x\ 10^3$$

Magnetic field strength (coded as 1.5T, 3T, or change from 1.5T to 3T) was used as a covariate for hippocampal volume level and slope within each class in the LCGA.

Biomarkers and Risk Factors

Based on previous literature and availability, we identified 38 biomarkers and risk factors available at baseline which have been identified to be associated with increased risk of AD. We included these biomarkers and risk factors in the machine learning prediction models for RG2 (see Table 2). For interpretive convenience, we sorted the biomarkers and risk factors into eight modalities: biospecimen (e.g., CSF t-tau; n = 6), demographic (e.g., sex; n = 3), genetic (*APOE,*

coded as ε2+ [ε2/ε2, ε2/ε3], ε3/ε3, and ε4+ [ε3/ε4, ε4/ε4] with ε2/ε4 carriers removed; *n* = 1), vascular and metabolic (e.g., systolic blood pressure; *n* = 5), lifestyle (e.g., smoking history; *n* = 2), comorbidities (e.g., cardiovascular disease; *n* = 17), familial background (e.g., paternal dementia history; *n* = 2) and cognitive status (e.g., MMSE; *n* = 2).

Statistical Analyses

RG1. Classes of LHC and RHC. We analyzed the longitudinal data with chronological age as the metric of change. Accordingly, age is included directly into the analyses and is essentially co-varied. We used LCGA, which implements an algorithm based on individual level (i.e., intercept) and slope, to identify differentiable classes of individual trajectories within the overall distribution of trajectories (Ram & Grimm, 2009). Analyses were conducted in Mplus 8.2 (Muthén & Muthén, 2018) and performed separately for LHC and RHC volume change data. The analysis plan specified the development of the most parsimonious one class (baseline) model, followed by the testing and comparison of four alternative *k*-class models to the *k*-1 models. LCGA can model non-linear trajectories; however, quadratic models were tested and removed from consideration due to poorer model fit. Thus, all tested models were random intercept, random slope linear growth models with the variance fully constrained within each class. We evaluated model fit in three steps only for models with entropy values greater than 0.8, which confirm that the model has satisfactory class separation and classification precision. Higher entropy is the best indicator of model separation, with values of 1 indicating perfect classification precision and separation between classes (Masyn, 2013b). First, we considered models which had lower values (compared to the baseline model) of the following recommended statistical fit indices: Akaike information criterion (AIC), Bayesian information criterion (BIC), and sample-size adjusted BIC (SABIC) (Masyn, 2013b). For this step, we plotted the values of

fit indices (i.e., AIC, BIC, SABIC) on the number of classes in a scree or elbow plot (Masyn, 2013b; Nylund, Asparouhob, & Muthén, 2007) to identify a possible inflection point (i.e., the point at which the values the slope changes). Second, as is recommended for LCGA research in which classes will be used for subsequent analyses (Little, 2013), we applied an a priori cut-off criterion for model selection which stipulated that candidate models would have greater than 10% of the sample in each class. This ensured that the subsequent prediction analyses (in the second research goal) would have sufficient participants in each identified class for stable and robust multiple-group analyses and solutions. As a consequence of this model selection criterion, possible low prevalence classes of potential clinical interest were not identified or studied. We aimed to represent as much as possible the broader distribution of initially cognitively normal aging adults and account for any existing heterogeneity using this recommended approach (Masyn, 2013b). Third, we consulted related and neighboring literature to ensure that class parameters for the final model were consistent with theoretical expectations. Based on complementary findings in the episodic memory literature, we expected to find a three class model for hippocampal volume trajectories (G. P. McFall et al., 2019).

RG2. Important Predictors of LHC and RHC Class Membership. Prediction analyses were also conducted separately for LHC and RHC and used the full pool of 38 AD-related biomarkers and risk factors. Using RFA (*R* 3.2.5, "Party*"* package) (Hothorn, Buehlmann, Dudoit, Molinaro, & Van Der Laan, 2006), we simultaneously tested these biomarkers and risk factors for relative importance in discriminating the lowest vs. highest hippocampal trajectory classes. We used the conditional probabilities provided in the LCGA to determine class membership for individuals. Specifically, the models determined each individual's LHC and RHC volume at every wave (i.e., level) and the slope of volume change (Lanza, Collins,

Lemmon, & Schafer, 2007) and then assigned them to the class to which they had the highest probability of membership. The conditional probabilities for membership assignment were very high for both LHC (M = 0.96; % > 0.8 = 92.3) and RHC (M = 0.97, % > 0.8 = 92.8).

Due to its robustness to overfitting and ability to accommodate a large number of predictors, RFA was selected as the optimal technique for simultaneous testing of a large number of mixed-type (i.e., categorical and continuous) variables (G. P. McFall et al., 2019). Unlike conventional statistical methods (e.g., multinomial logistic regression), which require conservative correction approaches, RF prediction models are equipped with provisions that lead to accurate and stable prediction solutions with many predictors (Couronné, Probst, & Boulesteix, 2018; Hapfelmeier & Ulm, 2013). Combining multiple classification predictions and regression trees (*ntree*) based on a random sample of participants and predictor variables (*mtry*), RFA is a recursive partitioning multivariate data exploration technique. Each forest was comprised of *ntree* = 1000 (sufficient for good model stability) and each potential split evaluated a random sample of the square root of the total number of predictors (biomarkers and risk factors; *mtry* = 6) (G. P. McFall et al., 2019). We utilized the *cforest* function in the "Party" package to determine biomarker and risk factor importance based on their conditional permutation accuracy importance (*varimp* function; conditional = TRUE), utilizing an algorithm that averages the prediction weight of each of the variable across all 1000 permutations (Couronné et al., 2018; Hapfelmeier & Ulm, 2013; C. Strobl, Boulesteix, Zeileis, & Hothorn, 2007). Interactions between predictors are taken into account with each permutation when variable importance is determined, although specific interactions are not reported (Hapfelmeier & Ulm, 2013). Specifically, conditional permutation importance provides a measure of the association between the outcome (i.e., hippocampal trajectory class) and each predictor based on

the values of other predictors (Carolin Strobl, Boulesteix, Kneib, Augustin, & Zeileis, 2008). The conditional variable importance method is especially advantageous in that it accounts for potentially correlated predictors to avoid typically occurring multicollinearity issues (Gregorutti, Michel, & Saint-Pierre, 2017; Carolin Strobl et al., 2008; Toloşi & Lengauer, 2011). As such, results regarding ranked predictor importance are presented and discussed in the context of all included predictors. After removing biomarkers and risk factors that were of lowest importance, the final RFA consisted of 16 variables (*mtry* = 4). Important variables were determined based on observation of an 'elbow' in the RFA plot. The *cforest* function also computes out-of-bag estimates, which can be used in place of cross-validation procedures (Hastie, Tibshirani, & Friedman, 2009). For both LHC and RHC volume trajectory models, we reported the concordance statistic (C), which is equivalent to the area under the curve. In non-medical prediction analyses an area under the curve or C value of 0.5 is considered to be chance, between 0.6 and 0.7 is considered to be a medium effect size, and 0.8 or greater is considered a strong effect size (G. P. McFall et al., 2019). In order to clarify the direction of relationship between the identified important predictors and hippocampal trajectory class membership, we report post-hoc correlational analyses as well as group means frequencies. These were interpreted independently from other predictors and do not represent formal probabilities of risk.

Missing biomarker and risk factor data was addressed as follows. Across the biomarker and risk factor modalities, with one exception, missing data rates were very low (range = 0 to 3.9% for LHC; 0 to 2.6% for RHC). The exception was the biospecimen modality (range = 38.2-55.6% for LHC; 35.3-50.0% for RHC). Details by biomarker and risk factor are provided in Table 2. Missing data were imputed using the "missForest" package as recommended in R (Daniel J. Stekhoven & Bühlmann, 2012; Waljee et al., 2013). This package is especially

recommended in the case of mixed-type missing data. Used together with the "RandomForest" package in R, the "missForest" package utilizes a random forest trained on the data matrix for missing value prediction (Daniel J Stekhoven, 2011; Daniel J. Stekhoven & Bühlmann, 2012).

Results

RG1: LHC and RHC Trajectory Classes

Left Hippocampal Volume Trajectories. Model fit statistics for all analyses are presented by number of classes in Table 3. All tested models had acceptable entropy values (i.e., > 0.8). The two-, three-, and five-class models were selected as possible candidate models as they had lower AIC, BIC and SABIC values than the baseline model and sufficient participants in each class. We selected the three-class model as the final model following the inspection of a scree plot (see Supplementary Materials, Figure 1) and in the context of past findings in the related domain of memory aging trajectory analyses (G. P. McFall et al., 2019). The three-class model is portrayed in Figure 1c, with parameter means (level and slope) reported in Table 4. Discriminated and ranked by a combination of both level and slope, from highest to lowest volume in the trajectory distribution, the three classes can be characterized as follows. Class 1 (n = 100; the group at the top of the distribution) was characterized by the highest combination of level and slope, followed by Class 2 (n = 173), the group in the middle of the distribution, and Class 3 (n = 78), the group at the bottom of the distribution. Informally, the classes appear to differ more in level than in slope (with Class 2 and 3 having the steeper slopes), but both parameters contributed to the latent class solution. Specifically, the LCGA algorithm identifies distinguishable trajectory classes based on simultaneous consideration of level and slope, both of which are essential parameters in model identification. It is important to note that the resulting trajectory classes are statistically differentiated even though they may not appear visually as

dramatically distinct at their edges. This between-class distinction is clearly indicated by the entropy values (revealing good class separation) and the level and slope parameters (and 95% confidence intervals) for each class (see Table 4).

Right Hippocampal Volume Trajectories. Model fit statistics for all analyses are presented by number of classes in Table 3. Similar to the LHC models, all tested models had acceptable entropy values (> 0.8). The four-class model was removed from consideration as the loglikelihood failed to replicate, indicating that no global solution was reached. The five-class model was removed from consideration due to insufficient participants in one class (9%). The two- and three-class models were selected as possible candidate models as they had lower AIC, BIC and SABIC values than the baseline model and sufficient participants in each class. As with LHC trajectories, we selected the three-class model as the final model based on past findings and inspection of the scree plot of relative fit indices for the inflection point (see Supplementary Materials, Figure 2). Thus, we identified three unique classes of RHC volume trajectories within the overall sample (Figure 1f). Parameter means (level and slope) are reported in Table 4. Discriminated and ranked by a combination of level and slope, from highest to lowest volume in the trajectory distribution, the classes can be characterized as follows. Class 1 (n = 96; the group at the top of the distribution) was characterized by the highest combination of level and decline, followed by Class 2 (n = 167), the group in the middle of the distribution, and Class 3 (n = 88), the group at the bottom of the distribution. Comparable to the LHC trajectory class distribution, the classes appear to differ in level more than slope; however, both parameters contributed to the latent class solution. Informally, the level (but not slope) of each RHC class appears to be consistently higher than that of the corresponding LHC class.

RG2: Important Predictors of LHC and RHC Class Membership

We performed RFA to identify biomarkers and risk factors that best discriminated between the highest (Class 1) and lowest (Class 3) trajectory classes within LHC and RHC volume separately.

Left Hippocampal Volume Trajectory Classes. The higher and lower LHC volume trajectory classes were discriminated by seven biomarkers and risk factors from four modalities: biospecimen (plasma Aβ1-40, plasma tau, plasma Aβ1-42), demographic (sex, education), co-morbidities (geriatric depression scale [GDS] score), and lifestyle (body mass index; $C = 0.80$; Figure 2a). As informed by post-hoc correlational analyses, we found that individuals belonging to the lower LHC volume trajectory class were more likely to have lower levels of plasma Aβ1-40, Aβ1-42 and tau, greater number of years of education, higher GDS scores (indicating more depressive symptoms), a lower BMI, and be male (see Table 5 for biomarker/risk factor frequencies and means per class).

Right Hippocampal Volume Trajectory Classes. The higher and lower RHC volume trajectory classes were discriminated by three biomarkers and risk factors from the following two modalities: demographic (sex, education) and biospecimen (plasma Aβ1-42; $C = 0.78$; Figure 2b). As informed by post-hoc correlational analyses, we found that individuals belonging to the lower RHC trajectory class were more likely to be male, have lower levels of plasma Aβ1-42, as well as have greater number of years of education (see Table 5 for biomarker frequencies and means per class).

Discussion

This study applied data-driven technologies to longitudinal imaging data to (a) extract computationally separable classes based on individual level and slope from LHC and RHC

trajectory distributions and (b) subsequently identify key AD-related biomarkers and risk factors that discriminate between the higher and lower trajectory classes. To our knowledge, no previous study has used these technologies to (a) identify trajectory classes based on separate LHC and RHC volume change in a sample of predominantly cognitively normal older adults and (b) assemble and test a large pool of putative biomarker and risk factor predictors of trajectory class.

Overall, the class structures (number and membership) and constituent trajectory characteristics (levels and slopes) for the two hemispheres were similar. One exception is that RHC volumes appeared consistently higher (in level) for each corresponding class. This RHC advantage is consistent with previous research indicating that RHC volumes are generally more preserved at corresponding ages than LHC volumes in cognitively normal older adults (J. Barnes et al., 2005; Cherbuin et al., 2010; Cherbuin, Sargent-Cox, Easteal, Sachdev, & Anstey, 2015). Our results provide a new and discriminating indicator of this advantage; namely, the advantage can be observed at all corresponding classes (higher, middle, and lower) of aging change. For both hemispheres, the slope means across classes were relatively similar; however, the two lowest classes (middle, lowest) exhibited steeper slopes than the highest class. This pattern was expected as the current sample consisted of uniformly cognitively normal older adults at baseline and who remained clinically non-impaired over 96% of the analyzed longitudinal observations. Notably, even in the more limited heterogeneity of a cognitively unimpaired older adult sample (as compared to a more clinically diverse sample), our analytic approach detected discriminable classes of HC volumetric change. In addition, although there was some overlap between the participants classified into the LHC and RHC classes, there were a substantial number of individuals (n = 93) who were uniquely classified (e.g., were in the lowest LHC but not the

lowest RHC) in the two hemispheric analyses. These findings provide further evidence for the consideration of LHC and RHC differences in future research.

As increasing hippocampal atrophy is associated with incipient clinical progression (Apostolova et al., 2012; Apostolova et al., 2010; Byun et al., 2015), two potential implications of our data-driven latent class approach could be considered. First, these classes of hippocampal trajectories could be provisionally considered as "secondary phenotypes" of brain aging in that they (a) differ in objective and salient brain aging trajectory characteristics and (b) may be associated with differential outcomes or clinical phenotypes such as cognitive impairment or AD. A post-hoc informal check of the current data revealed that cognitive performance over time decreased in a stepwise manner across hippocampal trajectory classes (see Supplementary Materials for ADAS-Cognition and ADNI Memory Composite scores by wave). In addition, higher scores on the Clinical Dementia Rating (CDR) were somewhat more prevalent in the lowest classes and none of the participants with a CDR of 1 were classified in the highest trajectory classes. Similarly, a recent study identifying four spatiotemporal trajectory subtypes of tau deposition found that longitudinal MMSE outcomes differed between subtypes (Vogel et al., 2021). The interpretation was that data-driven groups based on other AD-related biomarkers (tau) have also identified differences in cognitive trajectories (Vogel et al., 2021). Taken together, the present and complementary findings chart an important direction for future research, in which studies with comprehensive clinical outcome information could provide insights into AD or impairment risk based on long-term pre-clinical trajectory class membership. Second, members of higher trajectory classes may have lower exposure to AD risk factors. We investigated these implications in the next research goal by testing associations with AD biomarkers and risk factors.

Accordingly, we tested predictor importance for a roster of 38 multi-modal AD risk factors and biomarkers. The machine learning technology (RFA) evaluated the relative importance of all of the predictors in a quantitatively competitive context. The leading predictors of extreme classes (higher vs. lower) were thus identified for their prediction importance with both independent and interactional contributions considered. The present prediction models do not establish mechanisms of association, but instead identify the risk factors that emerge in data-driven analyses from a large panel of potential predictors and thereby point to promising future directions of both validation and mechanistic research. The full roster of predictors was presented earlier and listed (by modality) in Table 2. Three aspects of the results are discussed: (a) the subset of predictors that were observed for both LHC and RHC, (b) any predictors that were selectively associated with either hemisphere, and (c) notable predictors (e.g., factors that have been associated in candidate biomarker studies) that did not emerge in the present analyses. In all cases, we refer to any available candidate biomarker and risk factor literature to establish the context. Three important predictors from two modalities were robust across the hemispheres: demographic (sex, education) and biospecimen (plasma Aβ1-42). Four additional predictors were observed selectively in the LHC analyses. We characterize the three common predictors briefly and then discuss the unique predictors for LHC.

Regarding predictors in common for LHC and RHC classes, the sex factor indicated that being male was associated with membership in the lower trajectory classes. For hippocampal atrophy in cognitively unimpaired aging, a common result is that, for given ages, males experience more overall atrophy than females (Fraser, Shaw, & Cherbuin, 2015). Our results conducted separately on LHC and RHC extend this pattern to both hemispheres. As an illustration, for both LHC and RHC we noted that membership of the upper (less atrophied) class

was predominantly female (64-70%) whereas the lower class membership was predominantly male (66.7-68.2%). Notably, our current multimodal approach highlights the importance of sex relative to other established AD biomarkers and risk factors in predicting differential hippocampal atrophy. This female advantage is concordant with (a) findings in the cognitively asymptomatic aging literature, whereby cognitively normal females often perform at higher levels than males, and (b) our post-hoc check regarding cognitive trajectories for this sample (see Supplementary Materials). Specifically, mean memory scores for the lowest HC trajectory classes (predominantly male) were lower than for the highest trajectory classes (predominantly female), which is consistent with the growing evidence of a male disadvantage in asymptomatic memory aging (Shannon M Drouin, McFall, & Dixon, 2021; Laws, Irvine, & Gale, 2016; McDermott et al., 2017). However, it should be noted that this female advantage may be reversed in persons living with AD or even preclinical AD. For example, studies have found that females with AD exhibit more rapid hippocampal atrophy (B. A. Ardekani, Convit, & Bachman, 2016) and similar associations have been reported for females with AD-related neuropathology (Koran et al., 2017). In contrast, we found that in predominantly cognitively unimpaired individuals, men made up a higher proportion of the hippocampal trajectory class characterized by the lowest level and steepest decline (i.e., most atrophy). Thus, future research can aim to resolve whether there is (a) a selectively accelerated rate of hippocampal volume loss for preclinical and clinical (where AD-related neuropathology, such as low CSF AB42 levels, would be evident) females or (b) some other factor accounts for the contrasting observations.

More years of education was associated with the lowest (most atrophied) classes of both LHC and RHC volume trajectories. In cognitively unimpaired older adults, non-significant cross-sectional associations between hippocampal size (volume and thickness) and education have

been reported (Seo et al., 2011; Shpanskaya et al., 2014). In contrast, education has been previously identified as a potential protective factor in the AD epidemiological literature (Livingston et al., 2020). Longitudinal findings regarding associations with cognitive reserve (including education) have also been mixed (R. A. Dixon & M. E. Lachman, 2019; Whitwell, Dickson, et al., 2012). These inconsistencies may originate from a number of study-related differences, including: (a) design (cross-sectional vs. longitudinal), (b) measurement (years of schooling vs. attainment), (c) cohort (education differing across generations), (d) study sample (cognitively normal vs. clinical; higher vs lower education), (e) analytic approaches (most often single variable vs. multi-variable prediction models), (f) study role (correlate, covariate, and even AD protective factor), and (g) outcome (cognitive differences/changes, brain differences/changes). In the current ADNI sample, the majority of participants were relatively highly educated (*M* years of total schooling at baseline = 16.3). Previous findings regarding the moderation of hippocampal volume by education (Noble et al., 2012) indicate that these effects are diminished among those with higher education attainment. A relevant previous result (Piras et al., 2011) led us to explore whether the commonly used proportional approach to correcting for head size (Shen, Zhou, Chen, & Zhang, 2019; Sundermann, Tran, Maki, & Bondi, 2018; Voevodskaya et al., 2014) could lead to potential overcorrections in volume estimates for highly educated samples. Specifically, the common approach corrects the numerator (hippocampal volume) by the denominator (intracranial volume). In a post-hoc check we observed a positive correlation between intracranial volume and education (Piras et al., 2011). We suggest (a) careful monitoring of education effects in cognitively normal brain aging, (b) further specific attention to intracranial HC volume corrections when education levels are high, and (c) increasing

attention to education effects in research on other brain regions and related biomarkers (e.g., hippocampal to cortex atrophy ratio (Whitwell, Dickson, et al., 2012)).

Lower levels of plasma Aβ1-42 were associated with the lower trajectory classes for both LHC and RHC. Although a conventional biomarker of AD, Aβ1-42 has been found to be more strongly related to overall neurodegeneration (versus AD specifically) as increased levels in the brain and decreased levels in CSF also occur in other neurodegenerative diseases (Jack Jr et al., 2018). Evidence for brain atrophy associations with plasma levels of Aβ1-42 have been mixed. For example, higher plasma Aβ1-42 levels and lower volumes of hippocampal subfields have been linked in older adults with, but not those without, subjective complaints (Cantero, Iglesias, Van Leemput, & Atienza, 2016). In a separate study using a large sample of cognitively normal older adults, decreased levels of plasma Aβ1-42 were associated with smaller hippocampal volumes and increased risk of dementia (Hilal et al., 2018). Similarly, plasma levels of Aβ1-42 were found to be lower in amnesic MCI individuals as compared to cognitively normal older adults (Shi et al., 2019). Our results contribute to the existing and emerging evidence that (a) lower Aβ1-42 levels are a detectable biomarker of emerging neurodegeneration (hippocampal trajectory classes) in initially cognitively normal individuals and (b) less invasive biomarker collection procedures (e.g., plasma) provide reliable indicators of this early trend toward neurodegeneration (Hampel, O'Bryant, et al., 2018; Jack Jr et al., 2018).

Four additional predictors discriminated LHC trajectory classes only. From the biospecimen modality, plasma Aβ1-40 and plasma tau predicted class membership uniquely for the LHC. Specifically, lower levels of both plasma Aβ1-40 and plasma t-tau were associated with membership to the lowest LHC trajectory class. Our findings support and extend previous reports of lower levels of plasma Aβ1-40 in preclinical AD and AD-related neurodegeneration

(Hilal et al., 2018; Shi et al., 2019). Specifically, our results indicate that lower baseline levels of plasma Aβ1-40 predict trajectories associated with more left (but not right) hippocampal atrophy prior to detectable disease stages. For plasma t-tau, increased levels have been associated with lower gray matter volumes in Aβ+ (but not Aβ-) older adults (Deters et al., 2017) as well as higher risk of incident dementia (Pase et al., 2019). However, our results suggest that lower plasma t-tau may be differentially associated with "secondary phenotypes" of clustered individuals representing different patterns of longitudinal atrophy in cognitively normal adults. A possible explanation is the potential effect of age on plasma t-tau levels. In a recent study, older adults (compared to middle-aged adults) were found to have higher levels of plasma t-tau after controlling for sex and *APOE* (Chiu et al., 2017). Although not directly testable in the present data, the average age of the lowest class LHC class (M_{W1} = 73.9, M_{W2} = 74.3, M_{W3} = 74.8, M_{W4} = 75.7, M_{W5} = 77.0, M_{W6} = 78.6) was somewhat lower than that of the highest LHC class (M_{W1} = 75.1, M_{W2} = 75.6, M_{W3} = 75.9, M_{W4} = 76.7, M_{W5} = 78.2, M_{W6} = 79.5) at each time point. It is possible that the reported age-related effects extend to a higher age range and to subtler age differences, representing an important area of future investigation.

Depressive symptoms (at a non-clinical level) were a selective predictor of LHC trajectory classes, with higher mean GDS score associated with the lowest trajectory class. This result is concordant with previous literature in which depression has been linked with increased AD risk (Livingston et al., 2017). Similarly, depressive symptoms have been associated with increased limbic and prefrontal atrophy over a four-year follow-up in cognitively normal older adults (Lebedeva et al., 2018). The left hippocampus (but not the right hippocampus) has also been found to be reduced in major depression disorder in adults (Bremner et al., 2000). In our sample, only 2% of individuals were considered mildly depressed at baseline and no individuals

had GDS scores indicating moderate or severe depression. The present findings suggest that the association between mild depressive symptomology and prefrontal/limbic atrophy also extends to the left hippocampus. Although the mechanism of this relationship remains largely unknown, it is possible that such mood or affect symptomology is associated with the subtle changes in cognition as a function of emerging hippocampal and cortical atrophy (Mosti, Rog, & Fink, 2019). Another perspective is that hippocampal atrophy may be directly affecting networks that are associated with mood and impact depressive symptomology through numerous mechanisms such as estrogen depletion and deregulation of certain neural circuits (Elbejjani et al., 2014).

A lower body mass index (BMI) was associated with the lower LHC, but not RHC, trajectory class. BMI associations with brain and cognitive aging are complex (Alosco et al., 2017; K. Anstey, Cherbuin, Budge, & Young, 2011; Bischof & Park, 2015). A previous studying using BMI as a predictor of HC volumetric change reported a negative association between hippocampal volume (across hemispheres, but with stronger effects for the LHC) and BMI (Cherbuin, Sargent-Cox, Fraser, Sachdev, & Anstey, 2015). Participants of that study were, on average, a decade younger than those of the current study. Our findings indicate that a protective effect of higher BMI persists in an older cohort, and further support that this effect occurs more strongly in the LHC. Potential protective effects of increased BMI in older age (vs. midlife or young-old cohort) have been reported in the context of AD risk (Atti et al., 2008; Luchsinger & Mayeux, 2007) and cognitive decline (L. Bohn et al., 2020) and may act similarly for risk reduction for hippocampal atrophy. Notably, it appears that higher BMI might be an important AD risk factor in midlife, but this association reverses towards protection or risk-reduction in later life and older age, perhaps due to weight changes occurring in preclinical AD phases (Dye, Boyle, Champ, & Lawton, 2017; Suemoto, Gilsanz, Mayeda, & Glymour, 2015).

We tested 38 biomarkers and risk factors as potential predictors of trajectory class membership. Our analytic approach considered all predictors simultaneously in a computationally competitive context. In addition to the seven predictors of trajectory classes, we note that there were 31 AD-related predictors that did not successfully emerge in either (LHC or RHC) of the analyses. Within the biospecimen modality, plasma measures of Aβ and tau outperformed CSF Aβ and tau to discriminate between hippocampal trajectories. Although CSF measures of Aβ have been consistently reported as sensitive biomarkers of MCI and AD, recent developments have identified less invasive and lower cost alternatives such as blood-based biomarkers (Hampel, O'Bryant, et al., 2018). Potentially, these peripheral biomarkers are more useful in predicting specific pathological changes and broader neurodegeneration, such as hippocampal atrophy. Alternatively, it is possible that the present plasma markers are better suited as predictors of non-clinical aging outcomes (i.e., hippocampal classes representing a dynamic distribution of cognitively normal longitudinal trajectories) as compared to related findings for CSF markers and associations with AD diagnosis and clinical progression patterns. For the genetic modality, although *APOE* genetic risk is the most important genetic risk factor for sporadic AD (Michaelson, 2014), it did not appear as one of the important or leading predictors of the lowest HC atrophy class (although it was among the lesser contributing predictors). This may point to an attenuated importance of single genetic factors within an interactive network of wide-ranging AD risk factors. The inclusion of a polygenic AD-related risk score may have revealed more predictive utility in the context of other risk-related AD predictors and should be investigated in future research (Badhwar et al., 2020b). Within the vascular/metabolic modality, no factors reached sufficient variable importance to be considered important predictors despite past findings suggesting possible associations (Cooper et al., 2016;

G. P. McFall et al., 2015a). For the demographic modality, chronological age was not found to be an important predictor of the lowest hippocampal trajectory class membership. Instead, our findings indicate that, when available, certain aging-related mechanistic predictors may be more important than age per se for predicting adverse brain aging outcomes in predominantly cognitively normal samples. This provides additional support to the growing evidence that markers of biological age (vs. chronological age) are important to consider in predictions of exacerbated decline in non-demented aging (DeCarlo, Tuokko, Williams, Dixon, & MacDonald, 2014; Levine et al., 2018; S. W. MacDonald, DeCarlo, & Dixon, 2011; J. W. Wu et al., 2021). Given the current analytic approach and the use of a conditional variable importance measure, we identified the most prominent predictors of hippocampal trajectory classes in the context of other previously identified and often closely related AD-related biomarkers and risk factors.

There were several limitations to the present study. First, previous reports have acknowledged some limited generalizability of the ADNI cohort due to convenience sampling and possible biases in recruited participants (e.g., familial history of AD) (Whitwell, Wiste, et al., 2012). However, these potentially at-risk individuals are key targets of clinical trials and prevention efforts. As our study aimed to identify biomarkers and risk factors associated with morphometric change in cognitively normal older adults, we have identified biomarker associations in individuals that are likely to be targeted for these purposes. Second, although variables included in the current study had few missing data (0-3.9%), there was a notable exception for biomarkers in the biospecimen modality. For the biospecimen biomarkers, missing data ranged from 35 to 51.3%. Missing data were imputed using the 'missForest' package in R which utilizes a random forest to iteratively predict missing values. The present imputation procedure and RFA models allowed for the inclusion of many predictors from multiple

modalities despite some with higher rates of missing data. We consider this a notable strength of our approach, as previous studies predicting AD risk have often employed fewer biomarker or risk factor predictors, possibly due to analytical restrictions (e.g., multiple comparison issues) (Gomar et al., 2011; Kwon, Gupta, & Lama, 2019; Shaffer et al., 2013). Replicating and validating these findings using additional biomarker data would be an important future step. Third, because of data limitations we were unable to investigate whether preclinical trajectory class membership would predict clinical diagnostic outcomes such as MCI or AD. As shown in Table 5, 96.3% of the analyzed longitudinal observations were with participants who were free of MCI or AD and over 99% included persons who were non-AD. In total, there were very few participants who transitioned to AD (n = 8) or MCI (n = 32, with 5 reverting back to CN) within the six waves under study—and together they contributed data for only 3.7% of the analyzed longitudinal observations (AD = 0.56%). By design, the present sample was selected initially to be cognitively asymptomatic (all were cognitively normal at baseline) and remained predominantly so throughout the study. The very small number of observations that could be characterized as impaired was appropriate for our objectives and expected in our design. No separate machine learning prediction analysis of this small cluster is possible due to severely imbalanced groups. However, a post-hoc check revealed that, in general, most of the individuals transitioning to impairment status were members of the lower trajectory classes. Accordingly, we suggest future work aimed at testing whether lower HC trajectory class membership is a reliable precursor condition for impairment and AD diagnosis. Fourth, the correlational analyses to clarify predictor directionality were focused more on describing associations with predictor variables than interpreting potential underlying mechanisms. Specific mechanisms should be further explored in future studies. Fifth, due to the ADNI MRI methods and protocols, almost all

participants from ADNI1 were scanned using 1.5T scanners and all participants from ADNI2 were scanned using 3T scanners. However, we found no significant associations between scanner strength and hippocampal trajectory classes. This indicates that scanner strength was properly corrected for at the modelling stage, as has been done in previous studies (Koran et al., 2017). Sixth, other (non-AD specific) pathologies and risk factors unavailable in this study may have contributed to the observed hippocampal volume and atrophy trajectories.

Conclusions

We used multi-wave MRI data from ADNI to identified three data-driven trajectory classes of left and right hippocampal volume in asymptomatic older adults. Our analytic approach, based on an algorithm of level and slope, revealed that the vast individual variability in hippocampal atrophy could be clustered into trajectory classes which capture the heterogeneous and dynamic nature of brain aging in cognitively normal older adults. We then applied machine learning technology to a large, multi-modal set of AD-related biomarkers and risk factors and identified the best predictors that discriminated lower versus higher hippocampal trajectory classes. The current findings identify several emerging and prominent risk factors and biomarkers associated with early stages of hippocampal atrophy, all of which merit further investigation in future mechanistic and clinical research.

References

Alosco, M. L., Duskin, J., Besser, L. M., Martin, B., Chaisson, C. E., Gunstad, J., . . . Tripodis, Y. (2017). Modeling the relationships among late-life body mass index, cerebrovascular disease, and Alzheimer's disease neuropathology in an autopsy sample of 1,421 subjects from the National Alzheimer's Coordinating Center Data Set. *Journal of Alzheimer's Disease, 57*(3), 953-968.

Anstey, K., Cherbuin, N., Budge, M., & Young, J. (2011). Body mass index in midlife and late-life as a risk factor for dementia: a meta-analysis of prospective studies. *Obesity Reviews, 12*(5), e426-e437.

Apostolova, L. G., Green, A. E., Babakchanian, S., Hwang, K. S., Chou, Y.-Y., Toga, A. W., & Thompson, P. M. (2012). Hippocampal atrophy and ventricular enlargement in normal aging, mild cognitive impairment and Alzheimer's disease. *Alzheimer Disease and Associated Disorders, 26*(1), 17.

Apostolova, L. G., Mosconi, L., Thompson, P. M., Green, A. E., Hwang, K. S., Ramirez, A., . . . de Leon, M. J. (2010). Subregional hippocampal atrophy predicts Alzheimer's dementia in the cognitively normal. *Neurobiology of Aging, 31*(7), 1077-1088.

Ardekani, B., Hadid, S., Blessing, E., & Bachman, A. (2019). Sexual dimorphism and hemispheric asymmetry of hippocampal volumetric integrity in normal aging and Alzheimer disease. *American Journal of Neuroradiology, 40*(2), 276-282.

Ardekani, B. A., Convit, A., & Bachman, A. H. (2016). Analysis of the MIRIAD data shows sex differences in hippocampal atrophy progression. *Journal of Alzheimer's Disease, 50*(3), 847-857.

Atti, A. R., Palmer, K., Volpato, S., Winblad, B., De Ronchi, D., & Fratiglioni, L. (2008). Late-life body mass index and dementia incidence: nine-year follow-up data from the Kungsholmen Project. *Journal of the American Geriatrics Society, 56*(1), 111-116.

Badhwar, A., McFall, G. P., Sapkota, S., Black, S. E., Chertkow, H., Duchesne, S., . . . Bellec, P. (2020). A multiomics approach to heterogeneity in Alzheimer's disease: focused review and roadmap. *Brain, 143*(5), 1315-1331.

Barnes, J., Scahill, R. I., Schott, J. M., Frost, C., Rossor, M. N., & Fox, N. C. (2005). Does Alzheimer's disease affect hippocampal asymmetry? Evidence from a cross-sectional and longitudinal volumetric MRI study. *Dementia and Geriatric Cognitive Disorders, 19*(5-6), 338-344.

Beltrán, J. F., Wahba, B. M., Hose, N., Shasha, D., Kline, R. P., & Initiative, A. s. D. N. (2020). Inexpensive, non-invasive biomarkers predict Alzheimer transition using machine learning analysis of the Alzheimer's Disease Neuroimaging (ADNI) database. *PLoS One, 15*(7), e0235663.

Bernard, C., Helmer, C., Dilharreguy, B., Amieva, H., Auriacombe, S., Dartigues, J.-F., . . . Catheline, G. (2014). Time course of brain volume changes in the preclinical phase of Alzheimer's disease. *Alzheimers. Dement., 10*(2), 143-151. e141.

Bischof, G. N., & Park, D. C. (2015). Obesity and aging: Consequences for cognition, brain structure and brain function. *Psychosomatic Medicine, 77*(6), 697.

Bohn, L., McFall, G. P., Wiebe, S. A., & Dixon, R. A. (2020). Body mass index predicts cognitive aging trajectories selectively for females: Evidence from the Victoria Longitudinal Study. *Neuropsychology, 34*(4), 388.

Bremner, J. D., Narayan, M., Anderson, E. R., Staib, L. H., Miller, H. L., & Charney, D. S. (2000). Hippocampal volume reduction in major depression. *American Journal of Psychiatry, 157*(1), 115-118.

Byun, M. S., Kim, S. E., Park, J., Yi, D., Choe, Y. M., Sohn, B. K., . . . Woo, J. I. (2015). Heterogeneity of regional brain atrophy patterns associated with distinct progression rates in Alzheimer's disease. *PloS One, 10*(11), e0142756.

Cantero, J. L., Iglesias, J. E., Van Leemput, K., & Atienza, M. (2016). Regional hippocampal atrophy and higher levels of plasma amyloid-beta are associated with subjective memory complaints in nondemented elderly subjects. *Journals of Gerontology Series A: Biomedical Sciences and Medical Sciences, 71*(9), 1210-1215.

Cherbuin, N., Réglade-Meslin, C., Kumar, R., Sachdev, P., & Anstey, K. J. (2010). Mild cognitive disorders are associated with different patterns of brain asymmetry than normal aging: The PATH through Life Study. *Front. Psychiatry, 1*, 11.

Cherbuin, N., Sargent-Cox, K., Easteal, S., Sachdev, P., & Anstey, K. J. (2015). Hippocampal atrophy is associated with subjective memory decline: The PATH Through Life study. *The American Journal of Geriatric Psychiatry, 23*(5), 446-455.

Cherbuin, N., Sargent-Cox, K., Fraser, M., Sachdev, P., & Anstey, K. (2015). Being overweight is associated with hippocampal atrophy: the PATH Through Life Study. *International Journal of Obesity, 39*(10), 1509-1514.

Chiu, M.-J., Fan, L.-Y., Chen, T.-F., Chen, Y.-F., Chieh, J.-J., & Horng, H.-E. (2017). Plasma tau levels in cognitively normal middle-aged and older adults. *Frontiers in Aging Neuroscience, 9*, 51.

Cooper, L. L., Woodard, T., Sigurdsson, S., van Buchem, M. A., Torjesen, A. A., Inker, L. A., . . . Mitchell, G. F. (2016). Cerebrovascular damage mediates relations between aortic stiffness and memory. *Hypertension, 67*(1), 176-182. doi:10.1161/hypertensionaha.115.06398

Couronné, R., Probst, P., & Boulesteix, A.-L. (2018). Random forest versus logistic regression: a large-scale benchmark experiment. *BMC Bioinformatics, 19*(1), 270.

Dale, A., Fischl, B., & Sereno, M. I. (1999). Cortical Surface-Based Analysis: I. Segmentation and Surface Reconstruction. *Neuroimage, 9*, 179-194.

Dale, A. M., & Sereno, M. I. (1993). Improved localizadon of cortical activity by combining EEG and MEG with MRI cortical surface reconstruction: a linear approach. *J Cogn Neurosci, 5*(2), 162-176.

De Leon, M., George, A., Golomb, J., Tarshish, C., Convit, A., Kluger, A., . . . Reisberg, B. (1997). Frequency of hippocampal formation atrophy in normal aging and Alzheimer's disease. *Neurobiology of Aging, 18*(1), 1-11.

DeCarlo, C. A., Tuokko, H. A., Williams, D., Dixon, R. A., & MacDonald, S. W. (2014). BioAge: Toward a multi-determined, mechanistic account of cognitive aging. *Ageing Research Reviews, 18*, 95-105. doi:10.1016/j.arr.2014.09.003

Deters, K. D., Risacher, S. L., Kim, S., Nho, K., West, J. D., Blennow, K., . . . Weiner, M. W. (2017). Plasma tau association with brain atrophy in mild cognitive impairment and Alzheimer's disease. *Journal of Alzheimer's Disease, 58*(4), 1245-1254.

Dixon, R. A., & Lachman, M. E. (2019). Risk and protective factors in cognitive aging: Advances in assessment, prevention, and promotion of alternative pathways. In G. R. Samanez-Larkin (Ed.), *The aging brain: Functional adaptation across adulthood* (pp. 217-263). Washington, DC: APA Books.

Dong, A., Honnorat, N., Gaonkar, B., & Davatzikos, C. (2015). CHIMERA: clustering of heterogeneous disease effects via distribution matching of imaging patterns. *IEEE Transactions on Medical Imaging, 35*(2), 612-621.

Drouin, S. M., McFall, G. P., & Dixon, R. A. (2021). Subjective memory concerns, poor vascular health, and male sex predict exacerbated memory decline trajectories: An integrative data-driven class and prediction analysis. *Neuropsychology*.

Durazzo, T. C., Meyerhoff, D. J., & Nixon, S. J. (2013). Interactive effects of chronic cigarette smoking and age on hippocampal volumes. *Drug and Alcohol Dependence, 133*(2), 704-711.

Dye, L., Boyle, N. B., Champ, C., & Lawton, C. (2017). The relationship between obesity and cognitive health and decline. *Proceedings of the Nutrition Society, 76*(4), 443-454.

Eavani, H., Habes, M., Satterthwaite, T. D., An, Y., Hsieh, M.-K., Honnorat, N., . . . Beason-Held, L. L. (2018). Heterogeneity of structural and functional imaging patterns of advanced brain aging revealed via machine learning methods. *Neurobiol Aging, 71*, 41-50.

Elbejjani, M., Fuhrer, R., Abrahamowicz, M., Mazoyer, B., Crivello, F., Tzourio, C., & Dufouil, C. (2014). Hippocampal atrophy and subsequent depressive symptoms in older men and women: results from a 10-year prospective cohort. *American Journal of Epidemiology, 180*(4), 385-393.

Falahati, F., Westman, E., & Simmons, A. (2014). Multivariate data analysis and machine learning in Alzheimer's disease with a focus on structural magnetic resonance imaging. *Journal of Alzheimer's Disease, 41*(3), 685-708.

Ferreira, D., Verhagen, C., Hernández-Cabrera, J. A., Cavallin, L., Guo, C.-J., Ekman, U., . . . Wahlund, L.-O. (2017). Distinct subtypes of Alzheimer's disease based on patterns of brain atrophy: Longitudinal trajectories and clinical applications. *Scientific Reports, 7*, 46263.

Fischl, B., & Dale, A. M. (2000). Measuring the thickness of the human cerebral cortex from magnetic resonance images. *Proc Natl Acad Sci U S A, 97*, 11050-11055.

Fischl, B., Liu, A., & Dale, A. M. (2001). Automated manifold surgery: constructing geometrically accurate and topologically correct models of the human cerebral cortex. *{IEEE} Medical Imaging, 20*(1), 70-80.

Fischl, B., Salat, D. H., Busa, E., Albert, M., Dieterich, M., Haselgrove, C., . . . Dale, A. M. (2002). Whole brain segmentation: automated labeling of neuroanatomical structures in the human brain. *Neuron, 33*, 341-355.

Fischl, B., Salat, D. H., van der Kouwe, A. J. W., Makris, N., Ségonne, F., Quinn, B. T., & Dale, A. M. (2004). Sequence-independent segmentation of magnetic resonance images. *Neuroimage, 23*, S69 - S84. doi:DOI: 10.1016/j.neuroimage.2004.07.016

Fischl, B., Sereno, M. I., & Dale, A. (1999). Cortical Surface-Based Analysis: II: Inflation, Flattening, and a Surface-Based Coordinate System. *Neuroimage, 9*, 195-207.

Fischl, B., Sereno, M. I., Tootell, R. B. H., & Dale, A. M. (1999). High-resolution intersubject averaging and a coordinate system for the cortical surface. *Hum Brain Mapp, 8*, 272-284. doi:10.1002/(SICI)1097-0193(1999)8:4<272::AID-HBM10>3.0.CO;2-4

Fischl, B., van der Kouwe, A., Destrieux, C., Halgren, E., Ségonne, F., Salat, D. H., . . . Dale, A. M. (2004). Automatically Parcellating the Human Cerebral Cortex. *Cerebral Cortex, 14*, 11-22. doi:10.1093/cercor/bhg087

Fox, N., Scahill, R., Crum, W., & Rossor, M. (1999). Correlation between rates of brain atrophy and cognitive decline in AD. *Neurology, 52*(8), 1687-1687.

Fox, N. C., & Schott, J. M. (2004). Imaging cerebral atrophy: Normal ageing to Alzheimer's disease. *The Lancet, 363*(9406), 392-394.

Fraser, M. A., Shaw, M. E., & Cherbuin, N. (2015). A systematic review and meta-analysis of longitudinal hippocampal atrophy in healthy human ageing. *Neuroimage, 112*, 364-374.

Glisky, E. L. (2007). Changes in cognitive function in human aging. *Brain aging: Models, methods, and mechanisms*, 3-20.

Gomar, J. J., Bobes-Bascaran, M. T., Conejero-Goldberg, C., Davies, P., Goldberg, T. E., & Initiative, A. s. D. N. (2011). Utility of combinations of biomarkers, cognitive markers, and risk factors to predict conversion from mild cognitive impairment to Alzheimer disease in patients in the Alzheimer's disease neuroimaging initiative. *Archives of general psychiatry, 68*(9), 961-969.

Gregorutti, B., Michel, B., & Saint-Pierre, P. (2017). Correlation and variable importance in random forests. *Statistics and Computing, 27*(3), 659-678.

Gunter, J. L., Bernstein, M. A., Borowski, B. J., Ward, C. P., Britson, P. J., Felmlee, J. P., . . . Jack, C. R. (2009). Measurement of MRI scanner performance with the ADNI phantom. *Medical Physics, 36*(6Part1), 2193-2205.

Habes, M., Grothe, M. J., Tunc, B., McMillan, C., Wolk, D. A., & Davatzikos, C. (2020). Disentangling heterogeneity in Alzheimer's disease and related dementias using data-driven methods. *Biological Psychiatry*.

Hampel, H., O'Bryant, S. E., Molinuevo, J. L., Zetterberg, H., Masters, C. L., Lista, S., . . . Blennow, K. (2018). Blood-based biomarkers for Alzheimer disease: mapping the road to the clinic. *Nature Reviews Neurology, 14*(11), 639-652.

Han, X., Jovicich, J., Salat, D., van der Kouwe, A., Quinn, B., Czanner, S., . . . Fischl, B. (2006). Reliability of MRI-derived measurements of human cerebral cortical thickness: The effects of field strength, scanner upgrade and manufacturer. *Neuroimage, 32*, 180-194.

Hapfelmeier, A., & Ulm, K. (2013). A new variable selection approach using random forests. *Computational Statistics & Data Analysis, 60*, 50-69.

Hastie, T., Tibshirani, R., & Friedman, J. (2009). *The elements of statistical learning: data mining, inference, and prediction*: Springer Science & Business Media.

Henneman, W., Vrenken, H., Barnes, J., Sluimer, I., Verwey, N., Blankenstein, M., . . . Barkhof, F. (2009). Baseline CSF p-tau levels independently predict progression of hippocampal atrophy in Alzheimer disease. *Neurology, 73*(12), 935-940.

Hilal, S., Wolters, F. J., Verbeek, M. M., Vanderstichele, H., Ikram, M. K., Stoops, E., . . . Vernooij, M. W. (2018). Plasma amyloid-β levels, cerebral atrophy and risk of dementia: a population-based study. *Alzheimer's Research & Therapy, 10*(1), 63.

Hothorn, T., Buehlmann, P., Dudoit, S., Molinaro, A., & Van Der Laan, M. (2006). Survival ensembles. *Biostatistics, 7*(3), 355-373. doi:10.1093/biostatistics/kxj011

Jack, C. R., Petersen, R. C., Xu, Y., O'Brien, P., Smith, G. E., Ivnik, R. J., . . . Kokmen, E. (2000). Rates of hippocampal atrophy correlate with change in clinical status in aging and AD. *Neurology, 55*(4), 484-490.

Jack, C. R., Shiung, M., Weigand, S., O'Brien, P., Gunter, J., Boeve, B. F., . . . Tangalos, E. G. (2005). Brain atrophy rates predict subsequent clinical conversion in normal elderly and amnestic MCI. *Neurology, 65*(8), 1227-1231.

Jack Jr, C. R., Bennett, D. A., Blennow, K., Carrillo, M. C., Dunn, B., Haeberlein, S. B., . . . Karlawish, J. (2018). NIA-AA research framework: Toward a biological definition of Alzheimer's disease. *Alzheimers. Dement., 14*(4), 535-562.

Jack Jr, C. R., Bernstein, M. A., Fox, N. C., Thompson, P., Alexander, G., Harvey, D., . . . Ward, C. (2008). The Alzheimer's disease neuroimaging initiative (ADNI): MRI methods. *Journal of Magnetic Resonance Imaging: An Official Journal of the International Society for Magnetic Resonance in Medicine, 27*(4), 685-691.

Jovicich, J., Czanner, S., Greve, D., Haley, E., van der Kouwe, A., Gollub, R., . . . Dale, A. (2006). Reliability in multi-site structural MRI studies: Effects of gradient non-linearity correction on phantom and human data. *Neuroimage, 30*, 436-443. doi:DOI: 10.1016/j.neuroimage.2005.09.046

Jung, N.-Y., Seo, S. W., Yoo, H., Yang, J.-J., Park, S., Kim, Y. J., . . . Lee, J. M. (2016). Classifying anatomical subtypes of subjective memory impairment. *Neurobiol Aging, 48*, 53-60.

Koran, M. E. I., Wagener, M., & Hohman, T. J. (2017). Sex differences in the association between AD biomarkers and cognitive decline. *Brain Imaging and Behavior, 11*(1), 205-213.

Kwon, G.-R., Gupta, Y., & Lama, R. K. (2019). Prediction and classification of Alzheimer's disease based on combined features from apolipoprotein-E genotype, cerebrospinal fluid, MR, and FDG-PET imaging biomarkers. *Frontiers in computational neuroscience, 13*, 72.

Lanza, S. T., Collins, L. M., Lemmon, D. R., & Schafer, J. L. (2007). PROC LCA: A SAS procedure for latent class analysis. *Structural Equation Modeling: A Multidisciplinary Journal, 14*(4), 671-694.

Laws, K. R., Irvine, K., & Gale, T. M. (2016). Sex differences in cognitive impairment in Alzheimer's disease. *World journal of psychiatry, 6*(1), 54.

Lebedeva, A., Sundström, A., Lindgren, L., Stomby, A., Aarsland, D., Westman, E., . . . Nyberg, L. (2018). Longitudinal relationships among depressive symptoms, cortisol, and brain atrophy in the neocortex and the hippocampus. *Acta Psychiatr Scand, 137*(6), 491-502.

Levine, M. E., Lu, A. T., Quach, A., Chen, B. H., Assimes, T. L., Bandinelli, S., . . . Li, Y. (2018). An epigenetic biomarker of aging for lifespan and healthspan. *Aging, 10*(4), 573.

Little, T. D. (2013). *Longitudinal structural equation modeling*. New York, NY: Guilford Press.

Livingston, G., Huntley, J., Sommerlad, A., Ames, D., Ballard, C., Banerjee, S., . . . Cooper, C. (2020). Dementia prevention, intervention, and care: 2020 report of the Lancet Commission. *The Lancet, 396*(10248), 413-446.

Livingston, G., Sommerlad, A., Orgeta, V., Costafreda, S. G., Huntley, J., Ames, D., . . . Cohen-Mansfield, J. (2017). Dementia prevention, intervention, and care. *The Lancet, 390*(10113), 2673-2734.

Luchsinger, J. A., & Mayeux, R. (2007). Adiposity and Alzheimer's disease. *Current Alzheimer Research, 4*(2), 127-134.

MacDonald, S. W., DeCarlo, C. A., & Dixon, R. A. (2011). Linking biological and cognitive aging: Toward improving characterizations of developmental time. *The Journals of Gerontology Series B: Psychological Sciences and Social Sciences, 66*(Suppl 1), i59-70. doi:10.1093/geronb/gbr039

Malpas, C. B. (2016). Structural neuroimaging correlates of cognitive status in older adults: a person-oriented approach. *Journal of Clinical Neuroscience, 30*, 77-82.

Masyn, K. E. (2013). Latent class analysis and finite mixture modeling. In *The Oxford handbook of quantitative methods* (pp. 551): Oxford University Press, Oxford.

McDermott, K. L., McFall, G. P., Andrews, S. J., Anstey, K. J., & Dixon, R. A. (2017). Memory resilience to Alzheimer's genetic risk: Sex effects in predictor profiles. *Journals of Gerontology. Series B: Psychological Sciences and Social Sciences, 72*(6), 937-946.

McFall, G. P., McDermott, K. L., & Dixon, R. A. (2019). Modifiable Risk Factors Discriminate Memory Trajectories in Non-Demented Aging: Precision Factors and Targets for Promoting Healthier Brain Aging and Preventing Dementia. *Journal of Alzheimer's Disease, 70*(s1), S101-S118. doi:10.3233/JAD-180571

McFall, G. P., Wiebe, S. A., Vergote, D., Westaway, D., Jhamandas, J., Bäckman, L., & Dixon, R. A. (2015). ApoE and pulse pressure interactively influence level and change in the aging of episodic memory: Protective effects among epsilon2 carriers. *Neuropsychology, 29*(3), 388-401. doi:10.1037/neu0000150

Melis, R. J. F., Haaksma, M. L., & Muniz-Terrera, G. (2019). Understanding and predicting the longitudinal course of dementia. *Curr Opin Psychiatry, 32*(2), 123-129. doi:10.1097/YCO.0000000000000482

Michaelson, D. M. (2014). APOE ε4: The most prevalent yet understudied risk factor for Alzheimer's disease. *Alzheimer's & Dementia, 10*(6), 861-868.

Minkova, L., Habich, A., Peter, J., Kaller, C. P., Eickhoff, S. B., & Klöppel, S. (2017). Gray matter asymmetries in aging and neurodegeneration: A review and meta-analysis. *Human Brain Mapping, 38*(12), 5890-5904.

Mosti, C. B., Rog, L. A., & Fink, J. W. (2019). Differentiating mild cognitive impairment and cognitive changes of normal aging. In *Handbook on the Neuropsychology of Aging and Dementia* (pp. 445-463): Springer.

Muthén, L., & Muthén, B. (2018). *Mplus users guide and Mplus version 8.2. Retrieved January 10, 2019*.

Nettiksimmons, J., Harvey, D., Brewer, J., Carmichael, O., DeCarli, C., Jack Jr, C. R., . . . Weiner, M. W. (2010). Subtypes based on cerebrospinal fluid and magnetic resonance imaging markers in normal elderly predict cognitive decline. *Neurobiology of Aging, 31*(8), 1419-1428.

Noble, K. G., Grieve, S. M., Korgaonkar, M. S., Engelhardt, L. E., Griffith, E. Y., Williams, L. M., & Brickman, A. M. (2012). Hippocampal volume varies with educational attainment across the life-span. *Frontiers in Human Neuroscience, 6*, 307.

Nylund, K. L., Asparouhob, T., & Muthén, B. O. (2007). Deciding on the number of classes in latent class analysis and growth mixture modeling: A Monte Carlo simulation study. *Structural Equation Modeling, 14*(4), 535-569. doi:10.1080/10705510701575396

Orban, P., Tam, A., Urchs, S., Savard, M., Madjar, C., Badhwar, A., . . . Dagher, A. (2017). Subtypes of functional brain connectivity as early markers of neurodegeneration in Alzheimer's disease. *bioRxiv*, 195164.

Pase, M. P., Beiser, A. S., Himali, J. J., Satizabal, C. L., Aparicio, H. J., DeCarli, C., . . . Seshadri, S. (2019). Assessment of plasma total tau level as a predictive biomarker for dementia and related endophenotypes. *JAMA Neurology, 76*(5), 598-606.

Petersen, R. C., Aisen, P., Beckett, L. A., Donohue, M., Gamst, A., Harvey, D. J., . . . Toga, A. (2010). Alzheimer's disease neuroimaging initiative (ADNI): clinical characterization. *Neurology, 74*(3), 201-209.

Pini, L., Pievani, M., Bocchetta, M., Altomare, D., Bosco, P., Cavedo, E., . . . Frisoni, G. B. (2016). Brain atrophy in Alzheimer's disease and aging. *Ageing research reviews, 30*, 25-48.

Piras, F., Cherubini, A., Caltagirone, C., & Spalletta, G. (2011). Education mediates microstructural changes in bilateral hippocampus. *Human Brain Mapping, 32*(2), 282-289.

Potvin, O., Mouiha, A., Dieumegarde, L., Duchesne, S., & Initiative, A. s. D. N. (2016). Normative data for subcortical regional volumes over the lifetime of the adult human brain. *Neuroimage, 137*, 9-20.

Ram, N., & Grimm, K. J. (2009). Growth mixture modeling: A method for identifying differences in longitudinal change among unobserved groups. *Int J Behav Dev, 33*(6), 565-576. doi:10.1177/0165025409343765

Raz, N., Ghisletta, P., Rodrigue, K. M., Kennedy, K. M., & Lindenberger, U. (2010). Trajectories of brain aging in middle-aged and older adults: Regional and individual differences. *Neuroimage, 51*(2), 501-511.

Reuter, M., Rosas, H. D., & Fischl, B. (2010). Highly Accurate Inverse Consistent Registration: A Robust Approach. *Neuroimage, 53*, 1181-1196. doi:10.1016/j.neuroimage.2010.07.020

Reuter, M., Schmansky, N. J., Rosas, H. D., & Fischl, B. (2012). Within-Subject Template Estimation for Unbiased Longitudinal Image Analysis. *Neuroimage, 61*, 1402-1418. doi:10.1016/j.neuroimage.2012.02.084

Ritter, K., Schumacher, J., Weygandt, M., Buchert, R., Allefeld, C., Haynes, J.-D., & Initiative, A. s. D. N. (2015). Multimodal prediction of conversion to Alzheimer's disease based on incomplete biomarkers. *Alzheimer's & Dementia: Diagnosis, Assessment & Disease Monitoring, 1*(2), 206-215.

Rusinek, H., De Santi, S., Frid, D., Tsui, W.-H., Tarshish, C. Y., Convit, A., & de Leon, M. J. (2003). Regional brain atrophy rate predicts future cognitive decline: 6-year longitudinal MR imaging study of normal aging. *Radiology, 229*(3), 691-696.

Sapkota, S., Huan, T., Tran, T., Zheng, J., Camicioli, R., Li, L., & Dixon, R. A. (2018). Alzheimer's biomarkers from multiple modalities selectively discriminate clinical status: Relative importance of salivary metabolomics panels, genetic, lifestyle, cognitive, functional health and demographic risk markers. *Frontiers in Aging Neuroscience, 10*, 296.

Segonne, F., Dale, A. M., Busa, E., Glessner, M., Salat, D., Hahn, H. K., & Fischl, B. (2004). A hybrid approach to the skull stripping problem in MRI. *Neuroimage, 22*, 1060-1075. doi:DOI: 10.1016/j.neuroimage.2004.03.032

Segonne, F., Pacheco, J., & Fischl, B. (2007). Geometrically accurate topology-correction of cortical surfaces using nonseparating loops. *IEEE Trans Med Imaging, 26*, 518-529.

Seo, S. W., Im, K., Lee, J.-M., Kim, S. T., Ahn, H. J., Go, S. M., . . . Na, D. L. (2011). Effects of demographic factors on cortical thickness in Alzheimer's disease. *Neurobiol Aging, 32*(2), 200-209.

Shaffer, J. L., Petrella, J. R., Sheldon, F. C., Choudhury, K. R., Calhoun, V. D., Coleman, R. E., . . . Initiative, A. s. D. N. (2013). Predicting cognitive decline in subjects at risk for Alzheimer disease by using combined cerebrospinal fluid, MR imaging, and PET biomarkers. *Radiology, 266*(2), 583-591.

Shen, S., Zhou, W., Chen, X., & Zhang, J. (2019). Sex differences in the association of APOE ε4 genotype with longitudinal hippocampal atrophy in cognitively normal older people. *European Journal of Neurology, 26*(11), 1362-1369.

Shi, Y., Lu, X., Zhang, L., Shu, H., Gu, L., Wang, Z., . . . Zhou, D. (2019). Potential value of plasma amyloid-β, total Tau, and neurofilament light for identification of early Alzheimer's disease. *ACS chemical neuroscience, 10*(8), 3479-3485.

Shpanskaya, K. S., Choudhury, K. R., Hostage Jr, C., Murphy, K. R., Petrella, J. R., Doraiswamy, P. M., & Initiative, A. s. D. N. (2014). Educational attainment and hippocampal atrophy in the Alzheimer's disease neuroimaging initiative cohort. *Journal of Neuroradiology, 41*(5), 350-357.

Sled, J. G., Zijdenbos, A. P., & Evans, A. C. (1998). A nonparametric method for automatic correction of intensity nonuniformity in MRI data. *IEEE Trans Med Imaging, 17*, 87-97.

Stekhoven, D. J. (2011). Using the missForest package. *R package*, 1-11.

Stekhoven, D. J., & Bühlmann, P. (2012). MissForest—non-parametric missing value imputation for mixed-type data. *Bioinformatics, 28*(1), 112-118. doi:10.1093/bioinformatics/btr597

Stricker, N. H., Dodge, H. H., Dowling, N. M., Han, S. D., Erosheva, E. A., Jagust, W. J., & Initiative, A. s. D. N. (2012). CSF biomarker associations with change in hippocampal volume and precuneus thickness: implications for the Alzheimer's pathological cascade. *Brain Imaging and Behavior, 6*(4), 599-609.

Strobl, C., Boulesteix, A.-L., Kneib, T., Augustin, T., & Zeileis, A. (2008). Conditional variable importance for random forests. *BMC Bioinformatics, 9*(1), 1-11. doi:10.1186/1471-2105-9-307

Strobl, C., Boulesteix, A. L., Zeileis, A., & Hothorn, T. (2007). Bias in Random Forest Variable Importance Measures: Illustrations, Sources and a Solution. *BMC Bioinformatics, 8*. doi:10.1186/1471-2105-8-25

Suemoto, C. K., Gilsanz, P., Mayeda, E. R., & Glymour, M. M. (2015). Body mass index and cognitive function: the potential for reverse causation. *International Journal of Obesity, 39*(9), 1383-1389.

Sundermann, E. E., Tran, M., Maki, P. M., & Bondi, M. W. (2018). Sex differences in the association between apolipoprotein E ε4 allele and Alzheimer's disease markers. *Alzheimer's & Dementia: Diagnosis, Assessment & Disease Monitoring, 10*, 438-447.

Sundermann, E. E., Tran, M., Maki, P. M., Bondi, M. W., & Initiative, A. s. D. N. (2018). Sex differences in the association between apolipoprotein E ε4 allele and Alzheimer's disease markers. *Alzheimer's & Dementia: Diagnosis, Assessment & Disease Monitoring, 10*, 438-447.

Tam, A., Dansereau, C., Iturria-Medina, Y., Urchs, S., Orban, P., Sharmarke, H., . . . Initiative, A. s. D. N. (2019). A highly predictive signature of cognition and brain atrophy for progression to Alzheimer's dementia. *Gigascience, 8*(5), giz055.

Toloşi, L., & Lengauer, T. (2011). Classification with correlated features: unreliability of feature ranking and solutions. *Bioinformatics, 27*(14), 1986-1994.

Valenzuela, M. J., Sachdev, P., Wen, W., Chen, X., & Brodaty, H. (2008). Lifespan mental activity predicts diminished rate of hippocampal atrophy. *PloS One, 3*(7).

Voevodskaya, O., Simmons, A., Nordenskjöld, R., Kullberg, J., Ahlström, H., Lind, L., . . . Initiative, A. s. D. N. (2014). The effects of intracranial volume adjustment approaches on multiple regional MRI volumes in healthy aging and Alzheimer's disease. *Frontiers in Aging Neuroscience, 6*, 264.

Vogel, J. W., Young, A. L., Oxtoby, N. P., Smith, R., Ossenkoppele, R., Strandberg, O. T., . . . Iturria-Medina, Y. (2021). Four distinct trajectories of tau deposition identified in Alzheimer's disease. *Nature Medicine, 27*(5), 871-881.

Wachinger, C., Salat, D. H., Weiner, M., Reuter, M., & Initiative, A. s. D. N. (2016). Whole-brain analysis reveals increased neuroanatomical asymmetries in dementia for hippocampus and amygdala. *Brain, 139*(12), 3253-3266.

Waljee, A. K., Mukherjee, A., Singal, A. G., Zhang, Y., Warren, J., Balis, U., . . . Higgins, P. D. (2013). Comparison of imputation methods for missing laboratory data in medicine. *BMJ Open, 3*(8), e002847. doi:10.1136/bmjopen-2013-002847

Whitwell, J. L., Dickson, D. W., Murray, M. E., Weigand, S. D., Tosakulwong, N., Senjem, M. L., . . . Petersen, R. C. (2012). Neuroimaging correlates of pathologically defined subtypes of Alzheimer's disease: a case-control study. *The Lancet Neurology, 11*(10), 868-877.

Whitwell, J. L., Wiste, H. J., Weigand, S. D., Rocca, W. A., Knopman, D. S., Roberts, R. O., . . . Initiative, A. D. N. (2012). Comparison of imaging biomarkers in the Alzheimer disease neuroimaging initiative and the Mayo Clinic Study of Aging. *Archives of Neurology, 69*(5), 614-622.

Wu, J. W., Yaqub, A., Ma, Y., Koudstaal, W., Hofman, A., Ikram, M. A., . . . Goudsmit, J. (2021). Biological age in healthy elderly predicts aging-related diseases including dementia. *Scientific Reports, 11*(1), 1-10.

Zhang, Y., Qiu, C., Lindberg, O., Bronge, L., Aspelin, P., Bäckman, L., . . . Wahlund, L.-O. (2010). Acceleration of hippocampal atrophy in a non-demented elderly population: the SNAC-K study. *International Psychogeriatrics, 22*(1), 14-25.

Zhao, W., Wang, X., Yin, C., He, M., Li, S., & Han, Y. (2019). Trajectories of the hippocampal subfields atrophy in the Alzheimer's disease: A structural imaging study. *Frontiers in Neuroinformatics, 13*, 13

Tables

Table 2-1. Baseline characteristics for the entire sample (*n* = 351)

	Whole	LHC (Highest)	LHC (Middle)	LHC (Lowest)	RHC (Highest)	RHC (Middle)	RHC (Lowest)
N	351	100	173	78	96	167	88
n in ADNI-1	214	60	113	41	55	105	54
n in ADNI-2	137	40	60	37	41	62	34
Sex (% Female)	48.7	64.0	46.8	33.3	69.8	45.5	31.8
Age *M* (*SD)*	74.8 (5.7)	75. 1 (5.9)	75.0 (2.6)	73.9 (5.6)	74.6 (6.2)	75.1 (5.5)	74.5 (5.4)
Education *M* (*SD*)	16.3 (2.7)	15.7 (2.6)	16.3 (2.9)	17.2 (2.4)	15.3 (2.8)	16.5 (2.7)	17.2 (2.4)
Mini Mental State Exam *M* (*SD*)	29.1 (1.0)	29.1 (1.2)	29.1 (1.0)	29.0 (1.1)	29.2 (1.2)	29.1 (1.1)	29.1 (1.0)
ADAS-Cog *M* (*SD*)	9.3 (4.3)	8.5 (3.9)	9.7 (4.4)	9.2 (4.6)	9.0 (4.0)	9.3 (4.4)	9.5 (4.7)

Table 2-2. Predictors by modality and measurement characteristics

Modalities	Biomarkers	Metric	% Missing for LHC	% Missing for RHC
Biospecimen	Plasma Aβ1-40[1]	pg/mL	47.2	44.6
	Plasma Aβ1-42[1]	pg/mL	46.6	44.0
	CSF Aβ1-42[2]	pg/mL	38.2	35.3
	CSF total-tau[2]	pg/mL	38.8	35.9
	CSF p-tau[2]	pg/mL	38.2	35.3
	Plasma tau[3]	pg/mL	55.6	50.0
Demographic	Age	Years	0	0
	Sex	Female/Male	0	0
	Education	Years	0	0
Genetic	*APOE*	ε2+, ε3/ε3, ε4+	0	0
Vascular/Metabolic	Systolic blood pressure	mm Hg	0	0
	Diastolic blood pressure	mm Hg	0	0
	Hypertension	140/90 mm Hg	0	0
	Subjective report of diabetes	Yes / no	0	0
	Glucose level at baseline	mg/dL	3.9	2.2
Lifestyle	Body mass index	kg/m^2	1.1	0.5
	History of smoking	Yes / no	0	0
Co-morbidities	Geriatric depression scale score	Mild (5-8), moderate (9-11), severe (12-15)	0	0
	Cardiovascular, alcoholism, psychiatric, neurological, head/eyes/ears/nose/throat, respiratory, hepatic, dermatologic connective tissue, musculoskeletal, endocrine-metabolic, gastrointestinal, hematopoietic-lymphatic, renal-genitourinary, allergies/drug sensitivities, malignancy, and/or major surgeries	Yes / no	0	0
Familial Background	Maternal dementia history	Yes / no	0.6	0
	Paternal dementia history	Yes / no	1.7	2.6
Cognitive Status	MMSE	0-30, >24 indicates no dementia	0	0

ADAS-Cog	0-70, ≥ 18 indicates cognitive impairment	0	0

[1]Plasma collection - University of Pennsylvania (UPENNPLASMA.csv); [2]CSF collection - University of Pennsylvania (UPENNBIOMK_MASTER.csv, median re-scaled values); [3]Plasma collection – Blennow Lab (BLENNOWPLASMATAU.csv).

Table 2-3. Latent class growth analyses model fit statistics and class proportions for left and right hippocampal volume

Volumetric Variable	Number of Classes	Class Proportions	AIC	BIC	SABIC	Entropy
Left Hippocampus	1	-	403.50	442.12	410.39	-
	2	0.49/0.51	-909.04	-851.13	-898.71	0.90
	3*	0.49/0.29/0.22	-1907.10	-1829.88	-1893.33	0.92
	4	Did not replicate	-	-	-	-
	5	0.10/0.26/0.22/0.13/0.30	-2707.13	-2591.31	-2686.48	0.89
Right Hippocampus	1	-	399.19	437.80	506.08	-
	2	0.46/0.54	-885.82	-827.91	-875.49	0.90
	3*	0.25/0.27/0.48	-1997.35	-1920.14	-1983.58	0.93
	4	0.12/0.34/0.23/0.31	-2450.80	-2354.28	-2433.59	0.92
	5	0.12/0.09/0.36/0.22/0.21	-2765.27	-2649.45	-2744.62	0.90

Note. AIC, Akaike information criteria; BIC, Bayesian information criteria; SABIC, Sample-size adjusted BIC.
* Identified as best model fit based on low AIC, BIC, SABIC and no class proportion less than 10%

Table 2-4. Final latent class growth analyses models statistics and parameters

Volumetric Variable	Class	*n* (%)	Level (Intercept) [95% CI]	Slope [95% CI]
Left Hippocampus	1	100 (28.5)	2.50 [2.50-2.51]	-0.02 [-0.025—0.021]
	2	173 (49.3)	2.14 [2.13-2.14]	-0.03 [-0.028—0.024]
	3	78 (22.2)	1.79 [1.78-1.80]	-0.03 [-0.030—0.022]
Right Hippocampus	1	96 (27.4)	2.53 [2.53-2.54]	-0.02 [-0.025—0.021]
	2	167 (47.6)	2.21 [2.20-2.21]	-0.03 [-0.028—0.023]
	3	88 (25.1)	1.83 [1.83-1.84]	-0.03 [-0.027—0.023]

Note. Class 1 refers to the higher group; Class 2 refers to the middle group; Class 3 refers to the lower group.

Table 2-5. Biomarker and risk factor means and frequencies for LHC and RHC trajectory classes

Significant Biomarker	Lowest LHC Trajectory Class	Highest LHC Trajectory Class	Lowest RHC Trajectory Class	Highest RHC Trajectory Class
N	78	100	88	96
Plasma Aβ1-40	139.72 (56.78)	171.46 (47.03)	142.23 (47.19)	168.31 (45.30)
Sex (%, female)	33.33	64.0	31.82	69.80
Plasma t-tau	2.41 (0.94)	2.65 (1.05)	2.50 (1.42)	2.55 (1.07)
Plasma Aβ1-42	34.71 (10.58)	41.00 (14.62)	34.35 (10.13)	42.04 (14.52)
Education, years (SD)	17.15 (2.42)	15.73 (2.56)	17.17 (2.43)	15.33 (2.73)
GDS	0.91 (1.27)	0.52 (0.88)	0.81 (1.19)	0.67 (1.01)
BMI	26.06 (4.47)	27.35 (4.69)	26.11 (4.43)	27.36 (5.07)
Follow-up Cognitive Status Documentation				
# of person-waves (observations)	398	496	442	473
% of person-waves that are non-AD	98.2	99.8	98.6	100
% of person-waves that are non-AD and non-MCI	93.0	98.6	92.5	98.7

Figures

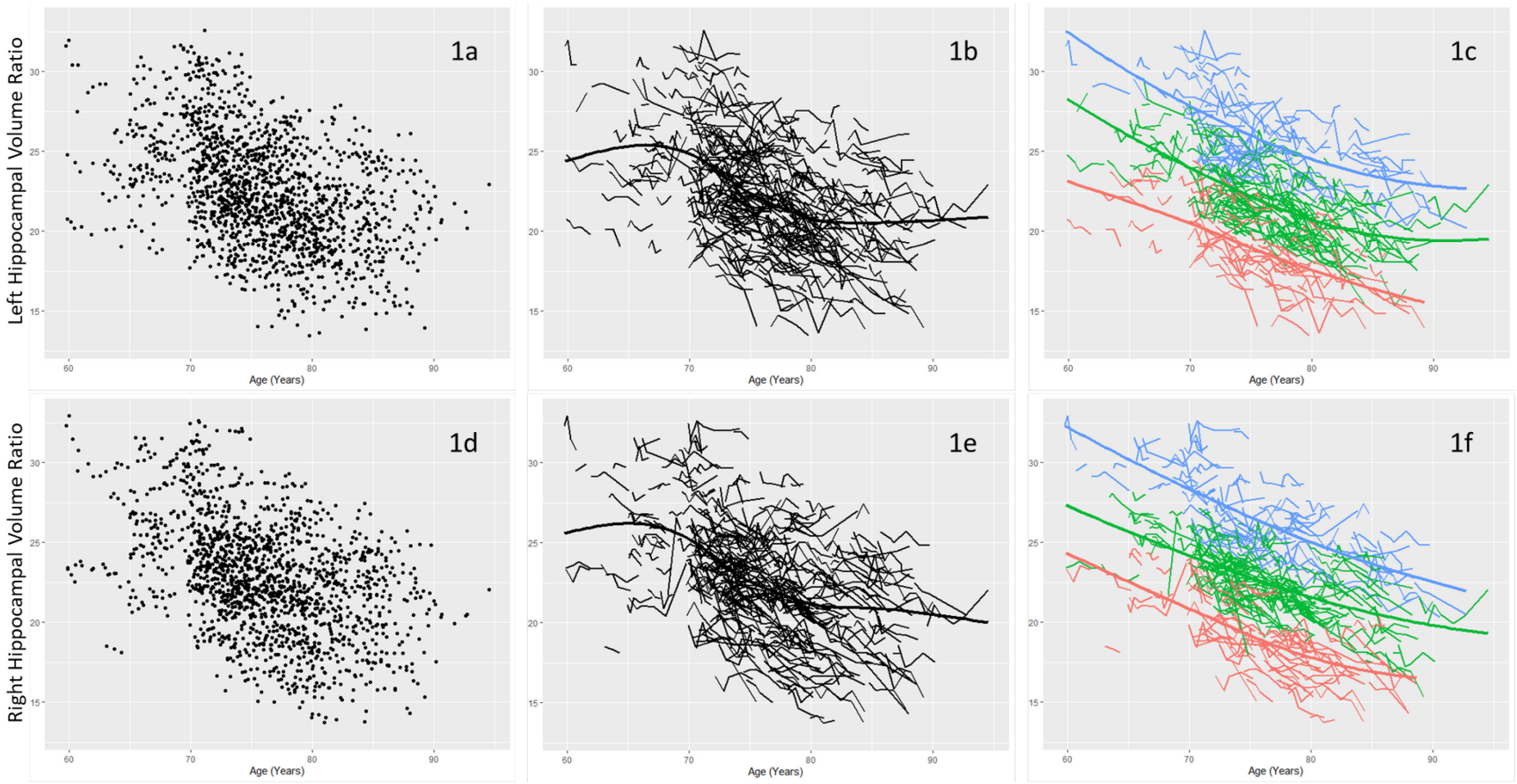

Figure 2-1. Distribution of left (1a) and right (1d) hippocampus volume data. Individual trajectories of left (1b) and right (1e) hippocampal volume. Three classes were identified within left (1c) and right (1f) hippocampal volume trajectories: **Class 1 (Highest, Least Atrophied)**, **Class 2 (Middle)**, and **Class 3 (Lowest, Most Atrophied)**. Hippocampal volume was corrected for head size using (hippocampal volume / intra cranial volume) x 10^3

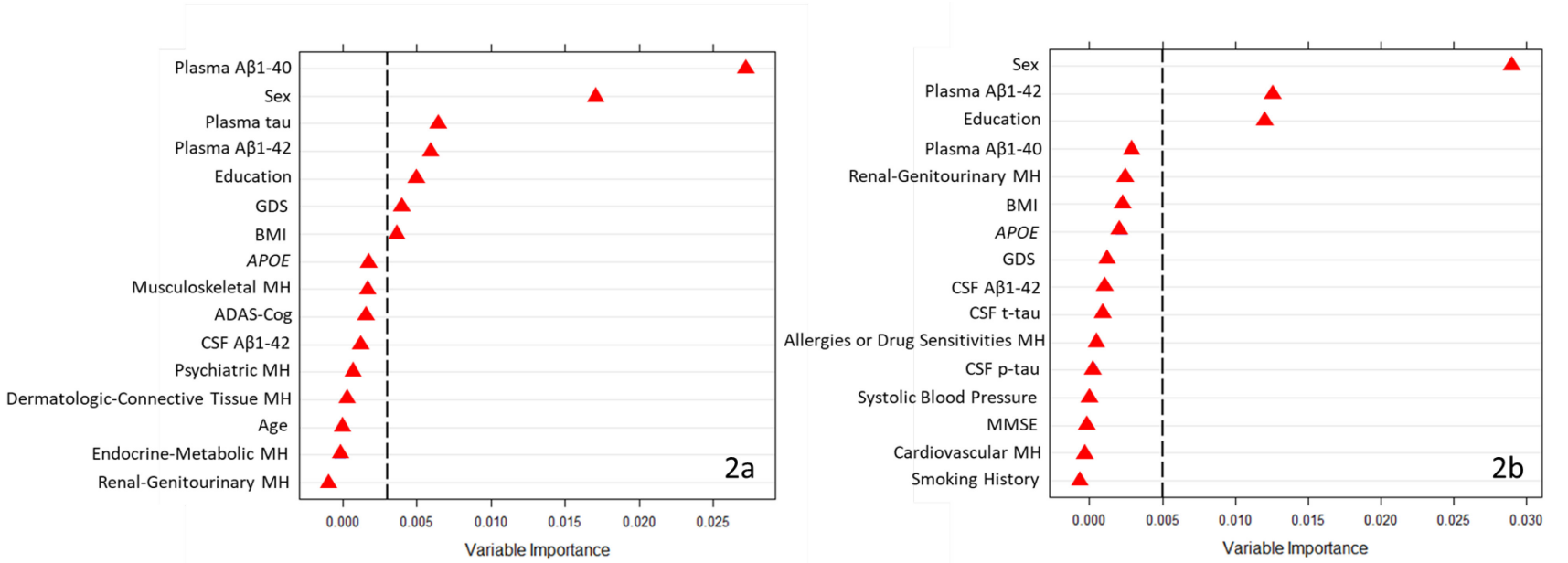

Figure 2-2. Variable importance (permutation accuracy) in the discrimination of the (2a) lowest (n = 78) vs. highest (n = 100) classes of left hippocampal volume trajectories (C = 0.80, *ntree* = 1000, *mtry* = 4), and (2b) lowest (n = 88) vs. highest (n = 96) classes of right hippocampal volume trajectories (C = 0.78, *ntree* = 1000, *mtry* = 4). *Note*. GDS, Geriatric Depression Scale score; BMI, body mass index; APOE, Apolipoprotein E genotype; MH, medical history; ADAS-Cog, Alzheimer's Disease Assessment Scale-Cognitive Subscale; CSF Aβ1-42, cerebrospinal fluid amyloid β-42; CSF t-tau, cerebrospinal fluid total tau; CSF p-tau, cerebrospinal fluid phosphorylated tau; MMSE, Mini-Mental State Examination score.

CHAPTER 3: STUDY 2

Cognitive Resilience, Cognitive Vulnerability, and Brain/Cognitive Stability in Older Adults with Varying Hippocampal Trajectory Patterns: Data-Driven Approaches to Detection and Prediction

Background

Defining Resilience, Vulnerability, and Stability in Brain/Cognitive Aging and Dementia.

Aging is characterized by vast and dynamic heterogeneity in individual brain and cognitive trajectories. In terms of interpretable change patterns, several general classes or types have been identified. These include (a) relatively higher and stable performance (i.e., sustained healthy or exceptional), (b) moderate levels with relatively shallow decline (i.e., typical or unimpaired) and (c) lower levels with steeper or accelerating decline (i.e., severely declining, at risk for impairment). Similarly, older adults also vary in the extent and magnitude of exposure to AD-related risk factors and adversities across the lifespan (but especially in midlife and later). Examples of such adversities can include established AD risk factors (e.g., smoking, Type 2 diabetes), neuropathology accumulation (e.g., Aβ accumulation), accelerated neurodegeneration (i.e., hippocampal atrophy), various lifestyle factors (e.g., diet) and increased genetic risk (e.g., presence of an *APOE* e4 allele). Resulting brain and cognitive aging trajectories as modified by incident and accumulated AD-related adversity have become a target of growing research attention. These heterogeneous pathways, each with varying levels of AD-related adversity and associated trajectory patterns include: cognitive resilience (i.e., stable/high cognitive trajectories despite high AD-related adversity), cognitive vulnerability (i.e., low/declining cognitive trajectories despite low AD-related adversity), and brain/cognitive stability (i.e., stable/high cognitive trajectories in conjunction with low AD-related adversity). Other schemes for representing these varying trajectory patterns cover similar phenomena with related methods, interpretations and terminology (K. J. Anstey & Dixon, 2021; Farrell, Kane, Bisset, Howlett, & Rutenberg, 2022; Montine et al., 2019; Stern et al., 2023). An important commonality among approaches to these change-related phenomena is the emphasis on

longitudinal data (e.g., Farrell et al., 2022).

Regarding resilience, increasing evidence has revealed that some aging adults in the face of pertinent adversities that exceed those of typical chronological aging—such as specific and objective elevated Alzheimer's disease (AD)-related neurodegeneration, neuropathology, or genetic risk—still exhibit sustained levels of cognitive function (Arenaza-Urquijo & Vemuri, 2018; R. Dixon & M. Lachman, 2019; Kaup et al., 2015; Latimer et al., 2017; McDermott et al., 2017; Melikyan et al., 2022; Montine et al., 2019; Ramanan et al., 2021). Characterized as 'cognitive resilience,' this phenomenon represents an opportunity for insight into pathways toward normal or even healthier brain and cognitive aging in the context of person-specific AD-related adversity. Evidence for cognitive resilience has emerged from studies whereby an important proportion of older adults with AD neuropathology *in vivo* or at autopsy did not exhibit cognitive decline in their lifetime (Arenaza-Urquijo & Vemuri, 2018; D. Hu et al., 2021; Melikyan et al., 2022; Selamawit Negash, A Bennett, S Wilson, A Schneider, & E Arnold, 2011; S. Negash, Xie, et al., 2013). Notably, findings from the Religious Orders Study indicate that over 75% of older adults without cognitive impairment had amyloid pathology at death (Bennett et al., 2012). Several other studies have also used observable criteria to define resilience, such as the presence of an *APOE* e4 risk allele (Ferrari et al., 2013; Kaup et al., 2015; McDermott et al., 2017; Zheng et al., 2023) and amyloid pathology (Ramanan et al., 2021; Rentz et al., 2017).. These studies have identified several predictors associated with the maintenance of cognitive function despite varying forms of AD-related adversities (e.g., genetic risk, neuropathology). Examples of observed predictors of cognitive resilience include full-scale intelligence quotient (higher), age (lower), favourable levels of physical activity (higher), and vascular health (better). Findings from these studies

point towards possible subsets of older adults with accumulated and varying levels of risk/protective exposures which allow for cognitive decline to be minimized, or forestalled in the face of different kinds of increased AD-related adversity (R. Dixon & M. Lachman, 2019).

Regarding vulnerability, this pathway represents the conceptual flipside to resilience, whereby aging individuals follow worse cognitive trajectories than would be expected based on (relatively low incidence or dosage of) observed (a) adversities such as accumulated AD risk or current neurodegeneration or (b) pertinent risk-reducing or protection factors. This subset of older adults exhibits unexpected moderate or severe declines in cognition without the apparent presence of prominent or assessed AD-related adversities, such as substantial hippocampal atrophy, increased neuropathology or genetic risk. Although such vulnerability is conceptually compelling, this potential pathway has rarely been directly targeted in brain and cognitive aging or dementia research. One reason may be that researchers rarely investigate or have access to all prominent (much less all possible) sources of accumulated adversity. It is possible that some older adults demonstrate objective evidence indicating the absence of specific AD-related adversities (i.e., the apparent presence of preserved brain health) yet still decline in cognitive performance. Alternatively, not all adversities may be associated with immediate, direct or severe detrimental cognitive effects, and not all aging individuals may accumulate sufficient or typical counterbalancing protection factors. Similarly, varying lifespan levels of exposures to, and accumulation of, different types and combinations of risk and protective factors may result in differing trajectories of cognitive change even in the context of less AD-related adversity. A methodological strategy that emphasizes the connection between the observed adversity (e.g., hippocampal atrophy) and the tested cognitive change function (e.g., episodic memory) may provide an opportunity for reliably

detecting and empirically testing this profile.

Regarding brain/cognitive stability, the phenomenon of stable brain and cognitive aging would be demonstrated by evidence reflecting a balancing of (a) low or absent specific adversities or vulnerabilities, (b) notable presence of risk-reduction or protection factors, and (c) observed long-term maintenance of relatively high levels and stable trajectories of cognitive performance into later life (R. Dixon & M. Lachman, 2019; Nyberg & Pudas, 2019). Specifically, this subset of older adults manages to both (a) maintain high levels of cognitive performance over extended years of aging and (b) experience minimal AD-related adversity, as assessed in the present categories of genetic risk (*APOE e4*), neurodegeneration (atrophy), or neuropathology (Nyberg & Pudas, 2019). In the case of brain/cognitive stability, favourable cognitive trajectories and absence of detected AD-related adversities are intrinsically linked, as there exists a strong association between brain health (e.g., very little neuropathology, preserved brain volume) and cognitive health (De Godoy et al., 2021; Gorbach et al., 2017; Pudas et al., 2013). For example, older adults with higher and stable hippocampal volume and function have been found to have higher performing memory (Gorbach et al., 2017; Lars Nyberg, Martin Lövdén, Katrine Riklund, Ulman Lindenberger, & Lars Bäckman, 2012; Pudas et al., 2013). In a previous study, a data-driven stable memory aging trajectory class was identified (G. P. McFall et al., 2019). Several precision factors (education, depressive symptoms, living status, body mass index, heart rate, social activity) were identified as predictors of stable memory aging. Accordingly, in the present study, we extend this approach by operationalizing brain/cognitive stability as the objective presence of a subgroup with relatively stable hippocampal volume combined with the observation of relatively higher and stable cognitive trajectories.

Risk and Protective Factors Associated with Resilience, Vulnerability, and Brain/Cognitive Stability

An important facet of emerging research has been the identification of risk and protective factors associated with differential trajectories of asymptomatic brain and cognitive aging, including patterns potentially representing the presently targeted phenomena of cognitive resilience, vulnerability and brain/cognitive stability (Aiello Bowles et al., 2019; R. Dixon & M. Lachman, 2019; S. M. Drouin et al., 2022; G. P. McFall et al., 2019). Specifically, risk and protective factors from multiple domains may contribute independently, interactively and differentially to affect pathways of cognitive and brain changes in the context of AD-related adversities (K. J. Anstey et al., 2021; R. Dixon & M. Lachman, 2019). Following the identification of patterns of cognitive resilience, vulnerability, and brain/cognitive stability, an important next goal is to determine the predictors that discriminate those who follow these patterns and those who do not. An important long-term consideration is which predictors are modifiable and which are non-modifiable, as preventative and intervention care can be appropriately targeted (Livingston et al., 2020).

In the case of cognitive resilience, both modifiable and non-modifiable risk factors have been identified in previous research. For example, occupational complexity has been found to predict cognitive resilience in people at neuropathological risk of AD (Boots et al., 2015). Physical and cognitive activities have also been previously linked to cognitive resilience (Casaletto et al., 2020). A recent study used a multi-modal dataset to identify predictors of cognitive resilience in older adults (Topiwala et al., 2019). Older adults were classified as resilient if they (a) were determined to have hippocampal atrophy according to a visual rating scale (Scheltens score > 0) and (b) scored up to 1.5 standard deviations below the

mean on all given cognitive tasks. Using logistic regression models, age, full-scale intelligence quotient, and social class were identified as predictors of cognitive resilience Moreover, Zheng and colleagues (2023) identified sex-specific predictors of resilience when defined by high and stable cognitive trajectories in the presence of an *APOE ε4* allele. Using logistic regression models, they found that resilience in male *APOE ε4* carriers was predicted by mild physical activity and employment at baseline, whereas only higher number of mental activities predicted resilience in female *APOE ε4* carriers (Zheng et al., 2023).

A form of cognitive vulnerability has been consistently reported in sex and gender research, whereby females have been found to exhibit more cognitive impairment than males for increasing AD-related pathology (L. L. Barnes et al., 2005; Mielke et al., 2014). Estrogen deficiency in post-menopausal women has been hypothesized as a possible contributing factor to the female vulnerability to AD pathology on cognition. Similarly, it is possible that other (at-risk) subsets of older adults who experience age-related cognitive decline despite having little AD pathology, neurodegeneration, or AD genetic risk. This may be due to specific independent or interactive risk factors which exacerbate existing cognitive declines even in the absence of AD-related adversity.

Specific risk and protective factors associated with long-term brain/cognitive stability have also been identified; however, relevant studies of this pattern have explored predictors of cognitive stability and brain stability separately and not simultaneously. Stable cognitive health longitudinally has been offered as a potential defining characteristic of "successful aging" (Nyberg & Pudas, 2019). Lin and colleagues (2017) identified a class of successful agers (i.e., high and stable cognitive trajectories over five years) which were predicted by female sex, lower AD genetic risk, and less AD-related neuropathology. Similarly, Josefsson and colleagues

(2012) found that successful memory aging (i.e., stability over 15 years) was predicted by higher education, female sex, higher levels of physical activity, the met allele of the catechol-O-methyltransferase gene, and cohabitation. Other modifiable lifestyle factors (e.g., leisure activities, occupational complexity) have been also found to be associated with stable cognitive and memory aging in other studies (L. Nyberg, M. Lövdén, K. Riklund, U. Lindenberger, & L. Bäckman, 2012). Stability in brain health has also been found to be associated with modifiable lifestyle factors, such as spatial navigation training (Lövdén et al., 2012). Female sex, lower education, and higher plasma $A\beta_{1-42}$ also predicted high and stable left and right hippocampal trajectories in a sample of cognitively unimpaired older adults (S. M. Drouin et al., 2022).

Methodological Issues: Design and Analytic Approaches to Risk and Protective Factor Research on Resilience, Vulnerability and Stability

Research investigating risk factors and predictors of cognitive resilience, cognitive vulnerability, and brain/cognitive stability presents two important methodological challenges. First, in order to explore factors associated with increased (or reduced) risk of these aging pathways, specific research attributes are required (but not always readily available) within large long-term studies on aging. These include longitudinal data with aging adults differing in both adversity (risk) exposure and cognitive trajectory patterns (Farrell et al., 2022). Specifically, the inclusion of multiple risk factors and biomarkers as predictors to represent potential mechanisms of healthier (resilience, stable) and adverse (vulnerability) brain and cognitive pathways (R. Dixon & M. Lachman, 2019; McDermott et al., 2017) is paramount and can be a major challenge to investigate. Second, the broader literature in this research area includes varying conceptual and operational definitions of the phenomena addressed in this dissertation. The present approach integrates longitudinal designs, objective and AD-related adversities, and subsequent

patterns of brain and cognitive aging pathways. Although related, other definitions of (and approaches to) cognitive resilience, vulnerability, and brain/cognitive stability have been proffered (Aiello Bowles et al., 2019; Arenaza-Urquijo & Vemuri, 2018; Bocancea et al., 2021; R. Dixon & M. Lachman, 2019; S. Negash, Wilson, et al., 2013; Nyberg & Pudas, 2019).

For the first methodological challenge, the inclusion of large multi-modal rosters of risk factors and biomarkers has become increasingly possible with available databases and new and emerging analytic approaches. Recently, data-driven and machine learning approaches have been deployed to adequately test large numbers of predictors simultaneously and overcome some of the challenges that accompany conventional statistical approaches. Notably, as compared with conventional statistical approaches in related literature, machine learning approaches allow for more flexible prediction analyses, such as the ability to include predictors with non-linear associations with the outcome of interest as well as accounting for potential higher-order interactions between predictors (Breiman, 2001; Jacobucci & Grimm, 2020). Most importantly in the context of risk factor research, such approaches can include a large number of predictor variables that can be considered in a computationally competitive context. As risk factors are often present in multiple numbers with varying degrees of interaction, data-driven approaches capable of managing these types of data have been encouraged and recently used in this research sector (Badhwar et al., 2020a; R. Dixon & M. Lachman, 2019). Examples of applications of these include the prediction of memory trajectories (G. P. McFall et al., 2019), hippocampal volume trajectories (S. M. Drouin et al., 2022), as well as MCI and AD prediction (Tanveer et al., 2020). A specific example includes a recent study by McDermott and colleagues (2017) where the authors used a data-driven approach to identify memory trajectory patterns displaying resilience to AD genetic risk. Subsequently, machine learning prediction analyses were used to

identify predictors of memory resilience in genetically at-risk older adults. Of the 22 multi-modal risk factors tested, 13 (nine unique) and five (one unique) were predictive for women and men respectively (McDermott et al., 2017). Kaup and colleagues (2015) also used random forest analyses to test predictors of cognitive resilience in *APOE* ε4 carriers stratified by race. Predictors for white *APOE* ε4 carriers included no recent negative life events, higher age, and more reading time predictors. Predictors for black *APOE* ε4 carriers included female sex and no type II diabetes. Higher literacy level and higher education were found to be common predictors (Kaup et al., 2015).

Similarly, data-driven and machine learning approaches have also been used to investigate a large number of predictors of healthy and stable memory aging simultaneously. For example, a recent study identified a group of stable memory aging adults using data-driven analyses (G. P. McFall et al., 2019). Education, depressive symptoms, living status, body mass index, heart rate, and social activity were identified as predictors of stable memory aging via a machine learning approach (G. P. McFall et al., 2019). As these data-driven and machine learning approaches allow for large numbers of predictors (needed to represent the dynamic and complex phenomenon of brain and cognitive aging), the current study deploys these types of analyses on a large multi-modal prediction roster for all three research goals.

For the second methodological challenge, we note that operational definitions of resilience that focus on cognitive maintenance in the documented context of specifically identified cognitive health-related adversities (e.g., amyloid pathology, AD genetic risk) are not universal. Indeed, some approaches and studies define resilience more generally as older adults remaining unimpaired or performing cognitively normal levels with advancing age as the principal (and only noted) ‘adversity’. For example, the common absence of cognitive

impairment in older adults aged 90+ has been previously used to operationalize resilience (Nienke Legdeur et al., 2018). A recent review provides a broad definition of resilience as "a general term that subsumes any concept that relates to the capacity of the brain to maintain cognition and function with aging and disease" (Stern et al., 2023, p.101). present perspective acknowledges that aging per se is a generic and universal adversity in that it is typically accompanied by brain and cognitive decrements. However, the present perspective aims to refine this generic perspective with a longitudinal approach and a more mechanistic operation that focuses on a specific and theoretically important adversities that are present in some but not all aging adults (Dixon & Lachman, 2019). In the context of aging adults, the presence (or absence) of an AD-related adversity is key to the present conceptualizations of cognitive resilience, vulnerability, and brain/cognitive stability (Aiello Bowles et al., 2019; R. Dixon & M. Lachman, 2019). For example, some of these operational approaches of cognitive resilience have included: (a) measuring the discordance between global cognition and global pathology (S. Negash, Wilson, et al., 2013), (b) high cognitive performance within two years of death despite high or intermediate neuropathology at autopsy (Aiello Bowles et al., 2019) and, (c) high cognitive trajectories despite AD genetic risk or other AD-related adversity (Kaup et al., 2015; McDermott et al., 2017). In the current study, we operationalize these trajectories based on stable or declining (adverse) hippocampal trajectories and cognitive trajectory patterns.

The Dissertation Study

In this study, we adapted an established approach consistent with the conceptual and methodological considerations detailed above (Kaup et al., 2015; McDermott et al., 2017). Specifically, among aging adults, cognitive resilience was operationally defined as relatively high and sustained cognitive (memory and executive function) trajectories despite objective

evidence of an AD-related adversity known to affect cognitive performance and change. Similarly, cognitive vulnerability was operationally defined as relatively low and declining cognitive trajectories despite little objective evidence of an AD-related adversity often associated with such decline patterns. Finally, brain/cognitive stability was operationally defined as relatively high and sustained cognitive trajectories in addition to no observed and objective evidence of an AD-related adversity.

Whereas some alternative approaches have based operational definitions on other AD-related adversities (i.e., genetic risk), in this study we used objective evidence of substantial hippocampal atrophy as the pivotal adversity. Although hippocampal atrophy occurs in normal brain aging, higher levels of atrophy and accelerated rates of volume loss have been established as important neurodegeneration biomarkers of incident Mild Cognitive Impairment (MCI) or AD. In addition, hippocampal atrophy is strongly associated with memory decline. Associations between hippocampal atrophy and executive function have also been previously reported (Milne et al., 2018; O'Shea et al., 2016). We used longitudinal imaging (MRI) and cognitive (memory, executive function) data in order to identify groups of older adults who are cognitively resilient (i.e., hippocampal atrophy with stable/high cognitive trajectories), cognitively vulnerable (i.e., stable hippocampal trajectories but low/declining cognitive trajectories), and brain/cognitive stable (i.e., stable hippocampal trajectories and stable/high cognitive trajectories).

Prior to the main research goals, we performed two pre-analytical foundational goals. The first was to identify statistically distinct classes of hippocampal volume trajectories. To accomplish this, we identified data-driven trajectory classes of left and right hippocampal volume (based on an algorithm of intercept and slope) in a large AD Neuroimaging Initiative

(ADNI) sample (n = 415) of older adults with up to six waves of MRI data. The second was to identify statistically distinct classes of cognitive trajectories. To accomplish this, the same sample was used to identify data-driven trajectory classes of two cognitive variables (episodic memory and executive function). With membership to both hippocampal and cognitive trajectory classes established, each individual in the sample was assigned to a group (i.e., resilient, vulnerable, stable) based on both of their respective hippocampal and cognitive memberships for the subsequent three main research goals. These groups, which are defined below, represent aging pathways, each potentially differentially affected and moderated by specific risk and protective factors.

For the first research goal, we focused on the cognitive resilience group (i.e., low and declining hippocampal trajectories combined with high and stable cognitive trajectories) as compared to the non-resilient group (i.e., low and declining hippocampal trajectories combined with low and declining cognitive trajectories). We used random forest classifier analyses to identify the leading predictors of cognitive resilience from a large roster of available multi-modal factors. For the second research goal, we focused on the cognitive vulnerable group (i.e., high and stable hippocampal trajectories combined with low and declining cognitive trajectories) as compared to the non-vulnerable (stable) group (i.e., high and stable hippocampal trajectories combined with high and stable cognitive trajectories). We used random forest analyses to identify the leading predictors of cognitive vulnerability from a large roster of available multi-modal factors. For the third research goal, we focused on the brain/cognitive stable group (i.e., high and stable hippocampal trajectories in conjunction with high and stable cognitive trajectories) as compared to the non-stable group (i.e., low and declining hippocampal trajectories in conjunction with low and declining cognitive trajectories). We used random forest

analyses to identify the leading predictors of brain/cognitive stability from a large roster of available multi-modal factors.

For all three research goals we used the same multi-modal roster of biomarkers and risk factors in order to allow for comparisons of predictors and prediction performance across these alternative pathways. Specific predictors of each of these alternative aging pathways may provide key insights into mechanisms behind resilient, stable, and vulnerable trajectories of cognitive and brain aging.

Methods

Data Source: Alzheimer's Disease Neuroimaging Initiative

Data used in preparation of this article were obtained and downloaded from the ADNI database (adni.loni.usc.edu on June 30 2020). The ADNI was launched in 2003 as a public-private partnership, led by Principal Investigator Michael W. Weiner, MD. The primary goal of ADNI has been to test whether serial magnetic resonance imaging (MRI), positron emission tomography (PET), other biological markers, and clinical and neuropsychological assessment can be combined to measure the progression of mild cognitive impairment (MCI) and early AD. For up-to-date information, see www.adni-info.org.

Participants

The initial source sample consisted of 415 initially cognitively normal participants (*M* age at baseline = 74.9, *SD* = 5.7, baseline range = 56.3-90.0 years, MMSE *M* = 29.1; ADAS-Cog *M* = 9.3, 49.9% Female) with at least one and up to six MRI scans processed by the Mayo clinic. The sample consisted of predominantly cognitively normal participants, with 88% of participants (*n* = 365) remaining so throughout the six waves. Of those who did not, 9.4% transitioned at least once to MCI (*n* = 39) and 2.7% transitioned at least once to AD (*n* = 11). See Table 1 for

full participant characteristics. Informed written consent was provided by all participants and IRB approval was obtained by our centers to conduct these analyses.

Measures: Magnetic Resonance Imaging (MRI)

MRI data were provided by the ADNI neuroimaging team with full details about the image processing found on adni.loni.usc.edu. Briefly, cortical reconstruction and volumetric segmentation was performed with the FreeSurfer image analysis suite, which is documented and freely available for download online (http://surfer.nmr.mgh.harvard.edu/). The FreeSurfer 6.0 longitudinal pipeline (Reuter et al., 2012) was used to process the sequential scans with procedure details extensively discussed elsewhere (A. Dale et al., 1999; A. M. Dale & Sereno, 1993; Fischl & Dale, 2000; Fischl et al., 2001; Fischl et al., 2002; Fischl, Salat, et al., 2004; Fischl, Sereno, & Dale, 1999; Fischl, Sereno, Tootell, et al., 1999; Fischl, van der Kouwe, et al., 2004; Xiao Han et al., 2006; Jovicich et al., 2006; Segonne et al., 2004). Quality control was conducted by the ADNI neuroimaging team and each brain segmentation was visually inspected through at least 20 evenly distributed coronal sections. In total, 17 images (0.6%) were removed due to failed segmentations.

For the current study, we used hippocampus (left and right) volume Z-scores derived from the MRI data for each participant by NOMIS (https://github.com/medicslab/NOMIS). NOMIS is a new open MRI tool designed to assess morphometric deviation from established norms in adults (Potvin et al., 2021). The left and right hippocampal volume z-scores were controlled for scanner vendor, magnetic field strength, image quality, and intracranial volume.

Measures: Memory and Executive Function

We used two composite variables developed and validated within ADNI to represent important domains of cognition in our analyses. The first composite variable was an established

memory composite variable (ADNI-Memory) to measure memory for up to six waves (7.1 years). This composite variable includes multiple indicators derived from the Rey Auditory Learning Test, AD Assessment Schedule (Cognition), Mini-Mental State Examination and Logical Memory tasks (Crane et al., 2012). The second composite variable was an established executive function composite variable (ADNI-EF) to measure executive function for up to six waves (7.1 years). This composite variable included the following indicators: WAIS-R Digit Symbol Substitution, Digit Span Backwards, Trails A and B, Category Fluency, and Clock Drawing (Gibbons et al., 2012). The memory and executive function composite variables were used simultaneously to represent cognition in our pre-analytic foundational goal. The pre-analytic foundational goal procedures are explained in detail below.

Measures: Risk Factors and Biomarkers

We implemented machine learning classifier models for testing AD-related biomarker and risk factor importance for predicting cognitive resilience, cognitive vulnerability, and cognitive and brain stability. Specifically, we selected 42 putative predictors from eight modalities: biological (e.g., CSF t-tau; $n = 6$), demographic (e.g., sex; $n = 4$), genetic (e.g., *APOE*; $n = 2$), vascular and metabolic (e.g., pulse pressure; $n = 8$), lifestyle (e.g., smoking history; $n = 3$), comorbidities (e.g., cardiovascular disease; $n = 17$), and familial background (e.g., paternal dementia history; $n = 2$). A full table with included biomarkers and risk factors is presented at the end of this chapter (see Table 2). Missing biomarker data across most modalities were generally quite low for the entire sample (range = 0 to 3.9%) with the exception of the biological modality in which only a subset of participants provided data due to the ADNI biosample collection design (range = 33.7 to 54.2%). Missing biomarker and risk factor data were handled using a sophisticated imputation approach (*IterativeImputer,* Python 3.9;

www.python.org*)* which utilizes regularized linear regression to impute missing data. Variables with the least missing data were imputed first and followed by variables with successively more missing data.

Analyses

Pre-analytic Foundational Goals: Data-Driven Classes of HC Volume and Cognition

We used latent class growth analyses (LCGA) in Mplus 8.2 in order to identify statistically separable trajectory classes of (a) hippocampal volume (left and right) and (b) cognition (memory and executive function) (Muthén & Muthén, 2018; Ram & Grimm, 2009). The first foundational analysis investigated hippocampal volume. In this analysis, left and right hippocampal volume were included in the same LCGA model but with separate intercept and slope parameters. The second foundational analysis investigated cognition. In this analysis, memory and executive function were also included simultaneously in the same LCGA model with separate intercept and slope parameters. This allowed us to classify individuals into hippocampal volume groups based on the simultaneous consideration left and right hippocampus trajectories and into cognitive groups based on the simultaneous consideration of memory and executive function trajectories.

LCGA utilizes a data-driven algorithm of level and slope in order to identify distinct classes based on growth patterns while constraining the variances of these parameters within each class. As the ADNI longitudinal data are distributed intra-individually across chronological age, we used age as the metric of change in the LCGA. Therefore, age is included directly in the analyses and the model co-varies for increasing age. As is recommended in the mixture modelling literature, we first identified a one-class baseline growth model. We then tested models with additional classes until model non-identification or the emergence of a small

(<10%) class. For models with adequate class separation (entropy values greater than 0.8), final model selection was informed by intercept and slope parameter interpretation as well as lower values of the following recommended statistical fit indices: Akaike information criterion (AIC), Bayesian information criterion (BIC), and sample-size adjusted BIC (SABIC) (Masyn, 2013a). In the case of similar model selection criteria, more parsimonious models were preferred (Masyn, 2013a). As LCGA utilizes maximum likelihood estimation methods for missing data, all participants are included in these analyses as long as they contributed at least one wave of both MRI and cognitive data.

Research Goal 1, 2 and 3: Data-Driven Prediction of Cognitive Resilience, Cognitive Vulnerability, and Brain/Cognitive Stability in Aging

Using a multi-modal set of 42 biomarkers, we tested three separate research goals: the prediction of (a) cognitive resilience, (b) cognitive vulnerability, and (c) brain/cognitive stability. We used three machine learning (ML) classifier algorithms in Python (3.9; www.python.org) (Pedregosa et al., 2011). The purpose of including three alternative algorithms for each research goal was to compare their performance in each analysis and select the best performing algorithm for final reporting and interpretation within each goal (G. P. McFall, Bohn, L., Drouin, S.M., Gee, M., Han, W., Li, L., Camicioli, R., & Dixon, R.A., 2023; Tseng et al., 2020), We selected random forest (RF; *sklearn RandomForestClassifier*), gradient boosting (GB; *sklearn* G*radientBoostingClassifier*) and K-Nearest Neighbours (KNN; *sklearn KNeighborsClassifier*). RF classification is an ensemble machine learning algorithm which combines multiple decision trees independently to classify an output (Géron, 2022; Pedregosa et al., 2011). For the RF algorithm, the predicted output is determined based on the aggregation of all the trees via majority voting. GB classification is also an ensemble machine learning algorithm which

combines multiple decision trees sequentially to classify an output. For the GB algorithm, the predicted output is determined by the sum of all trees which are individually weighted. KNN is a non-parametric machine learning algorithm which classifies outputs based on a distance metric (i.e., Euclidean distance). For the KNN algorithm, the classification of the output is based on the majority class of its K nearest neighbor as determined by the Euclidean distance (Géron, 2022; Pedregosa et al., 2011). All three machine learning algorithms account for possible interactions and allow for the inclusion of large number ($p > n$) of mixed-type predictors which is typically discouraged in conventional parametric statistical analyses (i.e., logistic regression) (Hapfelmeier & Ulm, 2013; Pedregosa et al., 2011).

For each research goal, we used stratified five-fold cross-validation to evaluate both internal and external validation. Cross-validation is recommended in the case of single or smaller samples unsuited for the creation of separate adequately large training and testing sets (Hastie et al., 2009). In five-fold cross validation, each pairwise dataset was subdivided into five folds, with four of the five folds used for training (internal validation) and the remaining fold used for testing (external validation). This process was repeated until all five folds have been used once for testing.

For each research goal, we built all three ML algorithms and estimated missing data within a *sklearn pipeline* simultaneously. This procedure allowed for all missing data to be imputed within each cross-validation fold and it avoided potential data leakage issues. The pipelines consisted of the following steps conducted at each fold: (a) missing data imputation (using *IterativeImputer*, a multivariate imputation approach) and (b) ML classification with three models (RF, GB, KNN). In addition, for each training fold, several combinations of possible hyperparameters were tested (via *sklearn GridSearchCV*) in order to identify the best

hyperparameters for each of the ML algorithms. For the RF and GB algorithms, the tested set of hyperparameters were 'n_estimators [100, 500, 750, 1000],' 'max_depth [3, 5, 10, 15, None],' and 'max_features [srqt, log2, None].' For the KNN algorithm, these were 'n_neighbors [3, 5, 7, 9],' 'weights [uniform, distance],' and 'algorithm [ball_tree, kd_tree, brute].' The average evaluation metrics (across cross-validation folds) for the RF, GB, and KNN algorithms were compared. Then, the ML algorithm with the best performing evaluation metrics on average was selected as the final model and was re-fit with the best identified hyperparameters.

We used the following evaluation indices (averaged across the cross-validation folds) to select the best performing ML algorithm: (a) area under the *ROC* curve (*AUC*), (b) accuracy (i.e., % correct classification), (c) precision (i.e., % of correct positive classifications), (d) recall (i.e., % of those in the positive class who are correctly predicted), and (e) F_1 score, a harmonic mean of precision and recall recommended for imbalanced samples. AUC values can be interpreted as follows: values between 0.6-0.7 are considered to have mild distinguishing power, values between 0.7-0.8 are considered to have moderate distinguishing power, and values over 0.8 are considered to have strong/excellent distinguishing power (Duan et al., 2020; Mandrekar, 2010). Ranging from 0-1, higher values of accuracy, precision, recall and F_1 indicate better classification.

For further interpretative purposes, we determined variable importance for each research goal using the final fitted ML models. We used Tree Shapley Additive exPlanation (SHAP) values (Lundberg, Erion, & Lee, 2018) to identify the leading predictors of cognitive resilience, cognitive vulnerability, and brain and cognitive stability. Originating from cooperative game theory, Tree SHAP values take into account both main effects and interaction effects (coalitions of all predictors) to estimate relative variable importance in the context of all other variables

included in the tree-based model. As such, each possible combination of variables is used to estimate the importance of individual variables (Lundberg et al., 2018).

In this study, we provide two established Tree SHAP plots: (a) SHAP waterfall plots and (b) SHAP summary plots. First, SHAP waterfall plots display the average absolute SHAP values as well as the composition (individual contribution) and cumulative (total contribution) ratio for each predictor on the model output. The SHAP waterfall plots were used to compare the leading predictors that explained (based on the cumulative ratio) a significant portion of the ML model. We begin by reporting the leading predictors corresponding to four cumulative ratio benchmarks: 40%, 50%, 60% and 70%. Second, SHAP summary plots provide information on predictor magnitude, prevalence and direction. Predictors are shown in descending order of importance. Each individual's SHAP value is plotted across the x-axis for each predictor. Positive SHAP values predict membership to the positive class (e.g., cognitive resilience, cognitive vulnerability, brain/cognitive stability) whereas negative SHAP values predict membership to the alternative (opposite) group. The absolute value of Tree SHAP values relates to the magnitude of the predictor effect, such that a higher absolute value (further to the right of the plot) indicates a stronger predictor effect. The colour of the dots display the value of the predictor (low = blue, high = red). We subsequently discuss and interpret the leading six predictors for each research goal using these SHAP summary plots. In sum, Tree SHAP values provide meaningful information on the (a) direction, (b) magnitude, and (c) prevalence of prediction effects for each predictor variable and are reported here for interpretative purposes.

Results

Pre-analytic Foundational Goals: Data-Driven Classes of HC Volume and Cognition

HC Volume Trajectory Classes. We tested the 2-, 3- and 4-class LCGA models of HC volume trajectories. In these 2-, 3- and 4-class models, left and right hippocampus volume were included within the same LCGA but were specified to load onto separate intercept and slope parameters. All three tested models had acceptable entropy (>0.8) and were considered candidate models (see Table 3 for detailed fit indices for all models). The 2-class model demonstrated excellent precision of classification with an entropy value of 0.93 and represented the inflection point of the AIC and BIC values across all tested models. The final 2-class solution parameter estimates for the intercept and slope values of LHC and RHC can be found in Table 4. Figure 1a displays the six-wave individualized trajectory plots for all HC measurements class. The highest class (n = 236) was characterized by a larger proportion of older adults with higher levels and relatively sustained hippocampal volume across time. The lowest class (n = 179) was characterized by a minority group of overall lower (more atrophied) hippocampal volume trajectories.

Memory and Executive Function Trajectory Classes. We tested 2-, 3- and 4-class LCGA models of memory and executive function trajectories. For the 2-, 3- and 4-class models, memory and executive function were specified to load onto separate intercept and slope parameters within the same LCGA. All three tested models had acceptable entropy (>0.8) and were considered candidate models (see Table 3 for detailed fit indices for all models). Similar to the HC trajectory models, the 2-class model demonstrated excellent precision of classification with an entropy value of 0.88 and represented the inflection point of the AIC and BIC values across all tested models. The final 2-class solution parameter estimates for memory and

executive function intercepts and slopes can be found in Table 5. Figure 1b displays the six-wave individualized trajectory plots for the memory and executive function composite variables by class. The highest class (n = 164) was characterized by a smaller proportion of older adults with higher levels and relatively sustained memory and executive function trajectories across time. The lowest class (n = 251) was characterized by a majority group of overall lower memory and executive function trajectories.

The integrated results of these two pre-analytic foundational analyses provided the bases for classifying individuals as members of one of four groups (see Table 6). Of the 179 participants classified as having AD-related adversity based on being in the lowest hippocampal trajectory class, 107 were also classified as in the lowest cognitive trajectory class (i.e., low/declining trajectories) and 72 were classified as being in the highest cognitive trajectory class (i.e., cognitive resilience). Of the 236 participants classified as having very little AD-related adversity based on being in the highest hippocampal trajectory class, 144 were also classified as in the lowest cognitive trajectory class (i.e., cognitive vulnerability) and 92 were classified as being in the highest cognitive trajectory class (i.e., brain and cognitive stability). The lowest/declining trajectory class was used as the prediction benchmark group for Research Goal 1 and 3. The resilient trajectory class was used as the prediction benchmark group for Research Goal 2.

Research Goal 1, 2 and 3: Data-Driven Prediction of Cognitive Resilience, Cognitive Vulnerability, and Stable Brain/Cognitive Aging

In a series of three pairwise comparisons, we used ML algorithms within a *sklearn* pipeline to identify important biomarkers which differentiate three pathways of brain and cognitive aging (i.e., cognitive resilience, cognitive vulnerability, and brain and cognitive

stability). For each research goal, we report the best fitting algorithm (RF, GB, KNN) and the best selected hyperparameters. We then report the leading predictors corresponding to four cumulative ratio benchmarks: 40%, 50%, 60%, and 70% (Table 7, 8, and 9). For comparison purposes, we center our discussion and interpretation on the leading six predictors for each analysis.

Research Goal 1: Predictors of Cognitive Resilience (vs. Low/Declining Trajectories). Three ML classification algorithms were tested to predict membership to the cognitive resilience group (vs. low/declining). These were RF (accuracy = 0.62, precision = 0.55, recall = 0.32, AUC = 0.63, F1 = 0.39), GB (accuracy = 0.62, precision = 0.53, recall = 0.38, AUC = 0.67, F1 = 0.44), and KNN (accuracy = 0.56 precision = 0.43, recall = 0.39, AUC = 0.53, F1 = 0.41). We identified GB ('max_depth': 5, 'max_features': 'log2', 'n_estimators': 100) as the best performing algorithm for the prediction of cognitive resilience (Table 10). Based on the SHAP waterfall plot (Figure 2), four predictors explained 40% of the ML model, six predictors explained 50% of the ML model, nine predictors explained 60% of the ML model, and 12 predictors explained 70% of the ML model. The leading predictors for each of these cumulative ratio benchmarks are shown in Table 7. The leading six predictors overall which discriminated cognitive resilience from low/declining trajectories originated from two domains of risk (i.e., biological and demographic). In order of importance, these predictors were: higher CSF Aβ1-42, higher education, lower plasma Aβ1-42, lower CSF p-tau, lower plasma Aβ1-40, and lower age (Figure 3).

Research Goal 2: Predictors of Cognitive Vulnerability (vs. Resilient Trajectories). Three ML classification algorithms were tested to predict membership to the cognitive vulnerability group (vs. cognitive resilience). These were RF (accuracy = 0.65, precision = 0.68, recall = 0.87, AUC = 0.70, F1 = 0.77), GB (accuracy = 0.61, precision = 0.67, recall = 0.80, AUC = 0.62, F1 =

0.73), and KNN (accuracy = 0.61, precision = 0.67, recall = 0.82, AUC = 0.53, F1 = 0.73). We identified RF ('max_depth': 5, 'max_features': 'None', 'n_estimators': 750) as the best performing algorithm for the prediction of cognitive resilience fairly (Table 10). Based on the SHAP waterfall plot (Figure 4), two predictors explained 40% of the ML model, three predictors explained 50% of the ML model, four predictors explained 60% of the ML model, and six predictors explained 70% of the ML model. The leading predictors for each of these cumulative ratio benchmarks are shown in Table 8. The leading six predictors overall which discriminated cognitive vulnerability from stable/sustained trajectories originated from four domains of risk (i.e., demographic, biological, vascular/metabolic, lifestyle). In order of importance, these predictors were: lower education, higher plasma Aβ1-40, higher BMI, higher age, lower glucose, higher plasma Aβ1-42 (Figure 5).

Research Goal 3: Predictors of Stable/Sustained Trajectories (vs. Low/Declining Trajectories). Three ML classification algorithms were tested to predict membership to the brain and cognitive stability group (vs. low/declining). These were RF (accuracy = 0.60, precision = 0.58, recall = 0.51, AUC = 0.64, F1 = 0.54), GB (accuracy = 0.58, precision = 0.54, recall = 0.23, AUC = 0.66, F1 = 0.32), and KNN (accuracy = 0.51, precision = 0.48, recall = 0.45, AUC = 0.56, F1 = 0.46). We identified RF ('max_depth': 'None', 'max_features': 'log2', 'n_estimators': 100) as the best performing algorithm for the prediction of cognitive resilience fairly (Table 10). Based on the SHAP waterfall plot (Figure 6), six predictors explained 40% of the ML model, eight predictors explained 50% of the ML model, 11 predictors explained 60% of the ML model, and 15 predictors explained 70% of the ML model. The leading predictors for each of these cumulative ratio benchmarks are shown in Table 9. The leading six predictors overall which discriminated stable/sustained trajectories from low/declining trajectories

originated from four domains of risk (i.e., genetic, biological, demographic, vascular/metabolic). In order of importance, these predictors were: higher CSF Aβ1-42, lower polygenic risk score, female sex, higher plasma Aβ1-42, higher pulse pressure, and lower age (Figure 7).

Discussion

We used a sequence of data-driven approaches in order to identify and predict three objectively observed brain and cognitive aging pathways: cognitive resilience, cognitive vulnerability, and brain and cognitive stability. We first used a data-driven approach based on the combination of intercept and slope to identify separable classes of hippocampal (left and right) volume and cognitive (memory and executive function) trajectories. Within one longitudinal sample of cognitively unimpaired aging adults, we identified and then selectively linked two coordinated sets of statistically separable trajectory classes: hippocampal volume (left, right) trajectories and cognitive (memory, executive function) trajectories. Based on each individual's combination of class memberships for hippocampal trajectories (high/low) and cognitive trajectories (high/low), we classified them into one of four groups: (a) cognitively resilient, (b) cognitively vulnerable, (c) brain and cognitively stable, and (d) low/declining. We expected and focused on the first three of these alternative pathways, with the latter serving as the benchmark group in two analyses. Subsequently, we applied three ML algorithms (RF, GB, KNN) and SHAP value explanation to identify and characterize the leading predictors of each of the three aging pathways. The identification of leading predictors of differential brain and cognitive aging pathways further our understanding of contributing factors to and potential mechanisms of different facets of both (a) declining (e.g., vulnerability) and (b) desirable/healthier (e.g., resilience, stability) aging trajectories. In this section, we discuss the leading risk factors and biomarkers which predicted cognitive resilience, cognitive vulnerability and brain and cognitive

stability. We first report the leading predictors which explained 40, 50, 60 and 70% of the ML model. Second, we interpret and focus on the top six predictors for each research goal and the associated amount of the model explained. Third, we discuss shared predictors across the prediction models (Figure 11).

For the first research goal, four predictors (CSF Aβ1-42, education, plasma Aβ1-42, CSF p-tau) explained 40% of the ML model. Six predictors (plasma Aβ1-40, age) explained 50% of the model. Nine predictors (*APOE*, BMI, smoking) explained 60% of the model. Twelve predictors (polygenic hazard score, medical history of allergies/drug sensitivities, cardiovascular medical history) explained 70% of the model. The leading six predictors of cognitive resilience to declining HC trajectory adversity explained 50% of the ML prediction model. These were: higher CSF Aβ1-42, higher education, lower plasma Aβ1-42, lower CSF p-tau, lower plasma Aβ1-40, and younger age were identified as leading predictors of cognitive resilience (vs. low/declining). We identified higher levels of CSF Aβ1-42 as the leading predictor of cognitive resilience. Previously, levels of CSF Aβ1-42 have been found to be inversely related to amyloid burden in the brain. Lower levels have been identified as key biomarkers of incipient AD or cognitive impairment in other neurodegenerative diseases (Hampel & Blennow, 2022; Jack Jr et al., 2018; Siderowf et al., 2010). Our results are indicative that older adults with less intensive doses of this prominent AD-related neuropathological burden (higher CSF levels) are more likely to exhibit cognitive resilience to adverse HC trajectories. Specifically, we note that in higher levels of CSF Aβ1-42, older adults with hippocampal atrophy may be less likely to exhibit cognitive impairment and decline. This suggests that resilience to declining cognitive trajectories in cognitively normal older adults is closely related to specific (amyloid) neuropathological burden rather than broad hippocampal neurodegeneration. Notably, older adults who may be considered to be at a higher risk of a

preclinical (higher amyloid burden) phase of disease are less likely to exhibit resilience to hippocampal atrophy.

Education (more years of schooling) was the second leading predictor of cognitive resilience. Education has been consistently associated with cognitive resilience in previous studies and related ADRD literature (Alipour & Goldust, 2016; Josefsson et al., 2012; Kaup et al., 2015; Stern, 2012). This association has been mainly explained via cognitive reserve, whereby older adults with higher educational attainment have gathered more cognitive reserve over their lifespan and are therefore more equipped to tolerate AD-related pathology and neurodegeneration with advancing age (K. J. Anstey, 2014; K. J. Anstey & Dixon, 2021; Kaarin J. Anstey, Ranmalee Eramudugolla, Diane E. Hosking, Nicola T. Lautenschlager, & Roger A. Dixon, 2015; Montine et al., 2019; Rogalski et al., 2020; Stern, 2012; Stern et al., 2023). Our current findings are in line with this interpretation; as in this sample of cognitively unimpaired aging adults, higher education was associated with belonging to a higher cognitive trajectory class in the context of hippocampal atrophy (i.e., resilience).

We identified lower levels of plasma Aβ1-42 as the third leading predictor of cognitive resilience. Associations between plasma measures of Aβ1-42 and cognitive impairment, neurodegeneration, and dementia risk have been inconsistent, leading to some contradictory interpretations (Alcolea et al., 2021; Chouraki et al., 2015; Lambert et al., 2009; van Oijen, Hofman, Soares, Koudstaal, & Breteler, 2006). These contradictory results have been noted to be likely due to the low concentration of proteins in plasma which requires extremely sensitive measurement approaches for detection and quantification (Alcolea et al., 2021). Some studies have found plasma Aβ1-42 to be associated with risk of AD and cognitive impairment in cognitively normal older adults (Lee et al., 2023). Specifically, higher levels of plasma Aβ1-42 has been found

to be associated with more cognitive decline or preclinical AD (MCI) in older adults (Lee et al., 2023; Mamo et al., 2008). In contrast, other studies have found that lower levels of plasma Aβ1-42 were associated with greater risk of converting to AD in MCI (Hanon et al., 2022) or greater hippocampal atrophy (Hilal et al., 2018). In our study, lower levels of plasma Aβ1-42 were predictive of cognitive resilience in cognitively normal older adults, providing additional evidence that lower levels of plasma Aβ1-42 may indicate protection from AD-related neurodegeneration

Of the six leading predictors, higher levels of CSF p-tau was the fourth leading predictor of cognitive resilience. Increased levels of CSF p-tau are an established AD biomarker and has been found to sensitively distinguish between normal aging adults, MCI, and AD (Hampel & Blennow, 2022). Increased levels of CSF p-tau have also been found to predict conversion from MCI to AD (Hampel & Blennow, 2022) and predict cognitive impairment in Parkinson's disease (X. Hu, Yang, & Gong, 2017). In the current study, we found that lower levels of CSF p-tau were associated with cognitive resilience. This is concurrent with previous findings in which higher levels of CSF p-tau were negatively associated with cognitive resilience defined as a longitudinal residual of cortical thickness and cognitive performance (Svenningsson, Ossenkoppele, Stomrud, Palmqvist, & Hansson, 2021). Our current results provide further evidence that levels of CSF p-tau are associated with cognitive resilience in the face of AD-related brain atrophy. However, we note that despite the CSF p-tau mean value being relatively normal for a cognitively normal sample (M = 30.5 pg/ml), the range (6.9-156 pg/ml) was somewhat unusual compared to other published ADNI studies (Duits et al., 2021; Toledo, Xie, Trojanowski, & Shaw, 2013).

Lower levels of plasma Aβ1-40 were the fifth leading predictor of cognitive resilience. Similarly to plasma Aβ1-42, associations between levels of plasma Aβ1-40 and risk of AD or cognitive impairment have been mixed (Alcolea et al., 2021; Chouraki et al., 2015; Lopez et al.,

2019; van Oijen et al., 2006). However, many studies have consistently identified positive associations between levels of plasma Aβ1-40 and risk of AD (van Oijen et al., 2006; Yang, Huang, Hsieh, & Huang, 2020). For example, plasma Aβ1-40 levels have been noted to be increased in those at risk of AD (i.e., familial history) and in those with more advanced dementia (as compared to mild dementia) (van Oijen et al., 2006; Yang et al., 2020). We found that plasma levels of Aβ1-40 were strongly associated with cognitive trajectory class; in that they indicate maintained higher cognitive levels over 7.1 years despite hippocampal atrophy.

The sixth leading predictor of cognitive resilience identified in this research goal was younger age. Older chronological age has been consistently reported as a reliable risk factor for pathological outcomes (e.g., impairment, cognitive decline, neurodegenerative disease) in brain and cognitive aging. Specifically, age is still considered the strongest risk factor for AD and is among the "triad" of AD risk factors (along sex and *APOE* genetic risk) (Clifford R Jack et al., 2015). Our results indicate that younger age is also predictive of cognitive resilience, and thus is related to maintenance of higher cognitive trajectories even in the face of objective AD-related adversity.

For the second research goal, we examined an under-explored (and relatively undesirable) aging trajectory pattern which is characterized here by low and declining cognitive trajectories in the context of intact hippocampal trajectories (little to no adversity due to this common potential source). Although not previously examined, our foundational analyses detected a substantial membership in a group meeting these empirical criteria. It is possible that this subset of older adults are experiencing objective declining trajectories due to other unexplained adversities, such as an accumulation of risk factors for non-AD-related cognitive impairment or preclinical phases of other neurodegenerative diseases characterized by exacerbated atrophy in other brain regions (e.g.,

frontotemporal dementia, lewy body dementia). Two predictors (education, plasma Aβ1-40) explained 40% of the ML model. Three predictors (BMI) explained 50% of the model. Four predictors (age) explained 60% of the model. Six predictors (glucose level, plasma Aβ1-42) explained 70% of the model. The leading six predictors of cognitive vulnerability explained 70% of the ML prediction model. These were: lower education, higher plasma Aβ1-40, higher BMI, older age, lower glucose, and higher plasma Aβ1-42 were identified as leading predictors of cognitive vulnerability (vs. cognitive resilience). The leading predictor was lower education. As higher education was also a predictor of cognitive resilience (i.e., the conceptual flipside and more desirable outcome to cognitive vulnerability), our finding that less education predicts cognitive decline even in those without hippocampal atrophy suggests that education has an important role in modifying risk for cognitive impairment and decline irrespective of AD-related brain atrophy.

Higher levels of plasma Aβ1-40 was the second leading predictor of cognitive vulnerability. This result is consistent with our findings in our first research goal, whereby lower levels of plasma Aβ1-40 predicted cognitive resilience. Higher levels of plasma Aβ1-40 have been previously associated with increased risk of AD and with severe cases of dementia (van Oijen et al., 2006; Yang et al., 2020). We extend these findings and show that plasma Aβ1-40 levels are associated with membership to a group of cognitively normal older adults characterized by low and declining cognitive trajectories but high and stable hippocampal trajectories. This may highlight a subgroup of individuals with higher levels of Aβ1-40 experiencing objective cognitive impairment due to other unmeasured adversities. For example, CSF levels of Aβ1-40 have been associated with risk of non-AD neurodegenerative diseases (e.g., frontotemporal dementia, cerebral amyloid angiopathy, multiple sclerosis) (Lehmann et al., 2020). Our results suggest that

these associations may also be true for plasma concentrations of Aβ1-40 and should be tested in clinical populations.

We identified higher BMI as the third leading predictor of cognitive vulnerability. Although obesity has been identified as a mid-life risk factor for dementia, associations in later life have been less clear (Livingston et al., 2020; Bohn et al., 2020; Michaud et al., 2018). Looking specifically at older adults aged 76 and over, one study found that higher BMI at baseline to be associated with more rapid cognitive decline (Michaud et al., 2018). Other studies have found opposite associations, with lower BMI being associated with higher risk of AD and dementia - likely due to the rapid weight loss that can occur in preclinical phases of AD (Nguyen, Killcross, & Jenkins, 2014). Notably, higher BMI in general has been consistently linked with other comorbid vascular and metabolic syndromes which put older adults at risk for cognitive decline (Alosco et al., 2017; Bischof & Park, 2015; Nash & Fillit, 2006).This indicates that the relationship between BMI and cognition which may be unrelated to typical AD-mechanistic cognitive decline (e.g., hippocampal atrophy) and related to unexamined adversities (e.g., increased vascular pathology).

Older age was the fourth leading predictor of cognitive vulnerability. Notably, we identified younger age as a leading predictor of cognitive resilience in our first research goal. As such, chronological age appears to predict opposing dynamics of brain and cognitive aging pathways: resilience and vulnerability. Specifically, older chronological age may predict cognitively vulnerability as it is likely associated with other aging risk factors which may increase risk of non-clinical cognitive decline. his result is concordant with previous findings suggesting that risk of negative or undesirable brain and cognitive aging outcomes (e.g., vulnerability, AD)

increases with age (Riedel, Thompson, & Brinton, 2016; Sliwinski, Hofer, Hall, Buschke, & Lipton, 2003).

We observed that lower glucose was the fifth leading predictor of cognitive vulnerability in the context of HC adversity. This could indicate that glucose levels affect brain health and cognitive health differently - in that lower levels predict stable hippocampal volumes but negatively affect cognitive function. The relationship between glucose levels and cognitive health has been reported as complex in related literatures. For example, higher fasting glucose and glycated hemoglobin have been associated with increased risk of AD, severe hypoglycemia (low blood glucose levels) has also been consistently associated with poorer cognitive outcomes (Feinkohl et al., 2014) (Wheeler et al., 2017). Our findings suggest that even non-severe and clinically normal lower glucose levels (M = 97.3 mg/dl for the cognitively vulnerable group) may be a risk factor for cognitive declining trajectories in a subgroup of older adults. Interestingly, a medical history of diabetes did not appear as a leading predictor in our analysis. This suggests that glycemic control – a key component of meeting the brain's energy demand – more precisely explains the relationship between metabolic health and cognitive and brain health (Wheeler et al., 2017).

We found that higher plasma Aβ1-42 was the sixth leading predictor of cognitive vulnerability. Notably, we identified a complementary result in our first research goal for the opposing dynamic to cognitive vulnerability (i.e., cognitive resilience), whereby lower levels of plasma Aβ1-42 were predictive of cognitive resilience. A previous cross-sectional study have found a positive association between plasma Aβ1-42 and hippocampal volume (Hilal et al., 2018). No studies have investigated plasma biomarkers of AD in the context of hippocampal volumes in conjunction with cognitive trajectories. Results from our first two research goals in parallel with

that of Hilal and colleagues (2018) suggest that higher circulating levels of Aβ1-42 may not only be indicative of more stable hippocampal trajectories, but also of simultaneous declining cognitive trajectories. This subset of older adults may thus be at-risk for further cognitive decline due to other risk factors or adversities that were unstudied in the present research (e.g., *APOE* genetic risk).

For the third research goal, six predictors (CSF Aβ1-42, polygenic hazard score, sex, plasma Aβ1-42, pulse pressure, age) explained 40% of the ML model. Eight predictors (BMI, diastolic blood pressure) explained 50% of the model. Eleven predictors (CSF p-tau, medical history of endocrine-metabolic disorders, pulse rate) explained 60% of the model. Fifteen predictors (geriatric depression scale score, CSF t-tau, systolic blood pressure) explained 70% of the model. The leading six predictors of brain and cognitive stability explained 70% of the ML prediction model. These were: higher CSF Aβ1-42, lower polygenic risk score, female sex, higher plasma Aβ1-42, higher pulse pressure, and younger age. As with cognitive resilience, higher levels of CSF Aβ1-42 (i.e., lower amounts of Aβ1-42 in the brain) were the leading predictor of brain and cognitive stability. We show that CSF Aβ1-42, a robust biomarker and neuropathological hallmark of AD, is associated with healthier and more desirable trajectories in aging (Hampel & Blennow, 2022; Jack Jr et al., 2018; Siderowf et al., 2010). As CSF Aβ1-42 also predicted cognitive resilience, our results highlight how older adults with less AD-related amyloid burden are more likely to either (a) maintain their brain and cognitive health, or alternatively (b) maintain their cognitive health despite declining brain health.

The second leading predictor of brain and cognitive stability was a lower polygenic risk score. The ADNI polygenic risk score was computed using *APOE* and 31 other genetic variants whereby a lower score indicates lower cumulative incidence rate of AD (Desikan et al., 2017). In

our study, brain and cognitive stability was predicted by a lower AD polygenic risk score. Older adults at lower genetic risk for AD were thus predicted to exhibit maintained hippocampal and cognitive trajectories (as compared to low and declining), even in cognitively normal populations. This is in line with previous findings in which being at AD risk via polygenic risk score, but not *APOE* e4, predicted worse cognitive trajectories in cognitively unimpaired older adults (Kauppi, Rönnlund, Nordin Adolfsson, Pudas, & Adolfsson, 2020). Polygenic risk scores relating to AD risk have also been associated with cortical thickness in cognitively normal populations (Sabuncu et al., 2012). Our results extend these findings in that polygenic risk applies to the healthier 'flipside' to aging decline and impairment: brain and cognitive stability. This finding supports the idea that understanding pathways away from AD risk represent an important facet of AD risk reduction. In brief, healthier aging pathways such as stability likely have similar mechanisms, risk factors, and biomarkers (in opposing direction) to AD-related impairment and decline – including genetic risk.

We identified female sex as the third leading predictor of brain and cognitive stability. Female sex has been consistently associated with better cognitive performance in older age and greater stability over time in cognitively normal older adults (de Frias, Nilsson, & Herlitz, 2006; Josefsson et al., 2012; T Howrey, A Raji, M Masel, & Kristen Peek, 2015; Z. Wu, Phyo, Al-Harbi, Woods, & Ryan, 2020). For example, a main predictor of longitudinal successful (stable) memory aging has been found to be female sex (Josefsson et al., 2012). Similarly, females have been reported to exhibit less hippocampal atrophy than males (Fraser et al., 2021) and female sex has been previously found to be a predictor of higher (less atrophied) hippocampal trajectory classes (S. M. Drouin et al., 2022). In this study, we confirm a dual advantage in which cognitively normal

females appear to both maintain better brain and cognitive health (i.e., stable vs declining trajectories) as compared to cognitively normal males.

Our study also identified that higher levels of plasma Aβ1-42 were the fourth leading predictor of stable (and desirable) brain and cognitive trajectories in older age. Lower levels have also been associated with adverse outcomes such as increased risk of transitioning to MCI (Rembach et al., 2014) and accelerated progression of white matter hyperintensities (Kaffashian, 2014).. Only one study has specifically investigated associations between hippocampal volume and plasma Aβ1-42, whereby lower levels of plasma Aβ1-42 were found to be associated with reduced hippocampal volumes at baseline (Hilal et al., 2018). Our results extend this previous association to longitudinal hippocampal volumes in conjunction with cognitive trajectories. In addition, our findings in our two previous research goals provide complementary evidence for associations between plasma Aβ1-42 and brain and cognitive trajectories. We found that lower levels of Aβ1-42 were predictive of cognitive resilience our first research goal, while higher levels were predictive of cognitive vulnerability in our second research goal. Importantly, a shared facet of membership to the cognitive vulnerability and brain and cognitive stability groups is relatively stable and high hippocampal trajectories. As such, our findings in this context indicate that levels of plasma Aβ1-42 may be more closely associated with declining hippocampal trajectories than cognitive changes.

We identified higher pulse pressure as the fifth leading predictor of brain and cognitive stability. Interestingly, higher pulse pressure – indicative of worse vascular health -- has been associated with worse cognitive outcomes previously (McFall et al., 2015). One reported phenomena reported relating to this risk factor is the age dependency of risk effects. Other studies have reported an attenuation of risk factor effects – including hypertension and vascular health --

with increasing age, and a possible reversal of risk in the oldest-old (80+ years) (N Legdeur et al., 2018). The mean age for the brain and cognitively stable group was 75.5 years, suggesting that this hypothesized attenuation and reversal may also occur at earlier ages than previously reported.

Younger age was the sixth leading predictor of brain and cognitive stability. Younger age has been previously identified as an important predictor of cognitive stability and successful cognitive aging (M. S. Albert et al., 1995; Cosco et al., 2014; Daffner, 2010; Josefsson et al., 2012; G. P. McFall et al., 2019). Although not a mechanistic marker of aging trajectories, these results show that an easily measured and reliably collected variable in large-scale longitudinal studies is predictive of objectively determined brain and cognitive aging trajectories.

Notably, several predictors were commonly identified across two or all of the prediction analyses—with generally complementary and mechanistically appropriate prediction directions. Plasma Aβ1-42 was a common predictor of all three aging pathways: cognitive resilience (lower), cognitive vulnerability (higher), and brain and cognitive stability (higher). Plasma Aβ1-40 was a common predictor of cognitive resilience (lower) and cognitive vulnerability (higher). Reflecting circulating levels of Aβ associated with amyloid deposition in the brain, these plasma markers may be especially useful markers of aging trajectories differentially associated with AD risk (or protection). Age was a common predictor of all three aging pathways: cognitive resilience (younger), cognitive vulnerability (older), and brain and cognitive stability (younger). Higher CSF Aβ1-42 was a common predictor of cognitive resilience and brain and cognitive stability. Education was a common predictor of both cognitive resilience (higher) and cognitive vulnerability (lower).

Strengths and Limitations

There were several limitations to the current study. First, we acknowledge the use of convenience sampling in ADNI (e.g., individuals with family history) which may lead to recruitment biases and limited generalizability of our findings (Whitwell, Wiste, et al., 2012). However, at-risk individuals are considered important targets of therapeutic and preventative protocols. In the current study, we have identified several biomarker and risk factor associations in older adults who represent an important target of prevention efforts as they represent potential higher risk (cognitive vulnerability) or lower risk (cognitive resilience, brain/cognitive stability) for exacerbated cognitive decline and other non-normative aging trajectories. Second, we included several predictor variables from the biospecimen modality which had considerable missing data (ranging from 33.7-50.4%). However, we used a sophisticated imputation approach in order to allow for the inclusion of these important AD-related biomarkers as predictors despite higher amounts of missing data. Specifically, missing data were imputed using the *IterativeImputer* package in Python (sklearn). This package deploys a multivariate imputer which utilizes Bayesian Ridge to predict missing values sequentially from most to least missing based on all included predictors. Missing data imputation was conducted within a cross-validation pipeline in order to avoid potential data leakage. Third, the performance of the ML algorithms for our three research goals ranged between mild to moderate in distinguishing power (AUC = 0.64 – 0.70). However, the leading predictors identified for each model were consistent with previous literature and could be interpreted in the expected direction for a cognitively normal sample. As such, our prediction models provided strong evidence for reliable biomarker and risk factor associations with all three aging pathways despite mild to moderate distinguishing power. It is likely that the predictor roster available within AD, which are highly relevant to the

prediction of AD and clinical status, may be less applicable to a cognitively normal sample when predicting alternative trajectories in older adults. Notably, some predictors that have previously appeared in resilience, vulnerability and stability literature that were unavailable within ADNI include: living status, social activity, novel cognitive activities, literacy level, negative life events, reading time, and grip strength. We anticipate that model performance would be strengthened by the inclusion of some of these predictors. Accordingly, future studies investigating cognitive resilience, cognitive vulnerability, and brain and cognitive stability should include a broader range of predictors from multiple risk modalities. Fourth, we report and interpret the leading predictors for the best ML algorithm for each research goal, but not those for the alternative (unselected) ML algorithms. We chose to report only the leading predictors for each best fitting ML algorithm as these represent the best suited algorithm with the strongest evaluation metrics. In addition, we note that previous reports using SHAP values to interpret ML prediction analyses have also followed a similar approach (Alabdullah et al., 2022; Ullah, Liu, Yamamoto, Zahid, & Jamal, 2023).

There were also several strengths to the current study. First, we used a data-driven approach to detect subgroups of older adults with varying hippocampal and cognitive trajectories. As such, individuals were classified into trajectory groups (cognitively resilient, cognitively vulnerable, low/declining, brain and cognitive stability) in an unbiased manner based on the simultaneous consideration of an objective presence or absence of an AD-related adversity (i.e., declining hippocampal trajectories) and their cognitive trajectory group membership. Second, we utilized a large roster of predictors originating from several AD-related areas of risk. Our data-driven approach allowed for a computationally competitive consideration of all predictors to identify the leading and most important for each prediction model. Third, we

tested three established ML algorithms (RF, GB, KNN) simultaneously within a *sklearn* pipeline with hyperparameter tuning to optimize our prediction model. This allowed for the selection of the best performing ML algorithm for each research goal. Our findings suggest that among these datasets, GB (RG1) and RF (RG2 and RG3) emerged as the best performing ML algorithms.

Conclusion

In this study, we identified several key predictors of cognitive resilience, cognitive vulnerability, and brain and cognitive stability in a computationally competitive context. The identification of these predictors is key to elucidating the complex and dynamic trajectories of brain and cognitive aging. Pathways towards (and away from) resilient, vulnerable, and stable aging trajectories represent an important facet of emerging research on healthier cognitive aging. Importantly, many of these predictors are modifiable and targetable (e.g., education, BMI, glucose, pulse pressure) and could help (a) encourage stable brain and cognitive trajectories despite potential AD-related risk factors and adversity and (b) prevent declining and vulnerable cognitive trajectories in the face of stable brain aging. Similarly, several predictors (amyloid level, genetic risk, age, sex) are important risk identification and stratification variables that can be used in both research and applied prevention contexts.

Tables

Table 3-1. Full sample baseline characteristics (*n* = 415)

Characteristics	Full Sample
N	415
n in ADNI-1	229
n in ADNI-2	186
Sex (% Female)	49.9
Age *M* (*SD)*	74.9 (5.7)
Education *M* (*SD*)	16.3 (2.7)
Mini Mental State Exam *M* (*SD*)	29.1 (1.1)
ADAS-Cog *M* (*SD*)	9.3 (4.1)

Table 3-2. Biomarkers and AD-related risk factors by modality

Modalities	Biomarkers	Metric
Biological	Plasma Aβ1-40	pg/mL
	Plasma Aβ1-42	pg/mL
	CSF Aβ1-42	pg/mL
	CSF total-tau	pg/mL
	CSF p-tau	pg/mL
	Plasma tau	pg/mL
Demographic	Age	Years
	Sex	Female/Male
	Race	White, black, Asian, Hispanic/Latino (dummy coded)
	Marital status	Partnered, not partnered
Genetic	*APOE*	ε2+, ε3/ε3, ε4+
	Polygenic hazard score	Vector product of 31 single nucleotide polymorphisms
Vascular/Metabolic	Systolic blood pressure	mm Hg
	Diastolic blood pressure	mm Hg
	Hypertension	140/90 mm Hg
	Subjective report of diabetes	Yes / no
	Glucose level at baseline	mg/dL
	Heart rate	Beats per minute
	Respiratory rate	Breaths per minute
Lifestyle	Body mass index	kg/m^2
	Education	Years
	History of smoking	Yes / no
Co-morbidities	Geriatric depression scale score	Mild (5-8), moderate (9-11), severe (12-15)
	Cardiovascular, alcoholism, psychiatric, neurological, head/eyes/ears/nose/throat, respiratory, hepatic, dermatologic connective tissue, musculoskeletal, endocrine-metabolic, gastrointestinal, hematopoietic-lymphatic, renal-genitourinary, allergies/drug sensitivities, malignancy, and/or major surgeries	Yes / no
Familial Background	Maternal dementia history	Yes / no
	Paternal dementia history	Yes / no

Table 3-3. Fit indices for HC volume and memory/executive function LCGA

	Number of Classes	AIC	BIC	SABIC	Entropy
HC Volume	1	12874.31	12938.77	12887.99	-
	2	10033.13	10117.72	10051.08	0.93
	3	8534.52	8639.25	8556.75	0.94
	4	7645.79	7770.66	7672.29	0.97
Cognition	1	7257.77	7322.23	7271.46	-
	2	6164.98	6249.57	6182.94	0.88
	3	5878.76	5983.50	5900.99	0.84
	4	5578.98	5703.86	5605.49	0.84

Table 3-4. Intercept and slope parameter estimates for the 2-class HC volume LCGA

HC Volume	**Intercept**	**Slope**
Highest Class	LHC: -0.56	LHC: -0.11
	RHC: -0.60	RHC: -0.11
Lowest Class	LHC: -2.27	LHC: -0.11
	RHC: -2.29	RHC: -0.12

Table 3-5. Intercept and slope parameter estimates for the 2-class Memory and Executive Function LCGA

Memory and Executive Function	**Intercept**	**Slope**
Highest Class	Memory: 1.55	Memory: -0.03
	Executive Function: 1.41	Executive Function: -0.05
Lowest Class	Memory: 0.78	Memory: -0.03
	Executive Function: 0.56	Executive Function: -0.05

Table 3-6. HC/cognitive classes and RFA groupings

	Lowest HC Trajectory Class (n = 179)	Highest HC Trajectory Class (n = 236)
Lowest Cognitive Trajectory Class (n = 251)	**Low/Declining Trajectories** (n = 107)	**Cognitive Vulnerability** (n = 144)
Highest Cognitive Trajectory Class (n = 164)	**Cognitive Resilience** (n = 72)	**Stable/Sustained Trajectories** (n = 92)

Table 3-7. Leading predictors of cognitive resilience identified by cumulative ratio criteria

	40%	50%	60%	70%
CSF Aβ1-42	✓	✓	✓	✓
Education	✓	✓	✓	✓
Plasma Aβ1-42	✓	✓	✓	✓
CSF p-tau	✓	✓	✓	✓
Plasma Aβ1-40		✓	✓	✓
Age		✓	✓	✓
APOE			✓	✓
BMI			✓	✓
Smoking			✓	✓
Polygenic Hazard Score				✓
Allergies/Drug Sensitivities Medical History				✓
Cardiovascular Medical History				✓

Table 3-8. Leading predictors of cognitive vulnerability identified by cumulative ratio criteria

	40%	50%	60%	70%
Education	✓	✓	✓	✓
Plasma Aβ1-40	✓	✓	✓	✓
BMI		✓	✓	✓
Age			✓	✓
Glucose Level				✓
Plasma Aβ1-42				✓

Table 3-9. Leading predictors of brain and cognitive stability identified by cumulative ratio criteria

	40%	50%	60%	70%
CSF Aβ1-42	✓	✓	✓	✓
Polygenic Hazard Score	✓	✓	✓	✓
Sex	✓	✓	✓	✓
Plasma Aβ1-42	✓	✓	✓	✓
Pulse Pressure	✓	✓	✓	✓
Age	✓	✓	✓	✓
BMI		✓	✓	✓
Diastolic Blood Pressure		✓	✓	✓
CSF p-tau			✓	✓
Endocrine-Metabolic Medical History			✓	✓
Pulse Rate			✓	✓
Plasma Aβ1-40				✓
Geriatric Depression Scale Score				✓
CSF t-tau				✓
Systolic Blood Pressure				✓

Table 3-10. Machine learning classification prediction model evaluation metrics for RG1, RG2 and RG3

		Accuracy	Precision	Recall	F1 Score	ROC AUC
RG1: Cognitive Resilience Prediction	Random Forest	0.62	0.55	0.32	0.39	0.63
	Gradient Boosting Classifier	**0.62**	**0.54**	**0.39**	**0.44**	**0.68**
	K-Nearest Neighbour	0.56	0.43	0.39	0.41	0.53
RG2: Cognitive Vulnerability Prediction	**Random Forest**	**0.65**	**0.69**	**0.87**	**0.77**	**0.70**
	Gradient Boosting Classifier	0.61	0.67	0.80	0.73	0.62
	K-Nearest Neighbour	0.61	0.67	0.82	0.73	0.53
RG3: Brain and Cognitive Stability Prediction	**Random Forest**	**0.61**	**0.59**	**0.51**	**0.54**	**0.64**
	Gradient Boosting Classifier	0.58	0.54	0.23	0.32	0.66
	K-Nearest Neighbour	0.51	0.48	0.45	0.46	0.56

Figures

Figure 3-1. HC (left and right) and cognitive (memory and executive function) trajectory plots

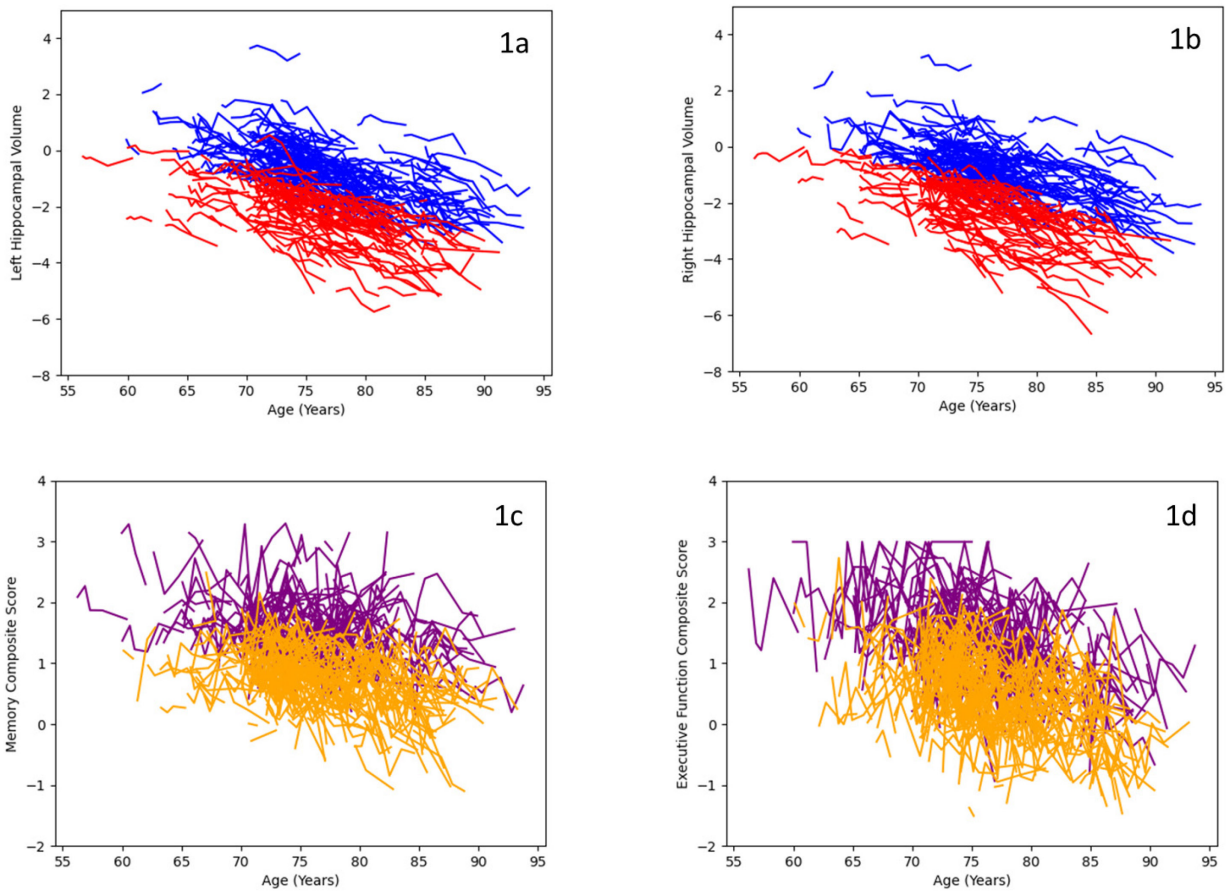

Figure 3-2. Waterfall plot for predicting cognitive resilience (RG1)

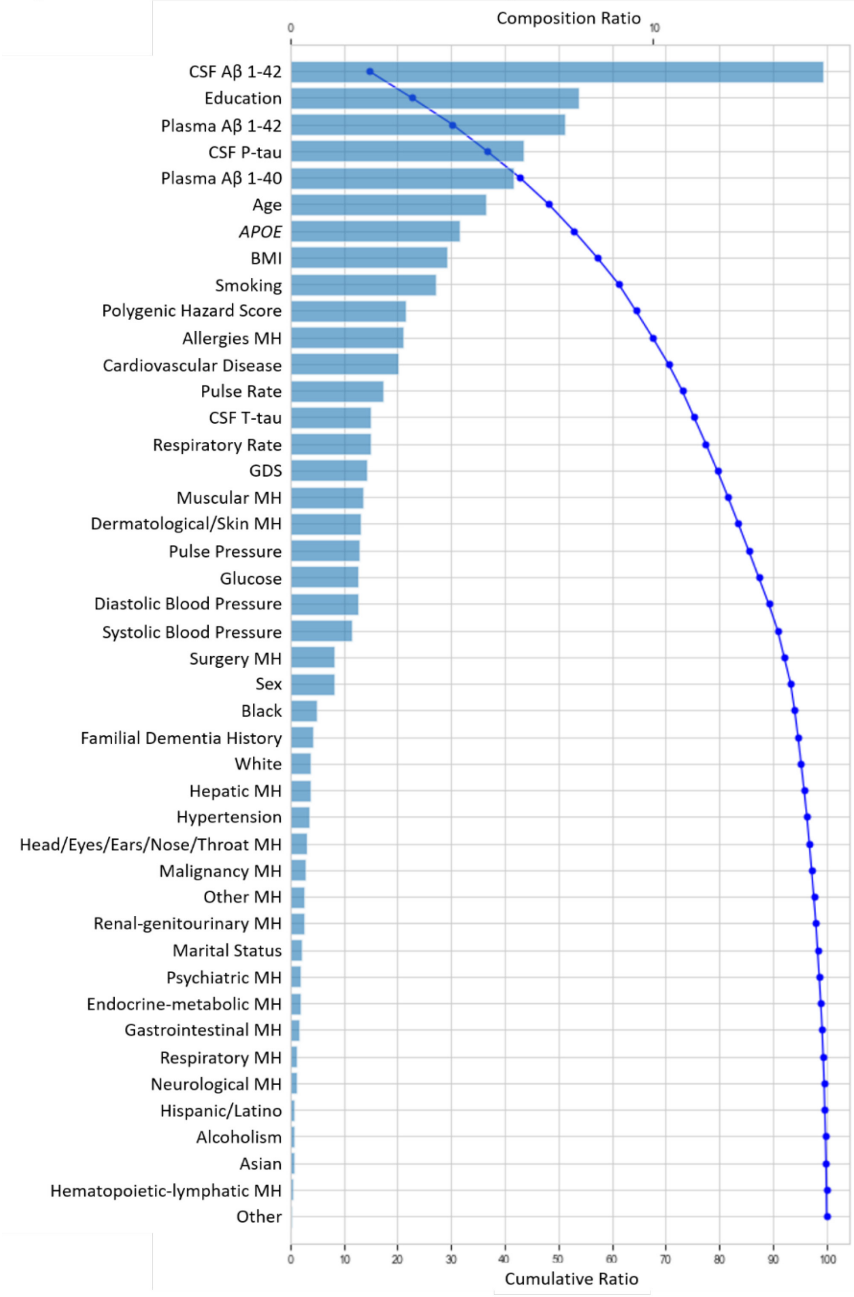

Figure 3-2. Tree SHAP Waterfall Plot showing the composition (top x-axis) and cumulative (bottom x-axis) ratios for the baseline predictors tested in the ML model. Predictors are shown in descending order of importance and their individual composition ratio (individual contribution to the model prediction) is indicated by the blue bars. The blue curved line indicates the cumulative ratio for each additional predictor.

Figure 3-3. SHAP summary plot for predicting cognitive resilience (RG1)

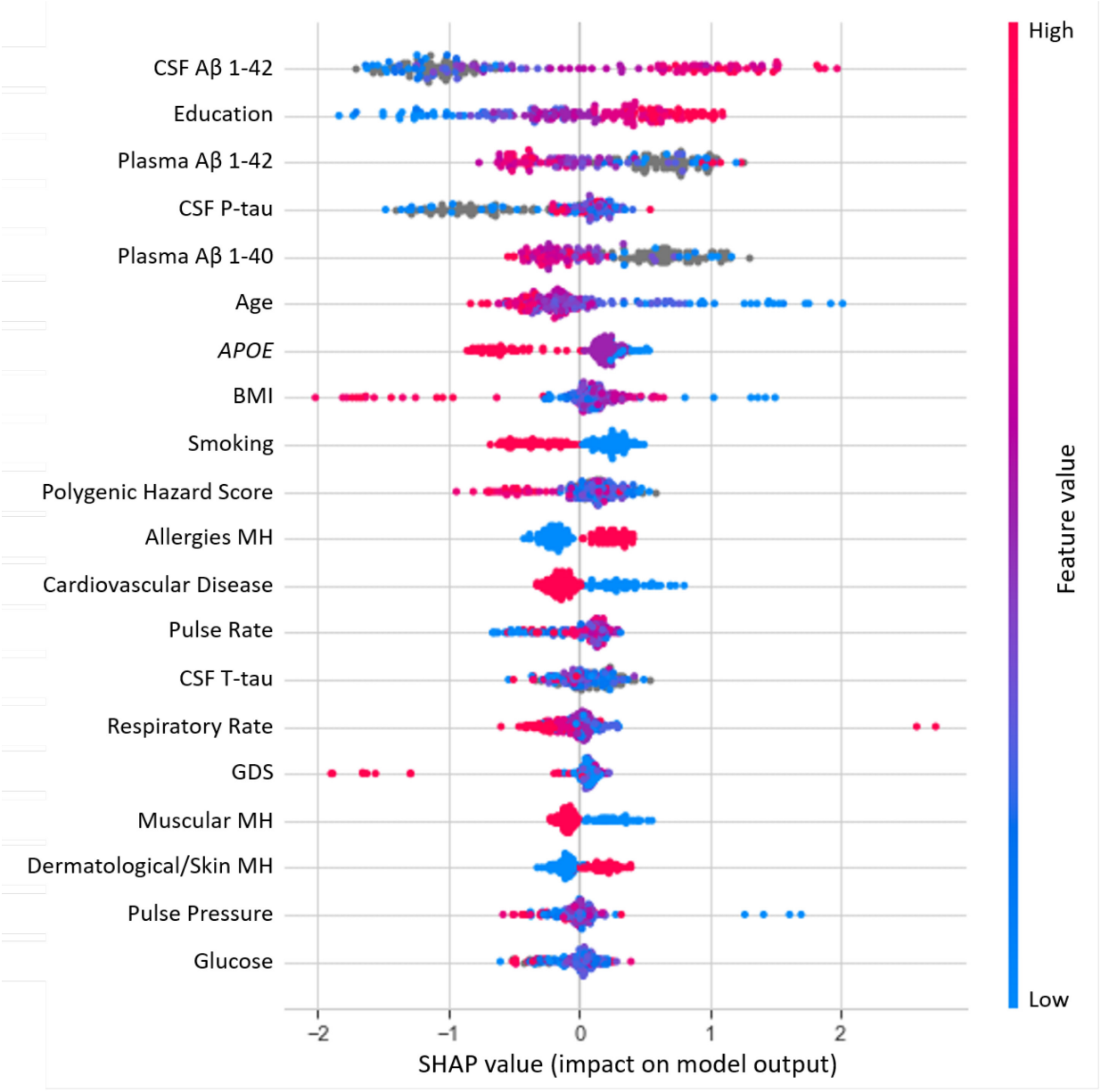

Figure 3-3. Tree SHAP Summary Plot showing the twenty most important predictors of cognitive resilience. Predictors are shown in descending order of importance. Each individual point on the plot represents a participant's Tree SHAP value for that predictor (bottom x-axis for scale). The position of the points indicates the effect on the model prediction. Specifically, Tree SHAP values over 0 (to the right of the figure) predict cognitive resilience. The colour of the dots indicates the direction of the effect for each predictor shown (red = higher values, blue = lower values, grey = imputed values).

Figure 3-4. Waterfall plot for predicting cognitive vulnerability (RG2)

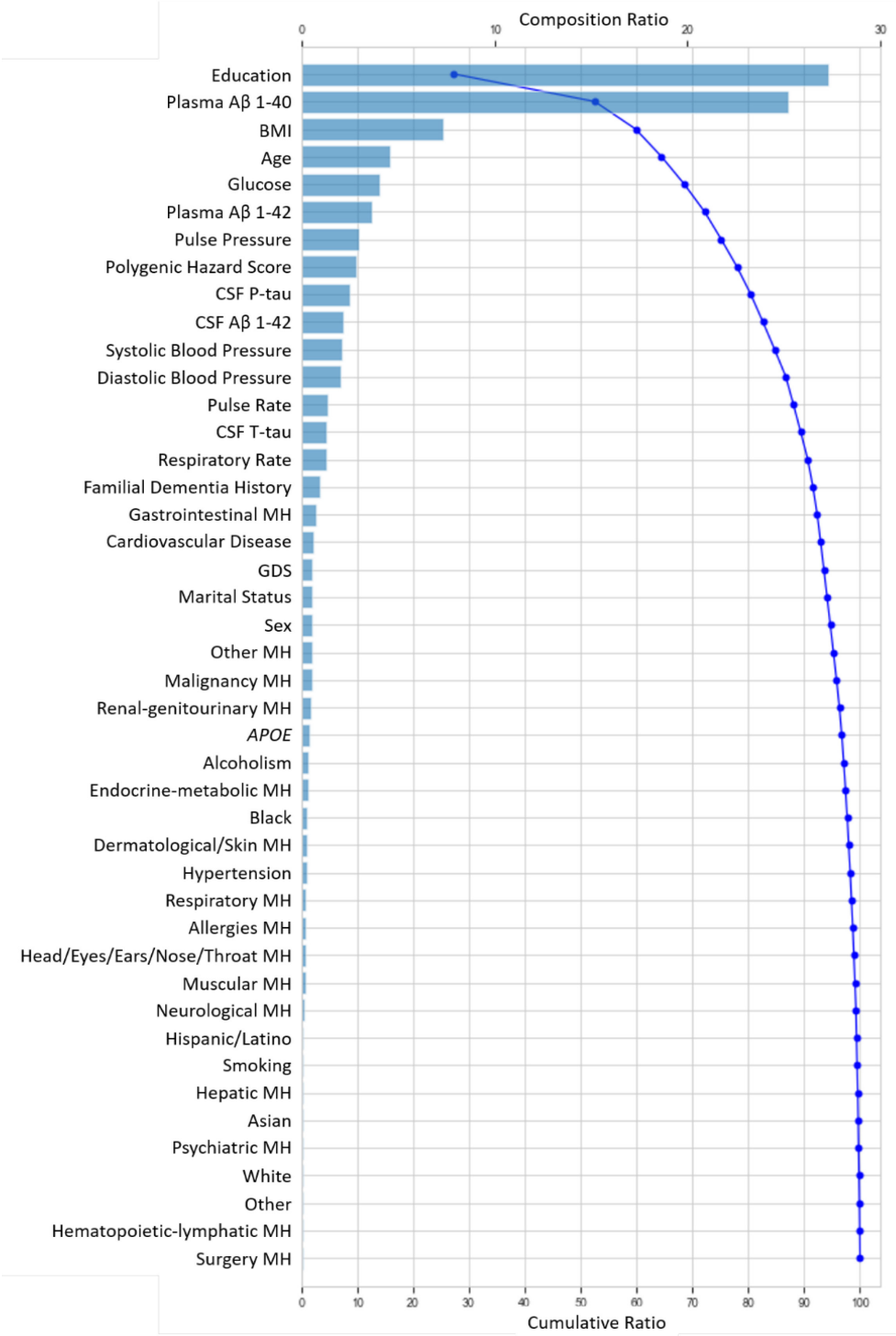

Figure 3-4. Tree SHAP Waterfall Plot showing the composition (top x-axis) and cumulative (bottom x-axis) ratios for the baseline predictors tested in the ML model. Predictors are shown in descending order of importance and their individual composition ratio (individual contribution to the model prediction) is indicated by the blue bars. The blue curved line indicates the cumulative ratio for each additional predictor.

Figure 3-5. SHAP summary plot for predicting cognitive vulnerability (RG2).

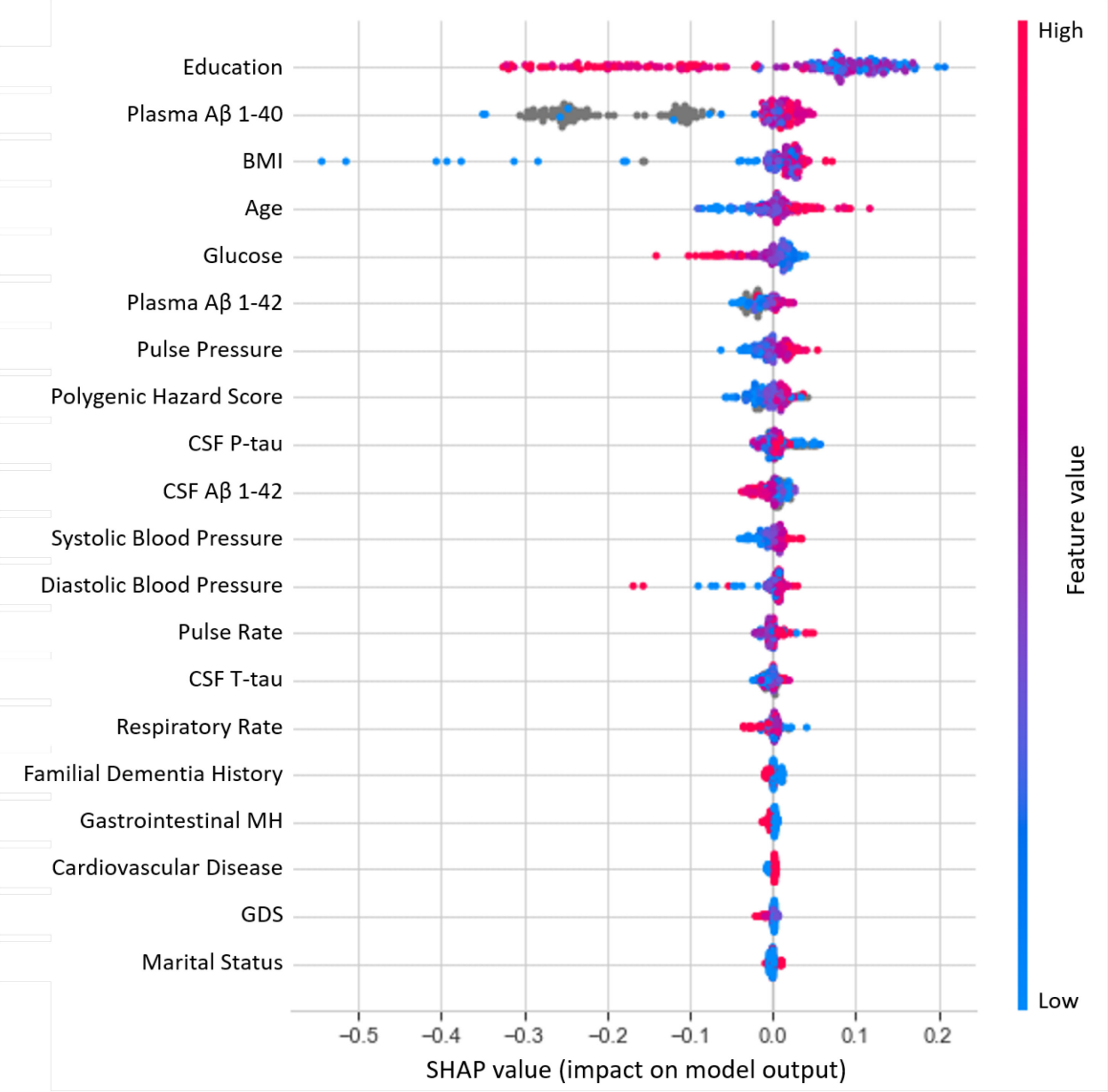

Figure 3-5. Tree SHAP Summary Plot showing the twenty most important predictors of cognitive vulnerability. Predictors are shown in descending order of importance. Each individual point on the plot represents a participant's Tree SHAP value for that predictor (bottom x-axis for scale). The position of the points indicates the effect on the model prediction. Specifically, Tree SHAP values over 0 (to the right of the figure) predict cognitive vulnerability. The colour of the dots indicates the direction of the effect for each predictor shown (red = higher values, blue = lower values, grey = imputed values).

Figure 3-6. Waterfall plot for predicting brain and cognitive stability (RG3).

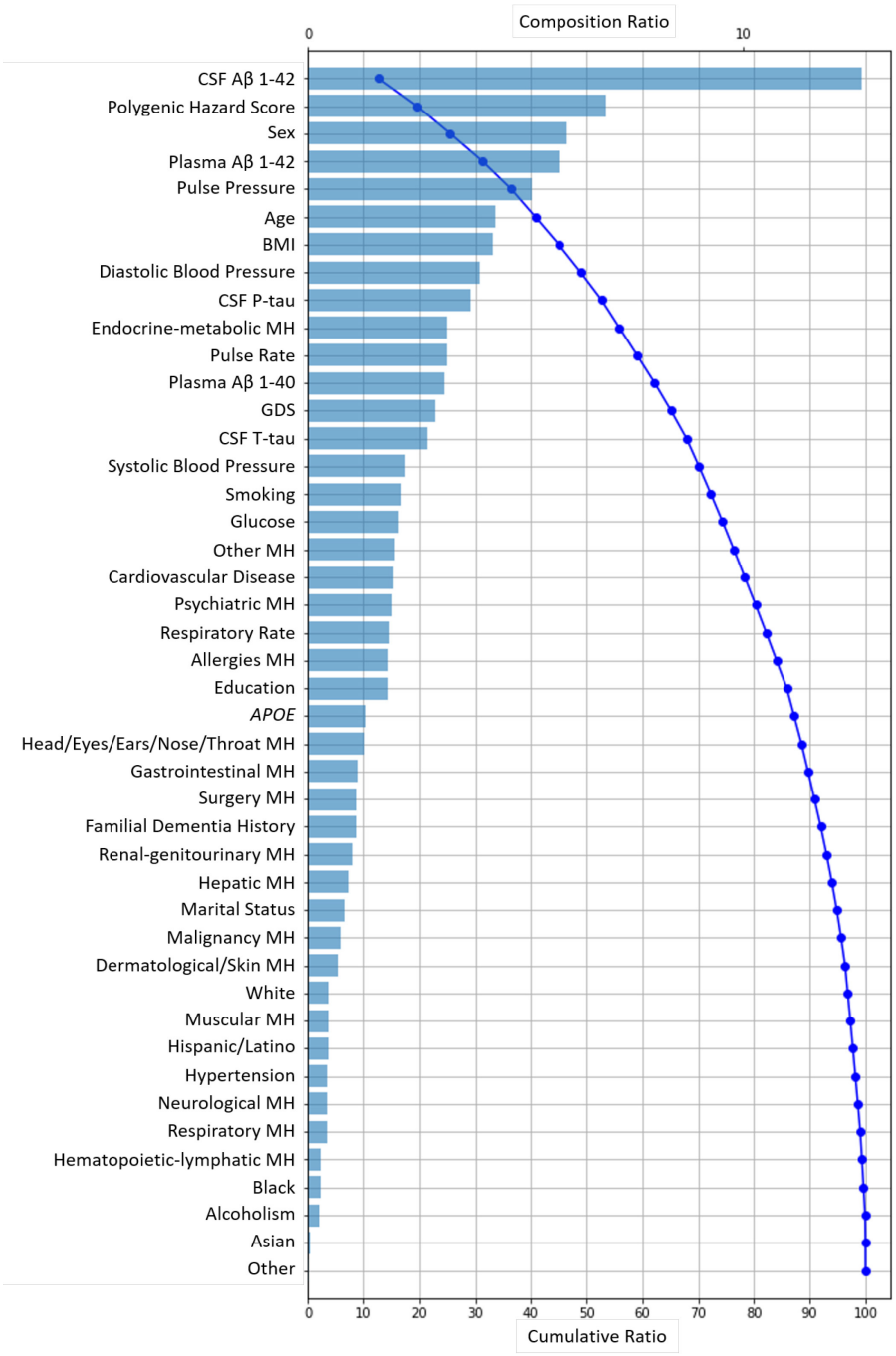

Figure 3-4. Tree SHAP Waterfall Plot showing the composition (top x-axis) and cumulative (bottom x-axis) ratios for the baseline predictors tested in the ML model. Predictors are shown in descending order of importance and their individual composition ratio (individual contribution to the model prediction) is indicated by the blue bars. The blue curved line indicates the cumulative ratio for each additional predictor.

Figure 3-7. SHAP summary plot for predicting brain and cognitive stability (RG3).

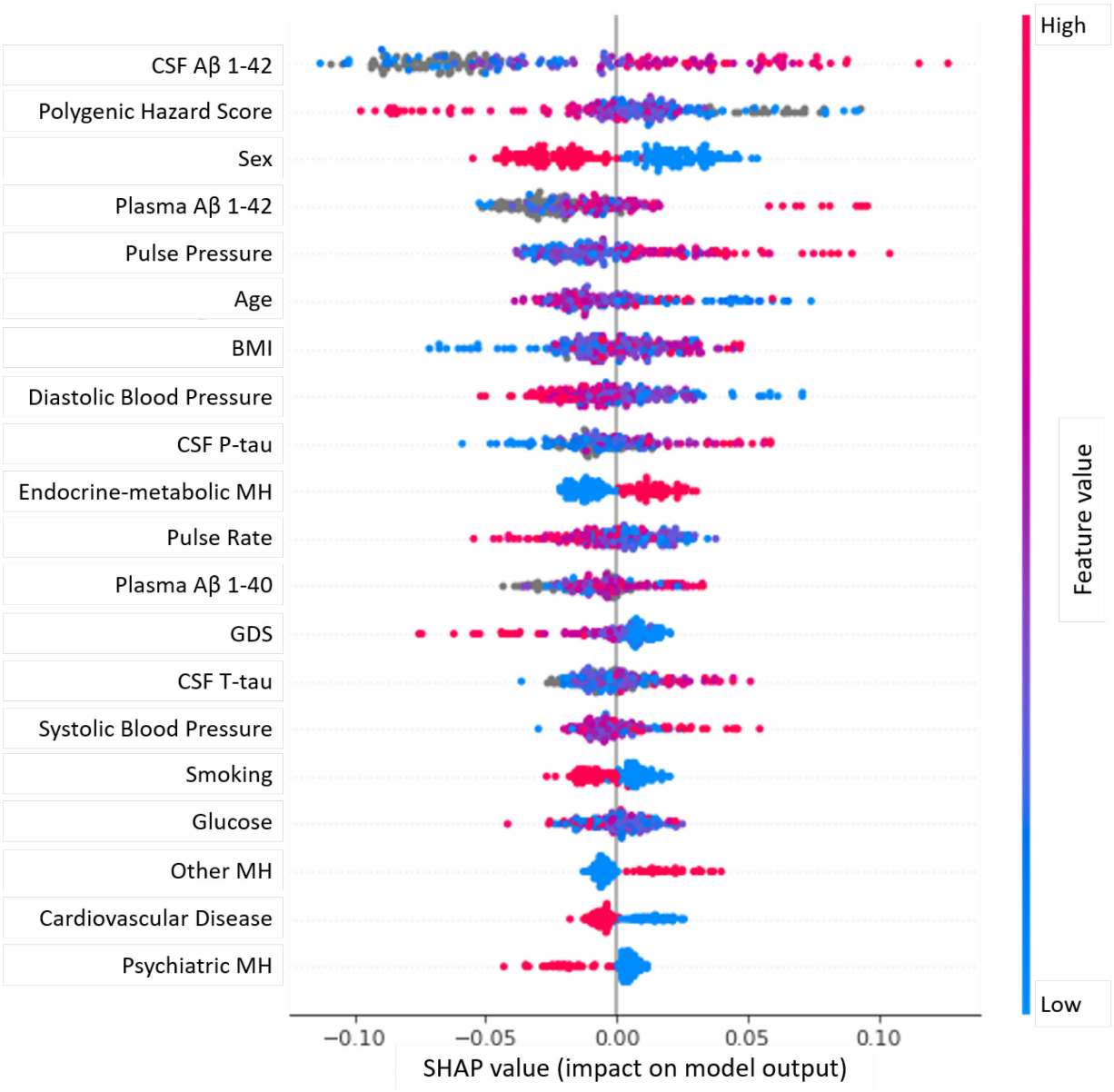

Figure 3-7. Tree SHAP Summary Plot showing the twenty most important predictors of brain and cognitive stability. Predictors are shown in descending order of importance. Each individual point on the plot represents a participant's Tree SHAP value for that predictor (bottom x-axis for scale). The position of the points indicates the effect on the model prediction. Specifically, Tree SHAP values over 0 (to the right of the figure) predict brain and cognitive stability. The colour of the dots indicates the direction of the effect for each predictor shown (red = higher values, blue = lower values, grey = imputed values).

Figure 3-8. Unique and shared predictors for cognitive resilience, cognitive vulnerability, and brain and cognitive stability

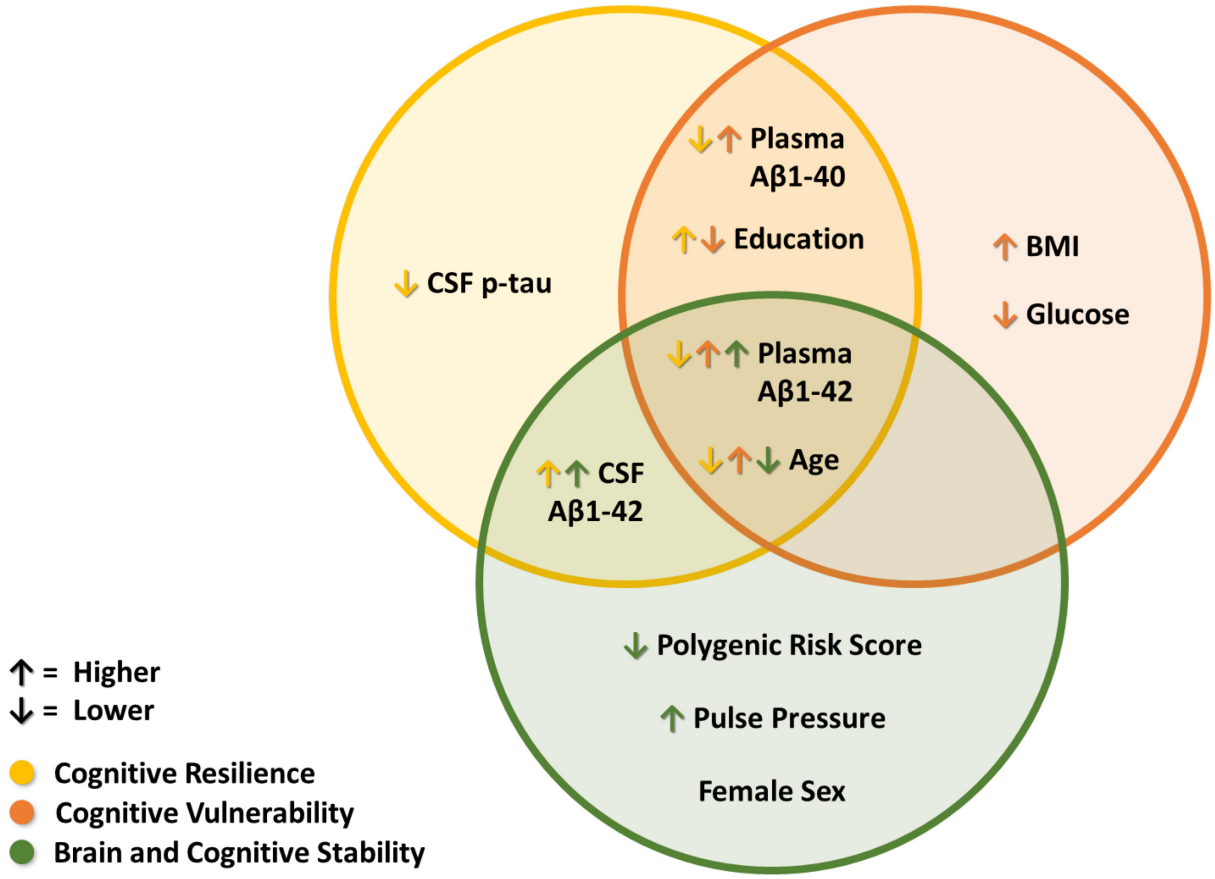

CHAPTER 4: STUDY 3

Data-Driven Predictions of Mild Cognitive Impairment and Alzheimer's Disease: Relative Importance of Multi-Modal and Omics Biomarkers and Risk Factors in the COMPASS-ND Study

Background

Currently the most common cause of dementia worldwide, Alzheimer's disease (AD) is characterized by specific neuropathology (beta-amyloid plaques and neurofibrillary tau tangles) as well as progressive cognitive and functional impairment (Barnes & Yaffe, 2011; Jack Jr et al., 2018; Livingston et al., 2020; X. Wang, Sun, Li, Cai, & Han, 2019; Zvěřová, 2019). The growing prevalence rates of AD point towards increasing societal and economics costs globally, projected to be $2 trillion by 2030 (Wimo et al., 2017). Marked by a lengthy prodromal period driven by accumulating multi-modal risk factors and indicated by advancing neuropathology and cognitive impairment, research attention has broadened to include the early detection of individuals or precision subtypes who are in earlier phases of the pathogenic process (K. J. Anstey et al., 2015; K. J. Anstey et al., 2020; Badhwar et al., 2020a; Iturria-Medina, Sotero, Toussaint, Mateos-Pérez, & Evans, 2016; Livingston et al., 2020; Tam et al., 2019; Vogel et al., 2021). The phase of aging prior to cognitive impairment, but with potentially accumulating AD risk, is referred to as asymptomatic or Cognitively Unimpaired (CU) aging. Aging persons in the CU phase may be experiencing moderate memory decline, early hippocampal (HC) atrophy, or even subjective concerns about their cognitive status. Mild Cognitive Impairment (MCI) is as a formally classifiable phase characterized by exacerbated cognitive decline with impaired performance (but not dementia), as well as increased risk of subsequent transition to AD (Marilyn S Albert et al., 2011; J.-Q. Li et al., 2016; Song, Poljak, Smythe, & Sachdev, 2009). Early identification of key characteristics and vulnerable individuals who are presently in either a CU or MCI phase but at risk of developing AD will aid in the precision understanding of the multi-modal networks potentially involved in AD-related neuropathological progression. In addition, such personalized and mechanistic advances may aid in the development of targeted

intervention and prevention protocols to delay or treat clinical impairment or disease onset (K. J. Anstey et al., 2020; Iturria-Medina et al., 2016; Röhr, Kivipelto, Mangialasche, Ngandu, & Riedel-Heller, 2022; Tam et al., 2019). Notably, it has been contended that efforts to delay or offset symptoms can have substantial benefits for controlling worldwide AD prevalence and costs (K. J. Anstey et al., 2020; Livingston et al., 2020).

Multi-Modal Risk Factors and Biomarkers Associated with MCI and AD

Accumulating research has identified risk factors and biomarkers associated with MCI and AD across a wide range of domains or modalities. Examples of these domains and their representative risk factors include brain health (lower HC volume), lifestyle (poor diet), vascular (hypertension), medical history (head injury), sensory (hearing), mental health (depression), metabolic (diabetes), cardiovascular (physical activity), education (years schooling), toxin exposure (smoking), engagement (cognitive activity), demographic (female sex/gender), biological (low CSF amyloid levels), and genetic (*APOE* e4 allele) (K. J. Anstey, Ee, Eramudugolla, Jagger, & Peters, 2019; Livingston et al., 2020). Risk factors from these modalities have been independently, or in combination, robustly associated with non-normative aging outcomes, including rapid cognitive decline, MCI and AD (K. J. Anstey et al., 2019; Livingston et al., 2020). The importance of risk factor management has been highlighted in recent reports. For example, 12 modifiable risk factors have been noted to be associated with 40% of dementias globally, providing specific modifiable targets that could substantially reduce dementia incidence (Livingston et al., 2020). As such, the identification of risk biomarkers and factors is key to the early detection of older adults at increased risk of AD and subsequent interventions and/or treatments.

Due to the large number and variegated types of potential predictors of AD risk,

researchers have encouraged approaches that allow for the investigation of multiple risk factors simultaneously. Notably, multi-modal predictions have been shown to (a) better represent the heterogeneous nature of MCI and AD as compared to individual single-domain predictors (K. J. Anstey et al., 2015; Badhwar et al., 2020a; Imtiaz, Tolppanen, Kivipelto, & Soininen, 2014; J.-Q. Li et al., 2016; Payton et al., 2018; Sapkota et al., 2018; Kristine Yaffe et al., 2019) and (b) provide valuable information on the relative importance of specific risk factors (G. P. McFall et al., 2019; Sapkota et al., 2021). For example, when evaluated simultaneously in a computationally competitive context, risk factors from five domains (genetic, lifestyle, cognition, functional health, metabolite panels) were found to discriminate between MCI and CU controls, while fewer risk domains were found to be statistically important when discriminating between cognitively normal and AD cohorts (Sapkota et al., 2018). Given that many diverse risk factors and biomarkers have been associated with AD risk, analytical approaches that include and evaluate risk factors simultaneously may help identify the leading predictors out of an established and heterogeneous set. In turn, the collection, examination, and preventative targeting of certain risk factors and biomarkers can be directed based on relative importance.

Omics-Based Predictors as Candidate Biomarkers of MCI and AD

Complementing the multi-modal risk factor research in the ADRD literature, there have been notable advances in the identification of biological and mechanistic markers which may also indicate increased AD risk. These include advances in ‘omics’ approaches which have especially supported the clarification of the multifactorial and heterogeneous nature of cognitive aging and AD (Badhwar et al., 2020a; Wilkins & Trushina, 2018) and have become an important approach in identifying and testing early dementia risk. As well-known and

established AD biomarkers (amyloid, tau, neurodegeneration) capture a crucial but circumscribed portion of the heterogeneous nature of AD etiology and disease-specific pathophysiology (Badhwar et al., 2020a), recent research has incorporated the investigation of broad biological patterns from emerging omics domains that may indicate mechanisms and level of differential risk for MCI or AD (Badhwar et al., 2020a). These omics approaches focus on a global or large-scale study of different biological systems (e.g., genes – genomics, lipids – lipidomics, metabolites – metabolomics) which may exhibit specific and identifiable perturbations or patterns of disease progression (Costa, Joaquim, Forlenza, Gattaz, & Talib, 2020; Hasin, Seldin, & Lusis, 2017). A recent focused review presented a graphical roadmap integrating omics analyses with machine learning technologies with the goal of addressing the etiological and clinical heterogeneity of Alzheimer's disease and related dementias (ADRD) (Badhwar et al., 2020a). Specifically, machine learning tools were noted to be especially advantageous in the cases of highly heterogeneous data, such as in ADRD (Badhwar et al., 2020a). Indeed, paired with sophisticated data-driven analytic approaches such as machine learning, the integrated study of multiple biological systems (i.e., 'multi-omics') provide a clearer characterization of the underlying disease process and identify new candidate biomarkers predictive of AD or AD risk based on novel biological pathways (Badhwar et al., 2020a; Hasin et al., 2017; Jia et al., 2021). These approaches are emerging as important complements to existing risk factor research. Specific to AD, metabolite and lipid biomarker panels have been developed from serum, saliva, and CSF via the application of data-driven algorithms (Badhwar et al., 2020a). These panels, which often vary in size, provide information on sets of molecules (in this case, metabolites or lipids) that are associated with clinical diagnoses of AD (Badhwar et al., 2020a) compared to heathy aging controls. For example, a

recent study identified a set of 24 serum lipids which accurately classified AD (Proitsi et al., 2017). Another recent study identified a smaller set of three metabolites, two acylcarnitines (dodecanedioylcarnitine [C12-DC], dodecanoylcarnitine [C12]) and one phosphatidylcholine (phosphatidylchline [PCaaC26:0]), which distinguished between AD and controls (Costa et al., 2020). Acylcarnitines are a lipid class important in the cholinergic cascade, via processes involving B-oxidation and acetyle coenzyme A (Costa et al., 2020). Notably, cholinergic dysfunction has been previously identified as an important pathophysiological component of AD (Hampel, Mesulam, et al., 2018). Similarly, disrupted phosphatidylcholine metabolism has been noted in AD through interactions with cholesterol transport and apolipoprotein E (Whiley et al., 2014). Other metabolite panels have been found to differentiate between AD and other types of dementias (Jia et al., 2021) and to be associated with preclinical signals of transitions from asymptomatic aging through MCI and AD (Hampel et al., 2021).

Moreover, metabolomics analyses have found that alterations in bile acids may occur in MCI and AD. Briefly, bile acids are derived from cholesterol and are produced in the liver to aid in lipid breakdown and clearance. Of specific interest to the disease pathophysiology of AD, bile acids represent the end product of cholesterol metabolism (i.e., an established mechanism of disease progression in AD) and are can be an indicator of key peripheral metabolic changes (Puglielli et al., 2003; Marksteiner et al., 2018; Nho et al., 2018). One study investigating plasma levels of bile acids found that lithocholic aid differentiated between AD and healthy controls while glycochenodeoxycholic acid, glycodeooxycholic acid and glycothithocholic acid differentiated between AD and MCI samples (Marksteiner et al., 2018). Similarly, lower serum concentrations of cholic acid and increased concentrations of deoxycholic acid were found in AD individuals as compared to controls (MahmoudianDehkordi et al., 2019). Higher

deoxycholic acid and cholic acid ratios in serum and brain tissue have also been consistently found to be associated with cognitive decline (MahmoudianDehkordi et al., 2019). Other studies have found similar associations between bile acid metabolites and AD-related neuropathology. Specifically, three bile acid ratios were found to be associated with CSF AB1-42 (glycodeoxycholic acid: cholic acid, taurochenodeoxycholic acid: cholic acid, clycolitocholic acid: chenodeoxycholic acid), and three bile acid metabolites were found to be associated with CSF p-tau (glycochenodeoxycholic acid, glycolithocolic acid, and taurolithocholic acid) (Nho et al., 2019)

The Relative Importance of Omics-Based Predictors in the Context of AD-Related Risk Factor Research

An important consideration for these approaches includes the potential added value of omics predictors as compared to other established, and perhaps more readily accessible, AD-related biomarkers and risk factors. For example, metabolite panels were identified as important predictors of clinical status (CU, MCI, AD) even among several established AD-related risk factors (Sapkota et al., 2018). This study followed an exhaustive metabolomics analysis that identified three leading biomarker panels from the same participants (Huan et al., 2018). In the multi-modal comparative prediction study, different metabolite panels involved with protein regulation were found to be important relative to other established AD risk factors for each pairwise comparison. Specifically, these panels were: (a) a 3-metabolite biomarker panel discriminating AD and CU (Methylguanosine, Histidinyl-Phenylalanine, Choline-cytidine), (b) a 3-metabolite biomarker panel discriminating AD and MCI (Amino-dihydroxybenzene, Glucosylgalactosyl hydroxylysine − H_2O, Aminobutyric acid + H_2., and (c) a 2-metabolite panel discriminating MCI and CU (Glucosylgalactosyl hydroxylysine − H_2O, Glutamine-carnitine). In

this study, the simultaneous consideration of metabolite panels and established AD-related risk factors provided additional evidence for the value of metabolomics-based predictors in addition to the advantages of multi-modal risk prediction models (Sapkota et al., 2018). In other fields, omics-based predictors have been found to improve prediction for diseases such as type II diabetes when used simultaneously in models with traditional risk factors (Liu et al., 2017). Importantly, omics-based predictors have emerged as powerful markers AD, and in conjunction with established risk factors, can serve as early indicators of increased risk in individuals who may benefit from targeted prevention and/or intervention protocols. Although a parallel study in Parkinson's disease dementia has been conducted with metabolomics markers integrated with multiple modalities of other predictors (G. P. McFall, Bohn, L., Drouin, S.M., Gee, M., Han, W., Li, L., Camicioli, R., & Dixon, R.A., 2023), no other studies in ADRD to date have investigated omics and established risk factors simultaneously to discriminate between cohorts or predict AD-related risk.

The Dissertation Study

In the current study, we leveraged a large roster of established AD-related multi-modal risk factors as well as previously identified metabolite and bile acid predictors from the Comprehensive Assessment of Neurodegeneration and Dementia Study (COMPASS-ND) dataset featuring three distinct cohorts (CU, MCI, AD) of older adults. COMPASS-ND is a comprehensive cross-sectional and multi-site Canadian study of older adults with several types of dementia and has collected extensive clinical, neuropsychological, MRI, and biofluid data. The large roster of multi-modal risk factors was selected based on (a) data availability and (b) previous findings in observational studies and reviews regarding MCI and AD risk. Beyond this roster, metabolomics (salivary and serum) and bile acid (serum) data were identified in a

previous study (S. Zhang, Drouin, Dixon, & Li, 2022; S. Zhang, Drouin, Li, & Dixon, 2022). Given that the performance of typical AD biomarkers (CSF amyloid and tau, PET neuroimaging) as early markers is still being explored, omics-based analyses may represent important a complementary approach for identifying (from a broad range of potential biomarkers) predictors associated with early perturbations in AD-related mechanistic pathways. These approaches could thus be a promising means of identifying candidate biomarkers for large-scale early screening of AD risk (Jia et al., 2021) and have thus far offered promising results (Badhwar et al., 2020; Hampel et al., 2021; Sapkota et al., 2018; Wilkins & Trushina, 2018).

The overall aim of this study was to test relative predictor importance of a multi-modal AD-related roster of biomarkers and risk factors, with focused attention on the comparative contributions of metabolite and bile acid biomarkers derived from a metabolomics analysis designed to identify leading predictors in discriminating between normal aging (CU) and two clinical classifications (MCI, AD). To accomplish this aim, we used machine learning technology to test predictor importance in three pairwise classification tasks (CU-MCI, MCI-AD, CU-AD) in two separate but comparable samples (Sample 1, Sample 2) extracted from the COMPASS-ND database.

Methods

Database

The COMPASS-ND Study is a large clinical cohort study of the Canadian Consortium of Neurodegeneration in Aging (Chertkow et al., 2019). This multi-site national study includes subsets of older adults (aged 50-90) with different clinically diagnosed neurodegenerative diseases as well as a CU comparison group. Participant conditions include Subjective Cognitive

Impairment (SCI), MCI, Subcortical Ischemic Vascular MCI, mild Alzheimer's disease, Dementia of Mixed Etiology, Lewy Body disease, Parkinson's dementia/MCI, and Frontotemporal dementia. The main goals of COMPASS-ND are (a) to identify those at early risk of dementia and (b) the early identification and detection of dementia. COMPASS-ND features a large roster of demographic, lifestyle, medical, functional, neuropsychological, biofluid, and imaging variables for recruited individuals (Chertkow et al., 2019).

Participants

The current study included two separate samples of older adults from three cohorts of the COMPASS-ND Study that were previously selected for metabolomics and bile acid analyses. For sample one (total n = 99, 57.6% Female, M age = 70.6, age range = 60.6-84.3), this included: (a) CU (n = 33), (b) MCI (n = 33), and (c) AD (n = 33) (S. Zhang, Drouin, Dixon, et al., 2022; S. Zhang, Drouin, Li, et al., 2022). For sample two (total n = 86, 50% Female, M age = 74.1, age range = 59.1-89.2, this included: (a) cognitively unimpaired (n = 32), (b) MCI (n = 33), and (c) AD (n = 21) (S. Zhang, Drouin, Dixon, et al., 2022; S. Zhang, Drouin, Li, et al., 2022). The three main cohorts in each sample are clinically comparable, with one deliberate exception: Whereas the CU cohort of Sample 1 includes persons with and without minor SCI, the CU cohort of Sample 2 includes only persons with no cognitive concerns. We present baseline descriptive statistics for the two samples divided by cohort in Table 1. Diagnostic status was determined by COMPASS-ND clinicians based on previously outlined criteria (Chertkow et al., 2019). Ethics approval was obtained from the Research Ethics Board of each participating study site and participants provided informed consent.

Measures

We assembled a predictor roster including both (a) established and emerging AD-related

biomarkers and risk factors originating from multiple domains available within the COMPASS-ND dataset and (b) metabolomics predictors derived from salivary and serum samples and bile acid predictors derived from serum samples only (as they were not detected in salivary samples).

AD-Related Risk Factors. Ninety-two predictors from this category were selected and assembled into a large multi-domain roster based on availability in the database and existing literature on AD-related biomarkers and risk or protective factors (R. Dixon & M. Lachman, 2019; Livingston et al., 2020). These predictors originated from ten risk domains: demographic (e.g., age, sex), lifestyle (e.g., physical activity, sleep), mental health (e.g., history of generalized anxiety disorder, history major depressive disorder), anthropometric measures (e.g., body mass index, waist circumference), sensory (e.g., olfaction, vision), function/gait (e.g., balance confidence, grip strength), vascular/metabolic (e.g., systolic blood pressure, heart rate), imaging (e.g., HC volume, EC volume), fluid biomarkers (e.g., triglycerides, Interleukin 6), and clinical health (e.g., HBA1C, platelet count). A complete list of included predictors from each risk domain and baseline descriptive data for each cohort is presented in Table 1.

Metabolomics: Selective Extraction of Leading Serum and Salivary Metabolite and Bile Acid Biomarkers. The metabolites and bile acids used in the current study were collected and identified from a series of metabolomics analyses conducted within two separate but similar 3-cohort samples (Sample 1, Sample 2) drawn from the COMPASS-ND database. The original metabolomics procedures and results are fully described in two technical reports (Zhang, Drouin, Dixon & Li, 2022; Zhang, Drouin, Li & Dixon, 2022). In brief, untargeted metabolomics (chemical isotope labeling liquid chromatography mass spectrometry platform; CIL LC-MS) analyses were applied to produce metabolite predictors derived from both salivary

and serum biofluids differentiating between three pairwise comparisons of cohorts of older adults within the two separate samples. The pairwise discriminations are: (1) CU-AD, referred to as predicting AD, (2) CU-MCI, referred to as predicting MCI, and (3) MCI-AD, referred to as predicting dementia. The identified metabolites for each sample are described below and presented in Table 3. For interpretative purposes, we have identified a working name (below and in Table 3) for each metabolite compound based on the two cohorts each discriminates for subsequent use in the dissertation. The assigned working name identifies the prediction goal (AD, MCI, or dementia), the biofluid analyzed (serum or saliva) and an alphanumeric label (ranging from 1 to 3 in Sample 1 or A to C in Sample 2). In every case, the three leading predictive metabolites were extracted, precisely identified, and labelled for convenience according to this nomenclature. However, we note that the leading metabolites are essentially equivalent in their predictive function and thus the ordering of the compounds (1,2,3 or A,B,C) does not reflect an interpretable ordinal ranking. Moreover, we note that the analytic context for each of the pairwise metabolomics analyses for both serum and saliva biofluids included over 7000 detected metabolite peaks. Thus, the leading three are promising putative biomarkers likely associated with mechanistic pathways of AD progression.

In the serum analyses for Sample 1, the leading three metabolites discriminating each pairwise comparison were selected. For the CU-AD comparison, these were 3beta Hydroxy-delta5-cholenic acid (AD Metabolite Serum 1), 20,26-Dihydroxyecdysone (AD Metabolite Serum 2), and N(gamma)-Acetyldiaminobutyric acid (AD Metabolite Serum 3). For the CU-MCI comparison, these were Erythronic acid (MCI Metabolite 1 Serum), O-Hydroxylaminobenzoic Acid (MCI Metabolite 2 Serum), and Hypoxanthine (MCI Metabolite 3 Serum). For the MCI-AD comparison, these were Methionyl-Hydroxyproline (Dementia

Metabolite 1 Serum), 2,3,6-Trihydroxypyridine (Dementia Metabolite 2 Serum) and Batatasin IV (Dementia Metabolite 3 Serum).

In the salivary analyses for Sample 1, the leading three salivary metabolites were selected from each comparison. For the CU-AD comparison, these were 4-Pyridoxolactone (AD Metabolite 1 Saliva), DL-Benzylsuccinic acid (AD Metabolite 2 Saliva), and 3-Hydroxyisoheptanoic acid (AD Metabolite 3 Saliva). For the CU-MCI comparison, these were Pyrocatechol (MCI Metabolite 1 Saliva), Hydroxyprolyl-Tryptophan (MCI Metabolite 2 Saliva), and 2-Hydroxy-3-(4-Hydroxyphenyl) Propenoic Acid (MCI Metabolite 3 Saliva). For the MCI-AD comparison, these were 2-Methylbenzaldehyde (Dementia Metabolite 1 Saliva), 3-Oxodecanoic acid (Dementia Metabolite 2 Saliva), and Ammeline (Dementia Metabolite 3 Saliva).

Finally, for Sample 1, the original metabolomics analyses identified 20 bile acids in the serum sample analyses and none in the salivary sample analyses. Based on previous research (MahmoudianDehkordi et al., 2019), we selected two serum-based bile acids for this study. These were cholic acid (CA), deoxycholic acid (DCA), and the deoxycholic acid:cholic acid ratio (DCA:CA ratio). These three measures are used only in the prediction models for serum.

As with Sample 1, we applied the same selection procedures for metabolite and bile acid biomarkers in Sample 2. Specifically, in the serum analyses for Sample 2, the leading three serum metabolites discriminating each pairwise comparison were selected. For the CU-AD comparison, these were 2,8-Dihydroxyadenine (AD Metabolite A Serum), Serotonin (AD Metabolite B Serum), and Uridine (AD Metabolite C Serum). For the CU-MCI comparison, these were 3-Mercaptolactate-cysteine disulfide (MCI Metabolite A Serum), N-Acetyl-2-Oxo-4-hydroxy-5-aminovaleric acid (MCI Metabolite B Serum), and Threonolactone (MCI

Metabolite C Serum). For the MCI-AD comparison, these were Ureidoacrylic Acid (Dementia Metabolite A Serum), Histidinyl-Aspartate (Dementia Metabolite B Serum), and 3-Methoxy-4-hydroxyphenylacetaldehyde O-glucuronide (Dementia Metabolite C Serum).

In the salivary analyses for Sample 2, the three leading metabolites were selected for each pairwise comparison. For the CU-AD comparison, these were Mandelic Acid (AD Metabolite A Saliva), 4-Hydroxybenzaldehyde-3-Hydroxybenzaldehyde (AD Metabolite B Saliva), and Carbapenem Biosynthesis Intermediate 5 (AD Metabolite C Saliva). For the CU-MCI comparison, these were Mandelic Acid (MCI Metabolite A Saliva), Diethanolamine (MCI Metabolite B Saliva), Phenylalanyl-Methionine (MCI Metabolite C Saliva). For the MCI-AD comparison, these were L-Pyrrolysine (Dementia Metabolite A Saliva), 2-Methyl-4-heptanone (Dementia Metabolite B Saliva), and Aspartyl-Glutamate (Dementia Metabolite C Saliva). Finally, for Sample 2, we selected the same two serum-based bile acids as with Sample 1: CA, DCA, and the DCA:CA ratio. These three measures are used only in the prediction models for serum.

RGs and Biomarker Prediction Analyses

Analyses Goal and Implementation. We implemented an analysis plan that follows a sequential set of six RGs. The sequence of analyses is designed to facilitate comparisons of each cohort pair (CU-AD, CU-MCI, MCI-AD) across the two samples. Accordingly, we separately analyzed and report the results for the parallel pairs of cohorts. The first RG was to test relative predictor importance in discriminating between CU and AD cohorts in Sample 1. The second RG was to test relative predictor importance in discriminating between CU and AD cohorts in Sample 2. The third RG was to test relative predictor importance in discriminating between CU and MCI cohorts in Sample 1. The fourth RG was to test relative predictor importance in

discriminating between CU and MCI cohorts in Sample 2. The fifth RG was to test relative predictor importance in discriminating between MCI and AD cohorts in Sample 1. The sixth RG was to test relative predictor importance in discriminating between MCI and AD cohorts in Sample 2. In order to consider CA/DCA and the DCA:CA ratio predictor variables adequately, all six RGs were conducted twice: (a) once with both bile acids independently included (CA and DCA) and (b) once including only the DCA:CA ratio. The best model (including CA/DCA independently or the DCA:CA ratio) for each RG was subsequently chosen as the final model and was reported in the dissertation. For both Sample 1 and 2, the final predictor roster included: 92 AD-related risk factors and biomarkers from COMPASS-ND, nine serum metabolite compound predictors, nine salivary metabolite compound predictors, and one (DCA:CA) or two (CA, DCA) bile acid predictors (total number of predictors = 111 and 112). Figure 1 shows a detailed flowchart of the analysis procedures for each RG.

Machine Learning (ML) Prediction Analyses. All prediction models depicted in the RGs were analyzed with three ML algorithms in Python 3.9 (scikit-learn package) (Pedregosa et al., 2011). The ML algorithms were random forest (RF; *sklearn RandomForestClassifier*), gradient boosting (GB; *sklearn* G*radientBoostingClassifier*) and K-Nearest Neighbours (KNN; *sklearn KNeighborsClassifier*). These algorithms are especially suitable for these RGs and data, as they allow for predictor interactions and the inclusion of large number ($p > n$) of mixed-type predictors (Hapfelmeier & Ulm, 2013; Pedregosa et al., 2011). Specifically, RF classification is an ensemble machine learning algorithm which determines a predicted classification based on an aggregation of multiple decision trees (Géron, 2022; Pedregosa et al., 2011). GB classification is an ensemble ML algorithm whereby decision trees are combined sequentially and are individually weighted in order to classify a final output. A key difference between RF and GB is

that for the former, decision trees are independent and built in parallel (Müller & Guido, 2016). Comparatively, in GB, the decision trees are built sequentially in order to correct previous errors in prediction (Müller & Guido, 2016). KNN is a non-parametric ML algorithm in which the predicted output is classified based on the majority class and its K-nearest neighbour as determined by a selected distance metric (i.e., Euclidean distance) (Géron, 2022; Pedregosa et al., 2011). We opted to test three ML algorithms equipped to deal with our specific data characteristics and then compare their performance to select the most suitable and best performing algorithm for each pairwise comparison.

For each analysis, we used (a) stratified five-fold cross-validation to evaluate both internal and external validation and (b) a *sklearn pipeline*. First, in five-fold cross validation, each dataset was subdivided into five folds, with four of the five folds used for training (internal validation) and the remaining fold used for testing (external validation). This process was repeated until all five folds have been used once for testing. Second, we tested and cross-validated all three ML algorithms and estimated missing data within a *sklearn pipeline.* The use of a *sklearn pipeline* allowed for all missing data to be imputed within each cross-validation fold to avoid all potential data leakage issues from the training set into the testing set. As such, at each fold, the *sklearn pipeline* consisted of: (a) missing data imputation (using *IterativeImputer*) and (b) ML classification and evaluation (via cross-validation) with three models (RF, GB, KNN). In addition, for each training fold, different combinations of hyperparameters were tested during the ML classification step (via *sklearn GridSearchCV*). This allowed us to identify and select the best hyperparameters (i.e., pre-defined parameters that control the ML algorithm behaviour and performance) for each of the ML algorithms within the pipeline. For the RF and GB algorithms, the tested set of hyperparameters were ‘n_estimators [100, 500, 750, 1000],’

'max_depth [3, 5, 10, 15, None],' and 'max_features [srqt, log2, None].' For the KNN algorithm, these were 'n_neighbors [3, 5, 7, 9],' 'weights [uniform, distance],' and 'algorithm [ball_tree, kd_tree, brute].' We report averaged (across five cross-validation folds) evaluation metrics for the RF, GB, and KNN algorithms. We then selected the best performing ML algorithm overall as the final model and this was re-fit with the best identified hyperparameters.

We used five averaged evaluation indices to select the best performing ML algorithm: (a) area under the *ROC* curve (*AUC*), (b) accuracy (i.e., % correct classification), (c) precision (i.e., % of correct positive classifications), (d) recall (i.e., % of those in the positive class who are correctly predicted), and (e) F_1 score, a harmonic mean of precision and recall recommended for imbalanced samples. AUC values can be interpreted as follows: values between 0.6-0.7 are considered to have mild distinguishing power, values between 0.7-0.8 are considered to have moderate distinguishing power, and values over 0.8 are considered to have strong/excellent distinguishing power (Duan et al., 2020; Mandrekar, 2010). Ranging from 0-1, higher values of accuracy, precision, recall and F_1 indicate better classification.

Predictor Importance. Following the selection of the best ML model for each RG, we aimed to identify the leading predictors of AD, MCI, and dementia in both samples. We leveraged Shapley Additive exPlanation (SHAP) values to determine variable importance in the prediction of (a) AD (RG 1 and 2), (b) MCI (RG 3 and 4), (c) dementia (RG 5 and 6) (Lundberg et al., 2018). SHAP values address the 'black-box' issue of ML models in that they provide interpretable explanations of ML algorithms by identifying the individual contribution of each variable in the prediction of the desired outcome. In this study, we report two established Tree SHAP plots: (a) SHAP waterfall plots, and (b) SHAP summary plots. SHAP waterfall plots display the composition (individual contribution) and cumulative (total contribution) ratio for

each predictor on the model prediction. The waterfall plots were used to determine and report the predictors corresponding to four cumulative ratio benchmarks: 40%, 50%, 60% and 70%. Subsequently, SHAP summary plots show predictors descending order of importance with SHAP values for each individual in the sample shown across the x-axis for each predictor. SHAP values over 0 predict membership to the positive class whereas SHAP values less than 0 predict membership to the alternative (opposite) group. For the CU-AD comparison, we considered AD the positive class. For the CU-MCI comparison, we considered MCI the positive class. For the MCI-AD comparison, we considered AD the positive class. Higher absolute SHAP values indicate greater magnitude of the predictor effect. The colour of the dots display the value of the predictor (low = blue, high = red).

Previous ML studies using SHAP values have reported and interpreted a large range (3-20) of the identified top predictors which explained a sizeable proportion of the model (% of variance explained). (L. Bohn, Drouin, S.M., McFall, G.P., Rolfson, D., Andrew, M.K., & Dixon, R.A., 2023; Gebreyesus, Dalton, Nixon, De Chiara, & Chinnici, 2023; Ju et al., 2021; J. Li et al., 2022; G. P. McFall, Bohn, L., Drouin, S.M., Gee, M., Han, W., Li, L., Camicioli, R., & Dixon, R.A., 2023; K. Wang et al., 2021; Zhou et al., 2022). We reported all predictors corresponding to a benchmark of 40% of the ML prediction model explained. Subsequently, we also report the number of predictors which correspond three larger cumulative ratio benchmarks of model explanation: 50%, 60% and 70%.

Results

The order of the RGs provides for sequential reporting that compares each cohort pair (CU-AD, CU-MCI, MCI-AD) across the two samples. For the prediction of AD, we report all predictors corresponding to 40% of the ML model explanation in Sample 1 (RG 1) and Sample 2

(RG 2). We then provide the number of predictors corresponding to 50%, 60%, and 70% of the ML model prediction of AD. For the prediction of MCI, we report all predictors corresponding to 40% of the ML model explanation in Sample 1 (RG 3) and Sample 2 (RG 4). We then provide the number of predictors corresponding to 50%, 60%, and 70% of the ML model prediction of MCI. For the prediction of dementia, we report all predictors corresponding to 40% of the ML model explanation in Sample 1 (RG 5) and Sample 2 (RG 6). We then provide the number of predictors corresponding to 50%, 60%, and 70% of the ML model prediction of dementia.

A detailed list of all leading predictors corresponding to 50%, 60% and 70% of the model explanation can be found in Tables 7 (for RG 1), 8 (for RG 2), 9 (for RG 3), 10 (for RG 4), 11 (for RG 5), and 12 (for RG 6). The SHAP Waterfall Plots depicting the exact composition and cumulative ratios for each predictor are shown in Figures 1 (for RG 1), 3 (for RG 2), 5 (for RG 3), 7 (for RG 4), 9 (for RG 5) and 11 (for RG 6).

Research Goal 1 (Sample 1, CU-AD). We tested three ML classification algorithms for the prediction of AD in Sample 1. In the analysis including CA and DCA (Table 4), these were RF (accuracy = 0.84, precision = 0.82, recall = 0.88, F1 = 0.84, AUC = 0.95), GB (accuracy = 0.68, precision = 0.76, recall = 0.40, F1 = 0.49, AUC = 0.94), and KNN (accuracy = 0.45, precision = 0.45, recall = 0.31, F1 = 0.35, AUC = 0.51). In the analysis including the DCA:CA ratio (Table 5), these were RF (accuracy = 0.83, precision = 0.82, recall = 0.88, F1 = 0.83, AUC = 0.89), GB (accuracy = 0.72, precision = 1.0, recall = 0.45, F1 = 0.61, AUC = 0.94), and KNN (accuracy = 0.57, precision = 0.58, recall = 0.52, F1 = 0.53, AUC = 0.53). The RF analysis (model #1) with CA and DCA (no ratio) was identified as the best performing algorithm ('max_depth': X, 'max_features': X, 'n_estimators': 100) for predicting AD (Table 6). Six predictors from three domains explained 40% of the prediction model and discriminated between

CU and AD in Sample 1: lower general olfaction score, lower right EC volume, lower left HC volume, lower left EC volume, lower right HC volume, and lower Dementia Metabolite 3 Saliva (Table 7; Figure 3). These predictors originated from the sensory, imaging, and metabolomics domains of risk. Specific to the metabolite predictors, one compound (Dementia Metabolite 3 Saliva) emerged when considering the 40% cumulative ratio benchmark for the model explanation. We also report the number of leading predictors corresponding to model explanations at three additional criteria: (a) 50% (nine predictors, four of which were metabolites), (b) 60% (15 predictors, seven of which were metabolites) and (c) 70% (24 predictors, nine of which were metabolites). A full list of predictors of AD in Sample 1 corresponding to 50%, 60% and 70% of the model explanation can be found in Table 7 and Figure 2.

Research Goal 2 (Sample 2, CU-AD). We tested three ML classification algorithms for the prediction of AD in Sample 2. In the analysis including CA and DCA (Table 4), these were RF (accuracy = 0.94, precision = 1.0, recall = 0.86, F1 = 0.92, AUC = 0.98), GB (accuracy = 0.87, precision = 1.0, recall = 0.68, F1 = 0.80, AUC = 0.98), and KNN (accuracy = 0.81, precision = 0.80, recall = 0.77, F1 = 0.77, AUC = 0.82). In the analysis including the DCA:CA ratio (Table 5), these were RF (accuracy = 0.86, precision = 0.93, recall = 0.71, F1 = 0.81, AUC = 0.98), GB (accuracy = 0.88, precision = 0.95, recall = 0.76, F1 = 0.84, AUC = 0.97), and KNN (accuracy = 0.74, precision = 0.75, recall = 0.63, F1 = 0.65, AUC = 0.80). The RF analysis (model #4) with CA and DCA (no ratio) was identified as the best performing algorithm ('max_depth': X, 'max_features': X, 'n_estimators': 100) for predicting AD (Table 6). Nine predictors from five domains explained 40% of the prediction model and discriminated between CU and AD in Sample 2: lower left HC volume, lower right HC volume, lower right EC volume,

higher age, higher IL6, lower general olfaction score, higher AD Metabolite A Serum, lower APOA, and lower cholesterol (Table 8, Figure 5). These predictors originated from the imaging, demographic, and clinical health, sensory, and metabolomics domains of risk. Specific to the metabolite predictors, one compound (AD Metabolite A Serum) emerged when considering the 40% cumulative ratio benchmark for the model explanation. We also report the number of leading predictors corresponding to model explanations at three additional criteria: (a) 50% (13 predictors, two of which were metabolites), (b) 60% (18 predictors, three of which were metabolites), and (c) 70% (26 predictors, four of which were metabolites). A full list of predictors of AD in Sample 2 corresponding to 50%, 60% and 70% of the model explanation can be found in Table 8 and Figure 4.

Research Goal 3 (Sample 1, CU-MCI). We tested three ML classification algorithms for the prediction of MCI in Sample 1. In the analysis including CA and DCA (Table 4), these were RF (accuracy = 0.66, precision = 0.73, recall = 0.58, F1 = 0.63, AUC = 0.71), GB (accuracy = 0.70, precision = 0.69, recall = 0.48, F1 = 0.58, AUC = 0.83), and KNN (accuracy = 0.47, precision = 0.39, recall = 0.29, F1 = 0.32, AUC = 0.50). In the analysis including the DCA:CA ratio (Table 5), these were RF (accuracy = 0.70, precision = 0.70, recall = 0.70, F1 = 0.69, AUC = 0.81), GB (accuracy = 0.65, precision = 0.83, recall = 0.42, F1 = 0.53, AUC = 0.78), and KNN (accuracy = 0.49, precision = 0.46, recall = 0.47, F1 = 0.46, AUC = 0.45). The RF analysis (model #25) with the DCA:CA ratio was identified as the best performing algorithm ('max_depth': 5, 'max_features': ‘sqrt’, 'n_estimators': 750) for predicting MCI (Table 6). Twelve predictors from three domains explained 40% of the prediction model and discriminated between CU and MCI in Sample 1: lower MCI Metabolite 1 Serum, lower MCI Metabolite 2 Serum, higher MCI Metabolite 1 Saliva, lower MCI Metabolite 3 Serum, lower HDL, lower SHBG,

lower MCI Metabolite 2 Saliva, higher AD Metabolite 1 Serum, lower left EC, lower APOA, lower sodium levels, and higher left HC volume (Table 9; Figure 7). These predictors originated from the metabolomics, clinical health, and imaging domains of risk. Specific to the metabolite predictors, six compounds (MCI Metabolite 1 Serum, MCI Metabolite 2 Serum, MCI Metabolite 1 Saliva, MCI Metabolite 3 Serum, MCI Metabolite 2 Saliva, AD Metabolite 1 Serum) emerged when considering the 40% cumulative ratio benchmark for the model explanation. We also report the number of leading predictors corresponding to model explanations at three additional criteria: (a) 50% (18 predictors, eight of which were metabolites), (b) 60% (24 predictors, 11 of which were metabolites), and (c) 70% (35 predictors, 15 of which were metabolites). A full list of predictors of MCI in Sample 1 corresponding to 50%, 60% and 70% of the model explanation can be found in Table 9 and Figure 6.

Research Goal 4 (Sample 2, CU-MCI). We tested three ML classification algorithms for the prediction of MCI in Sample 2. In the analysis including CA and DCA (Table 4), these were RF (accuracy = 0.80, precision = 0.83, recall = 0.76, F1 = 0.79, AUC = 0.86), GB (accuracy = 0.68, precision = 0.70, recall = 0.48, F1 = 0.51, AUC = 0.90), and KNN (accuracy = 0.62, precision = 0.67, recall = 0.64, F1 = 0.62, AUC = 0.69). In the analysis including the DCA:CA ratio (Table 5), these were RF (accuracy = 0.89, precision = 0.92, recall = 0.88, F1 = 0.89, AUC = 0.95), GB (accuracy = 0.78, precision = 0.96, recall = 0.60, F1 = 0.73, AUC = 0.95), and KNN (accuracy = 0.68, precision = 0.67, recall = 0.82, F1 = 0.73, AUC = 0.75). The RF analysis (model #28) with the DCA:CA ratio was identified as the best performing algorithm (‘max_depth’: 15, ‘max_features’: ‘log2’, ‘n_estimators’: 1000) for predicting MCI (Table 6). Thirteen predictors from five domains explained 40% of the prediction model and discriminated between CU and MCI in Sample 2: lower MCI Metabolite A Serum, lower AST, lower MCI

Metabolite B Serum, higher IL6, higher anion gap, higher systolic blood pressure, lower APOB, higher homocysteine, lower DHEAS, lower left HC volume, lower MCI Metabolite C Serum, lower number of reported spoken languages, and higher creatinine levels (Table 10; Figure 9). These predictors originated from the metabolomics, clinical health, vascular/metabolic, imaging, and demographic domains of risk. Specific to the metabolite predictors, three compounds (MCI Metabolite A Serum, MCI Metabolite B Serum, MCI Metabolite C Serum) emerged when considering the 40% cumulative ratio benchmark for the model explanation. We also report the number of leading predictors corresponding to model explanations at three additional criteria: (a) 50% (18 predictors, five of which were metabolites), (b) 60% (25 predictors, eight of which were metabolites), and (c) 70% (35 predictors, nine of which were metabolites). A full list of predictors of MCI in Sample 2 corresponding to 50%, 60% and 70% of the model explanation can be found in Table 10 and Figure 8.

Research Goal 5 (Sample 1, MCI-AD). We tested three ML classification algorithms for the prediction of dementia in Sample 1. In the analysis including CA and DCA (Table 4), these were RF (accuracy = 0.83, precision = 0.84, recall = 0.85, F1 = 0.84, AUC = 0.88), GB (accuracy = 0.69, precision = 0.68, recall = 0.48, F1 = 0.56, AUC = 0.84), and KNN (accuracy = 0.46, precision = 0.49, recall = 0.54, F1 = 0.49, AUC = 0.44). In the analysis including the DCA:CA ratio (Table 5), these were RF (accuracy = 0.81, precision = 0.80, recall = 0.85, F1 = 0.81, AUC = 0.91), GB (accuracy = 0.68, precision = 0.86, recall = 0.52, F1 = 0.59, AUC = 0.85), and KNN (accuracy = 0.44, precision = 0.43, recall = 0.49, F1 = 0.44, AUC = 0.43). The RF analysis (model #31) with CA and DCA (no ratio) was identified as the best performing algorithm ('max_depth': 3, 'max_features': ‘sqrt’, 'n_estimators': 500) for predicting dementia (Table 6). Nine predictors from four domains explained 40% of the prediction model and

discriminated between MCI and AD in Sample 1: lower general olfaction score, lower right HC volume, lower right EC volume, lower left HC volume, lower Dementia Metabolite 3 Serum, lower Dementia Metabolite 3 Saliva, higher Dementia Metabolite 2 Serum, lower systolic blood pressure, and lower diastolic blood pressure (Table 11; Figure 11). These predictors originated from the sensory, imaging, metabolomics, and vascular/metabolic domains of risk. Specific to the metabolite predictors, three compounds (Dementia Metabolite 3 Serum, Dementia Metabolite 3 Saliva, Dementia Metabolite 2 Serum) emerged when considering the 40% cumulative ratio benchmark for the model explanation. We also report the number of leading predictors corresponding to model explanations at three additional criteria: (a) 50% (13 predictors, five of which were metabolites), (b) 60% (19 predictors, seven of which were metabolites), and (c) 70% (27 predictors, eight of which were metabolites). A full list of predictors of dementia in Sample 1 corresponding to 50%, 60% and 70% of the model explanation can be found in Table 11 and Figure 10.

Research Goal 6 (Sample 2, MCI-AD). We tested three ML classification algorithms for the prediction of dementia in Sample 2. In the analysis including CA and DCA (Table 4), these were RF (accuracy = 0.76, precision = 0.87, recall = 0.48, F1 = 0.60, AUC = 0.82), GB (accuracy = 0.72, precision = 0.58, recall = 0.51, F1 = 0.53, AUC = 0.82), and KNN (accuracy = 0.58, precision = 0.46, recall = 0.34, F1 = 0.37, AUC = 0.55). In the analysis including the DCA:CA ratio (Table 5), these were RF (accuracy = 0.74, precision = 0.73, recall = 0.51, F1 = 0.55, AUC = 0.78), GB (accuracy = 0.82, precision = 0.93, recall = 0.57, F1 = 0.70, AUC = 0.86), and KNN (accuracy = 0.63, precision = 0.57, recall = 0.39, F1 = 0.45, AUC = 0.59). The GB analysis (model #35) with CA and DCA (no ratio) was identified as the best performing algorithm ('max_depth': 15, 'max_features': ‘sqrt’, 'n_estimators': 500) for predicting dementia

(Table 6). Nine predictors from seven domains explained 40% of the prediction model and discriminated between MCI and AD in Sample 2: lower right EC volume, lower left HC volume, lower right HC volume, higher age, lower glucose, lower Dementia Metabolite B Saliva, lower balance, lower physical activity, and lower diastolic blood pressure (Table 12; Figure 13). These predictors originated from the imaging, demographic, clinical health, metabolomics, gait/function, lifestyle, and vascular/metabolic domains of risk. Specific to the metabolite predictors, one compound (Dementia Metabolite B Saliva) emerged when considering the 40% cumulative ratio benchmark for the model explanation. We also report the number of leading predictors corresponding to model explanations at three additional criteria: (a) 50% (11 predictors, three of which were metabolites), (b) 60% (16 predictors, four of which were metabolites), and (c) 70% (23 predictors, eight of which were metabolites). A full list of predictors of dementia in Sample 2 corresponding to 50%, 60% and 70% of the model explanation can be found in Table 12 and Figure 12.

Discussion

In the current study with COMPASS-ND data, we tested pairwise cohort comparisons to predict AD (CU-AD), MCI (CU-MCI), and dementia (MCI-AD) using a large roster (p = 111 or 112) of AD-related risk factors, demographic, anthropometrics, biomarkers, imaging markers, as well as novel metabolites and bile acids. To this end, we applied three ML algorithms (RF, GB, KNN) and SHAP values in parallel to two separate clinical research samples (Samples 1 and 2), each of which included independent and equivalently characterized cohorts of participants fitting formal CU, MCI and AD classifications. The specific aim was to identify the leading predictors of AD, MCI, and dementia from the multi-domain roster.

Our first RG tested relative predictor importance in discriminating between CU and AD cohorts (predicting AD) in Sample 1. Our second RG tested relative predictor importance in discriminating between CU and AD cohorts (predicting AD) in Sample 2. Our third RG tested relative predictor importance in discriminating between CU and MCI cohorts (predicting MCI) in Sample 1. Our fourth RG tested relative predictor importance in discriminating between CU and MCI cohorts (predicting MCI) in Sample 2. Our fifth RG tested relative predictor importance in discriminating between MCI and AD (predicting dementia) cohorts in Sample 1. Our sixth RG tested relative predictor importance in discriminating between MCI and AD cohorts (predicting dementia) in Sample 2. Analyses for each RG were conducted twice to consider important AD-related bile acids (CA and DCA) independently and as a ratio (DCA:CA). We subsequently selected and report results for the best model (with or without the DCA:CA ratio) for each RG.

Although evidence for hallmark biomarkers of AD diagnosis has been rapidly accumulating, early predictors of AD etiology, mechanisms and pathways have been found to be highly variable and potentially represented by risk factors and biomarkers from multiple modalities operating independently and interactively. Accordingly, we compiled a large multi-modal roster (number of predictors = 92) of risk factors and biomarkers from the COMPASS-ND study. In addition to the available factors in the database, we included novel candidate biomarkers as selected from recent metabolomics analyses on blood and saliva from the same cohorts in both samples (Zhang, Drouin, Dixon & Li, 2022; Zhang, Drouin, Li & Dixon, 2022. We included in our roster of predictors the leading metabolite biomarker predictors of clinical status as well two selected bile acids. Specifically, we selected the top metabolite predictors from both the serum and salivary biofluid study samples, as well as two prominent bile acids (in two

forms, CA, DCA;DCA:CA ratio). These recently discovered biomarkers were included in a computationally competitive context vis-à-vis other established AD-related factors. For each comparison, both established (e.g., HC volume) and novel metabolomics (e.g., erythronic acid) biomarkers were tested identified as leading discriminating predictors.

Our findings suggest that several important risk domains (imaging, sensory, clinical health, demographic, vascular/metabolic, gait/function, lifestyle, and metabolomics) feature leading predictors of AD, MCI, and dementia. To illustrate, we focus our summary on the diversity of results obtained for the most restrictive model explanation criterion (40%). For the prediction of AD (RGs 1 and 2), six predictors from three domains (sensory, imaging, and metabolomics) and nine predictors from five domains (imaging, demographic, and clinical health, sensory, and metabolomics) explained 40% of the prediction model in Samples 1 and 2, respectively. In Sample 1, these leading predictors of AD included one metabolite which was previously identified as discriminating between MCI and AD: Dementia Metabolite 3 Saliva (Zhang, Drouin, Dixon & Li, 2022; Zhang, Drouin, Li & Dixon, 2022). In Sample 2, these included one metabolite that was previously identified as a leading serum metabolite discriminating between CU and AD: AD Metabolite A Serum in Sample 2 (Zhang, Drouin, Dixon & Li, 2022; Zhang, Drouin, Li & Dixon, 2022). The number of metabolomics predictors corresponding to model explanations of 50 to 70% ranged from four to nine in Sample 1 and two to four in Sample 2. Our selected bile acid markers did not emerge as predictors for any of the cumulative ratio benchmarks (40-70%) in either sample in the prediction of AD.

For the prediction of MCI (RGs 3 and 4), 12 predictors from three domains (metabolomics, clinical health, and imaging) and 13 predictors from five domains (metabolomics, clinical health, vascular/metabolic, imaging, and demographic) explained 40% of

the prediction model in Samples 1 and 2 respectively. In Sample 1, these leading predictors of MCI included six metabolites, five of which were previously found to discriminate between CU-MCI: MCI Metabolite 1 Serum, MCI Metabolite 2 Serum, MCI Metabolite 1 Saliva, MCI Metabolite 3 Serum, MCI Metabolite 2 Saliva, AD Metabolite 1 Serum (Zhang, Drouin, Dixon & Li, 2022; Zhang, Drouin, Li & Dixon, 2022). In Sample 2, these included three metabolites that were previously identified as the leading serum metabolites discriminating between CU and MCI: MCI Metabolite A Serum, MCI Metabolite B Serum, MCI Metabolite C Serum (Zhang, Drouin, Dixon & Li, 2022; Zhang, Drouin, Li & Dixon, 2022. The number of metabolomics predictors corresponding to model explanations of 50 to 70% ranged from eight to 15 in Sample 1 and five to nine in Sample 2. Our selected bile acid markers did not emerge as predictors for any of the cumulative ratio benchmarks (40-70%) in either sample in the prediction of MCI.

For the prediction of dementia (RGs 5 and 6), nine predictors from four domains (sensory, imaging, metabolomics, and vascular/metabolic) and nine predictors from seven domains (imaging, demographic, clinical health, metabolomics, gait/function, lifestyle, and vascular/metabolic domains) explained 40% of the prediction model in Samples 1 and 2, respectively. In Sample 1, these leading predictors of dementia included three metabolites which were previously identified as among the leading serum and salivary metabolites discriminating between MCI and AD: Dementia Metabolite 3 Serum, Dementia Metabolite 3 Saliva, Dementia Metabolite 2 Serum (Zhang, Drouin, Dixon & Li, 2022; Zhang, Drouin, Li & Dixon, 2022). In Sample 2, these included one metabolite which was previously identified as a leading salivary metabolite discriminating between MCI and AD: Dementia Metabolite B Saliva (Zhang, Drouin, Dixon & Li, 2022; Zhang, Drouin, Li & Dixon, 2022). The number of metabolomics predictors corresponding to model explanations of 50 to 70% ranged from five to eight in Sample 1 and

three to eight in Sample 2. Our selected bile acid markers did not emerge as predictors for any of the cumulative ratio benchmarks (40-70%) in either sample in the prediction of MCI.

Below, we further discuss and interpret a selection (i.e., the top five) of the leading predictors of AD, MCI, and dementia which originate from five risk domains. Specifically, these risk domains were imaging, sensory, clinical health, demographic, and metabolomics. Subsequently, we discuss additional predictors which correspond to the most restrictive model explanation criterion (40%) but were not among the top five predictors. Finally, we discuss the bile acid predictors (CA, DCA, and DCA:CA) which did not emerge as leading predictors in any of our analyses.

Volumetric Imaging Domain

Lower volume measurements for all four included MRI measurements (left HC volume, right HC volume, left EC volume, right EC volume) emerged as leading predictors of both AD and dementia. Specifically, in order of importance, right EC volume, left HC volume, left EC volume, and right HC volume were the second to fifth most important predictors of AD in Sample 1. Left HC volume, right HC volume, and right EC volume were the first to third most important predictors of AD in Sample 2. Right HC volume, right EC volume, and left HC volume were the second to fourth most important predictors of dementia in Sample 1. Right EC, left HC, and right HC were the first to third most important predictors of dementia in Sample 2. In previous studies, lower levels and steeper decline (atrophy) in both HC and EC volume have been suggestive of elevated risk for subsequent clinical transitions to MCI or AD (Apostolova et al., 2012; Byun et al., 2015; Pini et al., 2016). The HC is an important neurological site responsible for episodic and working memory. Similarly, the EC is an important medial temporal lobe structure with a major role in memory, cognition, spatial awareness, and navigation.

Notably, the EC is a pivotal structure connecting the HC with the rest of the brain – allowing for communication between the neocortex and the HC. Along with the HC, the EC has been reported to be one of the first and primary sites of neuropathology and neuronal loss in AD and is especially affected at earlier phases of the disease. Overall, atrophy and reduced metabolism in the HC and EC is considered a general neurodegeneration biomarker for AD. Volume and thickness differences for both of these structures have been repeatedly observed between normal controls, MCI, and AD (Apostolova et al., 2012; Apostolova et al., 2010; Bobinski et al., 1999; Devanand et al., 2012; Pini et al., 2016; Velayudhan et al., 2013). For example, smaller thickness measurements in these two regions have been identified in older adults with AD as compared to those with MCI or who are cognitively normal (Velayudhan et al., 2013). Our findings suggest that lower HC and EC volumes are consistent and leading predictors of AD and dementia. In some studies, atrophy of these regions has been found to be more pronounced and accelerated in those with AC (Devanand et al., 2012). The results of the current study suggest that volume differences in HC and EC may be too subtle to emerge as a leading predictor of MCI (in the CU-MCI comparison) when other AD-related risk factor and metabolomics data are available and used simultaneously.

Notably, we found that left EC volume was not among the leading five predictors of AD in Sample 2 or of dementia in either sample. Previous research has identified differences between the left and right HC between clinical cohorts (i.e., normal controls, subjective cognitive decline, MCI, and AD) (Zhao et al., 2019). It has also been noted that atrophy of the left HC is more commonly reported in normal aging and begins before atrophy of the right HC in MCI and AD (Donix et al., 2013). This suggests that right HC atrophy may occur only in later stages of disease and is more strongly associated with predictions of clinical transitions towards MCI and

AD. Similar findings have been found for other medial temporal lobe structures, including the EC (Donix et al., 2013).

Sensory Domain

One sensory predictor emerged as a leading predictor of both AD and dementia. Specifically, a lower olfactory score (i.e., worse olfactory function) was one of the leading five predictors in the CU-AD comparisons (Sample 1) and in the MCI-AD comparison (Sample 1). Olfactory dysfunction has been consistently reported as a key sensory predictor of cognitive changes in aging (Stuart WS MacDonald, Keller, Brewster, & Dixon, 2018) and one of the earliest clinical symptoms of AD (Djordjevic, Jones-Gotman, De Sousa, & Chertkow, 2008; Son et al., 2021; Zou, Lu, Liu, Zhang, & Zhou, 2016). Although also exhibited in normal aging, olfactory deficits in individuals with AD have been reported to be much more severe (Djordjevic et al., 2008). In addition, previous research has shown that greater olfactory deficits are associated with AD-related neurodegeneration in those with MCI and AD, such as left HC atrophy (Kjelvik et al., 2014). Importantly, the timing of olfactory deficits has been a key research question in recent literature, as early detection of AD could be improved if these deficits occurred early in the disease and could be detected reliably (Djordjevic et al., 2008; Son et al., 2021). In the current study, olfaction did not emerge as a leading predictor of MCI. These results indicate that although olfactory dysfunction is a strong predictor of AD and dementia, prediction of early (preclinical) stages of disease are not captured by this factor. As olfaction predicted dementia (MCI-AD comparison), it is likely that olfactory changes that are severe enough to emerge as a leading predictor occur during or after the MCI stage.

Clinical Health Domain

Several peripheral serum biomarkers were identified as leading predictors of AD, MCI, or dementia in the current study. These include higher levels of IL-6 (MCI and AD), lower HDL cholesterol (MCI), higher anion gap (MCI), lower glucose (dementia), and lower levels of AST (MCI). Specifically, higher IL-6 discriminated the CU-AD cohorts and the CU-MCI cohorts in Sample 2. Inflammatory pathways have been consistently linked in recent research to play an important role in AD pathogenesis. It has been hypothesized that several components of inflammatory pathways, such as microglial and astrocyte activation as well as cytokine overproduction contribute to neuronal damage seen in AD (Lyra e Silva et al., 2021; Stamouli & Politis, 2016). Increased levels of IL-6 have been reported in AD brain tissue post-mortem and have been inversely associated with cognitive performance (Lyra e Silva et al., 2021). Similarly, increased serum levels of IL-6 have been found in AD patients as compared to MCI or controls (Kim, Lee, & Kim, 2017). We extend this finding and demonstrate that IL-6 levels also discriminate between CU and MCI cohorts.

Several other peripheral markers of clinical health predicted MCI. Lower HDL cholesterol was identified as a leading predictor of the CU-MCI comparison in Sample 1. Several mechanistic links between cholesterol and risk of AD have been discussed in related ADRD literature, including inflammation and oxidative stress (Candore et al., 2010; Casserly & Topol, 2004; Hansen & Wang, 2023; Zarrouk et al., 2020) as well as vascular dysfunction and impairment (K. J. Anstey, Ashby-Mitchell, & Peters, 2017; Nordestgaard, Christoffersen, & Frikke-Schmidt, 2022; Z. Zhou et al., 2020). HDL, also known as ‘good’ cholesterol, has been associated with better cardiovascular outcomes and lower risk of MCI, AD, and other neurodegenerative diseases (Marsillach et al., 2020; Pillai et al., 2023). Increased LDL or total

cholesterol (hypercholesterolemia), on the other hand, has been posited to be a risk factor for AD (Vasantharekha, Priyanka, Swarnalingam, Srinivasan, & ThyagaRajan, 2017). Specifically, lower concentrations of HDL in CSF have been previously associated with better cognitive function (Martinez et al., 2023) while lower levels of serum HDL have been found to be associated with neurotoxicity (Marsillach et al., 2020; Martinez et al., 2023; Vasantharekha et al., 2017). Similarly, increased AD risk in older adults has been associated with higher levels of serum HDL cholesterol (Vasantharekha et al., 2017). On the other hand, other studies have reported no links between HDL cholesterol and dementia (K. J. Anstey et al., 2017). Our findings suggest that previous findings regarding HDL cholesterol and AD extend to MCI, and in the presence of other predictive factors, should be tested for associations with actual preclinical trajectories.

We also identified higher anion gap as a leading predictor of MCI in Sample 2. In a previous study, higher levels of anion gap have been found to be associated with lower scores on The Consortium to Establish a Registry for Alzheimer's Disease test (Supasitthumrong et al., 2019). Raised anion gap can indicate metabolic acidosis (increased blood acidity) or renal failure. Finally, lower levels of AST were also identified as a leading predictor of MCI in Sample 2. Elevated levels of AST can indicate live dysfunction or an underlying cardiovascular condition (e.g., myocardial infraction) (Javaid, Hasan, Zohra, & Hussain, 2012). Increased levels of AST have been fond to be associated with increased risk of MCI in a previous case-control study (X. Zhou et al., 2020). Similarly, a negative correlation between MMSE scores and AST has been reported previously in cognitively normal older adults (Sanke et al., 2014). A potential mechanism includes glucose metabolism dysfunction leading to the upregulation of alternative

energy sources which would lead to increased AST activity (Riemenschneider, Buch, Schmolke, Kurz, & Guder, 1997).

One marker of peripheral clinical health (lower glucose levels) emerged as one of the leading five predictors of dementia in Sample 2 (none in Sample 1). Previously, higher levels of glucose have been found to be associated with poorer memory function (Supasitthumrong et al., 2019). In the current study, we note that the SHAP Summary Plot (Figure 13) shows a significant number of imputed values as driving the prediction towards dementia which may contribute to this contradictory finding. Further research should explore the association between fasting glucose levels and AD.

Demographic Domain

Age was a leading predictor in Sample 2 for both the CU-AD and MCI-AD (dementia) comparisons. In both comparisons, older age predicted membership to the AD cohort. Older chronological age is associated with advancing frailty, increased disability, and the accumulation of different morbidities, all of which are associated with pathological clinical outcomes such as AD and dementia (L. Bohn, Drouin, S.M., McFall, G.P., Rolfson, D., Andrew, M.K., & Dixon, R.A., 2023; Riedel et al., 2016). Despite not capturing health status or a measure of an individual's 'healthspan,' our findings highlight that chronological age represents a key variable that can be used to reliably predict AD and dementia and is often collected in large-scale longitudinal studies. To note, biological sex (male/female) did not emerge as a leading predictor in any of the prediction models.

Metabolomics Domain

Precision medicine perspectives have highlighted the importance of incorporating biomarkers that go beyond the conventional markers of amyloid and tau in order to adequately

address AD heterogeneity. Several omics-based biomarkers have been identified as promising candidate biomarkers in previous studies, including individual metabolites (e.g., (dodecanedioylcarnitine, phosphatidylchline) and panels (e.g., (3-metabolite panel: Methylguanosine, Histidinyl-Phenylalanine, Choline-cytidine) (Bader et al., 2020; Habartová et al., 2019; Xianlin Han et al., 2011; Huan et al., 2018; Johnstone et al., 2012; Lista et al., 2013; Trushina & Mielke, 2014; Varma et al., 2018). Notably, a previous study incorporated metabolomics-based biomarkers in machine learning prediction models in a similar design (Sapkota et al., 2018; see also McFall et al., 2023, for a Parkinson's disease example). In the current study, we included the leading three serum and salivary metabolites discriminating between each pairwise comparison (CU-AD, CU-MCI, and MCI-AD) as identified in recent metabolomics analyses performed separately on the present cohorts. The full results of this recent metabolomics analyses are currently summarized in two technical reports (Zhang, Drouin, Dixon & Li, 2022; Zhang, Drouin, Li & Dixon, 2022). The present design resulted in nine salivary and nine serum metabolites discovered by these analyses and added to the present predictor roster.

For the CU-AD comparisons (RG 1 and RG 2), no metabolites emerged in the leading five predictors. For the CU-MCI comparisons (RG 3 and RG 4), six metabolites were identified as leading predictors (4 in Sample 1, 2 in Sample 2). The leading metabolite in Sample 1 was lower serum erythronic acid (MCI Metabolite 1 Serum). This compound was identified in a previous study as one of three leading metabolites discriminating between the CU-MCI cohort. Erythronic acid is a glucose-related metabolite and the diastereomer of threonic acid (Engelke et al., 2010). Higher urine concentrations have been associated with transaldolase deficiencies in pediatric populations (Engelke et al., 2010). Specific to AD and cognitive impairment, it has

been studied in both brain tissue and serum studies. Elevated levels of erythronic acid have been identified in the hippocampus and EC of AD patients (Xu et al., 2016). However, lower levels have been identified in plasma in individuals with schizophrenia and cognitive impairment as compared to those without cognitive impairment (Jiang et al., 2022). Briefly, it has been hypothesized that the downregulation of erythronic acid may be a contributor and indicator of cognitive decline and impairment (Jiang et al., 2022). Our results are concordant with this interpretation in that lower levels of serum erythronic acid predicted MCI. An extension is that erythronic acid was not a leading predictor of AD or dementia, suggesting that alterations in some metabolites that have been associated with cognitive impairment may be specific to pre-clinical (early) stages of disease.

Lower O-Hydroxyaminobenzoic acid (MCI Metabolite 2 Serum) and higher pyrocatechol (MCI Metabolite 1 Saliva) were also identified as leading predictors for the CU-MCI for Sample 1. The involvement of O-Hydroxyaminobenzoic acid in cognitive impairment, MCI, or AD has not been previously established. Our findings suggest that this metabolite compound is a leading (second most important) predictor of MCI and should be further investigated. Pyrocatechol is a metabolite involved in several degradation pathways, including chlorocyclohexane and chlorobenzene degradation, benzoate degradation, fluorobenzoate degradation, dioxin degradation, naphthalene degradation and aminobenzoate degradation. In a previous study exploring the effect of caffeine consumption on risk of AD, pyrocatechol (produced during coffee roasting from chlorogenic acid) was found to reduce Aβ production in SH-SY5Y cells (Fukuyama et al., 2018). Our findings provide additional support for a neuroprotective role (via reduced Aβ production) of pyrocatechol.

Lower serum hypoxanthine (MCI Metabolite 3 Serum) was also identified as a leading predictor in the CU-MCI comparison for Sample 1. Hypoxanthine is the catabolic intermediate of purine metabolism and is strongly associated with the uric acid cycle (Kaddurah-Daouk et al., 2013; Xu et al., 2016). Several purine derivatives have been identified as neuroprotective via anti-inflammatory and antioxidant mechanisms. These include uric acid, guanosine, and inosine. Previous findings have suggested that uric acid may have a neuroprotective effect (Kaddurah-Daouk et al., 2013). Hypoxanthine specifically has been found to be decreased in the brain tissue (Xu et al., 2016), saliva (Liang et al., 2015), and plasma (Chouraki et al., 2017) of AD patients – reflecting abnormal purine metabolism in AD individuals.

In addition, lower 3-Mercaptolactate-cysteine disulfide (MCI Metabolite A Serum) and lower N-Acetyl-2-Oxo-4-hydroxy-5-aminovaleric acid (MCI Metabolite B Serum) were identified as leading predictors of MCI in Sample 2. For the MCI-AD comparisons (RG 5 and RG 6), one metabolite compound (BatatsinIV [Dementia Metabolite 3 Serum]) was identified as a leading predictor of dementia in Sample 1. Though previously unexplored, these metabolic compounds were identified as discriminating metabolites between the MCI and CN and MCI and AD cohorts in the previous metabolomics study, respectively (Zhang, Drouin, Dixon & Li, 2022; Zhang, Drouin, Li & Dixon, 2022). Possible linkages to pathways of the AD clinical spectrum with 3-Mercaptolactate-cysteine disulfide, N-Acetyl-2-Oxo-4-hydroxy-5-aminovaleric acid, and BatatsinIV should be further explored.

Notably, our findings reveal a noteworthy pattern in the prediction of AD, MCI, and dementia using serum and salivary metabolites. When considering the leading five predictors for each RG, no metabolites emerged as leading predictors of AD, six metabolites emerged as

leading predictors of MCI, and one metabolite predicted dementia. All but one (pyrocatechol) metabolites originated from the serum analyses.

Additional Leading Predictors of AD, MCI, and Dementia

Several AD-related risk factors, biomarkers, and metabolite predictors contributed to 40% of the model explanation but were not among the leading five predictors discussed in the sections above. For RG 1 (predicting AD in Sample 1), this included one predictor from the metabolomics domain (ammeline). For RG 2 (predicting AD in Sample 2), this included predictors originating from the sensory (general olfaction score), metabolomics (2,8-Dihydroxyadenine [AD Metabolite A Serum]), and clinical health (APOA, cholesterol) domains. For RG 3 (predicting MCI in Sample 1), this included predictors from the clinical health (SHBG, APOA, sodium), metabolomics (Hydroxypropyl Tryptophan [MCI Metabolite 2 Saliva], 3-beta-Hydroxydelta-5-cholenic Acid [AD Metabolite 1 Serum]), and imaging (left EC volume, left HC volume) domains. For RG 4 (predicting MCI in Sample 2), this included predictors originating from the vascular/metabolic (Systolic BP), clinical health (APOB, homocysteine, DHEAS, creatinine), imaging (left HC volume), metabolomics (Threonolactone [MCI Metabolite C Serum]), and demographic (languages) domains. For RG 5 (predicting dementia in Sample 1), this included predictors originating from the metabolomics (Ammeline [Dementia Metabolite 3 Saliva], 2,3,6-Trihydroxypyridine [Dementia Metabolite 2 Serum]) and vascular/metabolic (systolic BP, diastolic BP) domains. For RG 6 (predicting dementia in Sample 2), this included predictors originating from the metabolomics (2-Methyl-4-Heptanone [Dementia Metabolite B Saliva]), gait/function (balance), lifestyle (physical activity), and vascular/metabolic (diastolic BP) domains.

Bile Acids (CA, DCA, DCA:CA)

In the current study, the included bile acids (CA or DCA) and the bile acid ratio (DCA:CA) did not appear as leading predictors in any of our analyses for any of the cumulative ratio benchmark values (40%, 50%, 60%, 70%). Specifically, the composition (individual contribution) of each of the bile acid variables (CA, DCA, or DCA:CA) were under 1%. Previous studies have found lower levels of CA and increased levels of DCA acid in AD as compared to cognitively normal older adults (MahmoudianDehkordi et al., 2019) and were a notable interest of the current study. Bile acids are thought to be associated with AD in several ways, including gut microbiota and cholesterol metabolism. First, the pathogenesis of AD has been more recently associated with disturbances in the brain-gut-microbiota (Mulak, 2021). Bile acids and gut microbiota have been closely associated in previous studies, as bile acids are important signaling molecules for a number of metabolic processes (Mulak, 2021). Second, in humans, cholesterol is cleared from the body through bile acid production. Alterations in bile acid profiles can be linked to dysfunctional cholesterol clearance which could contribute to AD pathophysiology (MahmoudianDehkordi et al., 2019; Shao et al., 2020). Our findings indicate that in the context of a other AD-related risk factors and biomarkers which included a large roster of metabolomics predictors, bile acids did not add significant contributions to the prediction model.

Limitations and Strengths

There were several limitations associated to our study. First, we conducted our analyses on two relatively small samples. The samples included three cohorts, which ranged from 32-33 (CN), 33-33 (MCI), and 21-33 (AD) per group. We note, however, that the samples were balanced in that they were selected to be relatively age- and sex-matched. In addition, the final

selected ML algorithms (RF and GB) are powerful ensemble methods, that when used in conjunction with five-fold cross-validation and hyperparameter tuning, are considered well-suited for smaller samples and large predictor sets as they are less prone to overfitting than other algorithms. Second, our CN cohort in Sample 1 consisted of CN and older adults with subjective cognitive impairment. However, the CN cohort in Sample 2 consisted of CN older adults only. Due to this, we decided to conduct and report analyses in both samples separately, as is common in biomarker research. Moreover, this design feature provided an opportunity to check the generalizability of mixed versus "pure" CN group. Third, although CSF markers are invited in the COMPASS-ND data collection, the volunteer uptake has been small. This fact produced high proportions of missing CSF data for the present study, and thus we were unable to include conventional AD CSF biomarkers (Aβ1-42, t-tau) in our predictor roster. Although we note that our classification models resulted in good to excellent discrimination between cohorts despite the exclusion of these key predictors, future studies should consider adding these predictors to test and report their relative importance within a large set of AD-related risk factors.

The present study also features several notable strengths. First, we used a comprehensive predictor roster featuring AD-related risk factors and biomarkers from 12 domains of risk. These included demographic, lifestyle, mental health, anthropometric, sensory, gait/function, vascular/metabolic, imaging, fluid biomarkers, clinical health, metabolites (serum and salivary), and bile acids. In total, our predictor roster included 111 or 112 predictors covering a breadth of risk domains. Second, we took several steps to optimize the final selected prediction models for each RG. These included: (a) testing a set of three ML algorithms (RF, GB, KNN) simultaneously within a *sklearn* pipeline, (b) using hyperparameter tuning to select the best possible hyperparameters, and (c) testing two predictor rosters (one with CA and DCA bile acids

independently and one with the DCA:CA ratio). Third, the evaluation metrics (precision, accuracy, recall, F1 score, ROC-AUC) for the final ML prediction models indicated strong classification performance. Notably, the ROC-AUC values ranged from 0.81 to 0.98 which suggest strong distinguishing power for all comparisons. Finally, the COMPASS-ND database features clinically well-characterized and deeply phenotyped cohorts, including but not limited to the AD spectrum.

Conclusions

The current study examined a large roster of AD-related risk factors and biomarkers in a computationally competitive context to identify the leading predictors of AD, MCI, and dementia. For each prediction, established AD-related risk factors and biomarkers (e.g., HC volume, age, sex) as well as candidate metabolomics (e.g., erythronic acid, ammeline, hypoxanthine) and bile acids (i.e., CA, DCA, DCA:CA) predictors were tested. We identified several factors from varied AD-related risk domains (volumetric imaging, sensory, clinical health, demographic, metabolomics) which emerged as the leading predictors of AD, MCI, and dementia. Notably, several candidate metabolite predictors significantly contributed to the prediction of all three diagnoses, but especially the subtle differences between CU and MCI older adults. Overall, our findings highlight that advancing our knowledge of the AD spectrum benefits from a comprehensive approach which integrates multi-modal risk factors and biomarkers with metabolomics data.

Table 4-1. Sample characteristics predictors organized by domain

Domain	Predictor	Sample 1 CU (*n* = 33)	Sample 1 MCI (*n* = 33)	Sample 1 AD (*n* = 33)	Sample 2 CU (*n* = 32)	Sample 2 MCI (*n* = 33)	Sample 2 AD (*n* = 21)
Demographic	Age, months	842.0	843.8	856.4	850.1	890.0	949.5
	Sex (% Female)	81.1	54.5	42.4	68.8	48.5	23.8
	Number of Languages Spoken	1.88	2.22	1.70	2.3	1.8	2.0
	Total Years of Education	15.9	15.4	16.0	16.1	15.8	14.8
Lifestyle	General physical activity score (PASE)	117.7	118.6	108.8	153.0	121.6	83.1
	Nutrition Risk Score	38.6	38.3	41.2	40.2	38.6	39.6
	PSQI Sleep Score	5.6	4.7	3.9	5.5	4.4	5.0
	Regular Smoking (% Yes)	54.5	33.3	30.3	56.3	38.7	45.0
	Alcohol Consumption (% 7+)	21.2	18.2	9.0	25.0	9.7	10.0
	Oral Health Score	2.7	2.4	3.2	2.8	2.7	2.5
	Current number of medications	5.3	5.7	5.5	6.3	6.1	7.6
	Current health perception (% Very Good)	54.5	33.3	60.6	53.1	30.3	38.1

Mental Health	Major depressive disorder (% Yes)	15.2	15.2	18.2	9.4	18.2	28.6
	Generalized anxiety disorder (% Yes)	3.0	15.2	18.2	12.5	12.1	4.8
	Other mood disorder (% Yes)	0	0	3.0	6.3	0.0	9.5
	Phobic disorder (% Yes)	0	3.0	0	3.1	0.0	0.0
	Post-traumatic stress disorder (% Yes)	0	3.0	0	6.3	0.0	0.0
	Suicide attempts (% Yes)	3.0	6.0	0	3.1	15.2	4.8
Anthropometric Measures	BMI	26.4	26.9	25.9	25.9	26.3	28.7
	Waist Circumference	92.2	95.4	93.8	91.4	91.3	96.2
	Hip Circumference	103.2	103.1	98.9	102.6	97.2	101.6
	Neck Circumference	35.1	36.8	37.5	36.1	34.9	38.7
Sensory	Olfaction Score	10.3	9.6	6.2	10.5	8.7	6.5
	Vision Score	0.1	0.14	0.16	0.14	0.19	0.23
	Hearing Score	6.8	8.7	4.2	5.1	8.6	7.2

Gait and Function	Balance confidence (ABC Score)	86.9	84.5	91.7			
	Grip Strength (*M* of left and right hand)	23.7	25.5	29.7	28.8	26.4	31.5
Vascular and Metabolic	1 minute Orthostatic Change (% Yes)	18.2	9.0	9.0	18.2	23.3	14.3
	3 minute Orthostatic Change (% Yes)	15.2	6.0	6.0	19.0	24.1	14.3
	Systolic Blood Pressure (*M* supine, seated, standing)	127.8	133.3	123.1	123.7	136.4	128.2
	Diastolic Blood Pressure (*M* of supine, seated, standing)	75.9	76.4	71.8	74.1	79.5	71.4
	Resting heart rate (*M* of supine, seated, standing)	69.1	69.3	66.5	68.7	68.7	65.2
Imaging	Hippocampus Snipe Left (Z-Score)	-0.23	-0.2	-1.3	0.07	-0.3	-1.04
	Hippocampus Snipe Right (Z-Score)	-0.3	-0.4	-1.1	-0.07	-0.3	-0.9
	Entorhinal Cortex Snipe Left (Z-Score)	-0.08	-0.3	-0.7	-0.2	-0.3	-0.6
	Entorhinal Cortex Snipe Right (Z-Score)	-0.1	-0.3	-1.0	0.01	-0.2	-0.8
Fluid Biomarkers	Albumin*, g/L*	43.1	43.4	44.2	42.5	42.8	41.5
	Alkaline Phosphatase*, U/L*	70.1	82.1	70.6	71.1	67.4	75.2
	Alpha1 Antitrypsin, *mg/dL*	125.6	128.1	122.2	124.5	129.4	132.9

Fluid Biomarkers	Alanine aminotransferase (ALT), *U/L*	14.4	36.0	18.6	18.5	15.7	14.2
	Anion Gap, *mmol/L*	12.4	12.8	11.7	9.3	12.5	12.1
	Aspartate Aminotransferase (AST), *U/L*	17.2	43.0	19.3	23.1	16.1	17.3
	Bicarbonate, *mmol/L*	26.1	25.8	26.2	27.4	25.1	25.1
	Bilirubin Total, *mmol/L*	9.8	7.8	9.8	8.6	9.1	10.5
	Chloride, *mmol/L*	101.3	99.3	100.3	100.9	102.0	102.2
	Cholesterol total, *mmol/L*	4.9	4.6	4.8	5.8	4.8	4.3
	Cortisol, *mmol/L*	336.3	322.3	344.9	365.4	342.0	331.6
	Creatinine, *mmol/L*	71.3	76.0	80.4	67.6	83.0	88.6
	Cystatin C, *mg/L*	1.0	1.0	1.1	0.9	1.2	1.2
	Dehydroepiandrosterone (DHEA) sulfate, *umol/L*	2.4	1.6	2.5	2.6	1.7	1.3
	Estradiol, *pmol/L*	44.5	61.2	71.3	51.5	66.8	91.0
	Ferritin, *ug/L*	124.9	196.4	183.2	173.9	141.3	165.0
	Follicle-stimulating hormone (FSH), *U/L*	56.7	49.6	40.1	48.9	41.8	21.5

Fluid Biomarkers	Glucose, *mmol/L*	5.3	5.7	5.6	5.2	6.0	5.3
	HDL cholesterol, *mmol/L*	1.7	1.5	1.6	1.7	1.5	1.3
	Homocysteine, *umol/L*	11.6	11.2	12.0	10.4	12.7	13.3
	Insulin, *pmol/L*	75.2	102.0	70.8	69.4	98.8	90.6
	LDL cholesterol, *mmol/L*	2.7	2.6	2.7	3.4	2.6	2.3
	Luteinizing hormone (LH), *U/L*	27.3	25.5	21.4	24.3	22.7	12.9
	Non-HDL cholesterol, *mmol/L*	3.2	3.1	3.4	4.0	3.4	2.9
	Potassium, *mmol/L*	4.4	4.2	4.4	4.3	4.4	4.2
	Prolactin, *ug/L*	9.8	9.8	10.2	9.6	11.5	12.0
	Sex hormone binding globulin, *nmol/L*	88.8	70.8	65.9	68.5	68.8	60.4
	Sodium, *mmol/L*	139.8	137.9	138.5	137.6	139.7	139.4
	Adrenocorticotropic Hormone (ACTH) , *pmol/L*	4.9	4.6	5.4	5.0	5.4	5.8
	Androstenedione, *nmol/L*	5.7	3.6	6.5	3.4	5.9	4.5
	High-sensitivity C-reactive protein, *mg/L*	1.4	5.2	2.1	1.9	1.5	2.1

Fluid Biomarkers	Insulin-like Growth Factor-1, *nmol/L*	17.0	17.8	26.1	17.2	15.3	17.8
	InterLuken 6, *ng/L*	4.0	3.5	3.6	3.2	4.2	2.7
	Apolipoprotein-A Quantitation, *g/L*	1.7	1.6	1.5	1.8	1.6	1.4
	Apolipoprotein-B Quantitation, *g/L*	0.9	0.9	1.0	1.1	0.9	0.9
	Ratio total cholesterol / HDL	3.1	3.2	3.3	3.6	3.6	3.4
	Triglycerides, *mmol/L*	1.1	1.4	1.4	1.3	2.0	1.4
	Thyroid stimulating hormone (TSH) , *mU/L*	2.4	3.1	2.5	2.8	2.6	3.12
	Urea, *mmol/L*	5.4	5.7	6.1	5.6	6.2	6.9
	Vitamin B12, *pmol/L*	405.4	482.1	387.9	511.5	392.3	483.1
	25-Hydroxy Vitamin D, *nmol/L*	405.4	482.1	387.9	105.1	84.0	77.0
Clinical Health (Clinical Blood Count)	HBA1C	5.6	6.0	5.7	5.5	5.8	5.6
	Hemoglobin	140.8	141.4	145.6	142.1	138.0	137.0
	Red blood count	4.6	4.7	4.7	4.7	4.5	4.6
	Hematocrit	0.4	0.4	0.4	0.4	0.4	0.4

Clinical Health (Clinical Blood Count)	Mean corpuscular volume	92.6	90.8	92.8	90.7	91.8	91.9
	Mean corpuscular hemoglobin concentration	331.1	333.1	330.7	340.1	332.6	328.8
	Red Cell Distribution Width	13.2	13.4	13.3	12.9	14.0	13.9
	Platelet count	234.2	229.1	227.0	246.6	234.4	208.1
	Mean platelet volume	9.8	10.3	10.4	9.8	9.7	10.6
	White blood count	5.5	5.7	6.0	5.2	6.1	6.2
	N neutrophils	3.1	3.2	3.6	3.0	3.5	4.0
	N lymphocytes	1.5	1.8	1.5	1.6	1.6	1.5
	N monocytes	0.4	0.4	0.5	0.4	0.5	0.5
	N eosinophils	0.2	0.2	0.2	0.2	0.2	0.1
	N basophils	0.03	0.02	0.03	0.03	0.02	0.04

Serum Metabolite Compounds (Sample 1)	Hypoxanthine	0.95	0.71	0.80	N/A	N/A	N/A
	N(gamma)-Acetyldiaminobutyric acid	1.1	0.92	0.89	N/A	N/A	N/A
	O-Hydroxylamino benzoic Acid	1.07	0.1	0.91	N/A	N/A	N/A
	3beta Hydroxy-delta5-cholenic acid	0.40	0.67	0.76	N/A	N/A	N/A
	Erythronic acid	1.1	0.79	0.92	N/A	N/A	N/A
	Methionyl-Hydroxyproline	0.52	0.57	0.42	N/A	N/A	N/A
	20,26-Dihydroxyecdysone	0.92	0.89	0.79	N/A	N/A	N/A
	2,3,6-Trihydroxypyridine	1.2	1.1	1.3	N/A	N/A	N/A
	Batatasin IV	0.9	0.95	0.83	N/A	N/A	N/A
Serum Metabolite Compounds (Sample 2)	Uridine	N/A	N/A	N/A	1.05	0.90	0.94
	Histidinyl-Asparatate	N/A	N/A	N/A	1.36	1.72	1.34
	Serotonin	N/A	N/A	N/A	1.35	1.0	0.55
	3-Mercaptolactate-cysteinedisulfide	N/A	N/A	N/A	1.20	0.67	0.84
	2,8-Dihydroxyadenine	N/A	N/A	N/A	1.10	1.21	1.33

Serum Metabolite Compounds (Sample 2)	Ureidocrylic Acid	N/A	N/A	N/A	0.75	0.65	1.56
	N-Acetyl-2-Oxo-4-Hydroxy-5-Amino Valeric aAid	N/A	N/A	N/A	1.03	0.65	0.78
	Threonolactone	N/A	N/A	N/A	1.06	0.74	0.77
	3-Methoxy-4-hydroxyphenyl actaldehyde Oglucuronide	N/A	N/A	N/A	0.54	0.68	0.53
Saliva Metabolite Compounds (Sample 1)	Pyrocatechol	0.57	0.93	0.79	N/A	N/A	N/A
	4-Pyridoxolactone	0.68	0.52	0.41	N/A	N/A	N/A
	Ammeline	1.75	2.46	1.12	N/A	N/A	N/A
	2-Hydroxy-3-(4-Hydoxyphenyl) Propenoic Acid	0.78	1.02	0.86	N/A	N/A	N/A
	DL-Benzylsuccinic acid	3.04	2.92	2.33	N/A	N/A	N/A
	Hydroxyprolyl-Tryptophan	0.84	0.62	0.74	N/A	N/A	N/A
	3-Hydroxyisoheptanic acid	1.99	1.88	1.40	N/A	N/A	N/A
	2-Methylbenzaldehyde	0.79	0.69	0.89	N/A	N/A	N/A
	3-Oxodecanoic Acid	1.05	0.92	1.17	N/A	N/A	N/A

Saliva Metabolite Compounds (Sample 2)	Aspartyl Glutamate	N/A	N/A	N/A	1.07	0.86	1.13
	Phenylalanyl Methionione	N/A	N/A	N/A	0.91	1.64	1.19
	4-Hydroxybenzaldehyde-3-Hydroxybenzadehyde	N/A	N/A	N/A	1.06	0.98	0.85
	Diethanolamine	N/A	N/A	N/A	0.85	1.9	0.87
	L-Pyrrolysine	N/A	N/A	N/A	1.39	1.03	1.75
	Carbapenem Biosynthesis Intermediate-5	N/A	N/A	N/A	0.66	0.77	0.87
	Mandelic Acid	N/A	N/A	N/A	1.23	0.86	0.69
	2-Methyl-4-Heptanone	N/A	N/A	N/A	0.99	1.02	0.95
Serum Bile Acids	Cholic Acid	0.73	0.55	0.61	0.56	0.62	0.85
	Deoxycholic Acid	0.58	0.92	0.90	0.80	0.93	1.41
	Deoxycholic Acid: Cholic Acid Ratio	3.26	4.82	5.26	2.78	3.81	4.73

Table 4-2. Predictors and working names and/or abbreviations

Domain	Predictor Name	Working Name
Demographic	Age, months	Age
	Sex (% Female)	Sex
	Number of Languages Spoken	Languages
	Total Years of Education	Education
Lifestyle	General physical activity score (PASE)	PASE
	Nutrition Risk Score	Nutrition
	PSQI Sleep Score	PSQI
	Regular Smoking (% Yes)	Smoking
	Alcohol Consumption (% 7+)	Alcohol
	Oral Health Score	Oral Health
	Current number of medications	Medication
	Current health perception (% Very Good)	Health Perception
Mental Health	Major depressive disorder (% Yes)	Depression
	Generalized anxiety disorder (% Yes)	Anxiety
	Other mood disorder (% Yes)	Mood Disorder
	Phobic disorder (% Yes)	Phobic Disorder
	Post-traumatic stress disorder (% Yes)	PTSD
	Suicide attempts (% Yes)	Suicide

Anthropometric Measures	BMI	BMI
	Waist Circumference	Waist Circumference
	Hip Circumference	Hip Circumference
	Neck Circumference	Neck Circumference
Sensory	Olfaction Score	Olfaction
	Vision Score	Vision
	Hearing Score	Hearing
Gait and Function	Balance confidence (ABC Score)	Balance
	Grip Strength (*M* of left and right hand)	Grip Strength
Vascular and Metabolic	1 minute Orthostatic Change (% Yes)	Orthostatic Change (1 min)
	3 minute Orthostatic Change (% Yes)	Orthostatic Change (3 min)
	Systolic Blood Pressure (*M* supine, seated, standing)	Systolic BP
	Diastolic Blood Pressure (*M* of supine, seated, standing)	Diastolic BP
	Resting heart rate (*M* of supine, seated, standing)	Heart rate
Imaging	Hippocampus Snipe Left (Z-Score)	Left Hippocampus
	Hippocampus Snipe Right (Z-Score)	Right Hippocampus
	Entorhinal Cortex Snipe Left (Z-Score)	Left Entorhinal
	Entorhinal Cortex Snipe Right (Z-Score)	Right Entorhinal
Fluid Biomarkers	Albumin*, g/L*	Albumin
	Alkaline Phosphatase*, U/L*	ALP
	Alpha1 Antitrypsin, *mg/dL*	AAT

	Alanine aminotransferase*, U/L*	ALT
Fluid Biomarkers	Anion Gap, *mmol/L*	Anion Gap
	Aspartate Aminotransferase*, U/L*	AST
	Bicarbonate, *mmol/L*	Bicarbonate
	Bilirubin Total, *mmol/L*	Bilirubin
	Chloride, *mmol/L*	Chloride
	Cholesterol total, *mmol/L*	Cholesterol
	Cortisol, *mmol/L*	Cortisol
	Creatinine, *mmol/L*	Creatinine
	Cystatin C, *mg/L*	Cystatin C
	Dehydroepiandrosterone sulfate, *umol/L*	DHEA
	Estradiol, *pmol/L*	Estradiol
	Ferritin, *ug/L*	Ferritin
	Follicle-stimulating hormone, *U/L*	FSH
	Glucose, *mmol/L*	Glucose
	HDL cholesterol, *mmol/L*	HDL
	Homocysteine, *umol/L*	Homocysteine
	Insulin, *pmol/L*	Insulin
	LDL cholesterol, *mmol/L*	LDL
	Luteinizing hormone, *U/L*	LH
	Non-HDL cholesterol, *mmol/L*	Non-HDL cholesterol

	Potassium, *mmol/L*	Potassium
	Prolactin, *ug/L*	Prolactin
	Sex hormone binding globulin, *nmol/L*	SHBG
Fluid Biomarkers	Sodium, *mmol/L*	Sodium
	Adrenocorticotropic Hormone, *pmol/L*	ACTH
	Androstenedione, *nmol/L*	Androstenedione
	High-sensitivity C-reactive protein, *mg/L*	hs-CRP
	Insulin-like Growth Factor-1, *nmol/L*	IGF-1
	InterLuken 6, *ng/L*	IL-6
	Apolipoprotein-A Quantitation, *g/L*	APOA
	Apolipoprotein-B Quantitation, *g/L*	APOB
	Ratio total cholesterol / HDL	Cholesterol ratio
	Triglycerides, *mmol/L*	Triglycerides
	Thyroid stimulating hormone, *mU/L*	TSH
	Urea, *mmol/L*	Urea
	Vitamin B12, *pmol/L*	B12
	25-Hydroxy Vitamin D, *nmol/L*	Vitamin D
Clinical Health (Clinical Blood Count)	HBA1C	HBA1C
	Hemoglobin	Hemoglobin
	Red blood count	RBC
	Hematocrit	Hematocrit

	Mean corpuscular volume	MCV
	Mean corpuscular hemoglobin concentration	MCHC
	Red Cell Distribution Width	RCDW
	Platelet count	PC
Clinical Health (Clinical Blood Count)	Mean platelet volume	MPV
	White blood count	WBC
	N neutrophils	Neutrophils
	N lymphocytes	Lymphocytes
	N monocytes	Monocytes
	N eosinophils	Eosinophils
	N basophils	Basophils
Serum Bile Acids	Cholic Acid	CA
	Deoxycholic Acid	DCA
	Deoxycholic Acid: Cholic Acid Ratio	DCA:CA

Table 4-3. Metabolites discriminating between CU-AD, CU-MCI, and MCI-AD in Sample 1 and Sample 2 and provisional AD-related pathways

Predictor Name	Comparison	Working Name	Pathway
3beta-Hydroxy-delta5-cholenic acid	Sample 1: CU-AD	AD Metabolite 1 Serum	
20,26-Dihydroxyecdysone	Sample 1: CU-AD	AD Metabolite 2 Serum	Insect hormone biosynthesis
N(gamma)-Acetyldiaminobutyric acid	Sample 1: CU-AD	AD Metabolite 3 Serum	Glycine, serine, and threonine metabolism
2,8-Dihydroxyadenine	Sample 2: CU-AD	AD Metabolite A Serum	Purine metabolism
Serotonin	Sample 2: CU-AD	AD Metabolite B Serum	Tryptophan metabolism
Uridine	Sample 2: CU-AD	AD Metabolite C Serum	Pyrimidine metabolism
4-Pyridoxolactone	Sample 1: CU-AD	AD Metabolite 1 Saliva	Vitamin B6 metabolism
DL-Benzylsuccinic acid	Sample 1: CU-AD	AD Metabolite 2 Saliva	
3-Hydroxyisoheptanoic acid	Sample 1: CU-AD	AD Metabolite 3 Saliva	
Mandelic Acid	Sample 2: CU-AD	AD Metabolite A Saliva	Aminobenzoate degradation
4-Hydroxybenzaldehyde/ 3-Hydroxybenzaldehyde	Sample 2: CU-AD	AD Metabolite B Saliva	Toluene degradation; Aminobenzoate degradation
Carbapenem Biosynthesis Intermediate 5	Sample 2: CU-AD	AD Metabolite C Saliva	Carbapenem biosynthesis
Erythronic acid	Sample 1: CU-MCI	MCI Metabolite 1 Serum	
O-Hydroxylaminobenzoic Acid	Sample 1: CU-MCI	MCI Metabolite 2 Serum	Aminobenzoate degradation
Hypoxanthine	Sample 1: CU-MCI	MCI Metabolite 3 Serum	Purine metabolism
3-Mercaptolactate-cysteine disulfide	Sample 2: CU-MCI	MCI Metabolite A Serum	

N-Acetyl-2-Oxo-4-hydroxy-5-aminovaleric acid	Sample 2: CU-MCI	MCI Metabolite B Serum	
Threonolactone	Sample 2: CU-MCI	MCI Metabolite C Serum	
Pyrocatechol	Sample 1: CU-MCI	MCI Metabolite 1 Saliva	Chlorocyclohexane and chlorobenzene degradation; Benzoate degradation; Fluorobenzoate degradation; Dioxin degradation; Naphthalene degradation; Aminobenzoate degradation
Hydroxyprolyl-Tryptophan	Sample 1: CU-MCI	MCI Metabolite 2 Saliva	
2-Hydroxy-3-(4-Hydroxyphenyl) Propenoic Acid	Sample 1: CU-MCI	MCI Metabolite 3 Saliva	Tyrosine metabolism
Mandelic Acid	Sample 2: CU-MCI	MCI Metabolite A Saliva	Aminobenzoate degradation
Diethanolamine	Sample 2: CU-MCI	MCI Metabolite B Saliva	Glycerophospholipid metabolism
Phenylalanyl-Methionine	Sample 2: CU-MCI	MCI Metabolite C Saliva	
Methionyl-Hydroxyproline	Sample 1: MCI-AD	Dementia Metabolite 1 Serum	
2,3,6-Trihydroxypyridine	Sample 1: MCI-AD	Dementia Metabolite 2 Serum	Nicotinate and nicotinamide metabolism
Batatasin IV	Sample 1: MCI-AD	Dementia Metabolite 3 Serum	
Ureidoacrylic Acid	Sample 2: MCI-AD	Dementia Metabolite A Serum	Pyrimidine metabolism
Histidinyl-Aspartate	Sample 2: MCI-AD	Dementia Metabolite B Serum	

3-Methoxy-4-hydroxyphenylacetaldehyde O-glucuronide	Sample 2: MCI-AD	Dementia Metabolite C Serum	
2-Methylbenzaldehyde	Sample 1: MCI-AD	Dementia Metabolite 1 Saliva	Xylene degradation
3-Oxodecanoic acid	Sample 1: MCI-AD	Dementia Metabolite 2 Saliva	
Ammeline	Sample 1: MCI-AD	Dementia Metabolite 3 Saliva	Atrazine degradation
L-Pyrrolysine	Sample 2: MCI-AD	Dementia Metabolite A Saliva	Lysine biosynthesis
2-Methyl-4-heptanone	Sample 2: MCI-AD	Dementia Metabolite B Saliva	
Aspartyl-Glutamate	Sample 2: MCI-AD	Dementia Metabolite C Saliva	

Table 4-4. Evaluation metrics for analyses including CA and DCA (no DCA:CA ratio)

	ML Algorithm	Model #	Accuracy	Precision	Recall	F1 Score	ROC-AUC
Research Goal 1 CU-AD (Sample 1)	**RF**	**1**	**0.84**	**0.82**	**0.88**	**0.84**	**0.95**
	GB	2	0.68	0.76	0.40	0.49	0.94
	KNN	3	0.45	0.45	0.31	0.35	0.51
Research Goal 2 CU-AD (Sample 2)	**RF**	**4**	**0.94**	**1.0**	**0.86**	**0.92**	**0.98**
	GB	5	0.87	1.0	0.68	0.80	0.98
	KNN	6	0.81	0.8	0.77	0.77	0.82
Research Goal 3 CU-MCI (Sample 1)	RF	7	0.66	0.73	0.58	0.63	0.71
	GB	**8**	**0.70**	**0.69**	**0.48**	**0.58**	**0.83**
	KNN	9	0.47	0.39	0.29	0.32	0.50
Research Goal 4 CU-MCI (Sample 2)	**RF**	**10**	**0.80**	**0.83**	**0.76**	**0.79**	**0.86**
	GB	11	0.68	0.70	0.48	0.51	0.90
	KNN	12	0.62	0.67	0.64	0.62	0.69
Research Goal 5 MCI-AD (Sample 1)	**RF**	**13**	**0.83**	**0.84**	**0.85**	**0.84**	**0.88**
	GB	14	0.69	0.68	0.48	0.56	0.84
	KNN	15	0.46	0.49	0.54	0.49	0.44
Research Goal 6 MCI-AD (Sample 2)	**RF**	**16**	**0.76**	**0.87**	**0.48**	**0.60**	**0.82**
	GB	17	0.72	0.58	0.51	0.53	0.82
	KNN	18	0.58	0.46	0.34	0.37	0.55

Note. **Bolded rows** indicate the best algorithm out of the tested three (RF, GB, KNN) for each research goal.

Table 4-5. Evaluation metrics for Analyses including DCA:CA ratio only

	ML Algorithm	Model #	Accuracy	Precision	Recall	F1 Score	ROC-AUC
Research Goal 1 CU-AD (Sample 1)	**RF**	**19**	**0.83**	**0.82**	**0.88**	**0.83**	**0.89**
	GB	20	0.72	1.0	0.45	0.61	0.94
	KNN	21	0.57	0.58	0.52	0.53	0.53
Research Goal 2 CU-AD (Sample 2)	RF	22	0.86	0.93	0.71	0.81	0.98
	GB	**23**	**0.88**	**0.95**	**0.76**	**0.84**	**0.97**
	KNN	24	0.74	0.75	0.63	0.65	0.80
Research Goal 3 CU-MCI (Sample 1)	**RF**	**25**	**0.70**	**0.70**	**0.70**	**0.69**	**0.81**
	GB	26	0.65	0.83	0.42	0.53	0.78
	KNN	27	0.49	0.46	0.47	0.46	0.45
Research Goal 4 CU-MCI (Sample 2)	**RF**	**28**	**0.89**	**0.92**	**0.88**	**0.89**	**0.95**
	GB	29	0.78	0.96	0.60	0.73	0.95
	KNN	30	0.68	0.67	0.82	0.73	0.75
Research Goal 5 MCI-AD (Sample 1)	**RF**	**31**	**0.81**	**0.80**	**0.85**	**0.81**	**0.91**
	GB	32	0.68	0.86	0.52	0.59	0.85
	KNN	33	0.44	0.43	0.49	0.44	0.43
Research Goal 6 MCI-AD (Sample 2)	RF	34	0.74	0.73	0.51	0.55	0.78
	GB	**35**	**0.82**	**0.93**	**0.57**	**0.70**	**0.86**
	KNN	36	0.63	0.57	0.39	0.45	0.59

Note. **Bolded rows** indicate the best algorithm out of the tested three (RF, GB, KNN) for each research goal.

Table 4-6. Final reported ML models for each research goal

	Selected Final ML Algorithm	Selected Final Model	Selected Final Model #
Research Goal 1 CU-AD (Sample 1)	RF	With CA and DCA (no ratio)	1
Research Goal 2 CU-AD (Sample 2)	RF	With CA and DCA (no ratio)	4
Research Goal 3 CU-MCI (Sample 1)	RF	With DCA:CA ratio	25
Research Goal 4 CU-MCI (Sample 2)	RF	With DCA:CA ratio	28
Research Goal 5 MCI-AD (Sample 1)	RF	With CA and DCA (no ratio)	31
Research Goal 6 MCI-AD (Sample 2)	GB	With DCA:CA ratio	35

*Note***.** The selected final model # refers to the assigned model number shown in Tables 4 and 5.

Table 4-7. Leading predictors for Research Goal 1 including CA and DCA (no DCA:CA ratio) for CU-AD for **Sample 1**

Predictor	Benchmark % (Model Explained)			
	40%	50%	60%	70%
General Olfaction Score	X	X	X	X
Right Entorhinal Cortex Volume	X	X	X	X
Left Hippocampal Volume	X	X	X	X
Left Entorhinal Cortex Volume	X	X	X	X
Right Hippocampal Volume	X	X	X	X
Ammeline[1]	X	X	X	X
DL-Benzylsuccinic acid[2]		X	X	X
3-Hydroxyisoheptanoic acid[3]		X	X	X
20,26-Dihydroxyecdysone[4]		X	X	X
APOA			X	X
Hypoxanthine[5]			X	X
O-Hydroxylamino Benzoic Acid[6]			X	X
Estradiol			X	X
N-gamma-Acetyldiaminobutryic acid[7]			X	X
Num E			X	X
Erythronic Acid[8]				X
Num N				X
3-beta Hydroxydelta5cholenic acid[9]				X
SHBG				X
PSQI				X
Num M				X
Oral Health				X
Diastolic BP				X
AST				X

[1]Dementia Metabolite 3 Saliva
[2]AD Metabolite 2 Saliva
[3]AD Metabolite 3 Saliva
[4]AD Metabolite 2 Serum
[5]MCI Metabolite 3 Serum

[6]MCI Metabolite 2 Serum
[7]AD Metabolite 3 Serum
[8]MCI Metabolite 1 Serum
[9]AD Metabolite 1 Serum

Table 4-8. Leading predictors for Research Goal 2 including CA and DCA (no DCA:CA ratio) for CU-AD for **Sample 2**

Predictor	Benchmark % (Model Explained)			
	40%	50%	60%	70%
Left Hippocampal Volume	X	X	X	X
Right Hippocampal Volume	X	X	X	X
Right Entorhinal Cortex Volume	X	X	X	X
Age	X	X	X	X
IL6	X	X	X	X
General Olfaction Score	X	X	X	X
2,8-Dihydroxyadenine[1]	X	X	X	X
APOA	X	X	X	X
Cholesterol	X	X	X	X
Left Entorhinal Cortex Volume		X	X	X
Mandelic Acid[2]		X	X	X
Num N		X	X	X
RDWCV		X	X	X
MPV			X	X
MCHC			X	X
Creatinine			X	X
3-Mercaptolactatecysteinedisulfide[3]			X	X
ACTH			X	X
TSH				X
Balance				X
Bicarbonate				X
FSH				X
DHEAS				X
Estradiol				X
Uridine[4]				X
Vision				X

[1]AD Metabolite A Serum

[2]MCI Metabolite A Saliva
[3]MCI Metabolite A Serum
[4]AD Metabolite C Serum

Table 4-9. Leading predictors for Research Goal 3 including DCA:CA ratio for CU-MCI for **Sample 1**

Predictor	Benchmark % (Model Explained)			
	40%	50%	60%	70%
Erythronic Acid[1]	X	X	X	X
O-Hydroxylaminobenzoic Acid[2]	X	X	X	X
Pyrocatechol[3]	X	X	X	X
Hypoxanthine[4]	X	X	X	X
HDL	X	X	X	X
SHBG	X	X	X	X
Hydroxyprolyl Tryptophan[5]	X	X	X	X
3-beta-Hydroxydelta-5-cholenic Acid[6]	X	X	X	X
Left Entorhinal Cortex Volume	X	X	X	X
APOA	X	X	X	X
Sodium	X	X	X	X
Left Hippocampal Volume	X	X	X	X
2-Hydroxy-34-Hydroxyphenyl Propenoic Acid[7]		X	X	X
CRPH		X	X	X
ALT		X	X	X
BatatasinIV[8]		X	X	X
Ferritin		X	X	X
Num_B		X	X	X
Vision			X	X
Chloride			X	X
N-gamma-Acetyldiaminobutric Acid[9]			X	X
4-Pyridoxolactone[10]			X	X
TSH			X	X
2,3,6-Trihydroxypyridine[11]			X	X

Cholesterol				X
Systolic BP				X
MCV				X
Bilirubin				X
MPV				X
2-Methylbenzaldehyde[12]				X
AST				X
3-Hydroxyisoheptanoic Acid[13]				X
DL-Benzylsuccinic Acid[14]				X
Num L				X
Ammeline[15]				X

[1]MCI Metabolite 1 Serum
[2]MCI Metabolite 2 Serum
[3]MCI Metabolite 1 Saliva
[4]MCI Metabolite 3 Serum
[5]MCI Metabolite 2 Saliva
[6]AD Metabolite 1 Serum
[7]MCI Metabolite 3 Saliva
[8]Dementia Metabolite 3 Serum
[9]AD Metabolite 3 Serum
[10]AD Metabolite 1 Saliva
[11]Dementia Metabolite 2 Serum
[12]Dementia Metabolite 1 Saliva
[13]AD Metabolite 3 Saliva
[14]AD Metabolite 2 Saliva
[15]Dementia Metabolite 3 Saliva

Table 4-10. Leading Predictors for Research Goal 4 including DCA:CA ratio for CU-MCI for **Sample 2**

Predictor	Benchmark % (Model Explained)			
	40%	50%	60%	70%
3-mercaptolactate-cysteine disulfide[1]	X	X	X	X
AST	X	X	X	X
N-Acetyl-2-Oxo-4-hydroxy5aminovaleric acid[2]	X	X	X	X
IL6	X	X	X	X
Anion Gap	X	X	X	X
Systolic BP	X	X	X	X
APOB	X	X	X	X
Homocysteine	X	X	X	X
DHEAS	X	X	X	X
Left Hippocampal Volume	X	X	X	X
Threonolactone[3]	X	X	X	X
Languages	X	X	X	X
Creatinine	X	X	X	X
3-Methoxy-4-hydroxyphenylacetaldehydeOglucuronide[4]		X	X	X
Bicarbonate		X	X	X
RDWCV		X	X	X
Uridine[5]		X	X	X
SHBG		X	X	X
Cystatin C			X	X
Diethanolamine[6]			X	X
LDL			X	X
Histidinyl Aspartate[7]			X	X
Carbapenem Biosynthesis Intermediate-5[8]			X	X
Mandelic Acid[9]			X	X

Cholesterol			X	X
Left Entorhinal Cortex Volume				X
Num N				X
Sodium				X
Non-HDL				X
General Olfaction Score				X
Phenylalanyl Methionine[10]				X
Glucose				X
Prolactin				X
Age				X
Diastolic BP				X

[1]MCI Metabolite A Serum
[2]MCI Metabolite B Serum
[3]MCI Metabolite C Serum
[4]Dementia Metabolite C Serum
[5]AD Metabolite C Serum
[6]MCI Metabolite B Saliva
[7]Dementia Metabolite B Serum
[8]AD Metabolite C Saliva
[9]AD Metabolite A Saliva
[10]MCI Metabolite C Saliva

Table 4-11. Leading predictors for Research Goal 5 including CA and DCA (no DCA:CA ratio) for MCI-AD for **Sample 1**

Predictor	Benchmark % (Model Explained)			
	40%	50%	60%	70%
General Olfaction Score	X	X	X	X
Right Hippocampal Volume	X	X	X	X
Right Entorhinal Cortex Volume	X	X	X	X
Left Hippocampal Volume	X	X	X	X
BatatasinIV[1]	X	X	X	X
Ammeline[2]	X	X	X	X
2,3,6-Trihydroxypyridine[3]	X	X	X	X
Systolic BP	X	X	X	X
Diastolic BP	X	X	X	X
Left Entorhinal Cortex		X	X	X
Mentionyl Hydroxyproline[4]		X	X	X
3-Hydroxyisoheptanoic Acid[5]		X	X	X
3-Oxodecanoic Acid[6]		X	X	X
2-Methylbenzaldehyde[7]			X	X
Anion GAP			X	X
DL-Benzylsuccinic Acid[8]			X	X
Oral Health			X	X
LH			X	X
Nutrition			X	X
CRPH				X
FSH				X
Heart rate				X
DHEAS				X
Pyrocatechol[9]				X
Cortisol				X

MCV				X
Current health rating				X

[1]Dementia Metabolite 3 Serum
[2]Dementia Metabolite 3 Saliva
[3]Dementia Metabolite 2 Serum
[4]Dementia Metabolite 1 Serum
[5]AD Metabolite 3 Saliva
[6]Dementia Metabolite 2 Saliva
[7]Dementia Metabolite 1 Saliva
[8]AD Metabolite 2 Saliva
[9]MCI Metabolite 1 Saliva

Table 4-12. Leading predictors for Research Goal 6 including DCA:CA ratio for MCI-AD for **Sample 2**

Predictor	Benchmark % (Model Explained)			
	40%	50%	60%	70%
Right Entorhinal Cortex Volume	X	X	X	X
Left Hippocampal Volume	X	X	X	X
Right Hippocampal Volume	X	X	X	X
Age	X	X	X	X
Glucose	X	X	X	X
2-Methyl-4-Heptanone[1]	X	X	X	X
Balance	X	X	X	X
Physical Activity	X	X	X	X
Diastolic BP	X	X	X	X
Aspartyl Glutamate[2]		X	X	X
2,8-Dihydroxyadenine[3]		X	X	X
3-Methoxy-4-hydroxyphenylacetaldehydeOglucuronide[4]			X	X
General Olfaction Score			X	X
MPV			X	X
Urea			X	X
Neck circumference			X	X
L-Pyrrolysine[5]				X
Left Entorhinal Cortex Volume				X
Ureidoarcylic Acid[6]				X
Diethanolamine[7]				X
Vision				X
SHBG				X
Histidinyl Aspartate[8]				X

[1]Dementia Metabolite B Saliva
[2]Dementia Metabolite C Saliva
[3]AD Metabolite A Serum

[4]Dementia Metabolite C Serum
[5]Dementia Metabolite A Saliva
[6]Dementia Metabolite A Serum
[7]MCI Metabolite B Saliva
[8]Dementia Metabolite B Serum

Figures

Figure 4-1. Flowchart of the analysis procedures for predicting AD (Research Goals 1 and 2), MCI (Research Goals 3 and 4), and dementia (Research Goals 5 and 6)

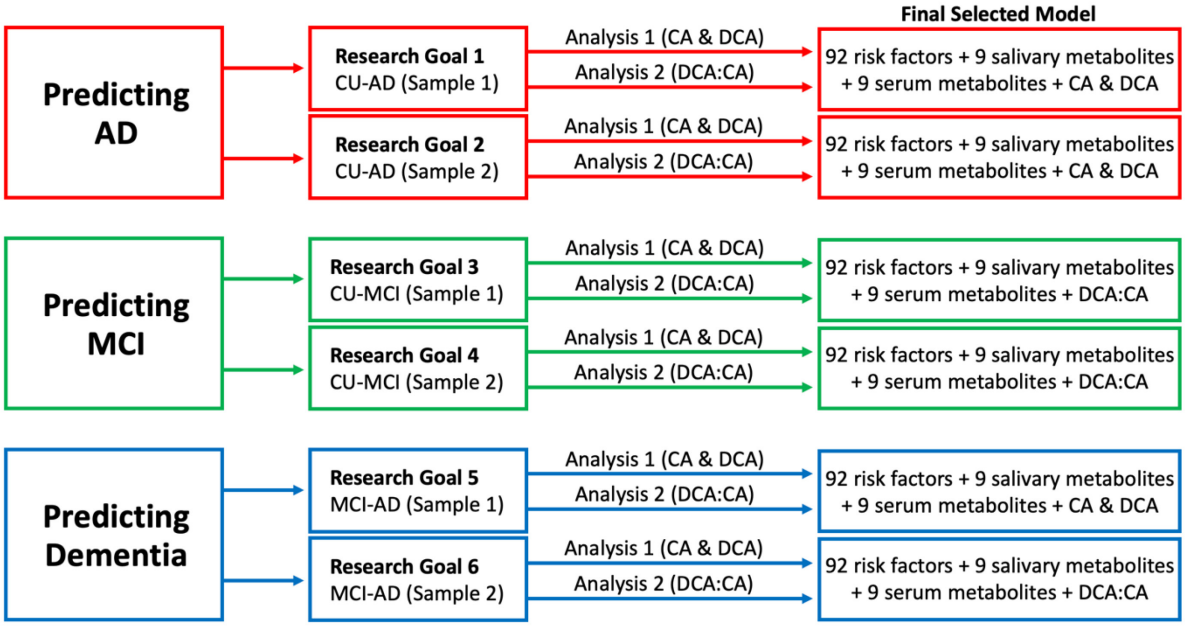

Figure 1. Flowchart illustrating the analyses conducted for each research goal. Each prediction (AD, MCI, dementia) was comprised of two research goals: one for each sample in the analysis. For each research goal, two analyses were conducted: including CA and DCA and including the DCA:CA ratio only. The final model that was selected and reported in the dissertation (with CA and DCA or with the ratio) for each research goal is shown in the far-right column.

Figure 4-2. SHAP Waterfall Plot for Research Goal 1 including CA and DCA (no DCA:CA ratio) for CU-AD for **Sample 1**

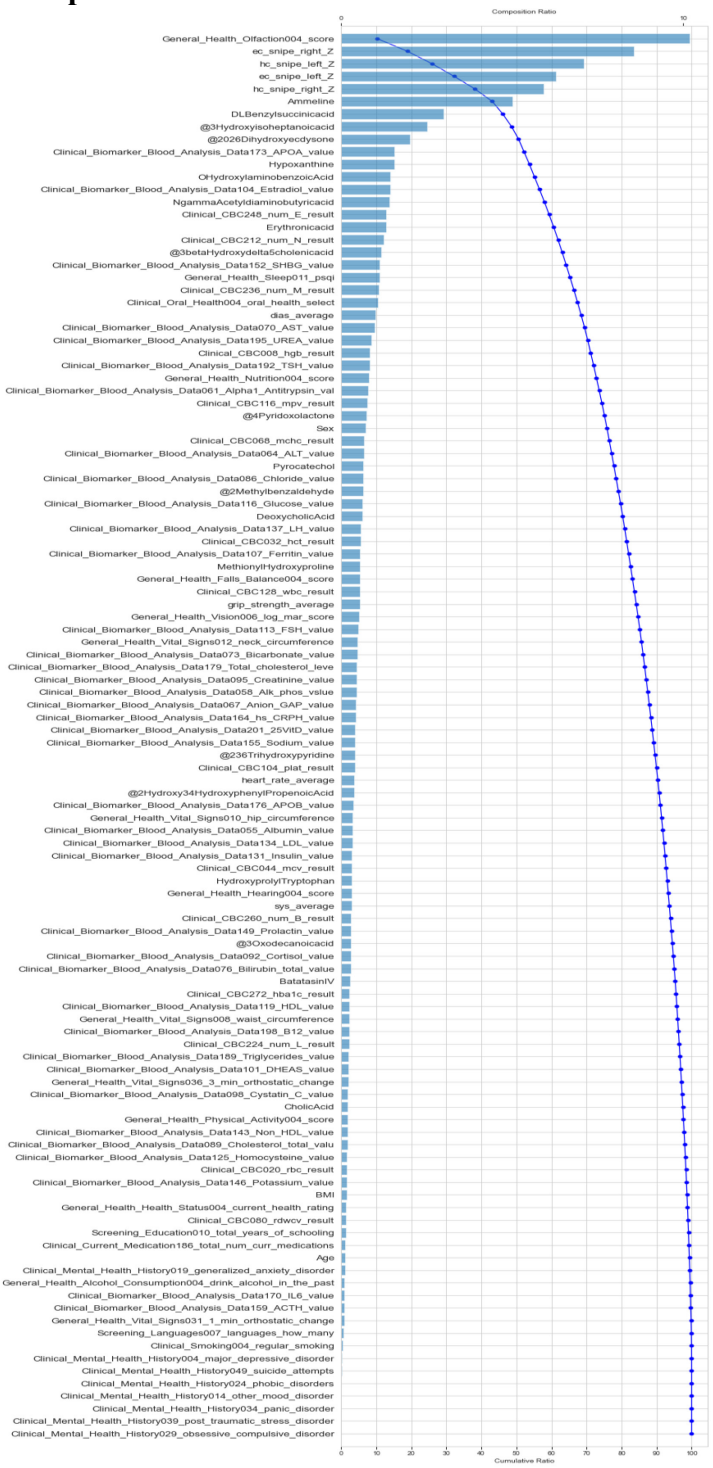

Figure 2. Tree SHAP Waterfall Plot showing the composition (top x-axis) and cumulative (bottom x-axis) ratios for the 112 baseline predictors tested in the random forest classifier model. Predictors are shown in descending order of importance and their individual composition ratio (individual contribution to the model prediction) is indicated by the blue bars. The blue curved line indicates the cumulative ratio for each additional predictor.

Figure 4-3. SHAP Summary Plot for Research Goal 1 including CA and DCA (no DCA:CA ratio) for CU-AD for **Sample 1**

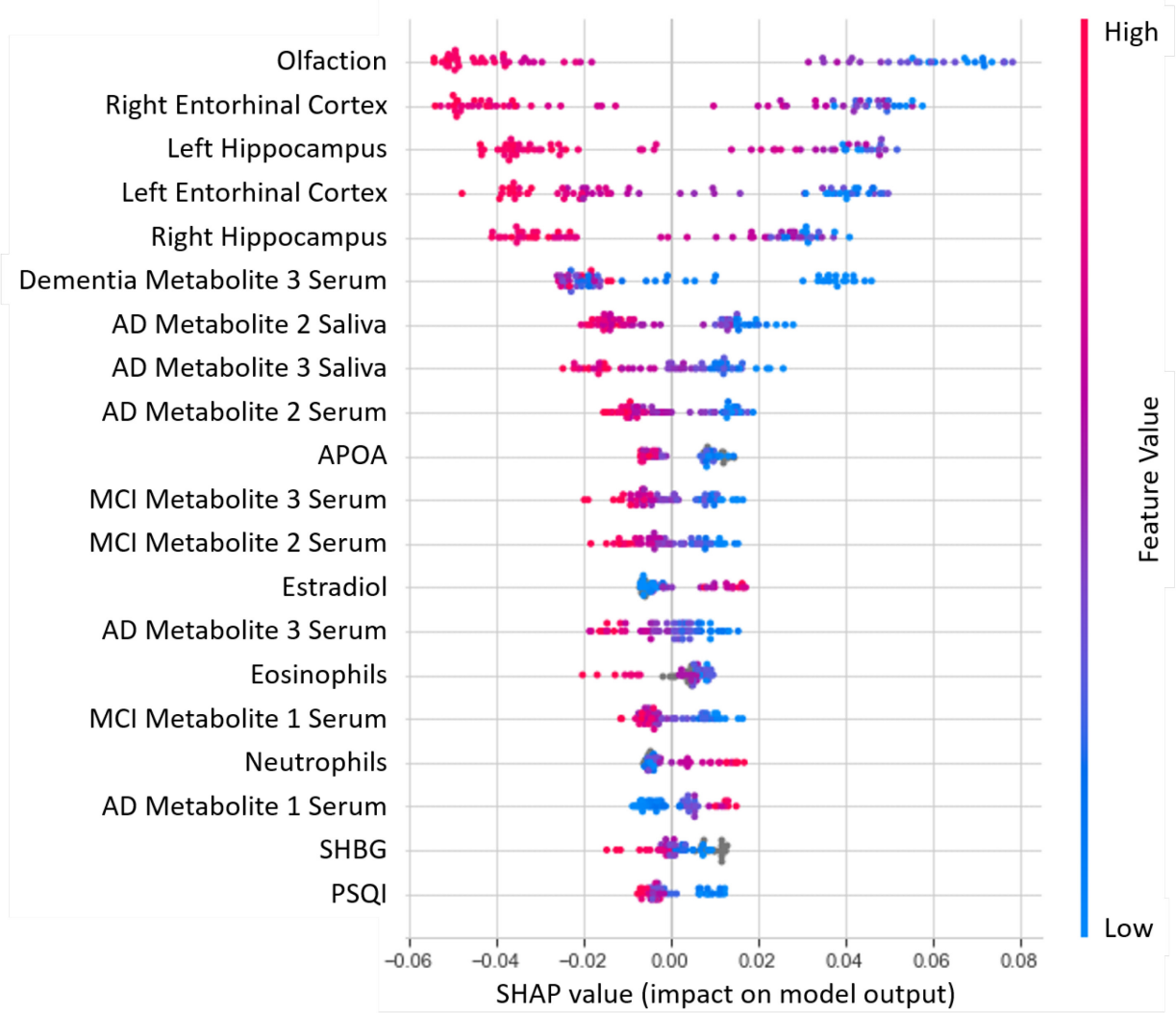

Figure 3. Tree SHAP Summary Plot showing the twenty most important predictors of AD in Sample 1. Predictors are shown in descending order of importance. Each individual point on the plot represents a participant's Tree SHAP value for that predictor (bottom x-axis for scale). The position of the points indicates the effect on the model prediction. Specifically, Tree SHAP values over 0 (to the right of the figure) predict AD. The colour of the dots indicates the direction of the effect for each predictor shown (red = higher values, blue = lower values, grey = imputed values).

Figure 4-4. SHAP Waterfall Plot for Research Goal 2 including CA and DCA (no DCA:CA ratio) for CU-AD for **Sample 2**

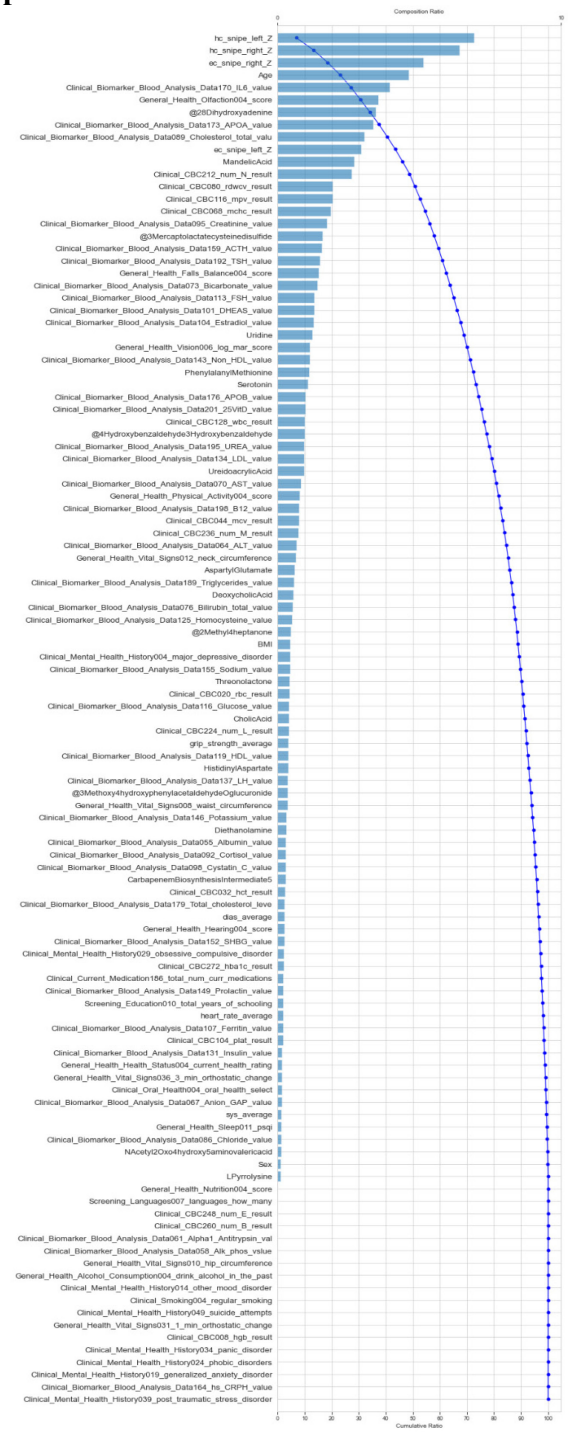

Figure 4. Tree SHAP Waterfall Plot showing the composition (top x-axis) and cumulative (bottom x-axis) ratios for the 112 baseline predictors tested in the random forest classifier model. Predictors are shown in descending order of importance and their individual composition ratio (individual contribution to the model prediction) is indicated by the blue bars. The blue curved line indicates the cumulative ratio for each additional predictor.

Figure 4-5. SHAP Summary Plot for Research Goal 2 including CA and DCA (no DCA:CA ratio) for CU-AD for **Sample 2**

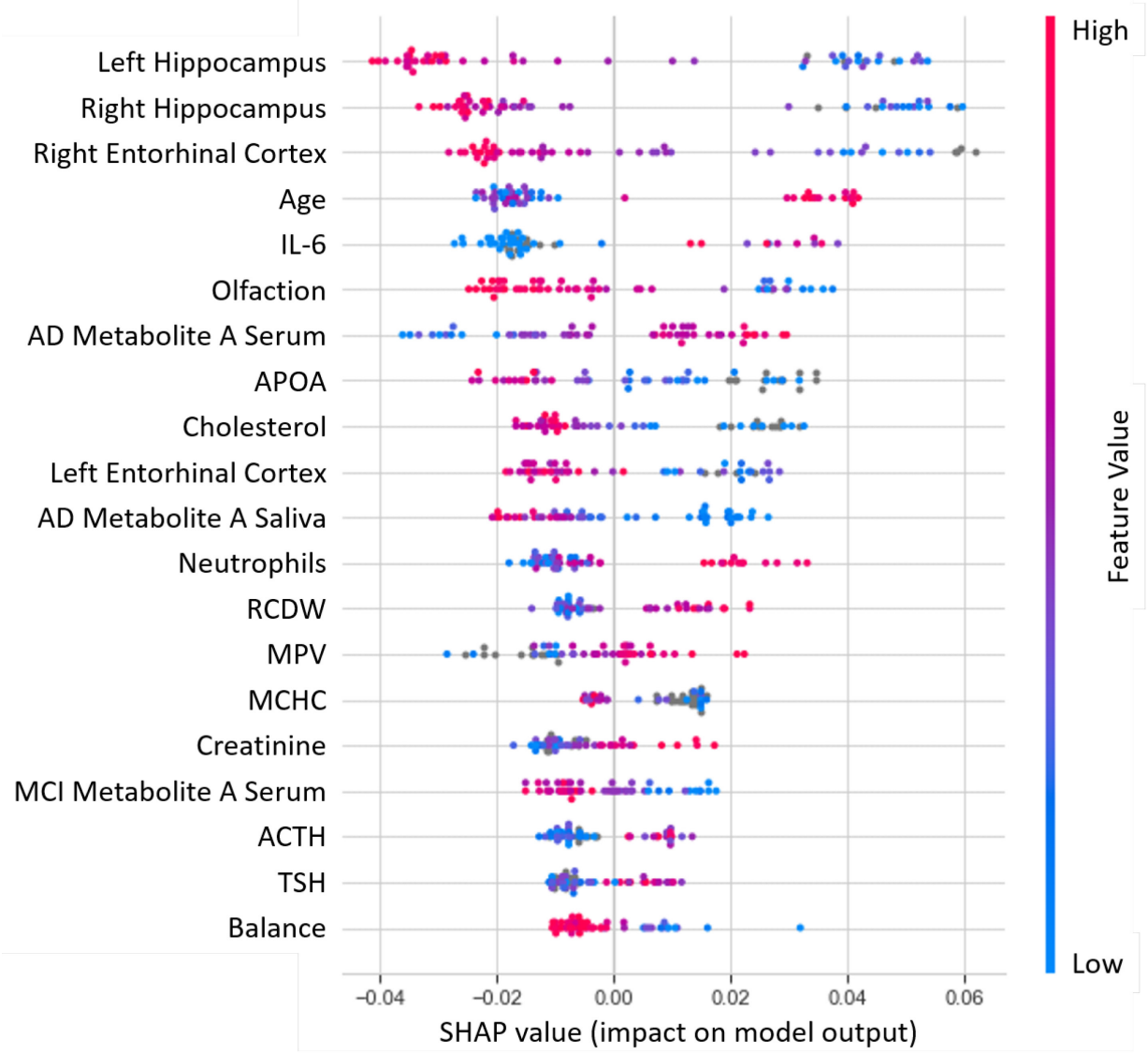

Figure 5. Tree SHAP Summary Plot showing the twenty most important predictors of AD in Sample 2. Predictors are shown in descending order of importance. Each individual point on the plot represents a participant's Tree SHAP value for that predictor (bottom x-axis for scale). The position of the points indicates the effect on the model prediction. Specifically, Tree SHAP values over 0 (to the right of the figure) predict AD. The colour of the dots indicates the direction of the effect for each predictor shown (red = higher values, blue = lower values, grey = imputed values).

Figure 4-6. SHAP Waterfall Plot for Research Goal 3 including DCA:CA ratio for CU-MCI for **Sample 1**

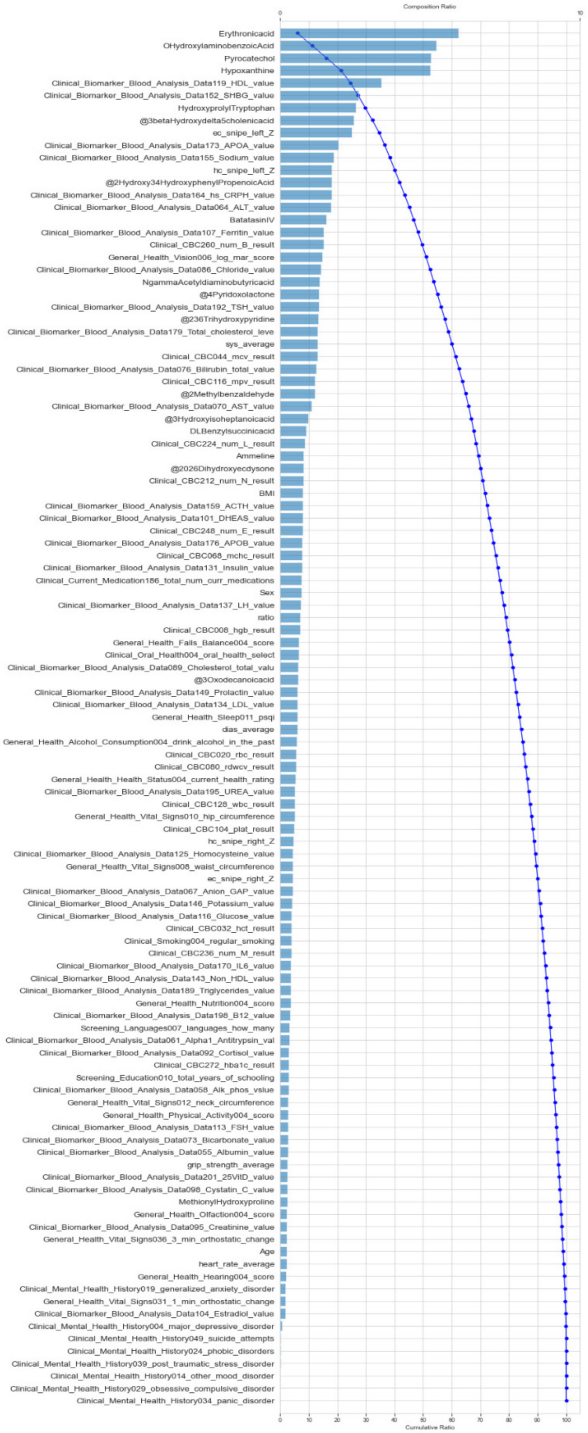

Figure 6. Tree SHAP Waterfall Plot showing the composition (top x-axis) and cumulative (bottom x-axis) ratios for the 111 baseline predictors tested in the random forest classifier model. Predictors are shown in descending order of importance and their individual composition ratio (individual contribution to the model prediction) is indicated by the blue bars. The blue curved line indicates the cumulative ratio for each additional predictor.

Figure 4-7. SHAP Summary Plot for Research Goal 3 for CU-MCI including DCA:CA ratio for **Sample 1**

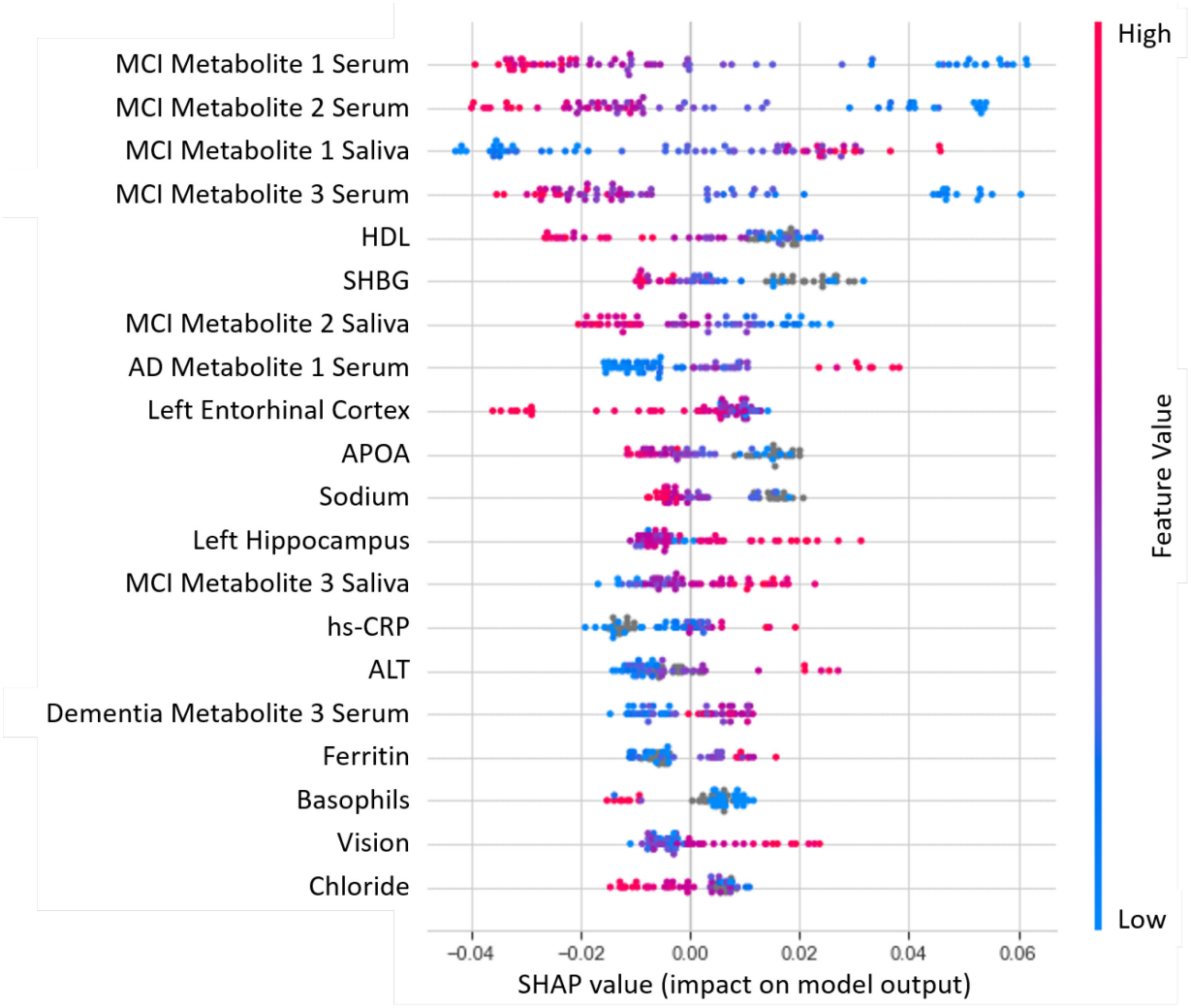

Figure 7. Tree SHAP Summary Plot showing the twenty most important predictors of MCI in Sample 1. Predictors are shown in descending order of importance. Each individual point on the plot represents a participant's Tree SHAP value for that predictor (bottom x-axis for scale). The position of the points indicates the effect on the model prediction. Specifically, Tree SHAP values over 0 (to the right of the figure) predict MCI. The colour of the dots indicates the direction of the effect for each predictor shown (red = higher values, blue = lower values, grey = imputed values).

Figure 4-8. SHAP Waterfall Plot for Research Goal 4 including DCA:CA ratio for CU-MCI for **Sample 2**

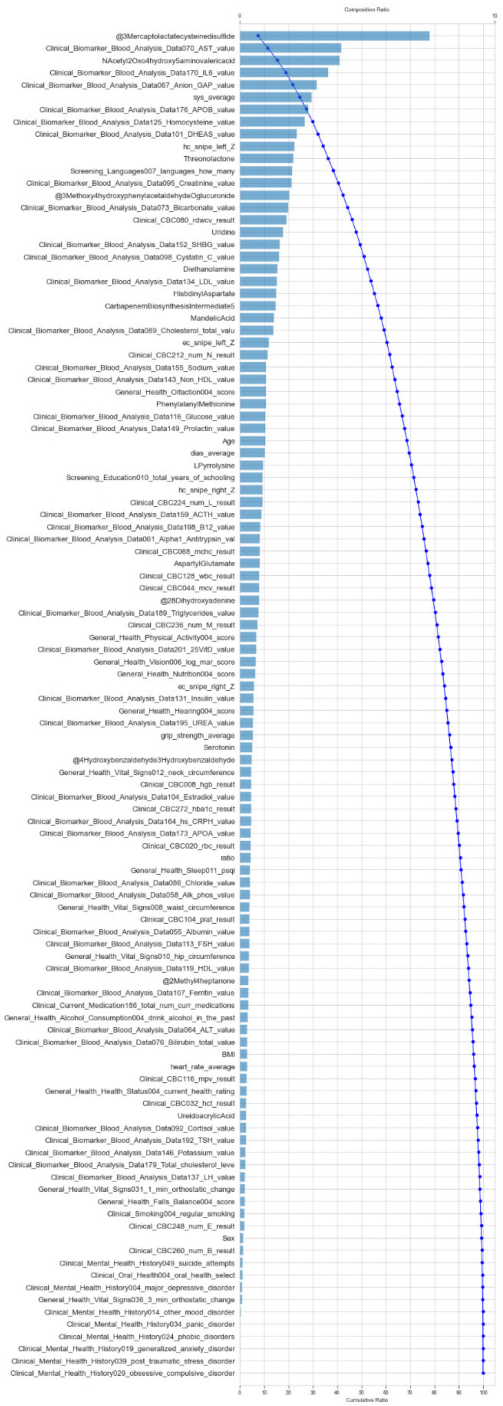

Figure 8. Tree SHAP Waterfall Plot showing the composition (top x-axis) and cumulative (bottom x-axis) ratios for the 111 baseline predictors tested in the random forest classifier model. Predictors are shown in descending order of importance and their individual composition ratio (individual contribution to the model prediction) is indicated by the blue bars. The blue curved line indicates the cumulative ratio for each additional predictor.

Figure 4-9. SHAP Summary Plot for Research Goal 4 including DCA:CA ratio for CU-MCI for **Sample 2**

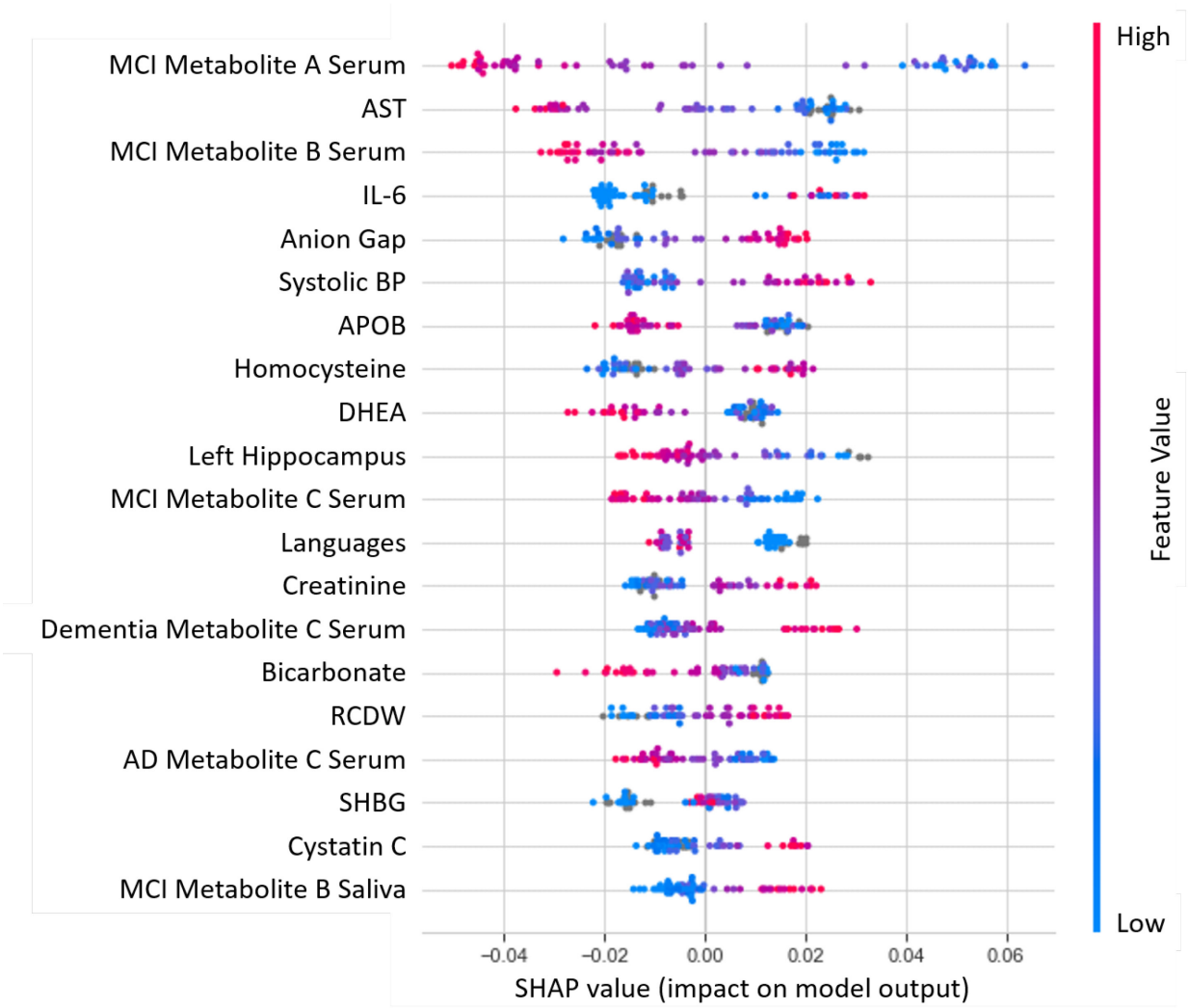

Figure 9. Tree SHAP Summary Plot showing the twenty most important predictors of MCI in Sample 2. Predictors are shown in descending order of importance. Each individual point on the plot represents a participant's Tree SHAP value for that predictor (bottom x-axis for scale). The position of the points indicates the effect on the model prediction. Specifically, Tree SHAP values over 0 (to the right of the figure) predict MCI. The colour of the dots indicates the direction of the effect for each predictor shown (red = higher values, blue = lower values, grey = imputed values).

Figure 4-10. SHAP Waterfall Plot for Research Goal 5 including CA and DCA (no DCA:CA ratio) for MCI-AD for **Sample 1**

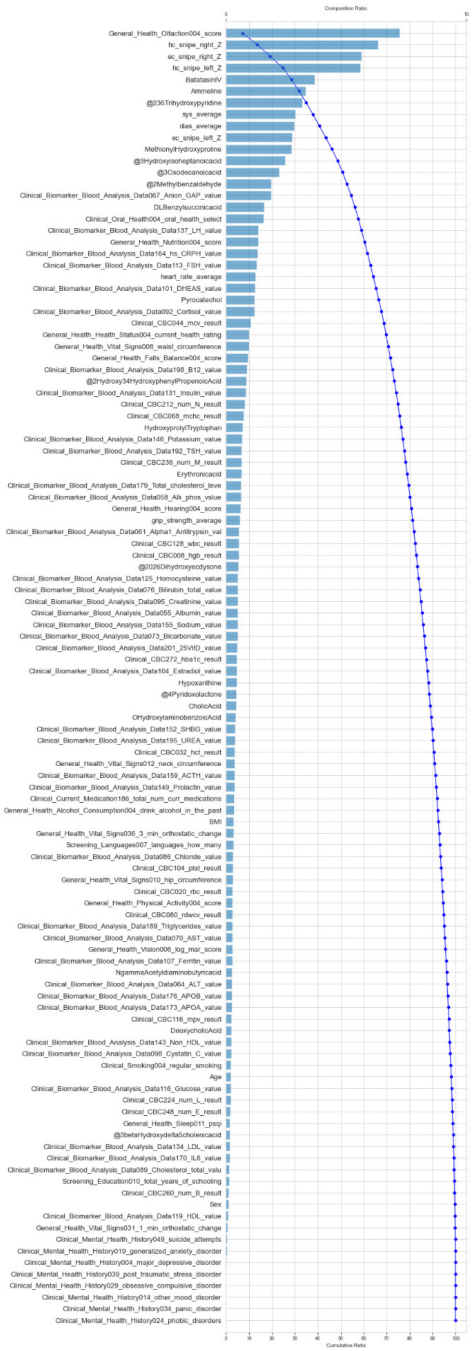

Figure 10. Tree SHAP Waterfall Plot showing the composition (top x-axis) and cumulative (bottom x-axis) ratios for the 112 baseline predictors tested in the random forest classifier model. Predictors are shown in descending order of importance and their individual composition ratio (individual contribution to the model prediction) is indicated by the blue bars. The blue curved line indicates the cumulative ratio for each additional predictor.

Figure 4-11. SHAP Summary Plot for Research Goal 5 including CA and DCA (no DCA:CA ratio) for MCI-AD for **Sample 1**

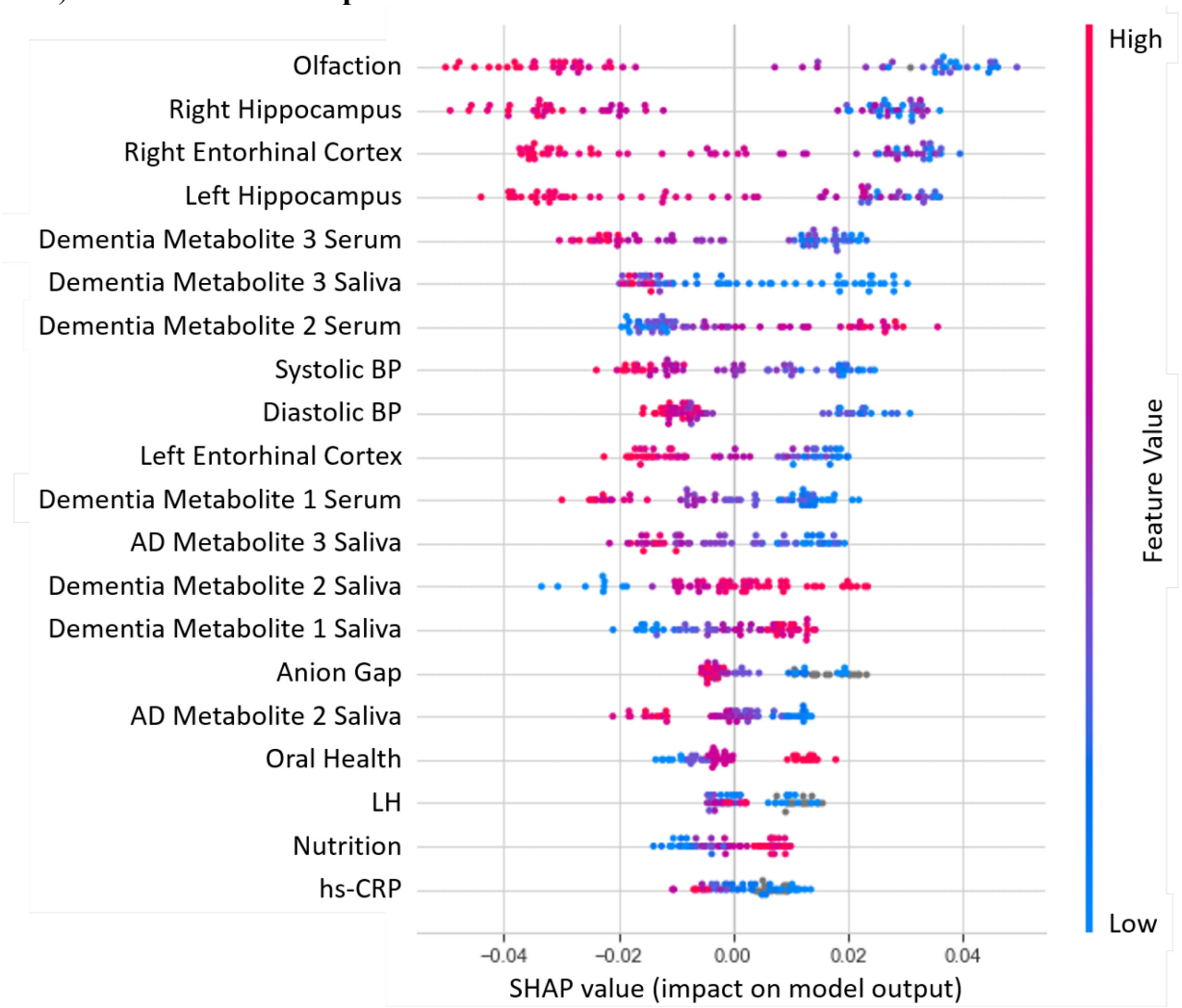

Figure 11. Tree SHAP Summary Plot showing the twenty most important predictors of dementia in Sample 1. Predictors are shown in descending order of importance. Each individual point on the plot represents a participant's Tree SHAP value for that predictor (bottom x-axis for scale). The position of the points indicates the effect on the model prediction. Specifically, Tree SHAP values over 0 (to the right of the figure) predict dementia. The colour of the dots indicates the direction of the effect for each predictor shown (red = higher values, blue = lower values, grey = imputed values).

Figure 4-12. SHAP Waterfall Plot for Research Goal 6 including DCA:CA ratio for MCI-AD for **Sample 2**

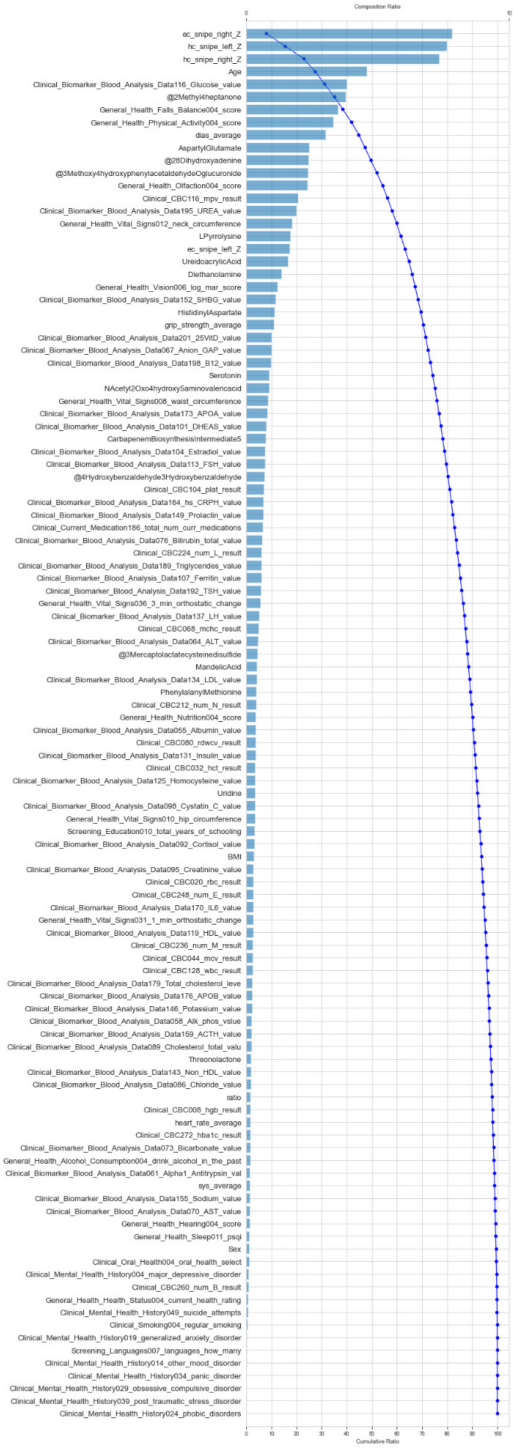

Figure 12. Tree SHAP Waterfall Plot showing the composition (top x-axis) and cumulative (bottom x-axis) ratios for the 111 baseline predictors tested in the random forest classifier model. Predictors are shown in descending order of importance and their individual composition ratio (individual contribution to the model prediction) is indicated by the blue bars. The blue curved line indicates the cumulative ratio for each additional predictor.

Figure 4-13. SHAP Summary Plot for Research Goal 6 including DCA:CA ratio for MCI-AD for **Sample 2**

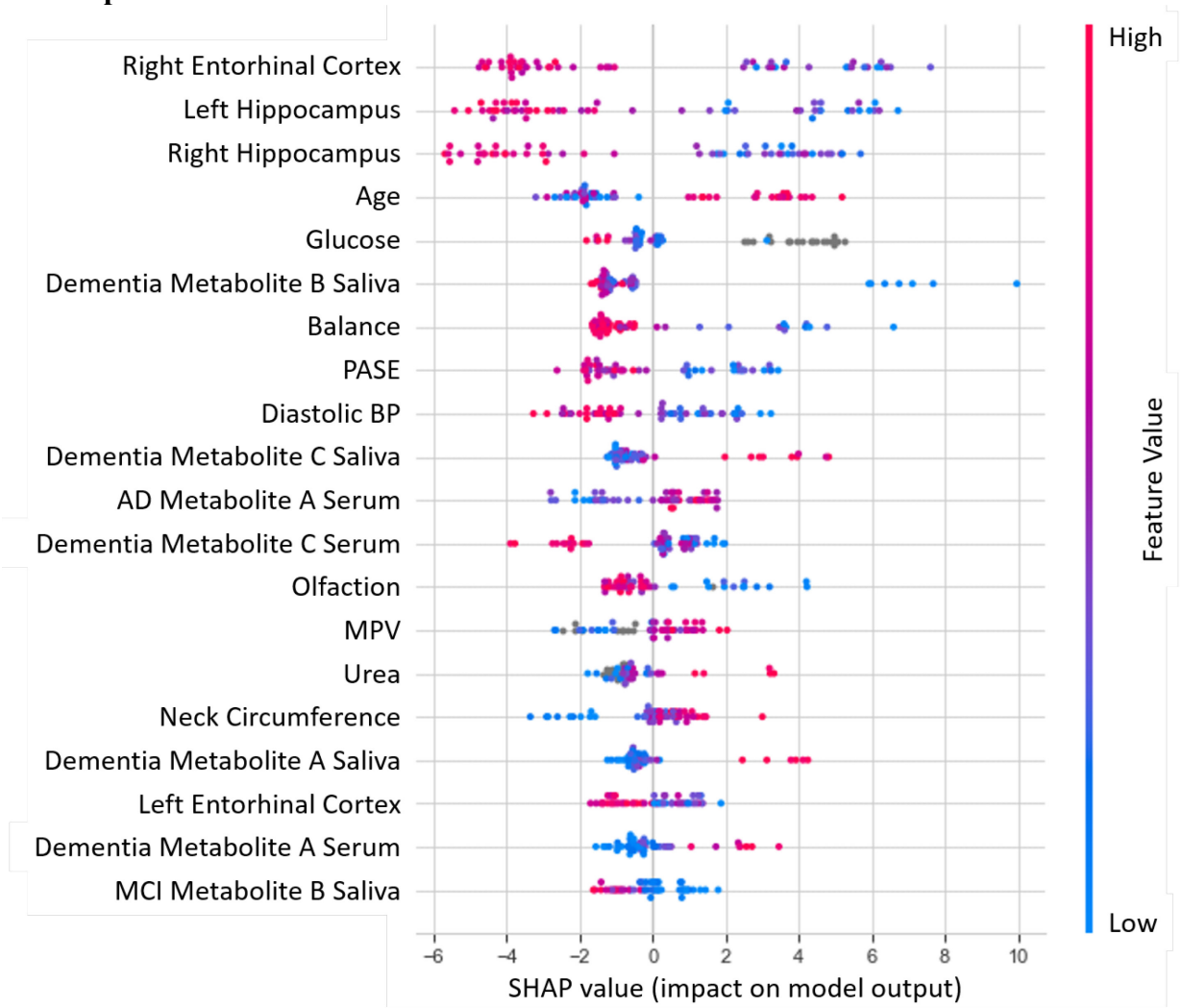

Figure 13. Tree SHAP Summary Plot showing the twenty most important predictors of dementia in Sample 2. Predictors are shown in descending order of importance. Each individual point on the plot represents a participant's Tree SHAP value for that predictor (bottom x-axis for scale). The position of the points indicates the effect on the model prediction. Specifically, Tree SHAP values over 0 (to the right of the figure) predict dementia. The colour of the dots indicates the direction of the effect for each predictor shown (red = higher values, blue = lower values, grey = imputed values).

Chapter 5: General Discussion

The dissertation work represents three thematically and analytically linked studies aimed at examining the heterogeneous trajectories and outcomes associated with brain and cognitive aging across asymptomatic phases and the AD clinical spectrum. We achieved this aim in a series of three data-driven studies featuring two large-scale datasets (one longitudinal [ADNI], one cross-sectional [COMPASS-ND]). The specific aims, results, and details of each of the three studies are discussed in Chapter Two, Three, and Four. The current chapter will provide a broad integrative overview of the findings and conclusions of the dissertation work.

In Study 1 (published as Drouin et al., 2022), we employed two analytic phases on longitudinal volumetric imaging (MRI) and baseline multi-modal biomarker data from ADNI for a sample of 351 cognitively normal older adults spanning a 35-year band of aging (60-95 years old). In the first analytic phase, we used a data-driven classification approach to longitudinal trajectory data. The aim was to identify statistically separable and distinct classes for both right and left hippocampal volume trajectories. We identified three separable classes (low, middle, high) of hippocampal volume trajectories for both the left and right hippocampus. These classes were statistically different in intercept (LHC Class 1: 2.5, LHC Class 2: 2.14, LHC Class 3: 1.79; RHC Class 1: 2.53, RHC Class 2: 2.21, RHC Class 3: 1.83) and slope (LHC Class 1: -0.02, LHC Class 2: -0.03, LHC Class 3: -0.03; RHC Class 1: -0.02, RHC Class 2: -0.03, RHC Class 3: -0.03). Our results were concordant with previous evidence of a more preserved right hippocampus in cognitively normal adults (i.e., higher intercept and slope across all classes) (J. Barnes et al., 2005; Cherbuin et al., 2010; Cherbuin, Sargent-Cox, Easteal, et al., 2015). An important extension of prior research is the evidence that cognitively normal older adults can be objectively classified into constituent trajectory classes of hippocampal volume change.

In the second phase, we used random forest classification to test a large multi-modal roster of AD-related biomarkers and risk factors in a computationally competitive machine learning context. As older adults belonging to the least atrophied (most preserved) hippocampal trajectory classes may have lower exposure to AD risk factors, our main aim was to detect the leading biomarkers and risk which predicted the highest (least atrophied) as compared to the lowest (most atrophied) hippocampal trajectory classes. Our results indicated that three biomarker predictors from two modalities were robust across hemispheres. These predictors were sex, plasma Aβ1-42, and education. Moreover, four biomarkers from three modalities uniquely predicted left hippocampal trajectory class. These predictors were plasma Aβ1-40, plasma t-tau, the geriatric depression scale score, and BMI. These findings provide novel information about (a) differential predictors of left and right hippocampal trajectory classes and (b) the leading predictors that emerge when considered in a computationally competitive context with other AD-related risk factors and biomarkers.

Several of the identified predictors in this study (i.e., sex, plasma Aβ1-42, plasma Aβ1-40, depressive symptoms, BMI) were consistent with previous results in the ADRD literature and extend these findings to be predictive of desirable HC trajectory patterns in cognitively normal older adults. Other predictors (i.e., education, plasma t-tau) revealed novel patterns of hippocampal trajectory classes that should be explored in future studies. In sum, Study 1 employed a two-phased data-driven analytic approach using cognitively normal adults to produce evidence for three underlying or latent classes of hippocampal atrophy. Our analytic approach, which was based on the simultaneous consideration of level and slope, produced trajectory classes which capture the individual variability in longitudinal hippocampal atrophy. We identified several AD-related biomarkers and risk factors and determined their relative

importance in discriminating between the potentially protective higher HC trajectory class and the potentially risk-elevated lower HC trajectory class.

In Study 2, we employed a sequential pre-analytic and analytic plan. First, we identified statistically discriminable classes of hippocampal (left and right) volume and cognitive (memory and executive function) trajectories. In this pre-analytic phase, we identified two classes of left and right hippocampal trajectories and two classes of cognitive trajectories. Based on each participant's membership to the identified data-driven classes, they were classified into one of four groups: cognitively resilient, cognitively vulnerable, brain and cognitively low/declining, or brain and cognitively stable. Older adults who were low on hippocampal trajectories, but high cognitive trajectories, were classified as cognitively resilient (n = 72). Older adults who were high and stable on hippocampal trajectories and but low on cognitive trajectories were classified as cognitively vulnerable (n = 144). Older adults who were low and declining for both hippocampal trajectories and cognitive trajectories were classified as brain and cognitively low/declining (n = 107). Older adults who were high and stable on both hippocampal trajectories and cognitive trajectories were classified as brain and cognitively stable (n = 92).

As our main analytic plan, we then used three ML algorithms to identify key predictors of these trajectory classes from a multi-modal roster of baseline risk factors and biomarkers. These ML algorithms were random forest (RF), gradient boosting (GB), and k-nearest neighbours (KNN). We then identified and interpreted the leading predictors of cognitive resilience (Research Goal 1), cognitive vulnerability (Research Goal 2), and brain and cognitive stability (Research Goal 3) using a set of ML algorithms (RF, GB, KNN) and Tree SHAP values.

For our first research goal, the GB model was selected as the best model and higher CSF Aβ1-42, higher education, lower plasma Aβ1-42, lower CSF p-tau, lower plasma Aβ1-40, and

lower age were the six leading predictors of cognitive resilience. Notably, conventional AD biomarkers such as CSF p-tau and CSF Aβ1-42 emerged as important predictors of this aging trajectory. Additionally, peripheral markers of amyloid deposition (plasma Aβ1-40 and plasma Aβ1-42) were also featured as top predictors. These results indicate that markers of amyloid and tau neuropathology (in CSF and serum) are also indicative of cognitive trajectories in the context of adverse hippocampal trajectories in cognitively normal older adults. Moreover, two demographic predictors (education and age) were amongst the six leading predictors – with education appearing as the second leading predictor after CSF Aβ1-42. Previous findings have consistently linked higher educational attainment with resilience to AD-related adversity – an association hypothesized to be related to cognitive reserve (K. J. Anstey, 2014; K. J. Anstey & Dixon, 2021; Kaarin J. Anstey et al., 2015; Stern, 2012).

For our second research goal, we identified the RF model as best performing. Lower education, higher plasma Aβ1-40, higher BMI, higher age, lower glucose, higher plasma Aβ1-42 were identified as the six leading predictors of cognitive vulnerability. In this study, we explore a unique and previously unexamined aging trajectory pattern characterized by low and declining cognitive trajectories coupled with intact hippocampal trajectories (i.e., little to no hippocampal adversity). Notably, in this research goal, lower education was identified as the leading predictor of cognitive vulnerability. Coupled with our findings in our first research goal, our findings provide further evidence that education is a strong and robust predictor of two opposing aging trajectories (cognitive resilience and cognitive vulnerability), whereby higher levels of this important early life factor provide a form of protection in the face of AD-related neurodegeneration (i.e., hippocampal atrophy) and lower levels may put older adults at risk of declining cognitive trajectories despite very little neurodegeneration.

For our third research goal, we identified RF as the best performing ML algorithm. We identified higher CSF Aβ1-42, lower polygenic risk score, female sex, higher plasma Aβ1-42, higher pulse pressure, and lower age as the six leading predictors of brain and cognitive stability. Although predictors of stability in cognition and brain health among aging adults has been independently investigated in the context of successful aging, predictors for aging trajectories characterized by the simultaneous stability in hippocampal volume and cognition had not been previously explored. Our results extend previous findings and identify predictors of trajectories characterized by high levels and stability in both favourable aging trajectories.

Younger age, lower AD genetic risk, and female sex have been previously linked with successful cognitive trajectories (Goveas et al., 2016; Josefsson et al., 2012; G. P. McFall et al., 2019). Our results indicate that these same predictors extend to cognitive and hippocampal stability. In addition, two conventional AD biomarkers emerged as important predictors of brain and cognitive stability (higher CSF Aβ1-42, higher plasma Aβ1-42). This finding underscores how factors contributing to brain and cognitive stability are likely to also be associated (in opposite directions) with increased risk of pathological aging outcomes, such as MCI and AD. The investigation of stable brain and cognitive trajectories can help provide a broader and more comprehensive perspective on heterogeneous aging trajectories, including pathological and non-normal outcomes. In sum, Study 2 employed an analytic phase consisting of two pre-analytic foundational goals (latent class growth analyses) followed by a series of three main research goals (machine learning algorithms). In a computationally competitive context, we identified several predictors from multiple AD-related risk domains associated with cognitive resilience, cognitive vulnerability, and brain and cognitive stability.

Study 1 and 2 utilized a similar roster of baseline predictors from ADNI (with the addition of polygenic risk score, race, marital status, heart rate and respiratory rate in Study 2). In addition, a similar sample of participants was used: however, Study 2 used a larger sample of cognitively normal individuals who provided MRI data that was processed using NOMIS. NOMIS is a MRI tool which generates Z-scores for volumetric measures. They represent deviations from normality while accounting for several confounding characteristics (i.e., sex, age, intracranial volume, image resolution, image contrast-to-noise ratio, and surface reconstruction defect holes) (Potvin et al., 2021). As such, the NOMIS processed data had less bias and variability in volumetric measures as it accounts for variations in scanner vendor, magnetic field strength, image quality, and intracranial volume. Four risk factors and biomarkers emerged as leading predictors in both studies. These were sex, plasma Aβ1-40, plasma Aβ1-42 and education. Female sex predicted the least atrophied class in Study 1 and brain and cognitive stability in Study 2. Our findings in Study 2 extend that of Study 1 in that female sex presents an advantage in both brain health in aging but also the maintenance of cognitive function.

Higher levels of plasma Aβ1-42 predicted the least atrophied class in Study 1 and predicted cognitive vulnerability and brain and cognitive stability in Study 2. Lower levels of AB1-42 predicted cognitive resilience. Similarly, higher levels of plasma Aβ1-40 predicted the least atrophied class in Study 1 and cognitive vulnerability in Study 2. Lower levels of plasma Aβ1-40 predicted resilience. Together, these findings indicate a robust prediction association between higher levels of Aβ1-42 and Aβ1-40 and stable hippocampal trajectories. Education followed an unexpected pattern in Study 1, whereby lower education predicted the least atrophied hippocampal trajectory class. Conversely, in Study 2, higher education predicted cognitive resilience and lower education predicted cognitive vulnerability. Study 2 results

provide further confirmation that the unexpected education association identified in Study 1 may have been due to the intracranial volume adjustment used to account for head size and sex. Special attention should be paid to intracranial volume controls in future studies as they may produce unexpected patterns between volume measurements and other AD-related factors. Plasma tau, depressive symptoms, and BMI only emerged as predictors in Study 1 when investigating hippocampal trajectory patterns. These findings highlight how AD-related predictors may be differentially associated with (a) hippocampal trajectories and (b) hippocampal trajectories considered simultaneously with cognitive trajectory patterns. In Study 3, we advance our approach by applying data-driven ML algorithms to examine the full AD spectrum (CN, MCI, AD) and associated predictors.

Study 3 was conducted in the context of the Canadian Consortium on Neurodegeneration in Aging study, using a database known as COMPASS-ND (Chertkow et al., 2019). We assembled a large (p = 111 and 112) predictor roster of multi-modal risk factors and biomarkers in conjunction with previously identified metabolite compounds and bile acids. Our overall research aim was to apply a set of three ML algorithms (RF, GB, KNN) to test the relative predictor importance of risk factors and biomarkers as well as candidate (saliva and serum) metabolite and (serum) bile acid data in discriminating between CU (n_1 = 33; n_2 = 32), MCI (n_1 = 33; n_2 = 33), and AD (n_1 = 33; n_2 = 21) cohorts. To do this, we conducted a series of three research goals in each sample (Research Goal 1 [AD], 3 [MCI], and 5 [Dementia]: Sample 1; Research Goal 2 [AD], 4 [MCI], and 6 [Dementia]: Sample 2).

In this summary we review the predictors identified and their associated domains of risk corresponding to the most restrictive model explanation criterion (40%; Results from additional criteria are reported in the chapter). For our first research goal, six predictors (one metabolite)

from three domains (sensory, imaging, and metabolomics) explained 40% of the model predicting AD in Sample 1. The leading five predictors for RG 1 were: lower general olfaction score, lower right EC volume, lower left HC volume, lower left EC volume, and lower right HC volume. For our second research goal, nine predictors (one metabolite) from five domains (imaging, demographic, and clinical health, sensory, and metabolomics) explained 40% of model predicting AD in Sample 2. The leading five predictors for RG 2 were: lower left HC volume, lower right HC volume, lower right EC volume, higher age, and higher IL-6.

For our third research goal, 12 predictors (six metabolites) from three domains (metabolomics, clinical health, and imaging) explained 40% of the model predicting MCI in Sample 1. The leading five predictors for RG 3 were: lower MCI Metabolite 1 Serum, lower MCI Metabolite 2 Serum, higher MCI Metabolite 1 Saliva, lower MCI Metabolite 3 Serum, and lower HDL. For our fourth research goal, 13 predictors (three metabolites) from five domains (metabolomics, clinical health, vascular/metabolic, imaging, and demographic) explained 40% of the model predicting MCI in Sample 2. The leading five predictors for RG 4 were: lower MCI Metabolite A Serum, lower AST, lower MCI Metabolite B Serum, higher IL-6, and higher anion gap.

For our fifth research goal, nine predictors (three metabolites) from four domains (sensory, imaging, metabolomics, and vascular/metabolic) explained 40% of the model predicting dementia in Sample 1. The leading five predictors for RG 5 were: lower general olfaction score, lower right HC volume, lower right EC volume, lower left HC volume, and lower Dementia Metabolite 3 Serum. For our sixth research goal, nine predictors (one metabolite) from seven domains (imaging, demographic, clinical health, metabolomics, gait/function, lifestyle, and vascular/metabolic) explained 40% of the model predicting dementia

in Sample 2. The leading five predictors for RG 6 were: lower right EC volume, lower left HC volume, lower right HC volume, higher age, and lower glucose.

Overall, several of the leading predictors of AD, MCI and dementia in this study have been identified in previous research in ADRD literature. Examples include HC and EC volume, age, IL-6, glucose, olfaction, anion gap, AST, and HDL (Chang et al., 2017; Fraser et al., 2021; Lim, Krajina, & Marsland, 2013; Lyra e Silva et al., 2021; Marsillach et al., 2020; Martinez et al., 2023; Supasitthumrong et al., 2019; Zhao et al., 2019). In addition, we identified several novel predictors of AD, MCI, and dementia originating from the metabolomics domain, which potentially reflect early changes in AD-related molecular pathways. Our results also indicate that metabolomics predictors seem to be especially important in the prediction of MCI, representing a potential preclinical window when metabolic perturbations are highly indicative of cognitive impairment. All metabolite compounds emerging within the leading five predictors were previously identified as one of the leading compounds discriminating between CU and MCI in previous metabolomics studies (Zhang, Drouin, Dixon & Li, 2022; Zhang, Drouin, Li & Dixon, 2022). Our results of this research goal provide evidence that these metabolite compounds (a) are the leading compounds predicting MCI (as opposed to the other tested compounds), and (b) have a stronger effect on the prediction of MCI than other AD-related risk factors and biomarkers (including imaging markers). Our findings underscore the importance of investigating established risk factors and biomarkers as well as novel metabolite predictors and their respective mechanisms alongside other AD-related risk factors. Future work should aim to further investigate these leading predictors and other predictors in the same domains of risk to advance our understanding of their mechanistic association with AD risk.

Study 3 demonstrates several differences and extensions in comparison to Studies 1 and 2. These include: (a) the predictor roster, (b) the ML classification performance, and (c) the nature of the predicted outcomes. In comparison to Studies 1 and 2, Study 3 utilized a much larger roster of predictors which were available within the COMPASS-ND dataset for all three cohorts. In addition, we were able to include eighteen important metabolomics predictors (nine serum and nine saliva metabolite compounds) and two bile acids and their ratio (CA, DCA, DCA:CA) to the predictor roster for Study 3. These metabolomics data bolstered an already comprehensive roster of AD-related risk factors and biomarkers, which expanded the data available within ADNI used in Studies 1 and 2. However, CSF Aβ and tau measures were unavailable within COMPASS-ND due to high rates of missing data (>50%). As in Studies 1 and 2, we anticipate that these biomarkers might have emerged as among the leading predictors in the pairwise comparisons if they were more widely available for participants in this study. Two predictors which were available in both datasets (ADNI and COMPASS-ND) emerged as leading predictors in Studies 2 and 3. These were age and glucose level. For age, lower age predicted cognitive resilience and brain/cognitive stability (Study 2) while higher age predicted cognitive vulnerability (Study 2), AD (Study 3), and dementia (Study 3). For glucose level, lower glucose levels predicted cognitive vulnerability (Study 2) and dementia (Study 3). There were no common predictors that emerged between Study 1 (predicting HC trajectory classes) and Study 3 (predicting AD, MCI, dementia). Importantly, many of the leading predictors of AD and dementia in Study 3 were HC volume (the outcome of interest in Study 1).

The notably stronger performance of the ML classification metrics (precision, accuracy, recall, AUC, F1) in Study 3 as compared to Study 1 and 2 can be attributed to two main factors. First, the predictor roster in COMPASS-ND was more extensive and included additional

established predictors of MCI and AD such as olfaction, clinical markers associated with key AD-related mechanisms (e.g., inflammation and IL-6), and emerging metabolites which had been previously identified as discriminating between cohorts in a previous study. Second, the goal of Study 1 and 2 was to predict distinct secondary phenotypes of aging (e.g., hippocampal trajectory classes, cognitive resilience, cognitive vulnerability, brain/cognitive stability) which are (a) less discriminable outcomes than objective clinical diagnoses (MCI, AD) used in Study 3, and (b) likely predicted by a broader array of risk factors, including lifestyle and health predictors (e.g., social activity, living status) (McFall et al., 2019; Josefsson et al., 2012). In Study 3, we use a similar approach to identifying leading predictors as in Studies 1 and 2 but extend our previous findings by deploying these methods predicting clinical cohorts. Our data-driven ML results contribute to and extend the literature on predictors that may be associated with increased risk of MCI and AD.

Future Directions

For Study 1, future work should aim to test whether objective hippocampal trajectory classes can be considered a valid precursor condition associated with future clinical transitions. Our informal check revealed that a larger proportion of those transitioning to MCI or AD within ADNI belonged to the lowest HC trajectory classes. Regarding Study 2, future studies should aim to include predictors from a wider breadth of risk domains in the investigation of cognitive resilience, cognitive vulnerability, and brain/cognitive stability. Our results indicated mild to moderate distinguishing power (AUC = 0.64 – 0.70), and we anticipate that the inclusion of risk factors previously associated with some of these trajectories would improve classification performance. For example, lifestyle factors such as physical activity and living status have been previously used to robustly predict memory maintenance (Josefsson et al., 2012). Similarly, factors such as social activities and lifestyle (cognitive, self-maintenance, social) activities were

found to be associated with stable and declining memory aging respectively (McFall et al., 2019). The approach deployed in Study 3 could be extended to include other diagnostic groups available within COMPASS-ND, including the Parkinson's disease dementia and mixed etiology cohorts. Specifically, clusters of risk factors and biomarkers may emerge as predictive of several dementia diagnoses while other predictors may emerge as specific to specific clinical diagnoses. In addition, several of the risk factors and biomarkers included in the current roster are known to have differing effects depending on *APOE* genotype and sex, for example. When sufficient data are available within COMPASS-ND, the stratification of the cohort groups by these known AD risk factors would likely reveal novel prediction patterns consistent with a precision medicine approach.

Significance and Conclusion

Overall, the dissertation research aimed to model and predict heterogeneous outcomes in brain and cognitive aging using a data-driven approach. In Study 1 (Drouin et al., 2022), we used a large sample of CN older adults (n = 351) and identified four trajectory classes of left and right HC volume. Subsequently, we identified the leading predictors that were associated with discriminating between the lowest and highest trajectory classes. In Study 2, we detected HC and cognitive trajectory classes within a large sample of older adults (n = 451). We classified individuals as being cognitive resilient, cognitively vulnerable, low/declining, or brain and cognitively stable based on the simultaneous consideration of their HC and cognitive trajectory class membership. We then identified the most important predictors of cognitive resilience, cognitive vulnerability, and brain and cognitive stability. In Study 3, we assembled a large multi-modal roster of AD-related risk factors and biomarkers as well as metabolomics and bile acid markers for two samples and three clinical cohorts (CU, MCI, AD). We identified the leading

predictors discriminating between CU-AD, CU-MCI, and MCI-AD for each sample and examined the relative importance of metabolomics predictors when considered in a computationally competitive context with other established risk factors. Together, these studies advance our understanding of important AD-related risk factors that may contribute to (a) increased risk of undesirable trajectories in cognitively normal aging (e.g., lowest HC trajectory classes, cognitive vulnerability), (b) desirable or protective trajectories in cognitively normal aging (e.g., highest HC trajectory classes, cognitive resilience, stable brain and cognitive aging), and (c) increased risk of MCI and AD.

References

Adav, S. S., & Wang, Y. (2021). Metabolomics Signatures of Aging: Recent Advances. *Aging and Disease, 12*(2), 646.

Aiello Bowles, E. J., Crane, P. K., Walker, R. L., Chubak, J., LaCroix, A. Z., Anderson, M. L., . . . Larson, E. B. (2019). Cognitive resilience to Alzheimer's disease pathology in the human brain. *Journal of Alzheimer's Disease, 68*(3), 1071-1083.

Alabdullah, A. A., Iqbal, M., Zahid, M., Khan, K., Amin, M. N., & Jalal, F. E. (2022). Prediction of rapid chloride penetration resistance of metakaolin based high strength concrete using light GBM and XGBoost models by incorporating SHAP analysis. *Construction and Building Materials, 345*, 128296.

Albert, M. S., DeKosky, S. T., Dickson, D., Dubois, B., Feldman, H. H., Fox, N. C., . . . Petersen, R. C. (2011). The diagnosis of mild cognitive impairment due to Alzheimer's disease: recommendations from the National Institute on Aging-Alzheimer's Association workgroups on diagnostic guidelines for Alzheimer's disease. *Alzheimer's & Dementia, 7*(3), 270-279.

Albert, M. S., Jones, K., Savage, C. R., Berkman, L., Seeman, T., Blazer, D., & Rowe, J. W. (1995). Predictors of cognitive change in older persons: MacArthur studies of successful aging. *Psychology and Aging, 10*(4), 578-589.

Alcolea, D., Delaby, C., Muñoz, L., Torres, S., Estellés, T., Zhu, N., . . . Santos-Santos, M. Á. (2021). Use of plasma biomarkers for AT (N) classification of neurodegenerative dementias. *Journal of Neurology, Neurosurgery and Psychiatry, 92*(11), 1206-1214.

Alipour, H., & Goldust, M. (2016). The association between blood pressure components and cognitive functions and cognitive reserve. *Clinical and Experimental Hypertension, 38*(1), 95-99. doi:10.3109/10641963.2015.1047946

Alosco, M. L., Duskin, J., Besser, L. M., Martin, B., Chaisson, C. E., Gunstad, J., . . . Tripodis, Y. (2017). Modeling the relationships among late-life body mass index, cerebrovascular disease, and Alzheimer's disease neuropathology in an autopsy sample of 1,421 subjects from the National Alzheimer's Coordinating Center Data Set. *Journal of Alzheimer's Disease, 57*(3), 953-968.

An, L., Li, Z., Yang, Z., & Zhang, T. (2011). Cognitive deficits induced by melamine in rats. *Toxicology Letters, 206*(3), 276-280.

An, L., & Sun, W. (2017). A brief review of neurotoxicity induced by melamine. *Neurotoxicity Research, 32*, 301-309.

Anstey, K., Cherbuin, N., Budge, M., & Young, J. (2011). Body mass index in midlife and late-life as a risk factor for dementia: a meta-analysis of prospective studies. *Obesity Reviews, 12*(5), e426-e437.

Anstey, K. J. (2014). Optimizing cognitive development over the life course and preventing cognitive decline: Introducing the Cognitive Health Environment Life Course Model (CHELM). *International Journal of Behavioral Development, 38*, 1-10. doi:10.1177/0165025413512255

Anstey, K. J., Ashby-Mitchell, K., & Peters, R. (2017). Updating the evidence on the association between serum cholesterol and risk of late-life dementia: review and meta-analysis. *Journal of Alzheimer's Disease, 56*(1), 215-228.

Anstey, K. J., & Dixon, R. A. (2021). Resilience in midlife and aging. In *Handbook of the Psychology of Aging* (pp. 287-300): Elsevier.

Anstey, K. J., Ee, N., Eramudugolla, R., Jagger, C., & Peters, R. (2019). A systematic review of meta-analyses that evaluate risk factors for dementia to evaluate the quantity, quality, and global representativeness of evidence. *Journal of Alzheimer's Disease, 70*(s1), S165-S186.

Anstey, K. J., Eramudugolla, R., Hosking, D. E., Lautenschlager, N. T., & Dixon, R. A. (2015). Bridging the translation gap: From dementia risk assessment to advice on risk reduction. *J Prev Alz Dis, 2*(3), 189-198. doi:10.14283/jpad.2015.75

Anstey, K. J., Eramudugolla, R., Hosking, D. E., Lautenschlager, N. T., & Dixon, R. A. (2015). Bridging the Translation Gap: From Dementia Risk Assessment to Advice on Risk Reduction. *J Prev Alzheimers Dis, 2*(3), 189-198. doi:10.14283/jpad.2015.75

Anstey, K. J., Peters, R., Mortby, M. E., Kiely, K. M., Eramudugolla, R., Cherbuin, N., . . . Dixon, R. A. (2021). Association of sex differences in dementia risk factors with sex differences in memory decline in a population-based cohort spanning 20–76 years. *Scientific Reports, 11*(1), 7710.

Anstey, K. J., Peters, R., Zheng, L., Barnes, D. E., Brayne, C., Brodaty, H., . . . Dodge, H. (2020). Future directions for dementia risk reduction and prevention research: an international research network on dementia prevention consensus. *Journal of Alzheimer's Disease, 78*(1), 3-12.

Apostolova, L. G., Green, A. E., Babakchanian, S., Hwang, K. S., Chou, Y.-Y., Toga, A. W., & Thompson, P. M. (2012). Hippocampal atrophy and ventricular enlargement in normal aging, mild cognitive impairment and Alzheimer's disease. *Alzheimer Disease and Associated Disorders, 26*(1), 17.

Apostolova, L. G., Mosconi, L., Thompson, P. M., Green, A. E., Hwang, K. S., Ramirez, A., . . . de Leon, M. J. (2010). Subregional hippocampal atrophy predicts Alzheimer's dementia in the cognitively normal. *Neurobiology of Aging, 31*(7), 1077-1088.

Ardekani, B., Hadid, S., Blessing, E., & Bachman, A. (2019). Sexual dimorphism and hemispheric asymmetry of hippocampal volumetric integrity in normal aging and Alzheimer disease. *American Journal of Neuroradiology, 40*(2), 276-282.

Ardekani, B. A., Convit, A., & Bachman, A. H. (2016). Analysis of the MIRIAD data shows sex differences in hippocampal atrophy progression. *Journal of Alzheimer's Disease, 50*(3), 847-857.

Arenaza-Urquijo, E. M., & Vemuri, P. (2018). Resistance vs resilience to Alzheimer disease: clarifying terminology for preclinical studies. *Neurology, 90*(15), 695-703.

Atti, A. R., Palmer, K., Volpato, S., Winblad, B., De Ronchi, D., & Fratiglioni, L. (2008). Late-life body mass index and dementia incidence: nine-year follow-up data from the Kungsholmen Project. *Journal of the American Geriatrics Society, 56*(1), 111-116.

Bader, J. M., Geyer, P. E., Müller, J. B., Strauss, M. T., Koch, M., Leypoldt, F., . . . Incesoy, E. I. (2020). Proteome profiling in cerebrospinal fluid reveals novel biomarkers of Alzheimer's disease. *Molecular Systems Biology, 16*(6), e9356.

Badhwar, A., McFall, G. P., Sapkota, S., Black, S. E., Chertkow, H., Duchesne, S., . . . Bellec, P. (2020a). A multiomics approach to heterogeneity in Alzheimer′ s Disease: Focused review and roadmap. *medRxiv*, 19008615.

Badhwar, A., McFall, G. P., Sapkota, S., Black, S. E., Chertkow, H., Duchesne, S., . . . Bellec, P. (2020b). A multiomics approach to heterogeneity in Alzheimer’s disease: focused review and roadmap. *Brain, 143*(5), 1315-1331.

Barnes, D. E., & Yaffe, K. (2011). The projected effect of risk factor reduction on Alzheimer's disease prevalence. *The Lancet Neurology, 10*(9), 819-828.

Barnes, J., Scahill, R. I., Schott, J. M., Frost, C., Rossor, M. N., & Fox, N. C. (2005). Does Alzheimer's disease affect hippocampal asymmetry? Evidence from a cross-sectional and longitudinal volumetric MRI study. *Dementia and Geriatric Cognitive Disorders, 19*(5-6), 338-344.

Barnes, L. L., Wilson, R. S., Bienias, J. L., Schneider, J. A., Evans, D. A., & Bennett, D. A. (2005). Sex differences in the clinical manifestations of Alzheimer disease pathology. *Archives of General Psychiatry, 62*(6), 685-691.

Baumgart, M., Snyder, H. M., Carrillo, M. C., Fazio, S., Kim, H., & Johns, H. (2015). Summary of the evidence on modifiable risk factors for cognitive decline and dementia: A population-based perspective. *Alzheimers Dement, 11*(6), 718-726. doi:10.1016/j.jalz.2015.05.016

Beltrán, J. F., Wahba, B. M., Hose, N., Shasha, D., Kline, R. P., & Initiative, A. s. D. N. (2020). Inexpensive, non-invasive biomarkers predict Alzheimer transition using machine learning analysis of the Alzheimer's Disease Neuroimaging (ADNI) database. *PLoS One, 15*(7), e0235663.

Bennett, D., Schneider, J., Buchman, A., Barnes, L., Boyle, P., & Wilson, R. (2012). Overview and findings from the rush Memory and Aging Project. *Current Alzheimer Research, 9*(6), 646-663.

Bernard, C., Helmer, C., Dilharreguy, B., Amieva, H., Auriacombe, S., Dartigues, J.-F., . . . Catheline, G. (2014). Time course of brain volume changes in the preclinical phase of Alzheimer's disease. *Alzheimers. Dement., 10*(2), 143-151. e141.

Bischof, G. N., & Park, D. C. (2015). Obesity and aging: Consequences for cognition, brain structure and brain function. *Psychosomatic Medicine, 77*(6), 697.

Bobinski, M., De Leon, M. J., Convit, A., De Santi, S., Wegiel, J., Tarshish, C. Y., . . . Wisniewski, H. M. (1999). MRI of entorhinal cortex in mild Alzheimer's disease. *The Lancet, 353*(9146), 38-40.

Bocancea, D. I., van Loenhoud, A. C., Groot, C., Barkhof, F., van der Flier, W. M., & Ossenkoppele, R. (2021). Measuring resilience and resistance in aging and Alzheimer disease using residual methods: a systematic review and meta-analysis. *Neurology, 97*(10), 474-488.

Bohn, L., Drouin, S.M., McFall, G.P., Rolfson, D., Andrew, M.K., & Dixon, R.A. (2023). Machine learning analyses identify frailty-related morbidities that discriminate four cohorts in the Alzheimer's disease spectrum: A COMPASS-ND study. *Manuscript in Progress*.

Bohn, L., McFall, G. P., Wiebe, S. A., & Dixon, R. A. (2020). Body mass index predicts cognitive aging trajectories selectively for females: Evidence from the Victoria Longitudinal Study. *Neuropsychology, 34*(4), 388.

Boots, E. A., Schultz, S. A., Almeida, R. P., Oh, J. M., Koscik, R. L., Dowling, M. N., . . . Bendlin, B. B. (2015). Occupational complexity and cognitive reserve in a middle-aged cohort at risk for Alzheimer's disease. *Archives of Clinical Neuropsychology, 30*(7), 634-642.

Boyle, P. A., Buchman, A. S., Wilson, R. S., Leurgans, S. E., & Bennett, D. A. (2009). Association of muscle strength with the risk of Alzheimer disease and the rate of

cognitive decline in community-dwelling older persons. *Archives of Neurology, 66*(11), 1339-1344. doi:10.1001/archneurol.2009.240

Breiman, L. (2001). Random forests. *Machine Learning, 45*(1), 5-32. doi:10.1023/A:1010933404324

Bremner, J. D., Narayan, M., Anderson, E. R., Staib, L. H., Miller, H. L., & Charney, D. S. (2000). Hippocampal volume reduction in major depression. *American Journal of Psychiatry, 157*(1), 115-118.

Byun, M. S., Kim, S. E., Park, J., Yi, D., Choe, Y. M., Sohn, B. K., . . . Woo, J. I. (2015). Heterogeneity of regional brain atrophy patterns associated with distinct progression rates in Alzheimer's disease. *PloS One, 10*(11), e0142756.

Candore, G., Bulati, M., Caruso, C., Castiglia, L., Colonna-Romano, G., Di Bona, D., . . . Pellicano, M. (2010). Inflammation, cytokines, immune response, apolipoprotein E, cholesterol, and oxidative stress in Alzheimer disease: therapeutic implications. *Rejuvenation Research, 13*(2-3), 301-313.

Cantero, J. L., Iglesias, J. E., Van Leemput, K., & Atienza, M. (2016). Regional hippocampal atrophy and higher levels of plasma amyloid-beta are associated with subjective memory complaints in nondemented elderly subjects. *Journals of Gerontology Series A: Biomedical Sciences and Medical Sciences, 71*(9), 1210-1215.

Casaletto, K. B., Rentería, M. A., Pa, J., Tom, S. E., Harrati, A., Armstrong, N. M., . . . Kramer, J. (2020). Late-life physical and cognitive activities independently contribute to brain and cognitive resilience. *Journal of Alzheimer's Disease, 74*(1), 363-376.

Casserly, I., & Topol, E. J. (2004). Convergence of atherosclerosis and Alzheimer's disease: inflammation, cholesterol, and misfolded proteins. *The Lancet, 363*(9415), 1139-1146.

Chang, C. Y., Lin, C. C., Tsai, C. F., Yang, W. C., Wang, S. J., Lin, F. H., & Fuh, J. L. (2017). Cognitive impairment and hippocampal atrophy in chronic kidney disease. *Acta Neurologica Scandinavica, 136*(5), 477-485.

Cherbuin, N., Réglade-Meslin, C., Kumar, R., Sachdev, P., & Anstey, K. J. (2010). Mild cognitive disorders are associated with different patterns of brain asymmetry than normal aging: The PATH through Life Study. *Front. Psychiatry, 1*, 11.

Cherbuin, N., Sargent-Cox, K., Easteal, S., Sachdev, P., & Anstey, K. J. (2015). Hippocampal atrophy is associated with subjective memory decline: The PATH Through Life study. *The American Journal of Geriatric Psychiatry, 23*(5), 446-455.

Cherbuin, N., Sargent-Cox, K., Fraser, M., Sachdev, P., & Anstey, K. (2015). Being overweight is associated with hippocampal atrophy: the PATH Through Life Study. *International Journal of Obesity, 39*(10), 1509-1514.

Chertkow, H., Borrie, M., Whitehead, V., Black, S. E., Feldman, H. H., Gauthier, S., . . . Rockwood, K. (2019). The comprehensive assessment of neurodegeneration and dementia: Canadian cohort study. *Canadian Journal of Neurological Sciences, 46*(5), 499-511.

Chetelat, G., & Fouquet, M. (2013). Neuroimaging biomarkers for Alzheimer's disease in asymptomatic APOE4 carriers. *Revista de Neurología, 169*(10), 729-736. doi:10.1016/j.neurol.2013.07.025

Chiu, M.-J., Fan, L.-Y., Chen, T.-F., Chen, Y.-F., Chieh, J.-J., & Horng, H.-E. (2017). Plasma tau levels in cognitively normal middle-aged and older adults. *Frontiers in Aging Neuroscience, 9*, 51.

Chouraki, V., Beiser, A., Younkin, L., Preis, S. R., Weinstein, G., Hansson, O., . . . Launer, L. (2015). Plasma amyloid-β and risk of Alzheimer's disease in the Framingham Heart Study. *Alzheimer's & Dementia, 11*(3), 249-257. e241.

Chouraki, V., Preis, S. R., Yang, Q., Beiser, A., Li, S., Larson, M. G., . . . Vasan, R. S. (2017). Association of amine biomarkers with incident dementia and Alzheimer's disease in the Framingham Study. *Alzheimer's & Dementia, 13*(12), 1327-1336.

Clark, C., Dayon, L., Masoodi, M., Bowman, G. L., & Popp, J. (2021). An integrative multi-omics approach reveals new central nervous system pathway alterations in Alzheimer's disease. *Alzheimer's Research & Therapy, 13*(1), 1-19.

Cooper, L. L., Woodard, T., Sigurdsson, S., van Buchem, M. A., Torjesen, A. A., Inker, L. A., . . . Mitchell, G. F. (2016). Cerebrovascular damage mediates relations between aortic stiffness and memory. *Hypertension, 67*(1), 176-182. doi:10.1161/hypertensionaha.115.06398

Cosco, T. D., Prina, A. M., Perales, J., Stephan, B. C., & Brayne, C. (2014). Operational definitions of successful aging: A systematic review. *International Psychogeriatrics, 26*(3), 373-381. doi:10.1017/s1041610213002287

Costa, A. C., Joaquim, H. P., Forlenza, O. V., Gattaz, W. F., & Talib, L. L. (2020). Three plasma metabolites in elderly patients differentiate mild cognitive impairment and Alzheimer's disease: A pilot study. *European Archives of Psychiatry and Clinical Neuroscience, 270*(4), 483-488.

Couronné, R., Probst, P., & Boulesteix, A.-L. (2018). Random forest versus logistic regression: a large-scale benchmark experiment. *BMC Bioinformatics, 19*(1), 270.

Crane, P. K., Carle, A., Gibbons, L. E., Insel, P., Mackin, R. S., Gross, A., . . . Harvey, D. (2012). Development and assessment of a composite score for memory in the Alzheimer's Disease Neuroimaging Initiative (ADNI). *Brain Imaging and Behavior, 6*(4), 502-516.

Cummings, J., Lee, G., Zhong, K., Fonseca, J., & Taghva, K. (2021). Alzheimer's disease drug development pipeline: 2021. *Alzheimer's & Dementia: Translational Research & Clinical Interventions, 7*(1), e12179.

Cummings, J. L., Tong, G., & Ballard, C. (2019). Treatment combinations for Alzheimer's disease: current and future pharmacotherapy options. *Journal of Alzheimer's Disease, 67*(3), 779-794.

Daffner, K. R. (2010). Promoting successful cognitive aging: A comprehensive review. *Journal of Alzheimer's Disease, 19*(4), 1101-1122. doi:10.3233/JAD-2010-1306

Dale, A., Fischl, B., & Sereno, M. I. (1999). Cortical Surface-Based Analysis: I. Segmentation and Surface Reconstruction. *Neuroimage, 9*, 179-194.

Dale, A. M., & Sereno, M. I. (1993). Improved localizadon of cortical activity by combining EEG and MEG with MRI cortical surface reconstruction: a linear approach. *J Cogn Neurosci, 5*(2), 162-176.

de Frias, C. M., Nilsson, L. G., & Herlitz, A. (2006). Sex differences in cognition are stable over a 10-year period in adulthood and old age. *Neuropsychol Dev Cogn, 13*(3-4), 574-587. doi:10.1080/13825580600678418

De Godoy, L. L., Alves, C. A. P. F., Saavedra, J. S. M., Studart-Neto, A., Nitrini, R., da Costa Leite, C., & Bisdas, S. (2021). Understanding brain resilience in superagers: a systematic review. *Neuroradiology, 63*(5), 663-683.

De Leon, M., George, A., Golomb, J., Tarshish, C., Convit, A., Kluger, A., . . . Reisberg, B. (1997). Frequency of hippocampal formation atrophy in normal aging and Alzheimer's disease. *Neurobiology of Aging, 18*(1), 1-11.

DeCarlo, C. A., Tuokko, H. A., Williams, D., Dixon, R. A., & MacDonald, S. W. (2014). BioAge: Toward a multi-determined, mechanistic account of cognitive aging. *Ageing Research Reviews, 18*, 95-105. doi:10.1016/j.arr.2014.09.003

Desikan, R. S., Fan, C. C., Wang, Y., Schork, A. J., Cabral, H. J., Cupples, L. A., . . . Holland, D. (2017). Genetic assessment of age-associated Alzheimer disease risk: Development and validation of a polygenic hazard score. *PLoS Medicine, 14*(3), e1002258.

Deters, K. D., Risacher, S. L., Kim, S., Nho, K., West, J. D., Blennow, K., . . . Weiner, M. W. (2017). Plasma tau association with brain atrophy in mild cognitive impairment and Alzheimer's disease. *Journal of Alzheimer's Disease, 58*(4), 1245-1254.

Devanand, D. P., Bansal, R., Liu, J., Hao, X., Pradhaban, G., & Peterson, B. S. (2012). MRI hippocampal and entorhinal cortex mapping in predicting conversion to Alzheimer's disease. *Neuroimage, 60*(3), 1622-1629.

Ding, X., Charnigo, R. J., Schmitt, F. A., Kryscio, R. J., Abner, E. L., & Alzheimer's Disease Neuroimaging, I. (2019). Evaluating trajectories of episodic memory in normal cognition and mild cognitive impairment: Results from ADNI. *PloS One, 14*(2), e0212435. doi:10.1371/journal.pone.0212435

Dixon, R., & Lachman, M. (2019). Risk and protective factors in cognitive aging: advances in assessment, prevention, and promotion of alternative pathways. In.

Dixon, R. A., & Lachman, M. E. (2019). Risk and protective factors in cognitive aging: Advances in assessment, prevention, and promotion of alternative pathways. In G. R. Samanez-Larkin (Ed.), *The aging brain: Functional adaptation across adulthood* (pp. 217-263). Washington, DC: APA Books.

Dixon, R. A., Small, B. J., MacDonald, S. W. S., & McArdle, J. J. (2012). Yes, memory declines with aging - but when, how, and why? In M. Naveh-Benjamin & N. Ohta (Eds.), *Memory and aging: Current issues and future directions* (pp. 325-347). New York, NY: Psychology Press.

Djordjevic, J., Jones-Gotman, M., De Sousa, K., & Chertkow, H. (2008). Olfaction in patients with mild cognitive impairment and Alzheimer's disease. *Neurobiology of Aging, 29*(5), 693-706.

Dong, A., Honnorat, N., Gaonkar, B., & Davatzikos, C. (2015). CHIMERA: clustering of heterogeneous disease effects via distribution matching of imaging patterns. *IEEE Transactions on Medical Imaging, 35*(2), 612-621.

Donix, M., Burggren, A. C., Scharf, M., Marschner, K., Suthana, N. A., Siddarth, P., . . . Ercoli, L. M. (2013). APOE associated hemispheric asymmetry of entorhinal cortical thickness in aging and Alzheimer's disease. *Psychiatry Research: Neuroimaging, 214*(3), 212-220.

Drouin, S. M., McFall, G. P., & Dixon, R. A. (2021). Subjective memory concerns, poor vascular health, and male sex predict exacerbated memory decline trajectories: An integrative data-driven class and prediction analysis. *Neuropsychology*.

Drouin, S. M., McFall, G. P., Potvin, O., Bellec, P., Masellis, M., Duchesne, S., . . . Alzheimer's Disease Neuroimaging, I. (2022). Data-Driven Analyses of Longitudinal Hippocampal Imaging Trajectories: Discrimination and Biomarker Prediction of Change Classes. *Journal of Alzheimer's Disease, 88*(1), 97-115. doi:10.3233/JAD-215289

Duan, J., Wang, X., Chi, J., Chen, H., Bai, L., Hu, Q., . . . Wang, X. (2020). Correlation between the variables collected at admission and progression to severe cases during hospitalization among patients with COVID-19 in Chongqing. *Journal of Medical Virology, 92*(11), 2616-2622.

Duits, F. H., Wesenhagen, K. E., Ekblad, L., Wolters, E., Willemse, E. A., Scheltens, P., . . . Tijms, B. M. (2021). Four subgroups based on tau levels in Alzheimer's disease observed in two independent cohorts. *Alzheimer's Research & Therapy, 13*(1), 1-25.

Durazzo, T. C., Meyerhoff, D. J., & Nixon, S. J. (2013). Interactive effects of chronic cigarette smoking and age on hippocampal volumes. *Drug and Alcohol Dependence, 133*(2), 704-711.

Dye, L., Boyle, N. B., Champ, C., & Lawton, C. (2017). The relationship between obesity and cognitive health and decline. *Proceedings of the Nutrition Society, 76*(4), 443-454.

Eavani, H., Habes, M., Satterthwaite, T. D., An, Y., Hsieh, M.-K., Honnorat, N., . . . Beason-Held, L. L. (2018). Heterogeneity of structural and functional imaging patterns of advanced brain aging revealed via machine learning methods. *Neurobiol Aging, 71*, 41-50.

Elbejjani, M., Fuhrer, R., Abrahamowicz, M., Mazoyer, B., Crivello, F., Tzourio, C., & Dufouil, C. (2014). Hippocampal atrophy and subsequent depressive symptoms in older men and women: results from a 10-year prospective cohort. *American Journal of Epidemiology, 180*(4), 385-393.

Engelke, U. F., Zijlstra, F. S., Mochel, F., Valayannopoulos, V., Rabier, D., Kluijtmans, L. A., . . . Wamelink, M. M. (2010). Mitochondrial involvement and erythronic acid as a novel biomarker in transaldolase deficiency. *Biochimica et Biophysica Acta (BBA)-Molecular Basis of Disease, 1802*(11), 1028-1035.

Ezzati, A., Zammit, A. R., Habeck, C., Hall, C. B., Lipton, R. B., & Initiative, A. s. D. N. (2019). Detecting biological heterogeneity patterns in ADNI amnestic mild cognitive impairment based on volumetric MRI. *Brain Imaging and Behavior*, 1-13.

Falahati, F., Westman, E., & Simmons, A. (2014). Multivariate data analysis and machine learning in Alzheimer's disease with a focus on structural magnetic resonance imaging. *Journal of Alzheimer's Disease, 41*(3), 685-708.

Farrell, S., Kane, A. E., Bisset, E., Howlett, S. E., & Rutenberg, A. D. (2022). Measurements of damage and repair of binary health attributes in aging mice and humans reveal that robustness and resilience decrease with age, operate over broad timescales, and are affected differently by interventions. *Elife, 11*, e77632.

Feinkohl, I., Aung, P. P., Keller, M., Robertson, C. M., Morling, J. R., McLachlan, S., . . . Price, J. F. (2014). Severe hypoglycemia and cognitive decline in older people with type 2 diabetes: the Edinburgh type 2 diabetes study. *Diabetes Care, 37*(2), 507-515.

Ferrari, C., Xu, W. L., Wang, H. X., Winblad, B., Sorbi, S., Qiu, C., & Fratiglioni, L. (2013). How can elderly apolipoprotein E ε4 carriers remain free from dementia? *Neurobiology of Aging, 34*(1), 13-21. doi:10.1016/j.neurobiolaging.2012.03.003

Ferreira, D., Verhagen, C., Hernández-Cabrera, J. A., Cavallin, L., Guo, C.-J., Ekman, U., . . . Wahlund, L.-O. (2017). Distinct subtypes of Alzheimer's disease based on patterns of brain atrophy: Longitudinal trajectories and clinical applications. *Scientific Reports, 7*, 46263.

Fischl, B., & Dale, A. M. (2000). Measuring the thickness of the human cerebral cortex from magnetic resonance images. *Proc Natl Acad Sci U S A, 97*, 11050-11055.

Fischl, B., Liu, A., & Dale, A. M. (2001). Automated manifold surgery: constructing geometrically accurate and topologically correct models of the human cerebral cortex. *{IEEE} Medical Imaging, 20*(1), 70-80.

Fischl, B., Salat, D. H., Busa, E., Albert, M., Dieterich, M., Haselgrove, C., . . . Dale, A. M. (2002). Whole brain segmentation: automated labeling of neuroanatomical structures in the human brain. *Neuron, 33*, 341-355.

Fischl, B., Salat, D. H., van der Kouwe, A. J. W., Makris, N., Ségonne, F., Quinn, B. T., & Dale, A. M. (2004). Sequence-independent segmentation of magnetic resonance images. *Neuroimage, 23*, S69 - S84. doi:DOI: 10.1016/j.neuroimage.2004.07.016

Fischl, B., Sereno, M. I., & Dale, A. (1999). Cortical Surface-Based Analysis: II: Inflation, Flattening, and a Surface-Based Coordinate System. *Neuroimage, 9*, 195-207.

Fischl, B., Sereno, M. I., Tootell, R. B. H., & Dale, A. M. (1999). High-resolution intersubject averaging and a coordinate system for the cortical surface. *Hum Brain Mapp, 8*, 272-284. doi:10.1002/(SICI)1097-0193(1999)8:4<272::AID-HBM10>3.0.CO;2-4

Fischl, B., van der Kouwe, A., Destrieux, C., Halgren, E., Ségonne, F., Salat, D. H., . . . Dale, A. M. (2004). Automatically Parcellating the Human Cerebral Cortex. *Cerebral Cortex, 14*, 11-22. doi:10.1093/cercor/bhg087

Fox, N., Scahill, R., Crum, W., & Rossor, M. (1999). Correlation between rates of brain atrophy and cognitive decline in AD. *Neurology, 52*(8), 1687-1687.

Fox, N. C., & Schott, J. M. (2004). Imaging cerebral atrophy: Normal ageing to Alzheimer's disease. *The Lancet, 363*(9406), 392-394.

Fransquet, P. D., & Ryan, J. (2018). Micro RNA as a potential blood-based epigenetic biomarker for Alzheimer's disease. *Clinical Biochemistry, 58*, 5-14.

Fraser, M. A., Shaw, M. E., & Cherbuin, N. (2015). A systematic review and meta-analysis of longitudinal hippocampal atrophy in healthy human ageing. *Neuroimage, 112*, 364-374.

Fraser, M. A., Walsh, E. I., Shaw, M. E., Abhayaratna, W. P., Anstey, K. J., Sachdev, P. S., & Cherbuin, N. (2021). Longitudinal trajectories of hippocampal volume in middle to older age community dwelling individuals. *Neurobiology of Aging, 97*, 97-105.

Fratiglioni, L. (1993). Epidemiology of Alzheimer’s disease. Issues of etiology and validity. *Acta Neurologica Scandinavica. Supplementum, 145*.

Fukumoto, N., Fujii, T., Combarros, O., Kamboh, M. I., Tsai, S. J., Matsushita, S., . . . Ingelsson, M. (2010). Sexually dimorphic effect of the Val66Met polymorphism of BDNF on susceptibility to Alzheimer's disease: New data and meta-analysis. *American Journal of Medical Genetics Part B: Neuropsychiatric Genetics, 153*(1), 235-242.

Fukuyama, K., Kakio, S., Nakazawa, Y., Kobata, K., Funakoshi-Tago, M., Suzuki, T., & Tamura, H. (2018). Roasted Coffee Reduces β-Amyloid Production by Increasing Proteasomal β-Secretase Degradation in Human Neuroblastoma SH-SY5Y Cells. *Molecular Nutrition & Food Research, 62*(21), 1800238.

Gebreyesus, Y., Dalton, D., Nixon, S., De Chiara, D., & Chinnici, M. (2023). Machine Learning for Data Center Optimizations: Feature Selection Using Shapley Additive exPlanation (SHAP). *Future Internet, 15*(3), 88.

Géron, A. (2022). *Hands-on machine learning with Scikit-Learn, Keras, and TensorFlow*: " O'Reilly Media, Inc.".

Gibbons, L. E., Carle, A. C., Mackin, R. S., Harvey, D., Mukherjee, S., Insel, P., . . . Crane, P. K. (2012). A composite score for executive functioning, validated in Alzheimer's Disease

Neuroimaging Initiative (ADNI) participants with baseline mild cognitive impairment. *Brain Imaging and Behavior, 6*(4), 517-527. doi:10.1007/s11682-012-9176-1

Giorgio, J., Landau, S. M., Jagust, W. J., Tino, P., Kourtzi, Z., & Initiative, A. s. D. N. (2020). Modelling prognostic trajectories of cognitive decline due to Alzheimer's disease. *NeuroImage: Clinical, 26*, 102199.

Glisky, E. L. (2007). Changes in cognitive function in human aging. *Brain aging: Models, methods, and mechanisms*, 3-20.

Gomar, J. J., Bobes-Bascaran, M. T., Conejero-Goldberg, C., Davies, P., Goldberg, T. E., & Initiative, A. s. D. N. (2011). Utility of combinations of biomarkers, cognitive markers, and risk factors to predict conversion from mild cognitive impairment to Alzheimer disease in patients in the Alzheimer's disease neuroimaging initiative. *Archives of general psychiatry, 68*(9), 961-969.

Gorbach, T., Pudas, S., Lundquist, A., Orädd, G., Josefsson, M., Salami, A., . . . Nyberg, L. (2017). Longitudinal association between hippocampus atrophy and episodic-memory decline. *Neurobiology of Aging, 51*, 167-176.

Goveas, J. S., Rapp, S. R., Hogan, P. E., Driscoll, I., Tindle, H. A., Smith, J. C., . . . Ockene, J. K. (2016). Predictors of optimal cognitive aging in 80+ women: the Women's Health Initiative Memory Study. *Journals of Gerontology Series A: Biomedical Sciences and Medical Sciences, 71*(Suppl_1), S62-S71.

Gregorutti, B., Michel, B., & Saint-Pierre, P. (2017). Correlation and variable importance in random forests. *Statistics and Computing, 27*(3), 659-678.

Gunter, J. L., Bernstein, M. A., Borowski, B. J., Ward, C. P., Britson, P. J., Felmlee, J. P., . . . Jack, C. R. (2009). Measurement of MRI scanner performance with the ADNI phantom. *Medical Physics, 36*(6Part1), 2193-2205.

Habartová, L., Hrubešová, K., Syslová, K., Vondroušová, J., Fišar, Z., Jirák, R., . . . Setnička, V. (2019). Blood-based molecular signature of Alzheimer's disease via spectroscopy and metabolomics. *Clinical Biochemistry, 72*, 58-63.

Habes, M., Grothe, M. J., Tunc, B., McMillan, C., Wolk, D. A., & Davatzikos, C. (2020). Disentangling heterogeneity in Alzheimer's disease and related dementias using data-driven methods. *Biological Psychiatry*.

Hampel, H., & Blennow, K. (2022). CSF tau and β-amyloid as biomarkers for mild cognitive impairment. *Dialogues in Clinical Neuroscience*.

Hampel, H., Mesulam, M.-M., Cuello, A. C., Farlow, M. R., Giacobini, E., Grossberg, G. T., . . . Snyder, P. J. (2018). The cholinergic system in the pathophysiology and treatment of Alzheimer's disease. *Brain, 141*(7), 1917-1933.

Hampel, H., Nisticò, R., Seyfried, N. T., Levey, A. I., Modeste, E., Lemercier, P., . . . Perry, G. (2021). Omics sciences for systems biology in Alzheimer's disease: State-of-the-art of the evidence. *Ageing Research Reviews, 69*, 101346.

Hampel, H., O'Bryant, S. E., Molinuevo, J. L., Zetterberg, H., Masters, C. L., Lista, S., . . . Blennow, K. (2018). Blood-based biomarkers for Alzheimer disease: mapping the road to the clinic. *Nature Reviews Neurology, 14*(11), 639-652.

Han, X., Jovicich, J., Salat, D., van der Kouwe, A., Quinn, B., Czanner, S., . . . Fischl, B. (2006). Reliability of MRI-derived measurements of human cerebral cortical thickness: The effects of field strength, scanner upgrade and manufacturer. *Neuroimage, 32*, 180-194.

Han, X., Rozen, S., Boyle, S. H., Hellegers, C., Cheng, H., Burke, J. R., . . . Kaddurah-Daouk, R. (2011). Metabolomics in early Alzheimer's disease: identification of altered plasma sphingolipidome using shotgun lipidomics. *PloS One, 6*(7), e21643.

Hanon, O., Vidal, J. S., Lehmann, S., Bombois, S., Allinquant, B., Baret-Rose, C., . . . Delmaire, C. (2022). Plasma amyloid beta predicts conversion to dementia in subjects with mild cognitive impairment: The BALTAZAR study. *Alzheimer's & Dementia*.

Hansen, S. B., & Wang, H. (2023). The shared role of cholesterol in neuronal and peripheral inflammation. *Pharmacology and Therapeutics*, 108486.

Hapfelmeier, A., & Ulm, K. (2013). A new variable selection approach using random forests. *Computational Statistics & Data Analysis, 60*, 50-69.

Hasin, Y., Seldin, M., & Lusis, A. (2017). Multi-omics approaches to disease. *Genome Biology, 18*(1), 1-15.

Hastie, T., Tibshirani, R., & Friedman, J. (2009). *The elements of statistical learning: data mining, inference, and prediction*: Springer Science & Business Media.

Heilman, K. M., & Nadeau, S. E. (2019). *Cognitive Changes and the Aging Brain*: Cambridge University Press.

Henneman, W., Vrenken, H., Barnes, J., Sluimer, I., Verwey, N., Blankenstein, M., . . . Barkhof, F. (2009). Baseline CSF p-tau levels independently predict progression of hippocampal atrophy in Alzheimer disease. *Neurology, 73*(12), 935-940.

Hersi, M., Irvine, B., Gupta, P., Gomes, J., Birkett, N., & Krewski, D. (2017). Risk factors associated with the onset and progression of Alzheimer's disease: A systematic review of the evidence. *Neurotoxicology, 61*, 143-187.

Hilal, S., Wolters, F. J., Verbeek, M. M., Vanderstichele, H., Ikram, M. K., Stoops, E., . . . Vernooij, M. W. (2018). Plasma amyloid-β levels, cerebral atrophy and risk of dementia: a population-based study. *Alzheimer's Research & Therapy, 10*(1), 63.

Hinrichs, C., Singh, V., Xu, G., Johnson, S. C., & Initiative, A. D. N. (2011). Predictive markers for AD in a multi-modality framework: an analysis of MCI progression in the ADNI population. *Neuroimage, 55*(2), 574-589.

Hothorn, T., Buehlmann, P., Dudoit, S., Molinaro, A., & Van Der Laan, M. (2006). Survival ensembles. *Biostatistics, 7*(3), 355-373. doi:10.1093/biostatistics/kxj011

Hu, D., Liu, C., Xia, K., Abramowitz, A., Wu, G., & Initiative, A. s. D. N. (2021). Characterizing the Resilience Effect of Neurodegeneration for the Mechanistic Pathway of Alzheimer's Disease. *Journal of Alzheimer's Disease, 84*(3), 1351-1362.

Hu, D. Y., Wu, M. Y., Chen, G. Q., Deng, B. Q., Yu, H. B., Huang, J., . . . Liu, J. Y. (2022). Metabolomics analysis of human plasma reveals decreased production of trimethylamine N-oxide retards the progression of chronic kidney disease. *British Journal of Pharmacology, 179*(17), 4344-4359.

Hu, X., Yang, Y., & Gong, D. (2017). Changes of cerebrospinal fluid Aβ 42, t-tau, and p-tau in Parkinson's disease patients with cognitive impairment relative to those with normal cognition: a meta-analysis. *Neurological Sciences, 38*, 1953-1961.

Huan, T., Tran, T., Zheng, J., Sapkota, S., MacDonald, S. W., Camicioli, R., . . . Li, L. (2018). Metabolomics analyses of saliva detect novel biomarkers of Alzheimer's disease. *Journal of Alzheimer's Disease, 65*(4), 1401-1416.

Imtiaz, B., Tolppanen, A.-M., Kivipelto, M., & Soininen, H. (2014). Future directions in Alzheimer's disease from risk factors to prevention. *Biochemical Pharmacology, 88*(4), 661-670.

Iturria-Medina, Y., Sotero, R. C., Toussaint, P. J., Mateos-Pérez, J. M., & Evans, A. C. (2016). Early role of vascular dysregulation on late-onset Alzheimer's disease based on multifactorial data-driven analysis. *Nature communications, 7*(1), 11934.

Jack, C. R., Petersen, R. C., Xu, Y., O'Brien, P., Smith, G. E., Ivnik, R. J., . . . Kokmen, E. (2000). Rates of hippocampal atrophy correlate with change in clinical status in aging and AD. *Neurology, 55*(4), 484-490.

Jack, C. R., Shiung, M., Weigand, S., O'Brien, P., Gunter, J., Boeve, B. F., . . . Tangalos, E. G. (2005). Brain atrophy rates predict subsequent clinical conversion in normal elderly and amnestic MCI. *Neurology, 65*(8), 1227-1231.

Jack, C. R., Wiste, H. J., Weigand, S. D., Knopman, D. S., Vemuri, P., Mielke, M. M., . . . Machulda, M. M. (2015). Age, sex, and APOE ε4 effects on memory, brain structure, and β-amyloid across the adult life span. *JAMA neurology, 72*(5), 511-519.

Jack, C. R., Wiste, H. J., Weigand, S. D., Knopman, D. S., Vemuri, P., Mielke, M. M., . . . Petersen, R. C. (2015). Age, sex, and APOE ε4 effects on memory, brain structure, and beta-amyloid across the adult life span. *JAMA Neurol, 72*(5), 511-519. doi:10.1001/jamaneurol.2014.4821

Jack Jr, C. R., Bennett, D. A., Blennow, K., Carrillo, M. C., Dunn, B., Haeberlein, S. B., . . . Karlawish, J. (2018). NIA-AA research framework: Toward a biological definition of Alzheimer's disease. *Alzheimers. Dement., 14*(4), 535-562.

Jack Jr, C. R., Bernstein, M. A., Fox, N. C., Thompson, P., Alexander, G., Harvey, D., . . . Ward, C. (2008). The Alzheimer's disease neuroimaging initiative (ADNI): MRI methods. *Journal of Magnetic Resonance Imaging: An Official Journal of the International Society for Magnetic Resonance in Medicine, 27*(4), 685-691.

Jacobucci, R., & Grimm, K. J. (2020). Machine learning and psychological research: The unexplored effect of measurement. *Perspectives on Psychological Science, 15*(3), 809-816.

Javaid, A., Hasan, R., Zohra, A., & Hussain, Z. (2012). A comparative study of the antihypertensive agents on serum liver enzymes ALT, AST and ALP of hypertensive and cardiac patients. *Journal of Basic & Applied Sciences, 8*, 468-472.

Jia, L., Yang, J., Zhu, M., Pang, Y., Wang, Q., Wei, Q., . . . Wang, Q. (2021). A metabolite panel that differentiates Alzheimer's disease from other dementia types. *Alzheimer's & Dementia*.

Jiang, Y., Sun, X., Hu, M., Zhang, L., Zhao, N., Shen, Y., . . . Yu, W. (2022). Plasma metabolomics of schizophrenia with cognitive impairment: a pilot study. *Frontiers in Psychiatry, 13*, 950602.

Johnstone, D., Milward, E. A., Berretta, R., Moscato, P., & Initiative, A. s. D. N. (2012). Multivariate protein signatures of pre-clinical Alzheimer's disease in the Alzheimer's disease neuroimaging initiative (ADNI) plasma proteome dataset. *PloS One, 7*(4), e34341.

Josefsson, M., de Luna, X., Pudas, S., Nilsson, L.-G., & Nyberg, L. (2012). Genetic and lifestyle predictors of 15-year longitudinal change in episodic memory. *Journal of the American Geriatrics Society, 60*(12), 2308-2312. doi:10.1111/jgs.12000

Jovicich, J., Czanner, S., Greve, D., Haley, E., van der Kouwe, A., Gollub, R., . . . Dale, A. (2006). Reliability in multi-site structural MRI studies: Effects of gradient non-linearity correction on phantom and human data. *Neuroimage, 30*, 436-443. doi:DOI: 10.1016/j.neuroimage.2005.09.046

Ju, C., Zhou, J., Lee, S., Tan, M. S., Liu, T., Bazoukis, G., . . . Wei, L. (2021). Derivation of an electronic frailty index for predicting short-term mortality in heart failure: a machine learning approach. *ESC heart failure, 8*(4), 2837-2845.

Jung, N.-Y., Seo, S. W., Yoo, H., Yang, J.-J., Park, S., Kim, Y. J., . . . Lee, J. M. (2016). Classifying anatomical subtypes of subjective memory impairment. *Neurobiol Aging, 48*, 53-60.

Kaddurah-Daouk, R., Zhu, H., Sharma, S., Bogdanov, M., Rozen, S., Matson, W., . . . Lei, Z. (2013). Alterations in metabolic pathways and networks in Alzheimer's disease. *Translational psychiatry, 3*(4), e244-e244.

Kaffashian, S. (2014). Plasma b-amyloid and MRI markers of cerebral small vessel disease.

Kaup, A. R., Nettiksimmons, J., Harris, T. B., Sink, K. M., Satterfield, S., Metti, A. L., . . . Yaffe, K. (2015). Cognitive resilience to apolipoprotein E ε4: Contributing factors in black and white older adults. *JAMA Neurol, 72*(3), 340-348. doi:10.1001/jamaneurol.2014.3978

Kauppi, K., Rönnlund, M., Nordin Adolfsson, A., Pudas, S., & Adolfsson, R. (2020). Effects of polygenic risk for Alzheimer's disease on rate of cognitive decline in normal aging. *Translational psychiatry, 10*(1), 250.

Kerchner, G. A., Berdnik, D., Shen, J. C., Bernstein, J. D., Fenesy, M. C., Deutsch, G. K., . . . Rutt, B. K. (2014). APOE ε4 worsens hippocampal CA1 apical neuropil atrophy and episodic memory. *Neurology, 82*(8), 691-697. doi:10.1212/WNL.0000000000000154

Kim, Y. S., Lee, K. J., & Kim, H. (2017). Serum tumour necrosis factor-α and interleukin-6 levels in Alzheimer's disease and mild cognitive impairment. *Psychogeriatrics, 17*(4), 224-230.

Kjelvik, G., Saltvedt, I., White, L. R., Stenumgård, P., Sletvold, O., Engedal, K., . . . Håberg, A. K. (2014). The brain structural and cognitive basis of odor identification deficits in mild cognitive impairment and Alzheimer's disease. *BMC Neurology, 14*(1), 1-10.

Kok, A. A., Aartsen, M. J., Deeg, D. J., & Huisman, M. (2015). Capturing the diversity of successful aging: An operational definition based on 16-year trajectories of functioning. *The Gerontologist*(Advance online publication). doi:10.1093/geront/gnv127

Koran, M. E. I., Wagener, M., & Hohman, T. J. (2017). Sex differences in the association between AD biomarkers and cognitive decline. *Brain Imaging and Behavior, 11*(1), 205-213.

Korolev, I. O., Symonds, L. L., & Bozoki, A. C. (2016). Predicting Progression from Mild Cognitive Impairment to Alzheimer's Dementia Using Clinical, MRI, and Plasma Biomarkers via Probabilistic Pattern Classification. *PloS One, 11*(2), e0138866. doi:10.1371/journal.pone.0138866

Kwon, G.-R., Gupta, Y., & Lama, R. K. (2019). Prediction and classification of Alzheimer's disease based on combined features from apolipoprotein-E genotype, cerebrospinal fluid, MR, and FDG-PET imaging biomarkers. *Frontiers in computational neuroscience, 13*, 72.

Lambert, J.-C., Schraen-Maschke, S., Richard, F., Fievet, N., Rouaud, O., Berr, C., . . . Buee, L. (2009). Association of plasma amyloid β with risk of dementia: the prospective Three-City Study. *Neurology, 73*(11), 847-853.

Lanza, S. T., Collins, L. M., Lemmon, D. R., & Schafer, J. L. (2007). PROC LCA: A SAS procedure for latent class analysis. *Structural Equation Modeling: A Multidisciplinary Journal, 14*(4), 671-694.

Latimer, C. S., Keene, C. D., Flanagan, M. E., Hemmy, L. S., Lim, K. O., White, L. R., . . . Montine, T. J. (2017). Resistance to Alzheimer disease neuropathologic changes and apparent cognitive resilience in the Nun and Honolulu-Asia Aging Studies. *Journal of Neuropathology and Experimental Neurology, 76*(6), 458-466.

Laws, K. R., Irvine, K., & Gale, T. M. (2016). Sex differences in cognitive impairment in Alzheimer's disease. *World journal of psychiatry, 6*(1), 54.

Lebedeva, A., Sundström, A., Lindgren, L., Stomby, A., Aarsland, D., Westman, E., . . . Nyberg, L. (2018). Longitudinal relationships among depressive symptoms, cortisol, and brain atrophy in the neocortex and the hippocampus. *Acta Psychiatr Scand, 137*(6), 491-502.

Lee, Y.-J., Lin, S.-Y., Peng, S.-W., Lin, Y.-C., Chen, T.-B., Wang, P.-N., & Cheng, I. (2023). Predictive Utility of Plasma Amyloid and Tau for Cognitive Decline in Cognitively Normal Adults. *The journal of prevention of Alzheimer's disease, 10*(2), 178-185.

Legdeur, N., Badissi, M., Carter, S. F., De Crom, S., Van De Kreeke, A., Vreeswijk, R., . . . Van Campen, J. P. (2018). Resilience to cognitive impairment in the oldest-old: design of the EMIF-AD 90+ study. *BMC Geriatrics, 18*, 1-16.

Legdeur, N., Heymans, M., Comijs, H., Huisman, M., Maier, A., & Visser, P. (2018). Age dependency of risk factors for cognitive decline. *BMC Geriatrics, 18*, 1-10.

Lehmann, S., Dumurgier, J., Ayrignac, X., Marelli, C., Alcolea, D., Ormaechea, J. F., . . . Vialaret, J. (2020). Cerebrospinal fluid A beta 1–40 peptides increase in Alzheimer's disease and are highly correlated with phospho-tau in control individuals. *Alzheimer's Research & Therapy, 12*(1), 1-12.

Levine, M. E., Lu, A. T., Quach, A., Chen, B. H., Assimes, T. L., Bandinelli, S., . . . Li, Y. (2018). An epigenetic biomarker of aging for lifespan and healthspan. *Aging, 10*(4), 573.

Li, J.-Q., Tan, L., Wang, H.-F., Tan, M.-S., Tan, L., Xu, W., . . . Yu, J.-T. (2016). Risk factors for predicting progression from mild cognitive impairment to Alzheimer's disease: a systematic review and meta-analysis of cohort studies. *Journal of Neurology, Neurosurgery and Psychiatry, 87*(5), 476-484.

Li, J., Liu, S., Hu, Y., Zhu, L., Mao, Y., & Liu, J. (2022). Predicting mortality in intensive care unit patients with heart failure using an interpretable machine learning model: retrospective cohort study. *Journal of Medical Internet Research, 24*(8), e38082.

Lim, A., Krajina, K., & Marsland, A. L. (2013). Peripheral inflammation and cognitive aging. *Mod Trends Pharmacopsychiatri, 28*, 175-187. doi:10.1159/000346362

Lin, F. V., Wang, X., Wu, R., Rebok, G. W., Chapman, B. P., & Initiative, A. s. D. N. (2017). Identification of successful cognitive aging in the Alzheimer's disease neuroimaging initiative study. *Journal of Alzheimer's Disease, 59*(1), 101-111.

Lipnicki, D. M., Sachdev, P. S., Crawford, J., Reppermund, S., Kochan, N. A., Trollor, J. N., . . . Brodaty, H. (2013). Risk Factors for Late-Life Cognitive Decline and Variation with Age and Sex in the Sydney Memory and Ageing Study. *PloS One, 8*(6), e65841. doi:10.1371/journal.pone.0065841

Lista, S., Faltraco, F., Prvulovic, D., & Hampel, H. (2013). Blood and plasma-based proteomic biomarker research in Alzheimer's disease. *Progress in Neurobiology, 101*, 1-17.

Little, T. D. (2013). *Longitudinal structural equation modeling*. New York, NY: Guilford Press.

Liu, J., Semiz, S., van der Lee, S. J., van der Spek, A., Verhoeven, A., van Klinken, J. B., . . . van Dijk, K. W. (2017). Metabolomics based markers predict type 2 diabetes in a 14-year follow-up study. *Metabolomics, 13*, 1-11.

Livingston, G., Huntley, J., Sommerlad, A., Ames, D., Ballard, C., Banerjee, S., . . . Cooper, C. (2020). Dementia prevention, intervention, and care: 2020 report of the Lancet Commission. *The Lancet, 396*(10248), 413-446.

Livingston, G., Sommerlad, A., Orgeta, V., Costafreda, S. G., Huntley, J., Ames, D., . . . Cohen-Mansfield, J. (2017). Dementia prevention, intervention, and care. *The Lancet, 390*(10113), 2673-2734.

Lopez, O. L., Chang, Y., Ives, D. G., Snitz, B. E., Fitzpatrick, A. L., Carlson, M. C., . . . DeKosky, S. T. (2019). Blood amyloid levels and risk of dementia in the Ginkgo Evaluation of Memory Study (GEMS): A longitudinal analysis. *Alzheimer's & Dementia, 15*(8), 1029-1038.

Lövdén, M., Schaefer, S., Noack, H., Bodammer, N. C., Kühn, S., Heinze, H.-J., . . . Lindenberger, U. (2012). Spatial navigation training protects the hippocampus against age-related changes during early and late adulthood. *Neurobiology of Aging, 33*(3), 620. e629-620. e622.

Luchsinger, J. A., & Mayeux, R. (2007). Adiposity and Alzheimer's disease. *Current Alzheimer Research, 4*(2), 127-134.

Lundberg, S. M., Erion, G. G., & Lee, S.-I. (2018). Consistent individualized feature attribution for tree ensembles. *arXiv preprint arXiv:1802.03888*.

Lyra e Silva, N. M., Gonçalves, R. A., Pascoal, T. A., Lima-Filho, R. A., Resende, E. d. P. F., Vieira, E. L., . . . Fortuna, J. T. (2021). Pro-inflammatory interleukin-6 signaling links cognitive impairments and peripheral metabolic alterations in Alzheimer's disease. *Translational psychiatry, 11*(1), 251.

MacDonald, S. W., DeCarlo, C. A., & Dixon, R. A. (2011). Linking biological and cognitive aging: Toward improving characterizations of developmental time. *The Journals of Gerontology Series B: Psychological Sciences and Social Sciences, 66*(Suppl 1), i59-70. doi:10.1093/geronb/gbr039

MacDonald, S. W., Keller, C. J., Brewster, P. W., & Dixon, R. A. (2018). Contrasting olfaction, vision, and audition as predictors of cognitive change and impairment in non-demented older adults. *Neuropsychology, 32*(4), 450.

MahmoudianDehkordi, S., Arnold, M., Nho, K., Ahmad, S., Jia, W., Xie, G., . . . Thompson, J. W. (2019). Altered bile acid profile associates with cognitive impairment in Alzheimer's disease—an emerging role for gut microbiome. *Alzheimer's & Dementia, 15*(1), 76-92.

Malpas, C. B. (2016). Structural neuroimaging correlates of cognitive status in older adults: a person-oriented approach. *Journal of Clinical Neuroscience, 30*, 77-82.

Mamo, J., Jian, L., James, A., Flicker, L., Esselmann, H., & Wiltfang, J. (2008). Plasma lipoprotein β-amyloid in subjects with Alzheimer's disease or mild cognitive impairment. *Annals of Clinical Biochemistry, 45*(4), 395-403.

Mandrekar, J. N. (2010). Receiver operating characteristic curve in diagnostic test assessment. *Journal of Thoracic Oncology, 5*(9), 1315-1316.

Mapstone, M., Lin, F., Nalls, M. A., Cheema, A. K., Singleton, A. B., Fiandaca, M. S., & Federoff, H. J. (2017). What success can teach us about failure: the plasma metabolome of older adults with superior memory and lessons for Alzheimer's disease. *Neurobiology of Aging, 51*, 148-155.

Marsillach, J., Adorni, M. P., Zimetti, F., Papotti, B., Zuliani, G., & Cervellati, C. (2020). HDL proteome and Alzheimer's disease: evidence of a link. *Antioxidants, 9*(12), 1224.

Martin, P., Kelly, N., Kahana, B., Kahana, E., B, J. W., Willcox, D. C., & Poon, L. W. (2014). Defining successful aging: A tangible or elusive concept? *Gerontologist, 55*(1), 14-25. doi:10.1093/geront/gnu044

Martinez, A. E., Weissberger, G., Kuklenyik, Z., He, X., Meuret, C., Parekh, T., . . . King, S. M. (2023). The small HDL particle hypothesis of Alzheimer's disease. *Alzheimer's & Dementia, 19*(2), 391-404.

Masyn, K. E. (2013a). 25 latent class analysis and finite mixture modeling. In *The Oxford handbook of quantitative methods* (pp. 551): Oxford University Press, Oxford.

Masyn, K. E. (2013b). Latent class analysis and finite mixture modeling. In *The Oxford handbook of quantitative methods* (pp. 551): Oxford University Press, Oxford.

Mazumder, M. K., Phukan, B. C., Bhattacharjee, A., & Borah, A. (2018). Disturbed purine nucleotide metabolism in chronic kidney disease is a risk factor for cognitive impairment. *Medical Hypotheses, 111*, 36-39.

McCarrey, A. C., An, Y., Kitner-Triolo, M. H., Ferrucci, L., & Resnick, S. M. (2016). Sex differences in cognitive trajectories in clinically normal older adults. *Psychology and Aging, 31*(2), 166-175. doi:10.1037/pag0000070

McDermott, K. L., McFall, G. P., Andrews, S. J., Anstey, K. J., & Dixon, R. A. (2017). Memory resilience to Alzheimer's genetic risk: Sex effects in predictor profiles. *Journals of Gerontology. Series B: Psychological Sciences and Social Sciences, 72*(6), 937-946.

McFall, G. P., Bäckman, L., & Dixon, R. A. (2019). Nuances in Alzheimer's Genetic Risk Reveal Differential Predictions of Non-demented Memory Aging Trajectories: Selective Patterns by APOE Genotype and Sex. *Current Alzheimer Research, 16*(4), 302-315.

McFall, G. P., Bohn, L., Drouin, S.M., Gee, M., Han, W., Li, L., Camicioli, R., & Dixon, R.A. (2023). owards identifying multi-modal predictors of incipient dementia in Parkinson's disease: A machine learning analysis. *Submitted for Publication*.

McFall, G. P., Drouin, S., Potvin, O., Dieumegarde, L., Collins, L. D., Bellec, P., . . . Dixon, R. A. (2020). Modeling Hippocampal Volume Trajectory Variability in Cognitively Healthy Aging: Moderation by Sex and APOE. *Neuroimage, Submited*.

McFall, G. P., McDermott, K. L., & Dixon, R. A. (2019). Modifiable Risk Factors Discriminate Memory Trajectories in Non-Demented Aging: Precision Factors and Targets for Promoting Healthier Brain Aging and Preventing Dementia. *Journal of Alzheimer's Disease, 70*(s1), S101-S118. doi:10.3233/JAD-180571

McFall, G. P., Wiebe, S. A., Vergote, D., Westaway, D., Jhamandas, J., Bäckman, L., & Dixon, R. A. (2015a). ApoE and pulse pressure interactively influence level and change in the aging of episodic memory: Protective effects among epsilon2 carriers. *Neuropsychology, 29*(3), 388-401. doi:10.1037/neu0000150

McFall, G. P., Wiebe, S. A., Vergote, D., Westaway, D., Jhamandas, J., Bäckman, L., & Dixon, R. A. (2015b). ApoE and pulse pressure interactively influence level and change in the aging of episodic memory: Protective effects among ε2 carriers. *Neuropsychology, 29*(3), 388-401. doi:10.1037/neu0000150

Melikyan, Z. A., Corrada, M. M., Leiby, A.-M., Sajjadi, S. A., Bukhari, S., Montine, T. J., & Kawas, C. H. (2022). Cognitive resilience to three dementia-related neuropathologies in an oldest-old man: A case report from The 90+ Study. *Neurobiology of Aging, 116*, 12-15.

Melis, R. J. F., Haaksma, M. L., & Muniz-Terrera, G. (2019). Understanding and predicting the longitudinal course of dementia. *Curr Opin Psychiatry, 32*(2), 123-129. doi:10.1097/YCO.0000000000000482

Michaelson, D. M. (2014). APOE ε4: The most prevalent yet understudied risk factor for Alzheimer's disease. *Alzheimer's & Dementia, 10*(6), 861-868.

Michaud, T. L., Siahpush, M., Farazi, P. A., Kim, J., Yu, F., Su, D., & Murman, D. L. (2018). The association between body mass index, and cognitive, functional, and behavioral declines for incident dementia. *Journal of Alzheimer's Disease, 66*(4), 1507-1517.

Mielke, M. M., Roberts, R. O., Savica, R., Cha, R., Drubach, D. I., Christianson, T., . . . Petersen, R. C. (2013). Assessing the temporal relationship between cognition and gait: slow gait predicts cognitive decline in the Mayo Clinic Study of Aging. *Journals of Gerontology. Series A: Biological Sciences and Medical Sciences, 68*(8), 929-937. doi:10.1093/gerona/gls256

Mielke, M. M., Vemuri, P., & Rocca, W. A. (2014). Clinical epidemiology of Alzheimer's disease: assessing sex and gender differences. *Clinical Epidemiology, 6*, 37-48. doi:10.2147/CLEP.S37929

Milne, N. T., Bucks, R. S., Davis, W. A., Davis, T. M., Pierson, R., Starkstein, S. E., & Bruce, D. G. (2018). Hippocampal atrophy, asymmetry, and cognition in type 2 diabetes mellitus. *Brain and behavior, 8*(1), e00741.

Minkova, L., Habich, A., Peter, J., Kaller, C. P., Eickhoff, S. B., & Klöppel, S. (2017). Gray matter asymmetries in aging and neurodegeneration: A review and meta-analysis. *Human Brain Mapping, 38*(12), 5890-5904.

Montine, T. J., Cholerton, B. A., Corrada, M. M., Edland, S. D., Flanagan, M. E., Hemmy, L. S., . . . White, L. R. (2019). Concepts for brain aging: resistance, resilience, reserve, and compensation. *Alzheimer's Research & Therapy, 11*(1), 1-3.

Mosti, C. B., Rog, L. A., & Fink, J. W. (2019). Differentiating mild cognitive impairment and cognitive changes of normal aging. In *Handbook on the Neuropsychology of Aging and Dementia* (pp. 445-463): Springer.

Mulak, A. (2021). Bile acids as key modulators of the brain-gut-microbiota axis in Alzheimer's disease. *Journal of Alzheimer's Disease, 84*(2), 461-477.

Müller, A. C., & Guido, S. (2016). *Introduction to machine learning with Python: a guide for data scientists*: " O'Reilly Media, Inc.".

Muthén, L., & Muthén, B. (2018). *Mplus users guide and Mplus version 8.2. Retrieved January 10, 2019*.

Nash, D. T., & Fillit, H. (2006). Cardiovascular disease risk factors and cognitive impairment. *The American journal of cardiology, 97*(8), 1262-1265.

Navigating the Path Forward for Dementia in Canada: The Landmark Study Report #1. (2022). Retrieved from

Negash, S., A Bennett, D., S Wilson, R., A Schneider, J., & E Arnold, S. (2011). Cognition and neuropathology in aging: multidimensional perspectives from the Rush Religious Orders Study and Rush Memory and Aging Project. *Current Alzheimer Research, 8*(4), 336-340.

Negash, S., Wilson, R. S., Leurgans, S. E., Wolk, D. A., Schneider, J. A., Buchman, A. S., . . . Arnold, S. E. (2013). Resilient brain aging: Characterization of discordance between Alzheimer's disease pathology and cognition. *Curr Alzheimer Res, 10*(8), 844-851. doi:10.2174/15672050113109990157

Negash, S., Xie, S., Davatzikos, C., Clark, C. M., Trojanowski, J. Q., Shaw, L. M., . . . Arnold, S. E. (2013). Cognitive and functional resilience despite molecular evidence of Alzheimer's disease pathology. *Alzheimers Dement, 9*(3), e89-95. doi:10.1016/j.jalz.2012.01.009

Nettiksimmons, J., Harvey, D., Brewer, J., Carmichael, O., DeCarli, C., Jack Jr, C. R., . . . Weiner, M. W. (2010). Subtypes based on cerebrospinal fluid and magnetic resonance imaging markers in normal elderly predict cognitive decline. *Neurobiology of Aging, 31*(8), 1419-1428.

Nguyen, J. C., Killcross, A. S., & Jenkins, T. A. (2014). Obesity and cognitive decline: role of inflammation and vascular changes. *Frontiers in Neuroscience, 8*, 375.

Nho, K., Kueider-Paisley, A., MahmoudianDehkordi, S., Arnold, M., Risacher, S. L., Louie, G., . . . Kastenmüller, G. (2019). Altered bile acid profile in mild cognitive impairment and Alzheimer's disease: relationship to neuroimaging and CSF biomarkers. *Alzheimer's & Dementia, 15*(2), 232-244.

Noble, K. G., Grieve, S. M., Korgaonkar, M. S., Engelhardt, L. E., Griffith, E. Y., Williams, L. M., & Brickman, A. M. (2012). Hippocampal volume varies with educational attainment across the life-span. *Frontiers in Human Neuroscience, 6*, 307.

Nordestgaard, L. T., Christoffersen, M., & Frikke-Schmidt, R. (2022). Shared risk factors between dementia and atherosclerotic cardiovascular disease. *International Journal of Molecular Sciences, 23*(17), 9777.

Nyberg, L., Lövdén, M., Riklund, K., Lindenberger, U., & Bäckman, L. (2012). Memory aging and brain maintenance. *Trends in Cognitive Sciences, 16*(5), 292-305.

Nyberg, L., Lövdén, M., Riklund, K., Lindenberger, U., & Bäckman, L. (2012). Memory aging and brain maintenance. *Trends in Cognitive Sciences, 16*(5), 292-305. doi:10.1016/j.tics.2012.04.005

Nyberg, L., & Pudas, S. (2019). Successful memory aging. *Annual Review of Psychology, 70*, 219-243.

Nylund, K. L., Asparouhob, T., & Muthén, B. O. (2007). Deciding on the number of classes in latent class analysis and growth mixture modeling: A Monte Carlo simulation study. *Structural Equation Modeling, 14*(4), 535-569. doi:10.1080/10705510701575396

O'Shea, A., Cohen, R., Porges, E. C., Nissim, N. R., & Woods, A. J. (2016). Cognitive aging and the hippocampus in older adults. *Frontiers in Aging Neuroscience, 8*, 298.

Olaya, B., Bobak, M., Haro, J. M., & Demakakos, P. (2017). Trajectories of Verbal Episodic Memory in Middle-Aged and Older Adults: Evidence from the English Longitudinal Study of Ageing. *Journal of the American Geriatrics Society, 65*(6), 1274-1281. doi:10.1111/jgs.14789

Orban, P., Tam, A., Urchs, S., Savard, M., Madjar, C., Badhwar, A., . . . Dagher, A. (2017). Subtypes of functional brain connectivity as early markers of neurodegeneration in Alzheimer's disease. *bioRxiv*, 195164.

Pase, M. P., Beiser, A. S., Himali, J. J., Satizabal, C. L., Aparicio, H. J., DeCarli, C., . . . Seshadri, S. (2019). Assessment of plasma total tau level as a predictive biomarker for dementia and related endophenotypes. *JAMA Neurology, 76*(5), 598-606.

Payton, N. M., Kalpouzos, G., Rizzuto, D., Fratiglioni, L., Kivipelto, M., Bäckman, L., & Laukka, E. J. (2018). Combining cognitive, genetic, and structural neuroimaging markers to identify individuals with increased dementia risk. *Journal of Alzheimer's Disease, 64*(2), 533-542.

Pedregosa, F., Varoquaux, G., Gramfort, A., Michel, V., Thirion, B., Grisel, O., . . . Dubourg, V. (2011). Scikit-learn: Machine learning in Python. *the Journal of machine Learning research, 12*, 2825-2830.

Perry, B. L., McConnell, W. R., Coleman, M. E., Roth, A. R., Peng, S., & Apostolova, L. G. (2021). Why the cognitive "fountain of youth" may be upstream: Pathways to dementia risk and resilience through social connectedness. *Alzheimer's & Dementia*.

Petersen, R. C., Aisen, P., Beckett, L. A., Donohue, M., Gamst, A., Harvey, D. J., . . . Toga, A. (2010). Alzheimer's disease neuroimaging initiative (ADNI): clinical characterization. *Neurology, 74*(3), 201-209.

Pettigrew, C., Soldan, A., Zhu, Y., Wang, M.-C., Moghekar, A., Brown, T., . . . Team, B. R. (2016). Cortical thickness in relation to clinical symptom onset in preclinical AD. *NeuroImage: Clinical, 12*, 116-122.

Pillai, J. A., Bena, J., Bekris, L., Kodur, N., Kasumov, T., Leverenz, J. B., & Kashyap, S. R. (2023). Metabolic syndrome biomarkers relate to rate of cognitive decline in MCI and dementia stages of Alzheimer's disease. *Alzheimer's Research & Therapy, 15*(1), 1-14.

Pini, L., Pievani, M., Bocchetta, M., Altomare, D., Bosco, P., Cavedo, E., . . . Frisoni, G. B. (2016). Brain atrophy in Alzheimer's disease and aging. *Ageing research reviews, 30*, 25-48.

Piras, F., Cherubini, A., Caltagirone, C., & Spalletta, G. (2011). Education mediates microstructural changes in bilateral hippocampus. *Human Brain Mapping, 32*(2), 282-289.

Potvin, O., Dieumegarde, L., Duchesne, S., Initiative, A. s. D. N., CIMA-Q, & groups, C. (2021). NOMIS: Quantifying morphometric deviations from normality over the lifetime of the adult human brain. *bioRxiv*, 2021.2001. 2025.428063.

Potvin, O., Mouiha, A., Dieumegarde, L., Duchesne, S., & Initiative, A. s. D. N. (2016). Normative data for subcortical regional volumes over the lifetime of the adult human brain. *Neuroimage, 137*, 9-20.

Prakash, M., Abdelaziz, M., Zhang, L., Strange, B. A., Tohka, J., & Initiative, A. s. D. N. (2021). Quantitative longitudinal predictions of Alzheimer's disease by multi-modal predictive learning. *Journal of Alzheimer's Disease, 79*(4), 1533-1546.

Prince, M., Wimo, A., Guerchet, M., Ali, G., Wu, Y., & Prina, M. (2015). World alzheimer report 2015. the global impact of dementia. alzheimer's disease international. *Alzheimer's Disease International (ADI), London*.

Proitsi, P., Kim, M., Whiley, L., Simmons, A., Sattlecker, M., Velayudhan, L., . . . Mecocci, P. (2017). Association of blood lipids with Alzheimer's disease: A comprehensive lipidomics analysis. *Alzheimer's & Dementia, 13*(2), 140-151.

Pudas, S., Persson, J., Josefsson, M., de Luna, X., Nilsson, L. G., & Nyberg, L. (2013). Brain characteristics of individuals resisting age-related cognitive decline over two decades. *Journal of Neuroscience, 33*(20), 8668-8677. doi:10.1523/jneurosci.2900-12.2013

Ram, N., & Grimm, K. J. (2009). Growth mixture modeling: A method for identifying differences in longitudinal change among unobserved groups. *Int J Behav Dev, 33*(6), 565-576. doi:10.1177/0165025409343765

Ramanan, V. K., Lesnick, T. G., Przybelski, S. A., Heckman, M. G., Knopman, D. S., Graff-Radford, J., . . . Jack, C. R. (2021). Coping with brain amyloid: genetic heterogeneity and cognitive resilience to Alzheimer's pathophysiology. *Acta Neuropathologica Communications, 9*(1), 1-14.

Raz, N., Ghisletta, P., Rodrigue, K. M., Kennedy, K. M., & Lindenberger, U. (2010). Trajectories of brain aging in middle-aged and older adults: Regional and individual differences. *Neuroimage, 51*(2), 501-511.

Rembach, A., Faux, N. G., Watt, A. D., Pertile, K. K., Rumble, R. L., Trounson, B. O., . . . Li, Q. X. (2014). Changes in plasma amyloid beta in a longitudinal study of aging and Alzheimer's disease. *Alzheimer's & Dementia, 10*(1), 53-61.

Rentz, D. M., Mormino, E. C., Papp, K. V., Betensky, R. A., Sperling, R. A., & Johnson, K. A. (2017). Cognitive resilience in clinical and preclinical Alzheimer's disease: the Association of Amyloid and Tau Burden on cognitive performance. *Brain Imaging and Behavior, 11*(2), 383-390.

Reuter, M., Rosas, H. D., & Fischl, B. (2010). Highly Accurate Inverse Consistent Registration: A Robust Approach. *Neuroimage, 53*, 1181-1196. doi:10.1016/j.neuroimage.2010.07.020

Reuter, M., Schmansky, N. J., Rosas, H. D., & Fischl, B. (2012). Within-Subject Template Estimation for Unbiased Longitudinal Image Analysis. *Neuroimage, 61*, 1402-1418. doi:10.1016/j.neuroimage.2012.02.084

Riedel, B. C., Daianu, M., Ver Steeg, G., Mezher, A., Salminen, L. E., Galstyan, A., . . . Initiative, A. s. D. N. (2018). Uncovering biologically coherent peripheral signatures of health and risk for Alzheimer's disease in the aging brain. *Frontiers in Aging Neuroscience*, 390.

Riedel, B. C., Thompson, P. M., & Brinton, R. D. (2016). Age, APOE and sex: triad of risk of Alzheimer's disease. *The Journal of steroid biochemistry and molecular biology, 160*, 134-147.

Riemenschneider, M., Buch, K., Schmolke, M., Kurz, A., & Guder, W. (1997). Diagnosis of Alzheimer's disease with cerebrospinal fluid tau protein and aspartate aminotransferase. *The Lancet, 350*(9080), 784.

Ritter, K., Schumacher, J., Weygandt, M., Buchert, R., Allefeld, C., Haynes, J.-D., & Initiative, A. s. D. N. (2015). Multimodal prediction of conversion to Alzheimer's disease based on incomplete biomarkers. *Alzheimer's & Dementia: Diagnosis, Assessment & Disease Monitoring, 1*(2), 206-215.

Rogalski, E. J., Sridhar, J., Martersteck, A., Makowski-Woidan, B., Engelmeyer, J., Parrish, T., . . . Weintraub, S. (2020). SuperAging: A model for studying mechanisms of resilience and resistance: Reserve and resilience: Opportunities and mechanisms for dementia prevention. *Alzheimer's & Dementia, 16*, e037932.

Röhr, S., Kivipelto, M., Mangialasche, F., Ngandu, T., & Riedel-Heller, S. G. (2022). Multidomain interventions for risk reduction and prevention of cognitive decline and dementia: current developments. *Current Opinion in Psychiatry, 35*(4), 285-292.

Rosano, C., Aizenstein, H. J., Newman, A. B., Venkatraman, V., Harris, T., Ding, J., . . . Yaffe, K. (2012). Neuroimaging differences between older adults with maintained versus declining cognition over a 10-year period. *Neuroimage, 62*(1), 307-313. doi:10.1016/j.neuroimage.2012.04.033

Rusanen, M., Rovio, S., Ngandu, T., Nissinen, A., Tuomilehto, J., Soininen, H., & Kivipelto, M. (2010). Midlife smoking, apolipoprotein E and risk of dementia and Alzheimer's disease: a population-based cardiovascular risk factors, aging and dementia study. *Dementia and Geriatric Cognitive Disorders, 30*(3), 277-284.

Rusinek, H., De Santi, S., Frid, D., Tsui, W.-H., Tarshish, C. Y., Convit, A., & de Leon, M. J. (2003). Regional brain atrophy rate predicts future cognitive decline: 6-year longitudinal MR imaging study of normal aging. *Radiology, 229*(3), 691-696.

Sabuncu, M. R., Buckner, R. L., Smoller, J. W., Lee, P. H., Fischl, B., Sperling, R. A., & Initiative, A. s. D. N. (2012). The association between a polygenic Alzheimer score and cortical thickness in clinically normal subjects. *Cerebral Cortex, 22*(11), 2653-2661.

Sachdev, P. S., Lipnicki, D. M., Crawford, J., Reppermund, S., Kochan, N. A., Trollor, J. N., . . . Brodaty, H. (2012). Risk profiles for mild cognitive impairment vary by age and sex: The Sydney Memory and Ageing Study. *The American Journal of Geriatric Psychiatry, 20*(10), 854-865. doi:http://dx.doi.org/10.1097/JGP.0b013e31825461b0

Sanke, H., Mita, T., Yoshii, H., Yokota, A., Yamashiro, K., Ingaki, N., . . . Tamura, Y. (2014). Relationship between olfactory dysfunction and cognitive impairment in elderly patients with type 2 diabetes mellitus. *Diabetes Research and Clinical Practice, 106*(3), 465-473.

Sapkota, S., Huan, T., Tran, T., Zheng, J., Camicioli, R., Li, L., & Dixon, R. A. (2018). Alzheimer's biomarkers from multiple modalities selectively discriminate clinical status: Relative importance of salivary metabolomics panels, genetic, lifestyle, cognitive, functional health and demographic risk markers. *Frontiers in Aging Neuroscience, 10*, 296.

Sapkota, S., McFall, G. P., Masellis, M., & Dixon, R. A. (2021). A multimodal risk network predicts executive function trajectories in non-demented aging. *Frontiers in Aging Neuroscience*, 602.

Schwarz, C. G., Gunter, J. L., Wiste, H. J., Przybelski, S. A., Weigand, S. D., Ward, C. P., . . . Dickson, D. W. (2016). A large-scale comparison of cortical thickness and volume methods for measuring Alzheimer's disease severity. *NeuroImage: Clinical, 11*, 802-812.

Sebastiani, P., Thyagarajan, B., Sun, F., Schupf, N., Newman, A. B., Montano, M., & Perls, T. T. (2017). Biomarker signatures of aging. *Aging Cell, 16*(2), 329-338.

Segonne, F., Dale, A. M., Busa, E., Glessner, M., Salat, D., Hahn, H. K., & Fischl, B. (2004). A hybrid approach to the skull stripping problem in MRI. *Neuroimage, 22*, 1060-1075. doi:DOI: 10.1016/j.neuroimage.2004.03.032

Segonne, F., Pacheco, J., & Fischl, B. (2007). Geometrically accurate topology-correction of cortical surfaces using nonseparating loops. *IEEE Trans Med Imaging, 26*, 518-529.

Seo, S. W., Im, K., Lee, J.-M., Kim, S. T., Ahn, H. J., Go, S. M., . . . Na, D. L. (2011). Effects of demographic factors on cortical thickness in Alzheimer's disease. *Neurobiol Aging, 32*(2), 200-209.

Seto, M., Weiner, R. L., Dumitrescu, L., & Hohman, T. J. (2021). Protective genes and pathways in Alzheimer's disease: moving towards precision interventions. *Molecular neurodegeneration, 16*(1), 1-16.

Shaffer, J. L., Petrella, J. R., Sheldon, F. C., Choudhury, K. R., Calhoun, V. D., Coleman, R. E., . . . Initiative, A. s. D. N. (2013). Predicting cognitive decline in subjects at risk for Alzheimer disease by using combined cerebrospinal fluid, MR imaging, and PET biomarkers. *Radiology, 266*(2), 583-591.

Shao, Y., Ouyang, Y., Li, T., Liu, X., Xu, X., Li, S., . . . Le, W. (2020). Alteration of metabolic profile and potential biomarkers in the plasma of Alzheimer's disease. *Aging and Disease, 11*(6), 1459.

Shen, S., Zhou, W., Chen, X., & Zhang, J. (2019). Sex differences in the association of APOE ε4 genotype with longitudinal hippocampal atrophy in cognitively normal older people. *European Journal of Neurology, 26*(11), 1362-1369.

Shen, S., Zhou, W., Chen, X., Zhang, J., & Initiative, A. s. D. N. (2019). Sex differences in the association of APOE ε4 genotype with longitudinal hippocampal atrophy in cognitively normal older people. *European Journal of Neurology, 26*(11), 1362-1369.

Sheppard, O., & Coleman, M. (2020). Alzheimer's Disease: Etiology, Neuropathology and Pathogenesis. *Exon Publications*, 1-21.

Shi, Y., Lu, X., Zhang, L., Shu, H., Gu, L., Wang, Z., . . . Zhou, D. (2019). Potential value of plasma amyloid-β, total Tau, and neurofilament light for identification of early Alzheimer's disease. *ACS chemical neuroscience, 10*(8), 3479-3485.

Shpanskaya, K. S., Choudhury, K. R., Hostage Jr, C., Murphy, K. R., Petrella, J. R., Doraiswamy, P. M., & Initiative, A. s. D. N. (2014). Educational attainment and hippocampal atrophy in the Alzheimer's disease neuroimaging initiative cohort. *Journal of Neuroradiology, 41*(5), 350-357.

Siderowf, A., Xie, S., Hurtig, H., Weintraub, D., Duda, J., Chen-Plotkin, A., . . . Clark, C. (2010). CSF amyloid β 1-42 predicts cognitive decline in Parkinson disease. *Neurology, 75*(12), 1055-1061.

Sled, J. G., Zijdenbos, A. P., & Evans, A. C. (1998). A nonparametric method for automatic correction of intensity nonuniformity in MRI data. *IEEE Trans Med Imaging, 17*, 87-97.

Sliwinski, M. J., Hofer, S. M., Hall, C., Buschke, H., & Lipton, R. B. (2003). Modeling memory decline in older adults: the importance of preclinical dementia, attrition, and chronological age. *Psychology and Aging, 18*(4), 658.

Small, B. J., Dixon, R. A., & McArdle, J. J. (2011). Tracking cognition–health changes from 55 to 95 years of age. *The Journals of Gerontology Series B: Psychological Sciences and Social Sciences, 66*(Suppl 1), i153-i161. doi:10.1093/geronb/gbq093

Son, G., Jahanshahi, A., Yoo, S.-J., Boonstra, J. T., Hopkins, D. A., Steinbusch, H. W., & Moon, C. (2021). Olfactory neuropathology in Alzheimer's disease: A sign of ongoing neurodegeneration. *BMB reports, 54*(6), 295.

Song, F., Poljak, A., Smythe, G. A., & Sachdev, P. (2009). Plasma biomarkers for mild cognitive impairment and Alzheimer's disease. *Brain Research Reviews, 61*(2), 69-80.

Stamouli, E., & Politis, A. (2016). Pro-inflammatory cytokines in Alzheimer's disease. *Psychiatrike= Psychiatriki, 27*(4), 264-275.

Stekhoven, D. J. (2011). Using the missForest package. *R package*, 1-11.

Stekhoven, D. J., & Bühlmann, P. (2012). MissForest—non-parametric missing value imputation for mixed-type data. *Bioinformatics, 28*(1), 112-118. doi:10.1093/bioinformatics/btr597

Stern, Y. (2012). Cognitive reserve in ageing and Alzheimer's disease. *The Lancet Neurology, 11*(11), 1006-1012. doi:http://dx.doi.org/10.1016/S1474-4422(12)70191-6

Stern, Y., Albert, M., Barnes, C. A., Cabeza, R., Pascual-Leone, A., & Rapp, P. R. (2023). A framework for concepts of reserve and resilience in aging. *Neurobiology of Aging, 124*, 100-103.

Stites, S. D., Cao, H., Harkins, K., & Flatt, J. D. (2022). Measuring sex and gender in aging and Alzheimer's research: Results of a national survey. *The Journals of Gerontology: Series B, 77*(6), 1005-1016.

Stricker, N. H., Dodge, H. H., Dowling, N. M., Han, S. D., Erosheva, E. A., Jagust, W. J., & Initiative, A. s. D. N. (2012). CSF biomarker associations with change in hippocampal

volume and precuneus thickness: implications for the Alzheimer's pathological cascade. *Brain Imaging and Behavior, 6*(4), 599-609.

Strobl, C., Boulesteix, A.-L., Kneib, T., Augustin, T., & Zeileis, A. (2008). Conditional variable importance for random forests. *BMC Bioinformatics, 9*(1), 1-11. doi:10.1186/1471-2105-9-307

Strobl, C., Boulesteix, A. L., Zeileis, A., & Hothorn, T. (2007). Bias in Random Forest Variable Importance Measures: Illustrations, Sources and a Solution. *BMC Bioinformatics, 8*. doi:10.1186/1471-2105-8-25

Suemoto, C. K., Gilsanz, P., Mayeda, E. R., & Glymour, M. M. (2015). Body mass index and cognitive function: the potential for reverse causation. *International Journal of Obesity, 39*(9), 1383-1389.

Sundermann, E. E., Tran, M., Maki, P. M., & Bondi, M. W. (2018). Sex differences in the association between apolipoprotein E ε4 allele and Alzheimer's disease markers. *Alzheimer's & Dementia: Diagnosis, Assessment & Disease Monitoring, 10*, 438-447.

Sundermann, E. E., Tran, M., Maki, P. M., Bondi, M. W., & Initiative, A. s. D. N. (2018). Sex differences in the association between apolipoprotein E ε4 allele and Alzheimer's disease markers. *Alzheimer's & Dementia: Diagnosis, Assessment & Disease Monitoring, 10*, 438-447.

Supasitthumrong, T., Tunvirachaisakul, C., Aniwattanapong, D., Tangwongchai, S., Chuchuen, P., Tawankanjanachot, I., . . . Maes, M. (2019). peripheral blood biomarkers coupled with the apolipoprotein e4 genotype are strongly associated with semantic and episodic memory impairments in elderly subjects with amnestic mild cognitive impairment and Alzheimer's disease. *Journal of Alzheimer's Disease, 71*(3), 797-811.

Svenningsson, A. L., Ossenkoppele, R., Stomrud, E., Palmqvist, S., & Hansson, O. (2021). Lower cognitive resilience against brain atrophy in cognitively unimpaired elderly is partly explained by Alzheimer's disease pathology. *Alzheimer's & Dementia, 17*, e055140.

T Howrey, B., A Raji, M., M Masel, M., & Kristen Peek, M. (2015). Stability in cognitive function over 18 years: Prevalence and predictors among older Mexican Americans. *Current Alzheimer Research, 12*(7), 614-621.

Taki, Y., Kinomura, S., Sato, K., Goto, R., Kawashima, R., & Fukuda, H. (2011). A longitudinal study of gray matter volume decline with age and modifying factors. *Neurobiology of Aging, 32*(5), 907-915.

Tam, A., Dansereau, C., Iturria-Medina, Y., Urchs, S., Orban, P., Sharmarke, H., . . . Initiative, A. s. D. N. (2019). A highly predictive signature of cognition and brain atrophy for progression to Alzheimer's dementia. *Gigascience, 8*(5), giz055.

Tanaka, T., Basisty, N., Fantoni, G., Candia, J., Moore, A. Z., Biancotto, A., . . . Ferrucci, L. (2020). Plasma proteomic biomarker signature of age predicts health and life span. *Elife, 9*, e61073.

Tanveer, M., Richhariya, B., Khan, R., Rashid, A., Khanna, P., Prasad, M., & Lin, C. (2020). Machine learning techniques for the diagnosis of Alzheimer's disease: A review. *ACM Transactions on Multimedia Computing, Communications, and Applications (TOMM), 16*(1s), 1-35.

Tatulian, S. A. (2022). Challenges and hopes for Alzheimer's disease. *Drug Discovery Today*.

Tierney, M. C., Curtis, A. F., Chertkow, H., & Rylett, R. J. (2017). Integrating sex and gender into neurodegeneration research: A six-component strategy. *Alzheimer's & Dementia: Translational Research & Clinical Interventions, 3*(4), 660-667.

Toledo, J. B., Xie, S. X., Trojanowski, J. Q., & Shaw, L. M. (2013). Longitudinal change in CSF Tau and Aβ biomarkers for up to 48 months in ADNI. *Acta Neuropathologica, 126*, 659-670.

Toloşi, L., & Lengauer, T. (2011). Classification with correlated features: unreliability of feature ranking and solutions. *Bioinformatics, 27*(14), 1986-1994.

Topiwala, A., Suri, S., Allan, C., Valkanova, V., Filippini, N., Sexton, C. E., . . . Singh-Manoux, A. (2019). Predicting cognitive resilience from midlife lifestyle and multi-modal MRI: A 30-year prospective cohort study. *PloS one, 14*(2), e0211273.

Trushina, E., & Mielke, M. M. (2014). Recent advances in the application of metabolomics to Alzheimer's Disease. *Biochimica et Biophysica Acta (BBA)-Molecular Basis of Disease, 1842*(8), 1232-1239.

Tseng, P.-Y., Chen, Y.-T., Wang, C.-H., Chiu, K.-M., Peng, Y.-S., Hsu, S.-P., . . . Lee, O. K.-S. (2020). Prediction of the development of acute kidney injury following cardiac surgery by machine learning. *Critical care, 24*(1), 1-13.

Ullah, I., Liu, K., Yamamoto, T., Zahid, M., & Jamal, A. (2023). Modeling of machine learning with SHAP approach for electric vehicle charging station choice behavior prediction. *Travel Behaviour and Society, 31*, 78-92.

Valenzuela, M. J., Sachdev, P., Wen, W., Chen, X., & Brodaty, H. (2008). Lifespan mental activity predicts diminished rate of hippocampal atrophy. *PloS One, 3*(7).

van Oijen, M., Hofman, A., Soares, H. D., Koudstaal, P. J., & Breteler, M. M. (2006). Plasma Aβ1–40 and Aβ1–42 and the risk of dementia: a prospective case-cohort study. *The Lancet Neurology, 5*(8), 655-660.

Varma, V. R., Oommen, A. M., Varma, S., Casanova, R., An, Y., Andrews, R. M., . . . Toledo, J. (2018). Brain and blood metabolite signatures of pathology and progression in Alzheimer disease: A targeted metabolomics study. *PLoS Medicine, 15*(1), e1002482.

Vasantharekha, R., Priyanka, H. P., Swarnalingam, T., Srinivasan, A. V., & ThyagaRajan, S. (2017). Interrelationship between Mini-Mental State Examination scores and biochemical parameters in patients with mild cognitive impairment and Alzheimer's disease. *Geriatrics & gerontology international, 17*(10), 1737-1745.

Velayudhan, L., Proitsi, P., Westman, E., Muehlboeck, J.-s., Mecocci, P., Vellas, B., . . . Spenger, C. (2013). Entorhinal cortex thickness predicts cognitive decline in Alzheimer's disease. *Journal of Alzheimer's Disease, 33*(3), 755-766.

Venugopalan, J., Tong, L., Hassanzadeh, H. R., & Wang, M. D. (2021). Multimodal deep learning models for early detection of Alzheimer's disease stage. *Scientific Reports, 11*(1), 1-13.

Voevodskaya, O., Simmons, A., Nordenskjöld, R., Kullberg, J., Ahlström, H., Lind, L., . . . Initiative, A. s. D. N. (2014). The effects of intracranial volume adjustment approaches on multiple regional MRI volumes in healthy aging and Alzheimer's disease. *Frontiers in Aging Neuroscience, 6*, 264.

Vogel, J. W., Young, A. L., Oxtoby, N. P., Smith, R., Ossenkoppele, R., Strandberg, O. T., . . . Iturria-Medina, Y. (2021). Four distinct trajectories of tau deposition identified in Alzheimer's disease. *Nature Medicine, 27*(5), 871-881.

Wachinger, C., Salat, D. H., Weiner, M., Reuter, M., & Initiative, A. s. D. N. (2016). Whole-brain analysis reveals increased neuroanatomical asymmetries in dementia for hippocampus and amygdala. *Brain, 139*(12), 3253-3266.

Waldstein, S. R., Rice, S. C., Thayer, J. F., Najjar, S. S., Scuteri, A., & Zonderman, A. B. (2008). Pulse pressure and pulse wave velocity are related to cognitive decline in the Baltimore Longitudinal Study of Aging. *Hypertension, 51*(1), 99-104. doi:10.1161/hypertensionaha.107.093674

Waljee, A. K., Mukherjee, A., Singal, A. G., Zhang, Y., Warren, J., Balis, U., . . . Higgins, P. D. (2013). Comparison of imputation methods for missing laboratory data in medicine. *BMJ Open, 3*(8), e002847. doi:10.1136/bmjopen-2013-002847

Wang, G., Zhou, Y., Huang, F.-J., Tang, H.-D., Xu, X.-H., Liu, J.-J., . . . Xu, W. (2014). Plasma metabolite profiles of Alzheimer's disease and mild cognitive impairment. *Journal of Proteome Research, 13*(5), 2649-2658.

Wang, K., Tian, J., Zheng, C., Yang, H., Ren, J., Liu, Y., . . . Zhang, Y. (2021). Interpretable prediction of 3-year all-cause mortality in patients with heart failure caused by coronary heart disease based on machine learning and SHAP. *Computers in Biology and Medicine, 137*, 104813.

Wang, M., Roussos, P., McKenzie, A., Zhou, X., Kajiwara, Y., Brennand, K. J., . . . Buxbaum, J. D. (2016). Integrative network analysis of nineteen brain regions identifies molecular signatures and networks underlying selective regional vulnerability to Alzheimer's disease. *Genome Medicine, 8*(1), 1-21.

Wang, X., Sun, Y., Li, T., Cai, Y., & Han, Y. (2019). Amyloid-β as a Blood Biomarker for Alzheimer's Disease: A Review of Recent Literature. *Journal of Alzheimer's Disease*(Preprint), 1-14.

Warzok, R. W., Kessler, C., Apel, G., Schwarz, A., Egensperger, R., Schreiber, D., . . . Walker, L. C. (1998). Apolipoprotein E4 promotes incipient Alzheimer pathology in the elderly. *Alzheimer Disease and Associated Disorders, 12*(1), 33-39.

Wheeler, M. J., Dempsey, P. C., Grace, M. S., Ellis, K. A., Gardiner, P. A., Green, D. J., & Dunstan, D. W. (2017). Sedentary behavior as a risk factor for cognitive decline? A focus on the influence of glycemic control in brain health. *Alzheimer's & Dementia: Translational Research & Clinical Interventions, 3*(3), 291-300.

Whiley, L., Sen, A., Heaton, J., Proitsi, P., García-Gómez, D., Leung, R., . . . Mecocci, P. (2014). Evidence of altered phosphatidylcholine metabolism in Alzheimer's disease. *Neurobiology of Aging, 35*(2), 271-278.

Whitwell, J. L., Dickson, D. W., Murray, M. E., Weigand, S. D., Tosakulwong, N., Senjem, M. L., . . . Petersen, R. C. (2012). Neuroimaging correlates of pathologically defined subtypes of Alzheimer's disease: a case-control study. *The Lancet Neurology, 11*(10), 868-877.

Whitwell, J. L., Wiste, H. J., Weigand, S. D., Rocca, W. A., Knopman, D. S., Roberts, R. O., . . . Initiative, A. D. N. (2012). Comparison of imaging biomarkers in the Alzheimer disease neuroimaging initiative and the Mayo Clinic Study of Aging. *Archives of Neurology, 69*(5), 614-622.

Wilkins, J. M., & Trushina, E. (2018). Application of metabolomics in Alzheimer's disease. *Frontiers in Neurology, 8*, 719.

Wimo, A., Guerchet, M., Ali, G.-C., Wu, Y.-T., Prina, A. M., Winblad, B., . . . Prince, M. (2017). The worldwide costs of dementia 2015 and comparisons with 2010. *Alzheimer's & Dementia, 13*(1), 1-7.

Wu, J. W., Yaqub, A., Ma, Y., Koudstaal, W., Hofman, A., Ikram, M. A., . . . Goudsmit, J. (2021). Biological age in healthy elderly predicts aging-related diseases including dementia. *Scientific Reports, 11*(1), 1-10.

Wu, Z., Phyo, A. Z. Z., Al-Harbi, T., Woods, R. L., & Ryan, J. (2020). Distinct cognitive trajectories in late life and associated predictors and outcomes: a systematic review. *Journal of Alzheimer's disease reports, 4*(1), 459-478.

Xu, J., Begley, P., Church, S. J., Patassini, S., Hollywood, K. A., Jüllig, M., . . . Unwin, R. D. (2016). Graded perturbations of metabolism in multiple regions of human brain in Alzheimer's disease: Snapshot of a pervasive metabolic disorder. *Biochimica et Biophysica Acta (BBA)-Molecular Basis of Disease, 1862*(6), 1084-1092.

Yaffe, K., Barnes, D. E., Rosenberg, D., Dublin, S., Kaup, A. R., Ludman, E. J., . . . Adams, K. J. (2019). Systematic multi-domain Alzheimer's risk reduction trial (SMARRT): study protocol. *Journal of Alzheimer's Disease, 70*(s1), S207-S220.

Yaffe, K., Fiocco, A. J., Lindquist, K., Vittinghoff, E., Simonsick, E. M., Newman, A. B., . . . Harris, T. B. (2009). Predictors of maintaining cognitive function in older adults: The Health ABC study. *Neurology, 72*(23), 2029-2035. doi:10.1212/WNL.0b013e3181a92c36

Yang, Y.-H., Huang, L.-C., Hsieh, S.-W., & Huang, L.-J. (2020). Dynamic blood concentrations of Aβ1–40 and Aβ1–42 in Alzheimer's disease. *Frontiers in Cell and Developmental Biology, 8*, 768.

Yu, J., Collinson, S. L., Liew, T. M., Ng, T.-P., Mahendran, R., Kua, E.-H., & Feng, L. (2019). Super-cognition in aging: cognitive profiles and associated lifestyle factors. *Applied Neuropsychology: Adult*.

Zahodne, L. B., Schupf, N., Brickman, A. M., Mayeux, R., Wall, M. M., Stern, Y., & Manly, J. J. (2016). Dementia risk and protective factors differ in the context of memory trajectory groups. *Journal of Alzheimer's Disease, 52*(3), 1013-1020. doi:10.3233/jad-151114

Zarrouk, A., Hammouda, S., Ghzaiel, I., Hammami, S., Khamlaoui, W., Ahmed, S. H., . . . Hammami, M. (2020). Association between oxidative stress and altered cholesterol metabolism in Alzheimer's disease patients. *Current Alzheimer Research, 17*(9), 823-834.

Zhang, S., Drouin, S., Dixon, R. A., & Li, L. (2022). Metabolomics analyses of MCI and AD cohorts in the COMPASS-ND study. . *Technical Report, The Metabolomics Innovation Centre, University of Alberta.* .

Zhang, S., Drouin, S., Li, L., & Dixon, R. A. (2022). Lipidomics analyses of MCI and AD cohorts in the COMPASS-ND study. . *Technical Report, The Metabolomics Innovation Centre, University of Alberta.* .

Zhang, Y., Qiu, C., Lindberg, O., Bronge, L., Aspelin, P., Bäckman, L., . . . Wahlund, L.-O. (2010). Acceleration of hippocampal atrophy in a non-demented elderly population: the SNAC-K study. *International Psychogeriatrics, 22*(1), 14-25.

Zhao, W., Wang, X., Yin, C., He, M., Li, S., & Han, Y. (2019). Trajectories of the hippocampal subfields atrophy in the Alzheimer's disease: A structural imaging study. *Frontiers in Neuroinformatics, 13*, 13.

Zheng, L., Eramudugolla, R., Cherbuin, N., Drouin, S. M., Dixon, R. A., & Anstey, K. J. (2023). Gender specific factors contributing to cognitive resilience in APOE ε4 positive older adults in a population-based sample. *Scientific Reports, 13*(1), 8037.

Zhou, F., Alsaid, A., Blommer, M., Curry, R., Swaminathan, R., Kochhar, D., . . . Tijerina, L. (2022). Predicting driver fatigue in monotonous automated driving with explanation using gpboost and SHAP. *International Journal of Human–Computer Interaction, 38*(8), 719-729.

Zhou, X., Wang, Q., An, P., Du, Y., Zhao, J., Song, A., & Huang, G. (2020). Relationship between folate, vitamin B12, homocysteine, transaminase and mild cognitive impairment in China: a case-control study. *International Journal of Food Sciences and Nutrition, 71*(3), 315-324.

Zhou, Z., Liang, Y., Zhang, X., Xu, J., Lin, J., Zhang, R., . . . Zhao, M. (2020). Low-density lipoprotein cholesterol and Alzheimer's disease: a systematic review and meta-analysis. *Frontiers in Aging Neuroscience, 12*, 5.

Zhu, H., & Kannan, K. (2019). Inter-day and inter-individual variability in urinary concentrations of melamine and cyanuric acid. *Environment International, 123*, 375-381.

Zou, Y.-m., Lu, D., Liu, L.-p., Zhang, H.-h., & Zhou, Y.-y. (2016). Olfactory dysfunction in Alzheimer’s disease. *Neuropsychiatric Disease and Treatment*, 869-875.

Zvěřová, M. (2019). Clinical aspects of Alzheimer's disease. *Clinical Biochemistry, 72*, 3-6.

Appendix A

Supplemental Material for Chapter 2 (as published in Drouin et al., 2022)

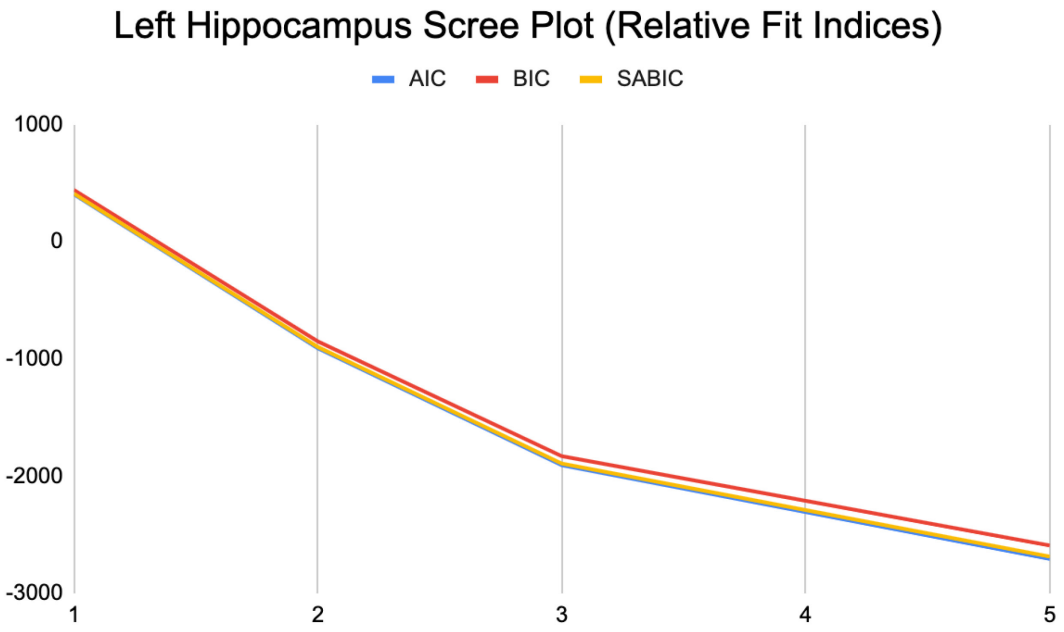

Supplementary Figure 1. Scree plot for the AIC, BIC, and SABIC values across the tested 1-, 2-, 3-, 4- and 5-class LCGA models for the LHC.

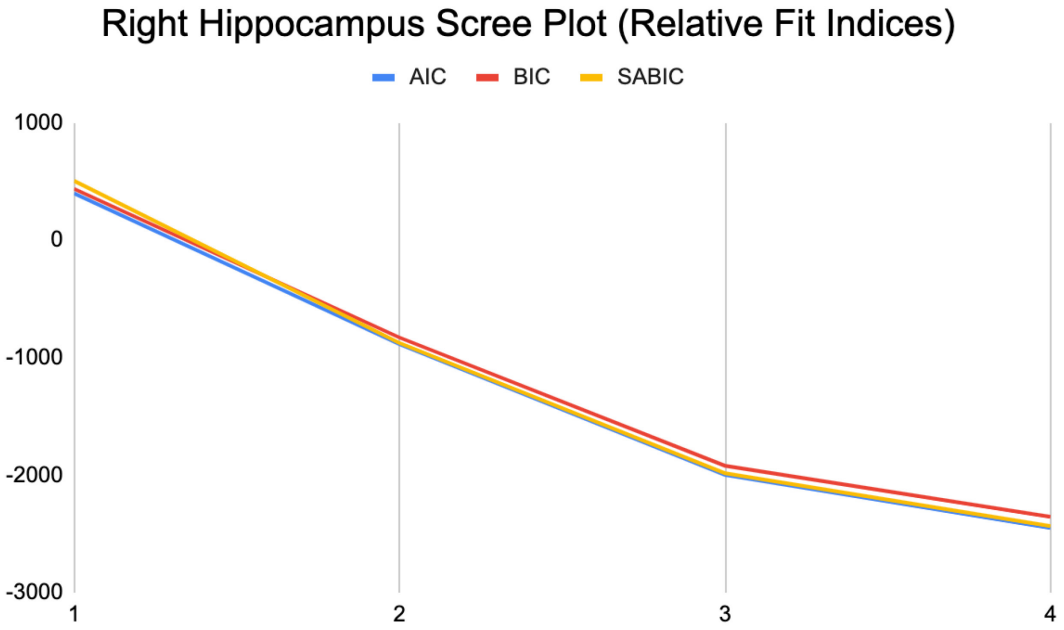

Supplementary Figure 2. Scree plot for the AIC, BIC, and SABIC values across the tested 1-, 2-, 3-, and 4-class LCGA models for the RHC.

	Lowest LHC Class	**Highest LHC Class**	**Lowest RHC Class**	**Highest RHC Class**
Wave 1, *Mean (SD)*	9.04 (4.49)	8.39 (3.77)	9.03 (4.60)	8.66 (3.90)
Wave 2, *Mean (SD)*	8.63 (4.69)	7.54 (3.44)	8.83 (4.91)	7.98 (3.50)
Wave 3, *Mean (SD)*	8.82 (4.61)	7.07 (3.56)	8.94 (4.89)	7.96 (3.70)
Wave 4, *Mean (SD)*	9.57 (5.13)	7.27 (3.11)	9.82 (5.83)	8.28 (3.69)
Wave 5, *Mean (SD)*	11.02 (6.28)	7.48 (3.55)	10.81 (6.59)	8.27 (3.44)
Wave 6, *Mean (SD)*	9.88 (6.54)	7.22 (3.39)	9.93 (6.27)	8.46 (3.73)

Supplementary Table 1. Mean (SD) Alzheimer's Disease Assessment Scale-Cognition scores by wave and hippocampal trajectory class.

	Lowest LHC Class	**Highest LHC Class**	**Lowest RHC Class**	**Highest RHC Class**
Wave 1, *Mean (SD)*	1.21 (0.61)	1.16 (0.49)	1.10 (0.61)	1.10 (0.46)
Wave 2, *Mean (SD)*	1.10 (0.64)	1.26 (0.58)	1.10 (0.64)	1.17 (0.55)
Wave 3, *Mean (SD)*	1.05 (0.61)	1.26 (0.56)	1.02 (0.59)	1.14 (0.54)
Wave 4, *Mean (SD)*	1.02 (0.61)	1.30 (0.54)	0.99 (0.62)	1.14 (0.56)
Wave 5, *Mean (SD)*	0.83 (0.61)	1.31 (0.56)	0.92 (0.71)	1.12 (0.45)
Wave 6, *Mean (SD)*	0.73 (0.88)	1.31 (0.61)	0.98 (0.77)	1.16 (0.54)

Supplementary Table 2. Mean (SD) Memory Composite scores by wave and hippocampal trajectory class.